

University of Alberta

**Mechanistic studies on the uptake and intracellular trafficking of
DNA complexes in primary cells using lipid-modified cationic
polymers as non-viral gene carrier**

by

Charlie Yu Ming Hsu

A thesis submitted to the Faculty of Graduate Studies and Research
in partial fulfillment of the requirements for the degree of

Doctor of Philosophy

in

Biomedical Sciences

Department of Biomedical Engineering

© Charlie Yu Ming Hsu

Fall 2012

Edmonton, Alberta

Permission is hereby granted to the University of Alberta Libraries to reproduce single copies of this thesis and to lend or sell such copies for private, scholarly or scientific research purposes only. Where the thesis is converted to, or otherwise made available in digital form, the University of Alberta will advise potential users of the thesis of these terms.

The author reserves all other publication and other rights in association with the copyright in the thesis and, except as herein before provided, neither the thesis nor any substantial portion thereof may be printed or otherwise reproduced in any material form whatsoever without the author's prior written permission.

for my mom and dad

給我的爸媽, 家安和秋媛

Abstract

This thesis work is aimed at addressing some of the fundamental questions surrounding the intracellular fate of plasmid DNA in clinically-relevant primary cells, when delivered with lipid-modified cationic polymers as gene carriers. We developed an optimized procedure for the transfection of primary cells, which included modifications designed to maximize the *in vitro* stability of the DNA-carrier complexes and enhance their transfection utility. These polymeric gene carriers bind to DNA through electrostatic interaction, which drives a self-assembly process that condenses DNA into sub-micron particles suitable for cellular uptake. This interaction is not DNA sequence or structurally specific, and thus able to package DNA molecules with different topologies and molecular weights with equal efficiency for uptake. However, circularized DNA performed better than its linearized equivalent in transfection, suggesting intracellular processing may be dependent on the physicochemical properties of the assembled complexes. Thus, we concentrated our effort on understanding the intracellular events leading to transfection. Using a linoleic acid substituted cationic polymer, we found that transfection efficiency is correlated with the amount of pDNA associated with the nucleus and that lipid-moieties is able to facilitate nuclear association of DNA to enhance transfection. Further, lipid modification altered the uptake pathways of the complexes from ones that are predominantly driven by macropinocytosis to ones that are mediated by clathrin. Endosome escape continues to be an inefficient process with these polymeric gene carriers, suggesting methods to promote cytosolic release may be the most effective approach to enhance their transfection efficiencies.

Acknowledgement

This project is funded by operating grants from the Natural Sciences and Engineering Research Council (NSERC) and Canadian Institutes of Health Research (CIHR)

I would like to acknowledge the generous financial support from NSERC for the Alexander Graham Bell Canada Graduate Scholarship, Alberta Innovates for the Graduate Studentship, Faculty of Medicine for the 75th Anniversary Award, CIHR Skeletal Regenerative Medicine Team for the Graduate Studentship, Ministry of Advanced Education for the Graduate Studentship, and Faculty of Graduate Studies and Research for the President's Doctoral Prize of Distinction, Queen Elizabeth II Masters' Graduate Studentship and Profiling Alberta's Graduate Student Award.

I would like to thank Dr. Derrick Rancourt (Biochemistry & Molecular Biology, University of Calgary) for the engaging discussions on professional development, Dr. Michael Hendzel (Oncology, University of Alberta) for the helpful thesis advice, Dr. Vanessa Incani and Dr. Remant Bahadur for synthesis of the polymers, Cezary Kucharski for the tissue culture work, Dorothy Rutkowski (Medical Microbiology and Immunology) for the tutorial on flow cytometry, Dr. Xuejun Sun (Experimental Oncology), Dr. Stephen Ogg (Medical Microbiology & Immunology) and Geraldine Barron (Alberta Health Services) for the technical assistance on confocal microscopy, and my colleagues in the Uludağ lab for the camaraderie.

Finally, my deepest gratitude goes out to my supervisor, Dr. Hasan Uludağ for his supervision, his patience, his mentorship, for the opportunity to work under his guidance, to travel the world, and for giving me a chance to learn and excel.

Table of Contents

Chapter 1	1
Scope of dissertation	
Chapter 2	5
Nucleic-acid based gene therapeutics: delivery challenges in non-viral gene carriers ¹	
2.1 Introduction	6
2.2 Barriers to nucleic acid based therapeutics	8
2.2.1 Overview of transfection pathway	9
2.2.2 Physicochemical properties and cell type dictate uptake pathways	10
2.2.3 Pathway dictates sorting and release of the cargo.....	15
2.2.4 Nuclear import.....	17
2.2.5 Sub-nuclear trafficking and post transcriptional events.....	19
2.2.6 Immune responses to nucleic acid and complexes.....	23
2.2.7 Limited duration of transgene expression.....	24
2.3 Strategies to improve transfection efficiencies	26
2.3.1 Stabilizing particles to facilitate uptake via transgene conducive pathway	26
2.3.2 Cell-specific targeting.....	27
2.3.3 Endosome escape and nucleocytoplasmic trafficking.....	28
2.4 References	32
Chapter 3	50
A simple and rapid non-viral approach to efficiently transfect primary tissue-derived cells using polyethylenimine ¹	
3.1 Introduction	51
3.1.1 Cationic polymers	51
3.1.2 Experimental design	53
3.1.3 Cell line.....	54
3.1.4 Complexation volume	54
3.1.5 Salt and solutes.....	55

3.1.6 DNA concentration, ratio of polymer-to-DNA, and polymer concentration	56
3.1.7 Effect of serum	57
3.1.8 Complex stability and incubation time.....	57
3.1.9 Cell density	58
3.1.10 Culturing condition.....	58
3.1.11 Choice of promoter and reporter gene construct	60
3.1.12 Limitations of the protocol.....	61
3.1.13 Optimization required for NHFF and rat bone marrow and human stromal cells.....	62
3.2 Reagent setup	64
3.3 Procedure	65
3.3.1 Revive frozen cell stock for sub-culturing	65
3.3.2 Cell seeding for transfection (24-well plate).....	66
3.3.3 Preparation of bPEI25/pDNA polyplexes for transfection.....	69
3.4 Analysis of GFP Expression by FACS.....	74
3.4 Typical results	78
3.5 References	89
Chapter 4	94
Effects of size and topology of DNA molecules on intracellular delivery with non-viral gene carriers ¹	
4.1 Introduction.....	95
4.2 Materials and methods	97
4.2.1 Chemicals and reagents.....	97
4.2.2 Preparation of different DNA Molecules (Figure 4.1)	98
4.2.3 Atomic force microscopy (AFM).....	99
4.2.4 Particle size measurement.....	100
4.2.5 Electrophoretic gel mobility assay (EMSA).....	100
4.2.6 Analysis of carrier-DNA binding.....	100
4.2.7 Analysis of carrier-DNA complex dissociation	101
4.2.8 Cell culture and DNA uptake	101

4.2.9 Transfection and assessment of GFP expression	102
4.2.10 Statistical analysis.....	103
4.3 Results	104
4.3.1 Particle formation.....	104
4.3.2 DNA binding	107
4.3.3 Complex dissociation.....	108
4.3.4 DNA delivery to rBMS.....	109
4.3.5 Effect of serum on DNA delivery.....	111
4.3.6 Transgene expression	114
4.4 Discussion	117
4.5 References	123
Chapter 5	127
Improved transfection efficiency of an aliphatic lipid substituted 2 kDa polyethylenimine is attributed to enhanced nuclear association and uptake in rat bone marrow stromal cell1	
5.1 Introduction	128
5.2 Materials and methods	130
5.2.1 Materials	130
5.2.2 Plasmid labeling.....	131
5.2.3 Cell culture and transfection	131
5.2.4 Complex preparation	132
5.2.5 Particle size measurement.....	132
5.2.6 Polyplex uptake and transfection efficiency	133
5.2.7 Nuclei isolation and quantification of nuclear-associated pDNA	133
5.2.8 Confocal microscopy and image quantification	134
5.2.9 Statistical analysis.....	134
5.3 Results	134
5.3.1 Polyplex sizes in transfection medium	134
5.3.2 Correlation between pDNA uptake and transgene expression.....	137
5.3.3 Nuclear-associated pDNA and transgene expression.....	142
5.3.4 CSLM image quantification of nuclear-associated plasmid DNA.....	146

5.3.5 Sub-cellular distribution of pDNA in GFP Positive and Negative Cells...	149
5.4 Discussion	152
5.5 References	158
Chapter 6	162
Cellular uptake pathways of lipid-modified cationic polymers in gene delivery to primary cells ¹	
6.1 Introduction	163
6.2 Materials and Methods	166
6.2.1 Materials.....	166
6.2.2 Cell culture.....	166
6.2.3 Plasmid DNA (pDNA) labeling.....	167
6.2.4 Cytotoxicity assessment of endocytosis inhibitors by MTT assay.....	167
6.2.5 Preparation of complexes for transfection.....	168
6.2.6 Transfection efficiency and gene expression kinetics.....	169
6.2.7 Uptake kinetics and inhibition of endocytosis.....	170
6.2.8 Laser scanning confocal fluorescent microscopy.....	171
6.2.9 Particle size measurements.....	172
6.2.10 Statistical analysis.....	173
6.3 Results	173
6.3.1 Particle sizes and transfection efficiencies in NHFF cells.....	173
6.3.2 Uptake kinetics of pDNA.....	176
6.3.3 Transgene expression kinetics.....	178
6.3.4 Effect of endocytosis inhibitors on transfection efficiency.....	181
6.3.5 Effect of endocytosis inhibitors on pDNA Uptake.....	184
6.3.6 Effect of endosome disruption on transfection.....	186
6.3.7 Intracellular distribution of complexes.....	187
6.4 Discussion	193
6.5 References	200
Chapter 7	206
General discussion, conclusions, future directions and perspectives	

7.1 General discussion.....	207
7.1 Future directions.....	210
7.2 Concluding remarks and perspectives	213
7.3 References.....	216
Appendix A	220
Delivering plasmid DNA with a non-viral polymeric carrier: plasmid persistence does not necessarily lead to transgene expression1	
Appendix B	225
Persistence of Plasmid DNA does not lead to sustained transgene expression in PEI mediated transfection in vitro: implication of transcriptional and post-transcriptional silencing1	
Appendix C	232
Transfection mediated by cationic polymer in vitro is enhanced by blocking NF-kB activation: involvement of the intracellular innate immune response in non-viral gene delivery1	
Appendix D	238
Modular genetic and epigenetic elements for targeted and sustained transgene expression in non-viral gene delivery system1	

List of Tables

Table 3.1	Volume of individual components in transfection solution	69
Table 3.2	Transfection protocol troubleshooting table	76
Table 4.1	Mean particle sizes (nm) obtained for the DNA molecules	106
Table 6.1	List of inhibitors and endosome disruptors used in this study.	183

List of Figures

Figure 2.1 Schematic overview of the transfection pathway.	11
Figure 2.2 Intensity histograms of particle sizes	12
Figure 2.3 Overview of ligand specificities of Toll-like receptors (TLRs).	23
Figure 3.1 Schematic overview of suggested transfection protocol.	53
Figure 3.2 Effect of complexation volume on transfection efficiency.	79
Figure 3.3 Effect of PEI-to-pDNA weight ratios used in complex formation on transfection efficiency.	80
Figure 3.4 Effect of centrifugation and incubation time on transfection efficiency.	81
Figure 3.5 Comparison of transfection efficiency of PEI2 in NHFF using complexation methods outlined in this protocol and other conventional methods.	83
Figure 3.6 Comparison of transfection efficiency of bPEI25 in NHFF using complexation methods outlined in this protocol and other conventional methods.	84
Figure 3.7 Comparison of transfection efficiency of bPEI25 in rBMSC using complexation methods outlined in this protocol and other conventional methods.	85
Figure 3.8 Comparison of transfection efficiency of bPEI25 in hBMSC using complexation methods outlined in this protocol and other conventional methods.	86
Figure 3.9 Comparison of transfection efficiency between bPEI25, PEI2 and Lipofectamine-2000™ in NHFF.	88
Figure 3.10 Comparison of transfection efficiency between bPEI25 and Lipofectamine-2000™ in rat bone marrow stromal cells.	88
Figure 4.1	96

Structure of the DNA molecules used in this study.

Figure 4.2	105
Tapping mode atomic force microscope amplitude topography of the three DNA molecules complexed with various gene carriers.	
Figure 4.3	107
Analysis of DNA binding to the gene carriers	
Figure 4.4	108
Dissociation kinetics of DNA-carrier complexes using heparin sulfate as the competitive polyanion.	
Figure 4.5	110
Delivery of c-DNA, l-DNA and pcr-DNA into rBMSC	
Figure 4.6	113
DNA delivery various cationic reagents in the presence and absence of serum.	
Figure 4.7	116
Transfection efficiency of c-DNA, l-DNA, and pcr-DNA using PEI as the gene carrier	
Figure 5.1	136
Typical intensity histogram of particle sizes.	
Figure 5.2	139
Transfection efficiency with PEI2, PEI2LA and PEI25 polyplexes in rBMSC	
Figure 5.3	140
The amount of cellular uptake of Cy5-fluorophore labeled pDNA polyplexes	
Figure 5.4	141
Two-dimensional histogram plotted with fluorescent intensity values	
Figure 5.5	143
Representative images of isolated intact nuclei from rBMSC viewed under a phase contrast microscope.	
Figure 5.6	143
Typical forward scatter (FSC-H) and side scatter (SSC-H) flow cytometry analysis of intact nuclei from rBMSC treated with PEI2LA complexes;	
Figure 5.7	144
The amount of nuclear-associated Cy5-labeled pDNA in rBMSC	
Figure 5.8	145
CLSM showing typical images of rBMSC nuclear-associated pDNA at 4 h after incubation with polyplexes	
Figure 5.9	146

Percentage of nuclei with pDNA associated	
Figure 5.10	148
Box plot histogram distribution in fluorescent intensity of pDNA associated with nuclei from rBMSC	
Figure 5.11	149
Representative CLSM images of GFP-positive (GFP+) cells transected	
Figure 5.12	151
Box plot histogram distribution in fluorescent intensity of pDNA associated with nuclei between transfected cells (GFP+) and non-transfected cells (GFP-)	
Figure 6.1	174
Comparison of transfection efficiency between complexes in different buffers.	
Figure 6.2	174
Hydrodynamic size ranges of complexes	
Figure 6.3	175
Transfection efficiency of PEI2LA, PEI25 and PEI2 in NHFF cells at various polymer-to-pDNA weight ratios.	
Figure 6.4	176
Fluorescent intensity of PEI2LA, PEI2 and PEI25 complexes.	
Figure 6.5	177
Uptake kinetics of PEI2LA, PEI25 and PEI2 complexes in NHFF cells.	
Figure 6.6	178
Kinetics of GFP expression during the first 72 h following the transfection with complexes.	
Figure 6.7	180
The effect of the endocytic inhibitors on transfection efficiency	
Figure 6.8	184
The effect of endocytic inhibitors on the level Cy3-pDNA uptake of PEI2LA, PEI2 and PEI25 complexes.	
Figure 6.9	186
Effects of the lysosomotropic agent chloroquine, the photosensitizer AlPcS2a and 0.45 M sucrose on the transfection efficiency of PEI2LA, PEI2, and PEI25 complexes.	
Figure 6.10	190
Fixed-cell confocal microscopy images showing the intracellular distribution of Cy3-pDNA	
Figure 6.11	191
Live-cell images acquired with a spinning disk confocal microscope of cells	

Figure 6.12	192
Wide-field microscopy images of cells pre-treated for 2 h with hypertonic media	
Scheme 6	198
A proposed model for the uptake and subsequent intracellular trafficking pathway of PEI2LA complexes in NHFF cells.	
Figure 7.1	214
A hypothetical map of DNA vector for the long-term targeted expression of transgene in mammalian cells.	
Appendix Figure A-1	222
Transfection efficiency of PLL-PA in rBMSC over a 21 day period.	
Appendix Figure A-2	223
Analysis of total RNA for the presence of AcGFP-specific mRNA transcript and GAPDH	
Appendix Figure A-3	223
Analysis of total DNA for the plasmid pIRES2-bFGF-AcGFP1 and GAPDH.	
Appendix Figure B-1	228
Mean fluorescence (FL1) of total cell population from Day 3 to Day 37.	
Appendix Figure B-2	229
RT-PCR on reverse transcribed cDNA to detect transgene expression	
Appendix Figure B-3	229
PCR on total DNA showing the presence of plasmid DNA	
Appendix Figure B-4	230
Transfection Efficiency in the presence of trichostatin A	
Appendix Figure C-1	234
Effect of various pathway inhibitors on transgene expression	

List of commonly used abbreviation

AFM	Atomic force microscopy
BMSC	Bone marrow stromal cell
c-DNA	Circular plasmid DNA
CHO	Chinese hamster ovary cells
CLSM	Confocal laser scanning microscope
CME	Clathrin-mediated endocytosis
CMF-HBSS	Calcium and magnesium free HBSS
CMV	Cytomegalovirus
COS7	African green monkey fibroblast-like kidney cells
CPZ	Chlorpromazine
DLS	Dynamic light scattering
DMEM	Dulbecco's modified Eagle's medium
DMSO	Dimethyl sulfoxide
DNA	Deoxyribonucleic acid
EDTA	Ethylenediaminetetraacetic acid
EMSA	Electro mobility shift assay
EtBr	Ethidium bromide
FBS	Fetal bovine serum
FITC	Fluorescein isothiocyanate
GFP	Green fluorescent protein
HBSS	Hank's balanced salt solution
HEK 293T	Human embryonic kidney cells
HeLa	Cervical cancer cell
HEPES	4-(2-hydroxyethyl)-1-piperazineethanesulfonic acid
kDa	Kilo dalton
LA	Linoleic acid
LFN2000	Lipofectamine-2000™
M β CD	Methyl- β -cyclodextrin
mRNA	Messenger RNA
MTT	3-(4,5-Dimethylthiazol-2-yl)-2,5-diphenyltetrazolium bromide
NES	Nuclear export signal
NHFF	Normal human foreskin fibroblast
NLS	Nuclear import signal
NPC	Nuclear pore complex
PAMM	Pathogen-associated molecular patterns
PCR	Polymerase chain reaction
pDNA	Plasmid DNA
PEG	Polyethylene glycol
PEI	Polyethyleneimine
PLL	Poly-L-lysine
PLL-PA	Palmitic acid substituted PLL
PS	Photosensitizer
S/MAR	Scaffold matrix attachment region
siRNA	Small interfering RNA
TLR	Toll-like receptor

Chapter 1

Scope of dissertation

Non-viral gene delivery systems encompass a wide variety of DNA transfer methods that ranges from cell permeating devices to natural and synthetic biocompatible materials. Cationic polymers are among one of the first biomaterials shown to be capable of condensing DNA into sub-micron complexes suitable for cellular uptake. Despite proof-of-concept evidence of gene delivery capability, clinical translation of cationic polymers has been hindered largely due to low efficacy *in vivo*. In order to develop a more effective gene carrier for clinical application, a basic understanding of the mechanism behind polymer-assisted gene delivery and the accompanying transfection pathway is needed. The work summarized herein is designed to address some of the fundamental question surrounding the intracellular fate of plasmid DNA using lipid-modified cationic polymers as gene carriers.

In **Chapter 1** (current chapter), we introduce the scope of the thesis and a synopsis of each of the chapter.

Chapter 2 provides an introductory overview of the barriers to transfection, focusing on key intracellular events that have been identified as rate-limiting steps. Specifically, we discuss the impact of uptake pathway on intracellular sorting with respect to endosome escape, nucleocytoplasmic transport, transgene expression and immune responses. A discussion of current strategies to improve transfection efficiency is presented. These rate-limiting steps provide a conceptual framework for the design of studies outlined in subsequent chapters.

In order to derive clinically relevant data, we have chosen tissue-derived rat bone marrow stromal cells and normal human foreskin fibroblast for all work outlined in this thesis since these primary cells display a physiology that is representative of actual clinical settings (as compared to cell lines). However, primary cells are more

unpredictable to work with as compared to established cultured cell lines. Not only are these cells more prone to damage, exhibit longer doubling time, and undergo limited passages (i.e., proliferation), they are also more selective in the type of conditions for transfection. In **Chapter 3**, we outlined a step-by-step protocol for the transfection of primary cells using cationic polymers. This optimized protocol was gradually developed in parallel with the mechanistic studies, as part of the continuing effort to improve transfection efficiencies and generate statistically significant quantitative data. While some aspects of this procedure were applied to all of the studies outlined in the chapters, the final optimized version in its published form was applied only to the studies in Chapter 6.

Non-viral gene carriers are unique from their viral counterpart in that packaging of the genetic cargo is facilitated through a self-assembly process initiated by electrostatic interaction between the cationic polymer and the anionic nucleic acid. This non-selective binding interaction permits a wide range of nucleic acid molecules to be condensed for delivery. Thus, in **Chapter 4**, we explored the effect of different topologies and molecular weights of DNA on uptake and transfection efficiency with focus on the physicochemical properties of the assembled complexes. The results from this study showed transfection efficiencies varied among the different forms of DNA and suggested intracellular factors may be more critical in determining transfection efficiency.

In light of the findings summarized in Chapter 4, we next directed our efforts towards understanding the intracellular events leading to transfection. In **Chapter 5**, we investigated the correlation between nuclear-associated plasmid DNA and transfection efficiency using a lipid-substituted cationic polymer as gene carrier. We employed several novel techniques for this study, including a minimally-invasive DNA

labeling technique, a rapid nuclei extract procedure for cytometry and multiplexed confocal microscopy for simultaneous analysis of nuclear import and transgene expression. Results from this chapter revealed a mechanistic role of lipid-moieties in nucleocytoplasmic transport and suggest hydrophobic modification may provide additional trafficking capabilities during gene delivery. We expanded on this notion and mapped the uptake pathway of the DNA delivered by lipid-polymer conjugates in **Chapter 6**. Using selective inhibitors of endocytosis, we determined that hydrophobic modification altered the uptake pathway and intracellular distribution of DNA complexes.

The results summarized in this thesis provide a preliminary view of the transfection pathway of a lipid-modified polymeric gene carrier in clinically-relevant cells. However, much work is needed to fully elucidate the intracellular pathway and biological responses to gene complexes, which is critical from both the safety standpoint and from the carrier design perspective. In **Chapter 7**, we provide a general discussion on the overall conclusions of the studies and suggest avenues to take that could increase the utility and efficacy of non-viral gene delivery systems.

Chapter 2

Nucleic-acid based gene therapeutics: delivery challenges in non-viral gene carriers¹

¹A portion of this chapter has been published in: Hsu C. Y., and Uludağ H., 2012, "Nucleic-acid based gene therapeutics: delivery challenges and modular design of nonviral gene carriers and expression cassettes to overcome intracellular barriers for sustained targeted expression.," *J Drug Targeting*, 20(4), pp. 301–328.

2.1 Introduction

The ability to alter or transform cellular physiology via the delivery of exogenous nucleic acid molecules to cells has been a common laboratory research tool to study gene functions. The therapeutic potential of this approach was not fully realized due to lack of reliable and practical methods to transfer and express recombinant DNA in the mammalian cells. By the 1980s, the concept of gene therapeutics has moved from the bench side to the bedside, when a series of clinical trials demonstrated therapeutic efficacy from the transplantation of virally transduced cells [1,2]. Gene therapy quickly became an intensely investigated field with the promising potential to devise treatment not only for genetic diseases, but also for a wide range of disorders, including metabolic disorders, infectious diseases, chronic illnesses, and cancer. The power of gene therapy is derived from the ability to manipulate cell physiology at genetic and epigenetic levels, accessing molecular processes that are previously unreachable by conventional pharmacological means. This allows particular pathways and factors to be targeted with unparalleled specificity, thereby greatly improving the efficacy in therapy and dramatically reducing side effects commonly associated with wide spectrum pharmacological compound.

As is common to all drug development processes, delivery is the foremost challenge for gene therapeutics. The large molecular weight and anionic charges prohibits nucleic acid molecules from entering the cell via passive diffusion across the negatively charged lipid bilayer of the plasma membrane, and thus calls for a facilitated uptake process. This challenge was initially met by engineering disarmed retroviruses, whose virulence factors that enable viral replication have been removed from the viral genome and replaced with the nucleic acid sequences coding for a protein with therapeutic potential [3]. Clinical translation of recombinant virus-based gene delivery vectors demonstrated promising results, with several trials reporting

long term remission of symptoms in patients suffering from difficult to treat genetic diseases such as severe combined immune deficiency [2]. However, the initial success of the gene therapy trials came into question when a few of the patients developed significant reactions to the administered vector. In one instance, patients developed leukemia-like symptoms, which was later determined to be the result of random vector integration at sensitive genomic sites, that transformed nearby genes into oncogenes [4]. In another trial, an acute inflammatory response was mounted against viral coat proteins [5], which lead to massive tissue damage that eventually resulted in death of the patient. These tragic conclusions prompted the community to re-examine the way viral safety is evaluated and subsequently spurred a shift in focus towards finding alternative non-viral gene transfer methods.

The development of synthetic non-viral gene delivery systems has been met with various technical and biological challenges. The essential features of gene carriers includes: (i) the ability to condense the negatively charged nucleic acid molecule into a compact size with an overall positive charge that are conducive to interaction with the plasma membrane and subsequent cellular uptake, (ii) protect genetic cargo from degradation by extracellular and intracellular nucleases, (iii) circumnavigate intracellular compartments to unload the cargo in the targeted sub-cellular domain, and (iv) minimize off-target associated toxicity, which includes genotoxicity, immunogenicity and cytotoxicity. Several types of cationic polymers and lipids have been explored for this purpose with varying levels of transfection efficiencies [6-9]. While these biocompatible materials meet some of the requirements of a gene carrier, they do not yet have the comprehensive capability to overcome the intracellular barriers that viruses have naturally evolved to evade. As such, non-viral gene delivery systems at present are inefficient for clinical application compared to viral vectors. Furthermore, while research into non-viral carriers are largely driven by the promise of

their theoretical safety profiles, the clinical data on their biodistribution and metabolism is limited. Thus, the promise of a safer gene delivery system in clinical application remains to be fulfilled. Finally, unlike conventional pharmacological compounds, nucleic acids are delivered as a pro-drug, where the activity, instructed by nucleic acid sequences, would depend on the physiology of the cell carrying out those instructions. There is thus an inherent disconnect between the pharmacokinetics of the nucleic acid complexes and the kinetics of the expressed transgene product. Determining the correlation between delivery efficiencies and therapeutic efficacy would necessarily involve re-tooling of existing methods.

Over the last two decades, strategies to improve non-viral gene delivery have largely borrowed approaches from conventional drug design, such as conjugate derivatization and liposome encapsulation. But unlike pharmaceutical compounds, nucleic acids can be modified through genetic recombination to insert functional elements that can self-modulate its own activities ranging from target specificity, bioavailability, intracellular trafficking, to regulated expression and sustained protein production, all without affecting the integrity or competency of the nucleic acid. In this chapter, we will provide an overview of the major physicochemical and biological barriers complicating delivery and expression.

2.2 Barriers to nucleic acid based therapeutics

Transfection pathway employed with non-viral carriers is a multi-step process that involves cell-surface binding, internalization, intracellular trafficking and, if appropriate, expression of the nucleic acids. Efforts to improve transfection efficiency have primarily focused on conjugate chemistry and carrier modification. Despite a large repository of novel carrier systems in the literature, only a limited subset has successfully translated to a setting appropriate for clinical testing (e.g., functionality in

primary cells or in animal models). Several barriers were identified along the transfection pathway; however, identification of dominant rate-limiting steps has been difficult to reconcile due to the ubiquity of the carriers and cell types used in the investigations. The distinction among rate-limiting steps is a systemic process aimed at simplifying the understanding of the events taking place. In practice, it is likely that no such line exists between each barrier and that the transfection pathway exists as one integral non-linear process. The list of barriers will likely differ for each type of carrier, delivery platform (*ex vivo* vs. *in vivo*), the types of nucleic acid cargo (DNA vs. RNA) and the types of genetic modification intended (expression vs. inhibition vs. repair). Below, we will focus our discussion on *ex vivo* transfection using cationic gene carriers for pDNA delivery to explore the overall transfection pathway that encompasses barriers common to most transfections.

2.2.1 Overview of transfection pathway

To facilitate delivery of genetic materials, carriers such as cationic polymers are first mixed with nucleic acid molecules in solution where the two species spontaneously bind to each other and assemble into positively charged sub-micron particles. These complexes, termed polyplexes or lipoplexes, can then be administered to the cell where they physically interact with the negatively charged plasma membrane and/or specific ligands on the cell surface. Cell binding induces an energy-dependent endocytosis whereby engulfed materials are enclosed in a membrane-bound vesicle called an “endosome” [10]; release from the endosome to the cytosolic domain is facilitated by the carrier through membrane destabilization. Following endosome escape, the nucleic acids navigate through the cytosolic milieu and traverse across the nuclear envelope into the nucleus where the pDNA may access the transcription machinery for expression. After transcription, the transgene mRNA is processed and

exported out of the nucleus, into the cytosol, and where it is translated by the ribosome to generate the protein product (**Figure 2.1**).

2.2.2 Physicochemical properties and cell type dictate uptake pathways

The pDNA-carrier complexes are characterized by size, zeta potential, morphology, chemical composition, spatial features, stability and polydispersity, which altogether define the physicochemical properties of the ensemble of complexes, and are used to predict carrier efficiency [8,11]. Prepared complexes are rarely homogeneous in size, charge, and stability [12]. Our previous studies have demonstrated that polyethyleneimine (PEI) polyplexes range in sizes that exhibit a bell shaped distribution when measured in a low serum transfection medium (**Figure 2.2a** and **Figure 2.2b**; [13]). These sizes may further change over time and especially upon interfacing medium with different solute concentration, ionic strength, and pH, as well as when encountering other charged molecules, such as those in the serum or on the cell-surface [14]. The size distributions would present the particles as a mixture of different species of molecules, which means the uptake of particles would likely proceed through multiple pathways.

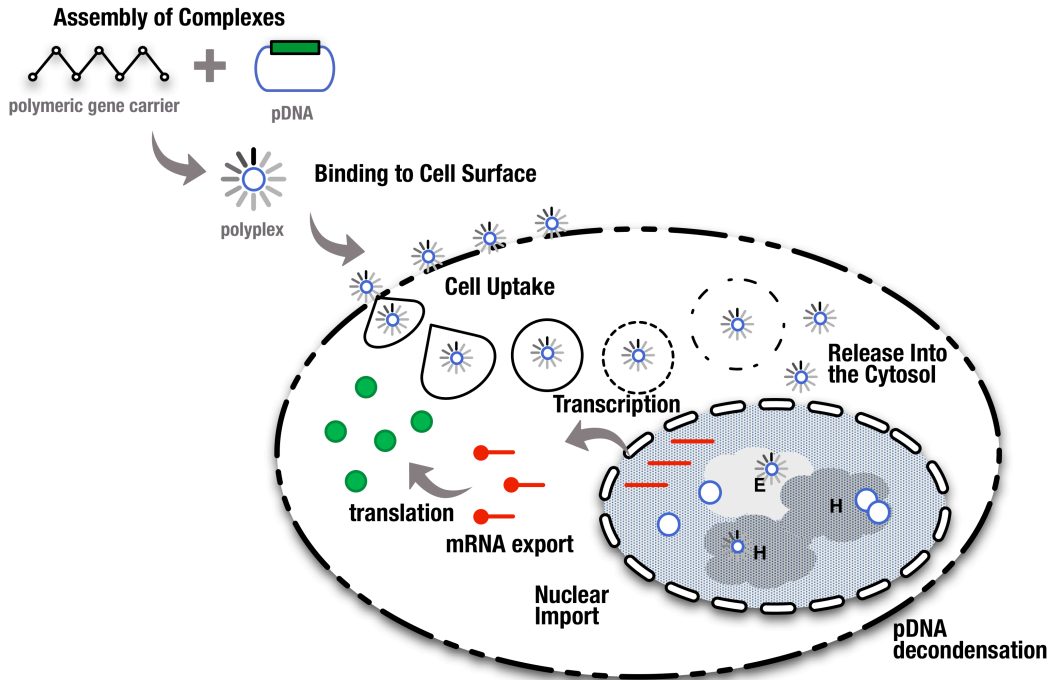


Figure 2.1
Schematic overview of the transfection pathway.

The initial step involves assembly of complexes between the gene carrier and the nucleic acid molecules. Complexes must be stable during delivery and exhibit uniformity in size distribution to better control internalization pathway. In the above figure, pDNA is condensed into sub-micron particles with an overall positive surface charge. This allows binding to the negatively charged cell surface and promote subsequent uptake via endocytosis. Release into the cytosol is facilitated by destabilization of endosome membrane with pH-responsive components of the gene carrier (i.e. proton sponge or endosomolytic peptide). Alternative, fusogenic peptide or pore-forming lipids can facilitate endosomal escape by fusion with the membrane. Once in cytosolic domain, the pDNA must be imported into the nucleus for transcription. This can be mediated by movement along the cytoskeleton network, or actively imported by importins through signal peptide or nuclear DNA targeting sequences. Transcriptional activity of the transgene is favored by intranuclear disposition within the euchromatin domain, as well as efficient de-condensation from the gene carrier. Long-term expression of the transgene will require replication and nuclear retention of the pDNA as well as avoiding the transgene clearance activity of the immune response. Adapted from[15].

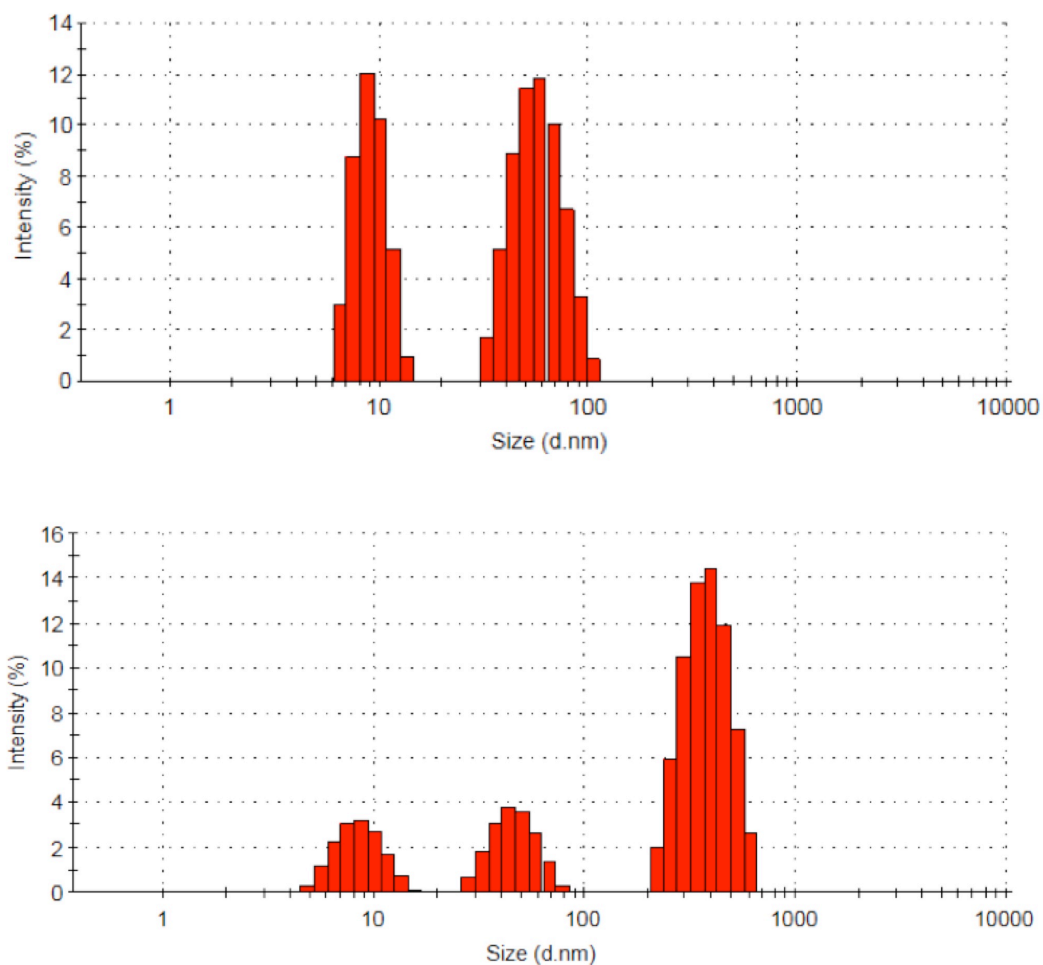


Figure 2.2

Intensity histograms of particle sizes

Obtained in (top) OptiMEM with 1% FBS (no pDNA complexes) and (bottom) PEI25/pDNA polyplex at polymer-to-DNA weight ratio of 2.5 at a pDNA concentration of 2 $\mu\text{g/ml}$, in OptiMEM + 1% FBS. The two distributions at approximately 10 nm and 80 nm in (a) are interpreted as signals from serum proteins. The additional third distribution in (b) is interpreted as the PEI25 polyplexes. Note that while polyplex particles have an average size of ~ 150 nm, the size distribution is significantly heterogeneous. Adapted from [13].

There are four mechanistically distinct endocytic pathways known: (i) clathrin-mediated, (ii) caveolae-dependent, (iii) macropinocytosis, and (iv) clathrin/caveolae-independent endocytosis [10,16,17]. These pathways differ in the size of the formed vesicles, the coat protein embedded in the endosome, which aids in subsequent sorting of the internalized molecule, and preference for the size of particles taken up. Clathrin-mediated endocytosis generally internalize particles that are <200 nm [18-21], while particles between 200 and 500 nm are preferentially taken up through the caveolae-mediated pathway [19]. This size preferences comes somewhat as a surprise considering that the reported size of caveolar vesicles are much smaller (50-60 nm) [22]. However, others have shown that large viruses, such as Newcastle disease virus (~300 nm) and the respiratory syncytial virus (~250 nm), are taken up via the caveolar endocytosis as well [23,24]. Therefore, the size of the cargo does not appear to be restricted by the size of the vesicles and vesicles may change in size to accommodate the cargo. Larger particles beyond the 500 nm are predominantly taken up by clathrin- and caveolae-independent endocytosis, such as macropinocytosis or even phagocytosis, in specialized phagocytic cells such as macrophages [10,25-27]. Thus, each of the uptake pathways is specialized for a particular size range. Since prepared complexes typically contain particles with different sizes, cellular uptake of particles is likely going to be a heterogeneous process involving multiple endocytic pathways contributing simultaneously in varying proportions.

Caveolae-mediated pathway plays an important role in cellular homeostasis and cargo transport, most notably in the transcytosis of serum proteins across the epithelial layer, in intracellular trafficking of cholesterol, and regulation of specific signaling cascades [28,29]. The flask shape and organization of caveolae is conferred by caveolin, which is

a class of cholesterol-binding protein, inserted as a loop into the leaflet of the plasmid membrane [30].

Cell physiology can dictate the qualitative and quantitative nature of receptors embedded on the cell surface. The expression of the receptors is dynamically regulated by the metabolic requirements of the cells, which are defined by cell type (e.g., epithelial or skeletal), cell lineage (e.g., pluripotent stem cells, mesenchymal stem cells, erythrocytes) and cell cycle (e.g., senescent versus dividing). In the case of epithelial cells, for example, up to 20% of the receptors for endocytosis are contributed by caveolae [31]. As such, the predominant endocytic pathways for a given molecule will differ among cells, and the proportion contributed by each of the endocytic pathways will be cell type dependent [32]. Indeed, Douglas *et al.* showed that, the predominant endocytic pathways for internalizing alginate/chitosan polyplexes differ among 293T, COS7 and CHO cells [33]. In the case of 293T, clathrin-dependent endocytosis was the major pathway, as clathrin inhibition led to a greater reduction in both complex internalization and transfection efficiency than caveolae inhibition. In contrast, transfection efficiency in COS7 cells was substantially reduced by caveolae inhibitors, whereas clathrin inhibitors had a minor impact. Furthermore, clathrin inhibitors had no effect on complex internationalization in CHO cells while caveolae inhibitors resulted in ~76% reduction, suggesting the presence of additional pathways in the uptake of complexes. Similarly, transfection of HUH-7 cells with linear PEI polyplexes involved both clathrin-mediated (70%) and caveolae-mediated (30%) endocytosis. The author further demonstrated pathway asymmetry in the uptake of particles with different sizes; smaller polyplexes were routed to both the clathrin and caveolae-mediated uptake pathway, while large particles proceeded through auxiliary pathways that were not interfered by clathrin or caveolae inhibitors [34]. Taken together, these recent findings point to an uptake process in which the predominant

endocytic pathways would depend on both the physicochemical properties of the complexes and the physiology of the cell.

2.2.3 Pathway dictates sorting and release of the cargo

The implication of the heterogeneity in endocytic pathways is that not all complexes internalized will contribute to transfection - some pathways may be transfection conducive while others lead to transgene inactivation. Clathrin-mediated endocytosis has consistently demonstrated to be conducive to transgene expression [33-35], though this may in part be dependent on carrier used and its mechanism of endosome disruption.

Clathrin-mediated endocytosis is thought to be involved in a number of cellular processes including intercellular communication, modulating signal transduction by regulating the expression of cell-surface protein receptors, and recycling/sorting of activated receptors [22]. During classical clathrin-mediated endocytosis, internalized vesicles are first uncoated and routed to sorting endosome by interacting with other vesicles through membrane-embedded signal molecules. They are subsequently recycled to either cell periphery or trafficked to the endolysosomal pathway for degradation [31]. In the latter case, sorting endosomes are directed to late endosomes, which undergo gradual acidification as proton pumps transport H⁺ into the lumen, and eventually fuse with lysosomes to degrade the engulfed material through hydrolytic enzyme digestion. The acidic environment inside lysosome is thought to be undesirable for internalized complexes as it leads to breakdown of the pDNA. However, routing to the endolysosomal pathway might be essential for endosomal escape and subsequent transgene expression [34,36]. The abundance of amine groups on cationic polymers such as PEI are thought to act as a "proton-sponge", whereby the acidic protons inside the lysosomal compartments are absorbed to buffer

the charge accumulation. The excessive proton and chloride inside the vesicle lead to an increase in osmotic pressure, which swell and ultimately ruptures the vesicles, releasing the complexes into the cytosol [37]. In contrast, caveolin-dependent macropinocytosis, and phagocytosis leads to formation of macropinosome and phagosome, respectively, which are not known to contain the membrane-embedded signal molecules necessary to interact with other vesicles for sorting and processing [10,17]. Instead, these vesicles often result in complexes sequestered in cytosol or possibly get exocytosed [36]. The lack of acidic environment in non-endosomolytic pathway deprives the opportunity for pH-responsive carriers to promote membrane destabilization required to escape the endosome. Further, it has been shown that microsphere beads with diameters of <200 nm were internalized preferentially through the clathrin-dependent endocytosis and were directed to the late endosomal/lysosomal compartments. Larger ~500 nm beads, however, entered cells predominantly through caveolin-mediated pathway and did not co-localize with endolysosomal markers [19]. Thus, it can be inferred that pH-responsive cationic carriers that form <200 nm particles (e.g., particles formulated with 25 kDa PEI) would give higher transfection efficiency than polymers that inherently form larger particles (e.g., particles formed with 2 kDa PEI), since the smaller polyplexes can take advantage of the pH changing environment to promote endosome escape, while the larger polyplexes become inactivated in non-acidic compartments. Conversely, pore-forming lipids and fusogenic peptides, which promote endosome escape via fusion with the vesicular membrane, do not require acidic compartment for endosomal disruption and may escape more efficiently in neutral non-degradative environment. In that case, the ideal particle size may be well above >200 nm, allowing them to be taken up by non-clathrin mediated uptake pathway. The desirable endocytic pathway will thus depend on the carrier as the chemical and structural features will determine both the mechanism of endosome disruption and size of the particles. It should be

noted that vesicle sorting may not be exclusively limited to one pathway since in some cell lines, vesicles can engage in pathway cross-talk whereby neutral caveosomal vesicles can fuse with acidic endosomes [38]. Regardless of the endocytic uptake pathways, the optimal transfection protocol would likely involve tuning the size of the particles with respect to cell type such that the complexes are internalized through the transgene conducive pathway.

2.2.4 Nuclear import

Once exogenous pDNA gets released into the cytosol, it must translocate across the nuclear membrane to access the main transcription machinery. The nuclear membrane is a double lipid bilayer that acts as a physical barrier to separate genomic materials from the cytoplasm. Bi-directional transport in and out of the nucleus is a tightly regulated process facilitated through a series of aqueous channels called the nuclear pore complex (NPC) that are embedded in the nuclear envelope. The NPC core structure is comprised of multiple units of nucleoporins that are arranged in an eight-fold rotational symmetry perpendicular to the membrane, forming a cylinder with hollow center. In its relaxed state, the cylinder has a diameter of 10 nm, which allows passive diffusion of molecules <60 kDa, such as ions, metabolites and some of the smaller proteins across the channel. The core diameter may further dilate or re-shape dynamically to accommodate transport of larger molecules during active transport [39,40]. The transport of larger molecules like proteins, RNA and DNA across the NPC is mediated through an energy-dependent process that generally involves the recognition of specific signal recognition motifs on the substrate by soluble transport receptors [41,42]. For RNA, transport signal is provided by adaptor proteins, which bind to mRNA to form a RNA-protein complex called the messenger ribonucleoprotein. For proteins, signal peptides termed the nuclear localization sequences (NLS) and nuclear export sequences (NES), are synthesized as part of the

protein pre-sequence, which may be buried (through either conformational changes or sequestered by binding to a repressor) as a mechanism to regulate its activity [43]. These evolutionarily conserved mechanisms of nuclear transport may provide viable strategies to artificially promote the import of pDNA into the nucleus.

Particle sizes of carrier-pDNA complexes are typically >100 nm, which are well above the NPC size cut-off. Without signal peptide or adaptor protein, entry into the nucleus would need to be facilitated by the carrier. The capability of gene carrier to mediate entry into the nucleus appears to vary among carriers - some are able to promote nuclear uptake as a complex [44-46], while others may dissociate in the cytosol, leaving pDNA to traverse across the nucleocytoplasmic pathway on its own [47,48]. The mechanism for gene carrier-assisted nuclear uptake is not very well described. Some carriers can directly facilitate entry by fusion with the nuclear membrane whereby a flip-flop mechanism allows the complex to translocate to the nucleoplasm side of the nuclear envelope [49]. Others may indirectly gain entry by riding along the cytoskeleton network, which spans the cytoplasm and extends into the nucleus [50]. Still, complexes may be permitted to enter the nucleus passively, provided that the spatial diameter can be condensed down to a size that is below the NPC molecular weight cut-off.

For carriers with limited nuclear delivery capability, import can still take place indirectly through processes associated with mitotic events. It is now widely regarded that transfection efficiency directly correlates with cell division and cell growth [46,51,52]. The strong correlation has been attributed to the mitotic phase (M-phase) of the cell cycle, whereby transient breakdown of nuclear membrane temporarily removes the physical barrier, to allow pDNA to interact and associate with nuclear components. Following re-assembly of the nuclear envelope, nuclear factors-

associated pDNA become opportunistically incorporated into the nucleoplasm [53-55]. However, a recent study suggested that transfection efficiency is also correlated to the synthesis phase (S-phase) of the cell cycle. S-phase of the cell cycle is characterized by replication of the genome, which is accompanied by synthesis of intranuclear histone proteins. The relative increase in the intranuclear concentration of cationic histones prior to cell division may facilitate dissociation and decondensation of pDNA from complexes through ionic exchange. Binding of histones to pDNA may further promote the formation of a nucleosome structure that enhance the transcription efficiency from pDNA templates (Akita et al. 2007). Though this correlation may be specific to lipoplexes, it is nevertheless conceivable that the heightened global transcriptional activity during the late S-phase could also increase the number of transcription initiation from the pDNA. In any case, it is likely that both M- and S-phases are correlated to better nuclear uptake and more frequent transgene expression, which would translate to higher transfection efficiencies.

Although the nuclear membrane remains a physical barrier for pDNA entry into nucleus, it is certainly not the final barrier; sub-nuclear trafficking and post-transcriptional events pose as major limiting steps as well. However, the post-nuclear events at present would appear stochastic at best, due to limited data on the kinetic in this part of the transfection pathway.

2.2.5 Sub-nuclear trafficking and post transcriptional events

Perhaps the least understood aspect of non-viral gene delivery is intranuclear trafficking of pDNA. The nucleus is a highly dynamic structure organized into compartments and domains that are closely associated with specific gene regulatory functions and transcriptional activity [56,57]. It is widely known that genes are defined into chromatin domains with euchromatin being transcriptionally active and

heterochromatin being transcriptionally repressed. Studies on lymphoid cells showed that inactivation of transgene expression correlates with its relocation to a heterochromatic nuclear site [58], suggesting the expression status of a gene can be strongly influenced by its nuclear localization. Indeed, comparative studies to evaluate the sub-nuclear localization of non-virally delivered pDNA and virally transduced adenovirus genomic DNA showed that the latter is preferentially localized with the euchromatin while pDNA were found primarily in the heterochromatin sites [59]. The ability for adenovirus to traffic to transcriptionally active domains are modulated by both cis and trans factors. *Trans*-acting viral core proteins such as protein V, protein VII and mu, complex with adenoviral DNA to facilitate entry into the nucleus; these core proteins can interact with nuclear sub-domains (e.g. PML body, nucleoli and the nuclear matrix) to exchange chromatin remodeling factors, loosening the chromatin structure within the transcriptional region of the genome to facilitate binding by transcription factors [60-62]. *Cis*-acting sequence elements or structural features on the adenoviral DNA are then bound by endogenous transcription factors or chromatin remodeling proteins to maintain the viral genome within euchromatin domains [63,64]. Similarly, Shaheen *et al.* found that the more efficient polycationic gene carrier containing 46 dimethylaminoethyl-modified polyrotaxane (46DMAE-ss-PRX), which formed a tighter condensed particle, was found to decondense and co-localize preferentially with euchromatin. In contrast, the less efficient sibling polymer 16DMAE-ss-PRX were found decondensed in the heterochromatins, suggesting that the condensation/decondensation efficiency in heterochromatin/euchromatin can be modulated by the number of cationic moieties per carrier [65]. Aside from these "euchromatin induction mechanism", the chromatin status of the exogenous pDNA may also be influenced by the nuclear uptake pathway. It has been suggested that complexes entering the nucleus through the NPC may be able to access the euchromatin more efficiently than those entering via other non-NPC entry ways such

as flip-flop fusion [59]. Thus, analogous to the dependence of transfection efficiency on the uptake pathways, transgene expression efficiency may be closely tied with the mechanism of nuclear import.

It is generally accepted that prior to being transcribed, pDNA must dissociate from the gene carrier and decondense into a transcriptionally favorable conformation [66]. Studies comparing the transcription efficiency between lipoplexes and adenovirus demonstrated that DNA decondensation accounts for the difference in efficiency between the two gene delivery systems [59,67]. Quantitative relationship between dissociation and expression activity were demonstrated by an *in vitro* transcription assay whereby low molecular weight cationic polymers, which dissociate better than high molecular weight polymers, supported higher transgene expression [66]. Similarly, lipoplexes formed with higher charge ratios resulted in lower transfection efficiency, despite exhibiting higher uptake and endosomal escape, hinting at the possibility that stronger compaction may reduce dissociation of DNA for transcriptional access [68,69]. In the case of PEI, however, transcription from pDNA polyplexes appears uninhibited in cell-free system [45], but *in vitro* transcription were inefficient at low and high nitrogen-to-phosphate (N/P) ratio, where particles tend to aggregate or be surrounded by excess polymers [70]. In short, transcription factors may play a tertiary role in the dissociation of complexes, but the releasing activity may be dependent on the properties of the particles.

The transcribed transgene mRNA needs to be processed and exported out of the nucleus. Presumably the export of transgene mRNA is not a rate-limiting step as it is naturally processed along with the endogenous transcripts, though data on this is currently limiting. However, free carriers may interact with RNA species, including the transgene mRNA, and compromise their utility downstream. Free carriers is a

byproduct of dissociated complexes, which could be found in either the cytoplasm or in the nucleus, potentially leaving a trail of free cationic residues for RNA interactions. Some studies showed that lipoplexes dissociated following escape from the endosome, while cationic polymers traveled with the pDNA as polyplexes into the nucleus and was dissociated through competitive interaction with endogenous biomacromolecules [66,71,72]. Comparative evaluation of post-nuclear events between Lipofectamine and adenovirus showed that translation of the transgene mRNA is inhibited in lipofection as a result of carrier interaction with mRNA species and accounts for the discrepancy in efficiency between viral and non-viral carriers [59]. Data on this for other carriers is limited, so that the impact of excess carriers inside the cells is not known. Regardless, a method to anchor or sequester dissociated carriers (e.g., biodegradable carriers) from binding to endogenous nucleic acids may enhance transfection efficiency as well as preserve cell viability.

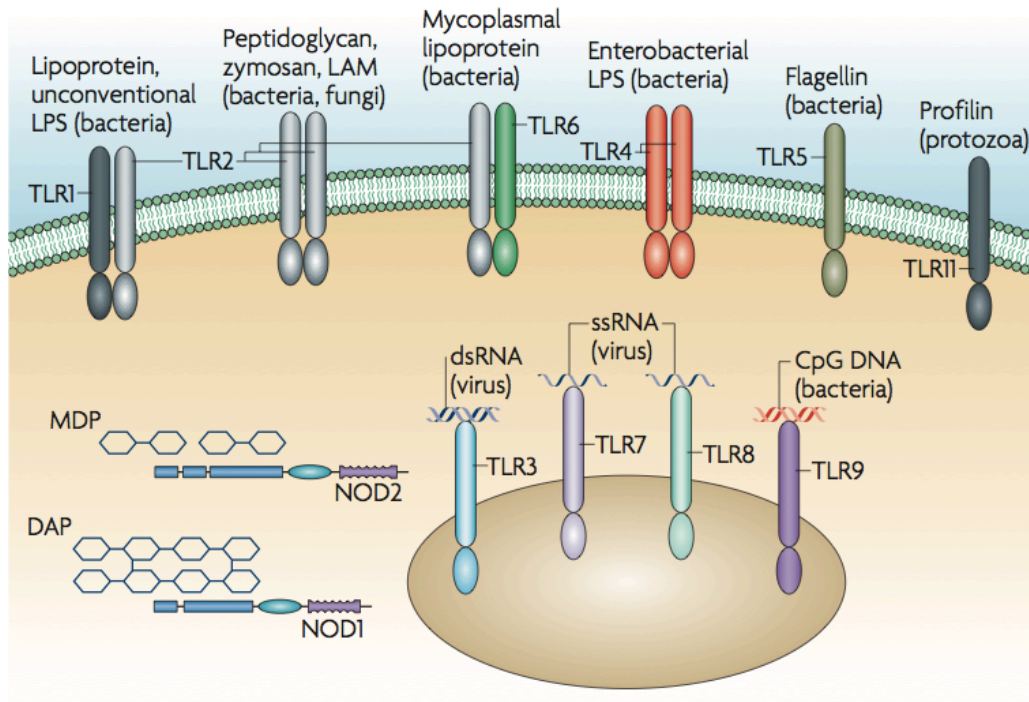


Figure 2.3

Overview of ligand specificities of Toll-like receptors (TLRs).

TLRs recognize pathogen-associated molecular patterns (PAMPs) to trigger a signal cascade that leads to the activation of the immune responses. TLR3 and TLR9 are involved in recognition of double-stranded (dsRNA) and unmethylated CpG motifs, respectively, which may be triggered during non-viral gene delivery of nucleic acid molecules. Adapted from [73]

2.2.6 Immune responses to nucleic acid and complexes

While initial excitement surrounding non-viral carriers stem from their superior safety profile compare to viral vectors, it is now widely known that systemic injection of lipoplexes and polyplexes induce innate immune response and cause tissue damage [74-78]. Immunogenicity of complexes is attributed to bacterial sequences on the pDNA backbone. These unmethylated CpG dinucleotide islands, which are typically present in much higher frequency in microbial genome, not only pose severe safety issues, including the dissemination of gene encoding the antibiotic selection factor and activation of cryptic expression signals [79], but can also be recognized as pathogen-associated molecular patterns (PAMM) in mammalian cells. The CpG-based PAMM can interact with toll-like receptors (TLR) to trigger a signal cascade that leads

to the activation of the innate immune response [80]. Out of the 10 TLR identified to-date, TLR3, TLR7, TLR8 and TLR9 are embedded in the endosomal membrane (**Figure 2.3**; [81]). These TLRs are specialized in recognizing pathogen-associated nucleic acids, such as dsRNA, ssRNA, dsDNA, and CpG-DNA [82]. TLR9 has been identified to be the receptor primarily responsible for detecting and triggering an immune response against CpG pDNA since systemic administration of lipoplexes in TLR9 deficient mice exhibited significantly lower production of proinflammatory cytokines [83]. Efforts to mask or remove PAMM by methylation of the CpG dinucleotides or excision of the bacterial vector backbone resulted in significant reduction in proinflammatory cytokine [84-86]. However, methylation alone is not sufficient to attenuate immune response [87], suggesting that other aspects of the nucleic acids (e.g., sequence, base modification, structural conformation) or even other cytosolic TLR-independent DNA sensors, such as the DLM-1/Z-DNA binding protein 1, can act in parallel to trigger inflammatory reactions [88,89]. It should be noted that sequential administration of pDNA and liposome carrier resulted in dramatic reduction in immune response in comparison to lipoplexes [90], suggesting the assembly of carrier and DNA into a complex may render higher immunogenic properties than either of the components alone. Further, comparative evaluation between different PEI polyplexes and lipoplexes showed that the former formulation resulted in dramatically reduced cytokine production, hinting carrier composition may play a factor its immunogenicity. Strategies to evade the immune response would involve removal or conformational shielding of immunogenic components, or re-directing complex uptake to avoid detection by intracellular sensors.

2.2.7 Limited duration of transgene expression

The practical consequences of an innate immune response to CpG DNA are not limited to tissue damage, but extend to the persistence of transgene expression. TLR-

triggered activation of innate immune responses results in the induction of interferon responses and renders cells in an antiviral state. Antiviral responses can include activities that range from inhibition of transcription [91], inactivation of translation initiation factor [92], induction of apoptosis [93], nuclease-mediated degradation of exogenous nucleic acids, inhibition of intracellular trafficking, and base modification to the transgene DNA to induce point mutation in the viral genome ([94]. Further, immunomodulation mediated by the interferon response can initiate a feedback loop that enhances the sensitivity of pathogen recognition and activate the adaptive immune response, which includes lymphocyte infiltration [95] that ultimately leads to the killing and systemic clearance of transfected cells.

Transgene expression can also be diminished over time due to lack of a mechanism to faithfully maintain plasmid copy number, especially in replicating cells. Typical mammalian expression cassette lacks sequence elements necessary for the replication and partitioning of pDNA among divided cells. As a consequence, the intracellular pDNA concentration will gradually decrease as cells multiply, eventually falling below the minimum that is sufficient to obtain expression. Furthermore, dissociated pDNA no longer protected by gene carrier is susceptible to degradation by intracellular nucleases. Any remaining pDNA left in the nucleus are subsequently subjected to epigenetic silencing through chromatinization or base methylation [96,97], repressing and attenuating transcription activity from the plasmid [96]. It was suggested that pDNA backbone acts as a focal point for heterochromatinization via the binding of histone proteins, which then spreads into the transcription unit in the plasmid, repressing the expression [98]. Thus, sustaining the expression of transgene would necessarily involve sequence elements that can promote the replication and nuclear retention of the plasmid, maintenance in a euchromatin state and reduction in immunological reactivity.

2.3 Strategies to improve transfection efficiencies

Strategies to improve the delivery of nucleic acid therapeutics can be divided into two thrusts: (i) those based on carrier design to control packaging, intracellular uptake/trafficking and release of the nucleic acid cargo, and (ii) those based on the design of nucleic acid cargo to mediate trafficking and expression of the transgene.

2.3.1 Stabilizing particles to facilitate uptake via transgene conducive pathway

A major hurdle prohibiting the efficient uptake of pDNA is the instability of complexes prior to exposure to cells. Complexes typically have an overall positive charge on the particle surface and thus may invite binding from other charged species [99-101]. These charge-charge interactions can arise during delivery, leading to premature dissociation of complexes, heterologous aggregation between particles and proteins, or homologous aggregation between complexes. Aggregation among complexes is supposedly driven by thermodynamically induced shielding of hydrophobic pockets within the complexes [12]. The result is formation of larger particles, which are less efficiently taken up by the cell, leading to a uptake pathway that may lead to the cytosolic sequestration of the complexes.

Preparation conditions aimed at reducing intermolecular interactions could favor the assembly of more uniform particles. Parameters such as mixing order of complex components, speed of mixing, ionic strength of solution, concentration of complexes, temperature, and pH are all factors that can be implemented to control aggregation [12,102]. For example, gradual drop-wise polymer addition to dilute nucleic acid solution results in smaller and more uniform particle sizes. Likewise, subsequent dilution of the complexes in larger volume combined with low temperature storage can slow down rate of aggregation. Acidic pH can increase the protonation of the

complex, leading to greater electrostatic repulsion among particles. Finally, enhancing the viscosity of complex solutions (e.g., by glycerol) can reduce the kinetic movement of molecules to reduce intermolecular interaction [12,103]. Homologous aggregation among particles has been attributed to the uncharged regions on particles, which promotes intermolecular interaction between particles to mask hydrophobic patches. Measures to counter hydrophobic interaction involves the addition of stabilizing agent, such as surfactants or sugars [102,104,105]. Optimized preparation methods and stabilizing agent may facilitate the formation of stable particles in storage, but these measures do not guarantee stability during delivery. That is, the physicochemical properties of the complexes may further change upon addition to transfection media or may interact with blood components *in vivo*. Perhaps the most widely cited approach to stabilize particles is the use of PEGylated carriers to sterically stabilize complexes' surfaces and shield complexes from blood components [106,107]. PEGylated liposomes have been a common pharmaceutical practice for many years and this approach was adapted to stabilize cationic complexes [108-112]. However, shielding surface charges may also reduce binding to cell surface, effectively reducing uptake efficiency[113]. PEGylation can also compromise the H⁺ buffering activity that is necessary to induce osmotic swelling inside the endosome [114]. Careful titration of different molecular weights of PEG chains may be necessary to balance the cost and benefit effect between particle stability and gene delivery efficiency [107]. However, a method to coat a layer of surfactant stabilizer that can be reversibly "ejected" upon binding to the cell surface may present be a more realistic approach to both the storage and delivery of gene formulation.

2.3.2 Cell-specific targeting

Strategies for cell-specific targeting typically utilize receptor-mediated endocytosis through the conjugation of appropriate ligands to the carrier. Ligands such as

antibodies, transferrin, folic acid, RGD peptides, carbohydrates and lipids have been employed, which has been reviewed elsewhere [106,115-122]. There may be several limitations to the use of ligand-conjugated carriers: (i) substitution of the cationic backbone can reduce binding affinity to anionic DNA, reducing the ability of the modified carrier to compact the DNA; (ii) the ligand needs to be properly displayed on the surface of the particles such that the receptor can recognize and bind to the complex; (iii) cell-specific receptors are typically presented at a lower proportion on the surface, thus, targeting to a specific subset of receptors may in effect, limit the level of nucleic acid uptake. It was estimated that at least $10^5 - 10^6$ plasmids per cell are required for transfection [123], if the number of plasmids taken up by the limited subset of cell-specific receptors falls below this range, than subsequent nuclear delivery and transgene expression would be reduced; (iv) the actual delivery efficiency of targeted carrier might be severely diminished due to the effect of the ligand on other intracellular barrier, such as endosome escape and nuclear uptake, and (v) the ligand, particularly antibodies and peptides, can potentially be immunogenic, compromising the safety profile of a non-viral delivery system [124]. While conceptually simple, ligand-based targeted delivery may enhance specificity at the expense of efficacy.

2.3.3 Endosome escape and nucleocytoplasmic trafficking

Methods to promote the release of complexes from endosomes largely rely on the composition of the carrier and its inherent reactive properties to disrupt of the enveloping membranes. This process can follow one of the following described mechanisms. i) The flip-flop mechanism suggests that increasing acidity in the endosome lumen causes the anionic phospholipids to flip inside out, inverting the intra-endosomal side of the membrane to the cytoplasmic side. The formation of charge neutral pairs between membrane and lipo-carrier leads to membrane

destabilization, allowing the lipoplex to penetrate into the cytoplasm, simultaneously dissociating pDNA from the cationic lipid [9,72,125]. ii) In the proton sponge effect, endosomolysis is promoted through adsorption of H⁺ by amine groups found on cationic polymers. Protonation induces an inflow of ions and water into the endosome lumen, leading to a gradual increase in osmotic pressure, swelling the vesicle, causing the membrane to destabilize and eventually rupture [126-128]. iii) For pore-forming cationic amphiphilic peptides, binding to lipid bilayer reduces the line tension in the membrane and causes the internal membrane tension to create pores in the lipid membrane, allowing the cargo to escape through the pores [129,130]. iv) Fusogenic peptides, on the other hand, can undergo conformational changes upon pH drop, which triggers the molecule to adopt a conformation suitable for fusion with the lipid bilayer [131]. For example, haemagglutinin, a peptide from the influenza virus coat, has an anionic hydrophilic coil at physiological pH, but adopts a hydrophobic helical conformation in the acidic pH inside the endosome, which allows the helical structure to embed into the membrane [132].

In addition to the inherent endosomolytic activity of the carriers, membrane disruptive components from a number of sources have been grafted onto the carriers to further enhance cytosolic release. These functional components have been derived from viruses ([133-136], bacteria [137-140], plants [141,142], mammalian (or endogenous) [143-146], as well as synthetic or recombinant peptides [147-152]. Attachment of these endosome-disruptive components is accomplished by either covalent linkages or through attractive interactions with the complex surface. Covalent linkage provides a more secure form of transit, ensuring the endosomolytic component arrive with the carrier in the sub-cellular compartment. However, there is often a minimum substitution density required to sufficiently induce membrane destabilization and high degree of carrier modification may diminish the DNA binding capacity, causing

the complexes to be less stable, similar to the problems faced with PEGylation and ligand-functionalization. Conjugation of functional devices could also lead to changes in the overall size of the complexes, which could in effect, re-direct the uptake to a pathway that may not allow the endosomolytic component to exert its activity. Finally, the functional component may be buried inside the core complex, rendering a spatial configuration that is sub-optimal to the activity of the conjugated device. Even though endosome entrapment is widely regarded as a rate-limiting step, the arrival at this barrier may merely be a consequence of mis-directed step (i.e., uptake down a transgene inactive pathway due to change in size). Some studies have demonstrated that endosome escape was not the rate limiting step [67], and that limited nucleocytoplasmic movement might impede the gene delivery.

Movement of endosomes across the cytoplasm is facilitated by microtubules along the cytoskeleton network which extends from the plasma membrane to the microtubule organizing centre (MTOC) located in close proximity to the nucleus [153-155]. Movement along the MTOC appears to be bi-directional - cargo may oscillate between the perinuclear region and the cell periphery [156,157]. Thus, the timing of endosome release relative to movement along the microtubules may be critical to subsequent nuclear uptake. If complexes are released distal to the nucleus, diffusive mobility of large pDNA (>2 kb) may be restricted in the crowded cytoskeleton mesh, limiting nuclear uptake [158]. If endosome escape coincides with localization around the perinuclear region, then cycle-dependent nuclear import may be enhanced. This prompts for a method to induce endosome escape that can be spatially triggered to the vicinity of the perinuclear region. Alternatively, pDNA movement can be facilitated by signal peptides [159], lipids [160] or adaptor proteins for sorting, targeting and anchoring to specific sub-cellular compartments [161]. We have recently demonstrated that a lipid-modified polymeric carrier exhibited enhanced trafficking to

the nuclear periphery [13], although it was not known whether the trafficking capability is an active process specific to the lipid moieties or a passive event that saw anchoring of the lipid group to nuclear membrane through hydrophobic interaction. Signal peptides are arguably the most widely used approach for sub-cellular trafficking. Even viruses have evolved to use specific peptide sequences to facilitate its interaction with dynein to move along the cytoskeleton network, which extends into the nucleoplasm, thereby gaining entry into the nucleus ([162,163]. Adapting endogenous mechanisms for protein import such as conjugating NLS to either the gene carrier or to the DNA vector has proven to be a viable strategy for promoting the nuclear uptake of complexes [164-166]. However, the positive effect of NLS has not been consistently demonstrated among research groups [167]. The problem, which is shared by conjugated carriers, is often the lack of proper spatial presentation of the ligand to its receptor. But more critically is the fact that other cellular barriers were not simultaneously tackled, which may inadvertently undermine the benefits of NLS. In that regard, a multifunctional gene delivery system that can incorporate all of the barrier-evading moieties in a spatially coordinated order would be ideal in overcoming multiple rate-limiting steps in the transfection pathway.

2.4 References

- [1] Rosenberg S. A., Anderson W. F., Blaese M., Hwu P., Yannelli J. R., Yang J. C., Topalian S. L., Schwartzentruber D. J., Weber J. S., and Ettinghausen S. E., 1993, "The development of gene therapy for the treatment of cancer," *Ann. Surg.*, **218**(4), pp. 455–63; discussion 463–4.
- [2] Blaese R. M., Culver K. W., Chang L., Anderson W. F., Mullen C., Nienhuis A., Carter C., Dunbar C., Leitman S., and Berger M., 1993, "Treatment of severe combined immunodeficiency disease (SCID) due to adenosine deaminase deficiency with CD34+ selected autologous peripheral blood cells transduced with a human ADA gene. Amendment to clinical research project, Project 90-C-195, January 10, 1992.," *Hum Gene Ther*, **4**(4), pp. 521–527.
- [3] Eglitis M. A., Kantoff P. W., Kohn D. B., Karson E., Moen R. C., Lothrop C. D., Blaese R. M., and Anderson W. F., 1988, "Retroviral-mediated gene transfer into hemopoietic cells.," *Adv. Exp. Med. Biol.*, **241**, pp. 19–27.
- [4] Hacein-Bey-Abina S., Kalle Von C., Schmidt M., McCormack M. P., Wulffraat N., Leboulch P., Lim A., Osborne C. S., Pawliuk R., Morillon E., Sorensen R., Forster A., Fraser P., Cohen J. I., de Saint Basile G., Alexander I., Wintergerst U., Frebourg T., Aurias A., Stoppa-Lyonnet D., Romana S., Radford-Weiss I., Gross F., Valensi F., Delabesse E., Macintyre E., Sigaux F., Soulier J., Leiva L. E., Wissler M., Prinz C., Rabbitts T. H., Le Deist F., Fischer A., and Cavazzana-Calvo M., 2003, "LMO2-associated clonal T cell proliferation in two patients after gene therapy for SCID-X1.," *Science*, **302**(5644), pp. 415–419.
- [5] Marshall E., 1999, "Gene therapy death prompts review of adenovirus vector.," *Science*, **286**(5448), pp. 2244–2245.
- [6] Midoux P., Breuzard G., Gomez J. P., and Pichon C., 2008, "Polymer-based gene delivery: a current review on the uptake and intracellular trafficking of polyplexes.," *Curr Gene Ther*, **8**(5), pp. 335–352.
- [7] Putnam D., 2006, "Polymers for gene delivery across length scales.," *Nat Mater*, **5**(6), pp. 439–451.
- [8] Park T. G., Jeong J. H., and Kim S. W., 2006, "Current status of polymeric gene

delivery systems.," *Adv Drug Deliv Rev*, **58**(4), pp. 467–486.

- [9] Wasungu L., and Hoekstra D., 2006, "Cationic lipids, lipoplexes and intracellular delivery of genes.," *J Control Release*, **116**(2), pp. 255–264.
- [10] Khalil I. A., Kogure K., Akita H., and Harashima H., 2006, "Uptake pathways and subsequent intracellular trafficking in nonviral gene delivery.," *Pharmacol. Rev.*, **58**(1), pp. 32–45.
- [11] Mintzer M. A., and Simanek E. E., 2009, "Nonviral vectors for gene delivery.," *Chem. Rev.*, **109**(2), pp. 259–302.
- [12] Sharma V. K., Thomas M., and Klibanov A. M., 2005, "Mechanistic studies on aggregation of polyethylenimine-DNA complexes and its prevention.," *Biotechnol Bioeng*, **90**(5), pp. 614–620.
- [13] Hsu C. Y. M., Hendzel M., and Uludağ H., 2011, "Improved transfection efficiency of an aliphatic lipid substituted 2 kDa polyethylenimine is attributed to enhanced nuclear association and uptake in rat bone marrow stromal cell.," *J Gene Med*, **13**(1), pp. 46–59.
- [14] Wightman L., Kircheis R., Rössler V., Carotta S., Ruzicka R., Kurska M., and Wagner E., 2001, "Different behavior of branched and linear polyethylenimine for gene delivery in vitro and in vivo.," *J Gene Med*, **3**(4), pp. 362–372.
- [15] Hsu C. Y. M. C., and Uludağ H. H., 2012, "Nucleic-acid based gene therapeutics: delivery challenges and modular design of nonviral gene carriers and expression cassettes to overcome intracellular barriers for sustained targeted expression.," *J Drug Targeting*, **20**(4), pp. 301–328.
- [16] Zhou R., Geiger R. C., and Dean D. A., 2004, "Intracellular trafficking of nucleic acids," *Expert Opin Drug Deliv*, **1**(1), pp. 127–140.
- [17] Medina-Kauwe L. K., Xie J., and Hamm-Alvarez S., 2005, "Intracellular trafficking of nonviral vectors.," *Gene Ther*, **12**(24), pp. 1734–1751.
- [18] Takei K., and Haucke V., 2001, "Clathrin-mediated endocytosis: membrane factors pull the trigger.," *Trends Cell Biol.*, **11**(9), pp. 385–391.

- [19] Rejman J., Oberle V., Zuhorn I. S., and Hoekstra D., 2004, "Size-dependent internalization of particles via the pathways of clathrin- and caveolae-mediated endocytosis.," *Biochem J*, **377**(Pt 1), pp. 159–169.
- [20] Ehrlich M., Boll W., Van Oijen A., Hariharan R., Chandran K., Nibert M. L., and Kirchhausen T., 2004, "Endocytosis by random initiation and stabilization of clathrin-coated pits.," *Cell*, **118**(5), pp. 591–605.
- [21] Cureton D. K., Massol R. H., Saffarian S., Kirchhausen T. L., and Whelan S. P. J., 2009, "Vesicular stomatitis virus enters cells through vesicles incompletely coated with clathrin that depend upon actin for internalization.," *PLoS Pathog.*, **5**(4), p. e1000394.
- [22] Conner S. D., and Schmid S. L., 2003, "Regulated portals of entry into the cell.," *Nature*, **422**(6927), pp. 37–44.
- [23] Werling D., Hope J. C., Chaplin P., Collins R. A., Taylor G., and Howard C. J., 1999, "Involvement of caveolae in the uptake of respiratory syncytial virus antigen by dendritic cells.," *J. Leukoc. Biol.*, **66**(1), pp. 50–58.
- [24] Cantín C., Holguera J., Ferreira L., Villar E., and Muñoz-Barroso I., 2007, "Newcastle disease virus may enter cells by caveolae-mediated endocytosis.," *J. Gen. Virol.*, **88**(Pt 2), pp. 559–569.
- [25] Kopatz I., Remy J.-S., and Behr J.-P., 2004, "A model for non-viral gene delivery: through syndecan adhesion molecules and powered by actin.," *J Gene Med*, **6**(7), pp. 769–776.
- [26] Vercauteren D., Piest M., van der Aa L. J., Soraj Al M., Jones A. T., Engbersen J. F. J., De Smedt S. C., and Braeckmans K., 2011, "Flotillin-dependent endocytosis and a phagocytosis-like mechanism for cellular internalization of disulfide-based poly(amido amine)/DNA polyplexes.," *Biomaterials*, **32**(11), pp. 3072–3084.
- [27] Grosse S., Aron Y., Thévenot G., François D., Monsigny M., and Fajac I., 2005, "Potocytosis and cellular exit of complexes as cellular pathways for gene delivery by polycations.," *J Gene Med*, **7**(10), pp. 1275–1286.

- [28] Anderson R. G., 1998, "The caveolae membrane system," *Annu. Rev. Biochem.*, **67**, pp. 199–225.
- [29] Razani B., Woodman S. E., and Lisanti M. P., 2002, "Caveolae: from cell biology to animal physiology," *Pharmacol. Rev.*, **54**(3), pp. 431–467.
- [30] Harris J., Werling D., Hope J. C., Taylor G., and Howard C. J., 2002, "Caveolae and caveolin in immune cells: distribution and functions," *Trends Immunol.*, **23**(3), pp. 158–164.
- [31] Maxfield F. R., and McGraw T. E., 2004, "Endocytic recycling," *Nat. Rev. Mol. Cell Biol.*, **5**(2), pp. 121–132.
- [32] Traub L. M., 2009, "Tickets to ride: selecting cargo for clathrin-regulated internalization," *Nat. Rev. Mol. Cell Biol.*, **10**(9), pp. 583–596.
- [33] Douglas K. L., Piccirillo C. A., and Tabrizian M., 2008, "Cell line-dependent internalization pathways and intracellular trafficking determine transfection efficiency of nanoparticle vectors," *Eur J Pharm Biopharm*, **68**(3), pp. 676–687.
- [34] Gersdorff von K., Sanders N. N., Vandenbroucke R., De Smedt S. C., Wagner E., and Ogris M., 2006, "The internalization route resulting in successful gene expression depends on both cell line and polyethylenimine polyplex type," *Mol Ther*, **14**(5), pp. 745–753.
- [35] van der Aa M. A. E. M., Huth U. S., Häfele S. Y., Schubert R., Oosting R. S., Mastrobattista E., Hennink W. E., Peschka-Süss R., Koning G. A., and Crommelin D. J. A., 2007, "Cellular uptake of cationic polymer-DNA complexes via caveolae plays a pivotal role in gene transfection in COS-7 cells," *Pharmaceutical research*, **24**(8), pp. 1590–1598.
- [36] Douglas K. L., 2008, "Toward development of artificial viruses for gene therapy: A comparative evaluation of viral and non-viral transfection," *Biotechnology Progress*, pp. 871–883.
- [37] Boussif O., Lezoualc'h F., Zanta M. A., Mergny M. D., Scherman D., Demeneix B., and Behr J. P., 1995, "A versatile vector for gene and oligonucleotide transfer into cells in culture and in vivo: polyethylenimine," *Proc Natl Acad Sci USA*,

92(16), pp. 7297–7301.

- [38] Pelkmans L., Bürli T., Zerial M., and Helenius A., 2004, "Caveolin-stabilized membrane domains as multifunctional transport and sorting devices in endocytic membrane traffic.," *Cell*, **118**(6), pp. 767–780.
- [39] Akey C. W., 1990, "Visualization of transport-related configurations of the nuclear pore transporter.," *Biophys. J.*, **58**(2), pp. 341–355.
- [40] Kiseleva E., Goldberg M. W., Allen T. D., and Akey C. W., 1998, "Active nuclear pore complexes in Chironomus: visualization of transporter configurations related to mRNP export.," *J. Cell. Sci.*, **111 (Pt 2)**, pp. 223–236.
- [41] Grünwald D., Singer R. H., and Rout M., 2011, "Nuclear export dynamics of RNA-protein complexes.," *Nature*, **475**(7356), pp. 333–341.
- [42] Rodriguez M. S., Dargemont C., and Stutz F., 2004, "Nuclear export of RNA.," *Biol. Cell*, **96**(8), pp. 639–655.
- [43] Lei E. P., and Silver P. A., 2002, "Protein and RNA export from the nucleus.," *Dev. Cell*, **2**(3), pp. 261–272.
- [44] Itaka K., Harada A., Yamasaki Y., Nakamura K., Kawaguchi H., and Kataoka K., 2004, "In situ single cell observation by fluorescence resonance energy transfer reveals fast intra-cytoplasmic delivery and easy release of plasmid DNA complexed with linear polyethylenimine.," *J Gene Med*, **6**(1), pp. 76–84.
- [45] Bieber T., Meissner W., Kostin S., Niemann A., and Elsasser H.-P., 2002, "Intracellular route and transcriptional competence of polyethylenimine-DNA complexes.," *J Control Release*, **82**(2-3), pp. 441–454.
- [46] Brunner S., Fürtbauer E., Sauer T., Kursu M., and Wagner E., 2002, "Overcoming the nuclear barrier: cell cycle independent nonviral gene transfer with linear polyethylenimine or electroporation.," *Mol Ther*, **5**(1), pp. 80–86.
- [47] de Semir D., Petriz J., Avinyó A., Larriba S., Nunes V., Casals T., Estivill X., and Aran J. M., 2002, "Non-viral vector-mediated uptake, distribution, and stability of chimeraplasts in human airway epithelial cells.," *J Gene Med*, **4**(3), pp. 308–

322.

- [48] Feng M., Lee D., and Li P., 2006, "Intracellular uptake and release of poly(ethyleneimine)-co-poly(methyl methacrylate) nanoparticle/pDNA complexes for gene delivery.," *Int J Pharm*, **311**(1-2), pp. 209–214.
- [49] Akita H., Ito R., Kamiya H., Kogure K., and Harashima H., 2007, "Cell cycle dependent transcription, a determinant factor of heterogeneity in cationic lipid-mediated transgene expression.," *J Gene Med*, **9**(3), pp. 197–207.
- [50] Wagstaff K. M., and Jans D. A., 2009, "Importins and beyond: non-conventional nuclear transport mechanisms.," *Traffic*, **10**(9), pp. 1188–1198.
- [51] Grosse S., Thévenot G., Monsigny M., and Fajac I., 2006, "Which mechanism for nuclear import of plasmid DNA complexed with polyethylenimine derivatives?," *J Gene Med*, **8**(7), pp. 845–851.
- [52] Männistö M., Rönkkö S., Mättö M., Honkakoski P., Hyttinen M., Pelkonen J., and Urtti A., 2005, "The role of cell cycle on polyplex-mediated gene transfer into a retinal pigment epithelial cell line.," *J Gene Med*, **7**(4), pp. 466–476.
- [53] Brunner S., Sauer T., Carotta S., Cotten M., Saltik M., and Wagner E., 2000, "Cell cycle dependence of gene transfer by lipoplex, polyplex and recombinant adenovirus.," *Gene Ther*, **7**(5), pp. 401–407.
- [54] Mortimer I., Tam P., MacLachlan I., Graham R. W., Saravolac E. G., and Joshi P. B., 1999, "Cationic lipid-mediated transfection of cells in culture requires mitotic activity.," *Gene Ther*, **6**(3), pp. 403–411.
- [55] Tseng W. C., Haselton F. R., and Giorgio T. D., 1999, "Mitosis enhances transgene expression of plasmid delivered by cationic liposomes.," *Biochim Biophys Acta*, **1445**(1), pp. 53–64.
- [56] Hendzel M. J., Kruhlak M. J., MacLean N. A., Boisvert F., Lever M. A., and Bazett-Jones D. P., 2001, "Compartmentalization of regulatory proteins in the cell nucleus.," *J. Steroid Biochem. Mol. Biol.*, **76**(1-5), pp. 9–21.
- [57] Jackson D. A., 2003, "The principles of nuclear structure.," *Chromosome Res.*,

11(5), pp. 387–401.

- [58] Baxter J., Merckenschlager M., and Fisher A. G., 2002, "Nuclear organisation and gene expression.," *Curr. Opin. Cell Biol.*, **14**(3), pp. 372–376.
- [59] Hama S., Akita H., Iida S., Mizuguchi H., and Harashima H., 2007, "Quantitative and mechanism-based investigation of post-nuclear delivery events between adenovirus and lipoplex.," *Nucleic Acids Res*, **35**(5), pp. 1533–1543.
- [60] Lee T. W. R., Blair G. E., and Matthews D. A., 2003, "Adenovirus core protein VII contains distinct sequences that mediate targeting to the nucleus and nucleolus, and colocalization with human chromosomes.," *J. Gen. Virol.*, **84**(Pt 12), pp. 3423–3428.
- [61] Lee T. W. R., Lawrence F. J., Dauksaite V., Akusjärvi G., Blair G. E., and Matthews D. A., 2004, "Precursor of human adenovirus core polypeptide Mu targets the nucleolus and modulates the expression of E2 proteins.," *J. Gen. Virol.*, **85**(Pt 1), pp. 185–196.
- [62] Matthews D. A., 2001, "Adenovirus protein V induces redistribution of nucleolin and B23 from nucleolus to cytoplasm.," *J. Virol.*, **75**(2), pp. 1031–1038.
- [63] de Jong R. N., Mysiak M. E., Meijer L. A. T., van der Linden M., and van der Vliet P. C., 2002, "Recruitment of the priming protein pTP and DNA binding occur by overlapping Oct-1 POU homeodomain surfaces.," *EMBO J.*, **21**(4), pp. 725–735.
- [64] Matsumoto K., Nagata K., Yamanaka K., Hanaoka F., and Ui M., 1989, "Nuclear factor I represses the reverse-oriented transcription from the adenovirus type 5 DNA terminus.," *Biochem Biophys Res Commun*, **164**(3), pp. 1212–1219.
- [65] Shaheen S. M., Akita H., Yamashita A., Katoono R., Yui N., Biju V., Ishikawa M., and Harashima H., 2011, "Quantitative analysis of condensation/decondensation status of pDNA in the nuclear sub-domains by QD-FRET.," *Nucleic Acids Res*, **39**(7), pp. e48–U108.
- [66] Schaffer D. V., Fidelman N. A., Dan N., and Lauffenburger D. A., 2000, "Vector unpacking as a potential barrier for receptor-mediated polyplex gene delivery.," *Biotechnol Bioeng*, **67**(5), pp. 598–606.

- [67] Hama S., Akita H., Ito R., Mizuguchi H., Hayakawa T., and Harashima H., 2006, "Quantitative comparison of intracellular trafficking and nuclear transcription between adenoviral and lipoplex systems," *Mol Ther*, **13**(4), pp. 786–794.
- [68] Saito Y., Kawakami S., Yabe Y., Yamashita F., and Hashida M., 2006, "Intracellular trafficking is the important process that determines the optimal charge ratio on transfection by galactosylated lipoplex in HEPG2 cells," *Biol Pharm Bull*, **29**(9), pp. 1986–1990.
- [69] Ahmad A., Evans H. M., Ewert K., George C. X., Samuel C. E., and Safinya C. R., 2005, "New multivalent cationic lipids reveal bell curve for transfection efficiency versus membrane charge density: lipid-DNA complexes for gene delivery," *J Gene Med*, **7**(6), pp. 739–748.
- [70] Honoré I., Grosse S., Frison N., Favatier F., Monsigny M., and Fajac I., 2005, "Transcription of plasmid DNA: influence of plasmid DNA/polyethylenimine complex formation," *J Control Release*, **107**(3), pp. 537–546.
- [71] Pollard H., Remy J. S., Loussouarn G., Demolombe S., Behr J. P., and Escande D., 1998, "Polyethylenimine but not cationic lipids promotes transgene delivery to the nucleus in mammalian cells," *J Biol Chem*, **273**(13), pp. 7507–7511.
- [72] Mui B., Ahkong Q. F., Chow L., and Hope M. J., 2000, "Membrane perturbation and the mechanism of lipid-mediated transfer of DNA into cells," *Biochim Biophys Acta*, **1467**(2), pp. 281–292.
- [73] Kaufmann S. H. E., 2007, "The contribution of immunology to the rational design of novel antibacterial vaccines," *Nat Rev Microbiol*, **5**(7), pp. 491–504.
- [74] Loisel S., Le Gall C., Doucet L., Ferec C., and Floch V., 2001, "Contribution of plasmid DNA to hepatotoxicity after systemic administration of lipoplexes," *Hum Gene Ther*, **12**(6), pp. 685–696.
- [75] Li S., Wu S. P., Whitmore M., Loeffert E. J., Wang L., Watkins S. C., Pitt B. R., and Huang L., 1999, "Effect of immune response on gene transfer to the lung via systemic administration of cationic lipidic vectors," *Am. J. Physiol.*, **276**(5 Pt 1), pp. L796–804.

- [76] Gautam A., Densmore C. L., and Waldrep J. C., 2001, "Pulmonary cytokine responses associated with PEI-DNA aerosol gene therapy," *Gene Ther*, **8**(3), pp. 254–257.
- [77] Sakurai H., Sakurai F., Kawabata K., Sasaki T., Koizumi N., Huang H., Tashiro K., Kurachi S., Nakagawa S., and Mizuguchi H., 2007, "Comparison of gene expression efficiency and innate immune response induced by Ad vector and lipoplex.," *J Control Release*, **117**(3), pp. 430–437.
- [78] Sakurai H., Kawabata K., Sakurai F., Nakagawa S., and Mizuguchi H., 2008, "Innate immune response induced by gene delivery vectors.," *Int J Pharm*, **354**(1-2), pp. 9–15.
- [79] Gill D. R., Pringle I. A., and Hyde S. C., 2009, "Progress and prospects: the design and production of plasmid vectors.," *Gene Ther*, **16**(2), pp. 165–171.
- [80] Kumar H., Kawai T., and Akira S., 2009, "Pathogen recognition in the innate immune response.," *Biochem J*, **420**(1), pp. 1–16.
- [81] Medzhitov R., 2001, "Toll-like receptors and innate immunity.," *Nature Reviews Immunology*, **1**(2), pp. 135–145.
- [82] Kawai T., and Akira S., 2008, "Toll-like receptor and RIG-I-like receptor signaling.," *Ann. N. Y. Acad. Sci.*, **1143**, pp. 1–20.
- [83] Zhao H., Hemmi H., Akira S., Cheng S. H., Scheule R. K., and Yew N. S., 2004, "Contribution of Toll-like receptor 9 signaling to the acute inflammatory response to nonviral vectors.," *Mol Ther*, **9**(2), pp. 241–248.
- [84] Whitmore M., Li S., and Huang L., 1999, "LPD lipopolyplex initiates a potent cytokine response and inhibits tumor growth.," *Gene Ther*, **6**(11), pp. 1867–1875.
- [85] Reyes-Sandoval A., and Ertl H. C. J., 2004, "CpG methylation of a plasmid vector results in extended transgene product expression by circumventing induction of immune responses.," *Mol Ther*, **9**(2), pp. 249–261.
- [86] Hyde S. C., Pringle I. A., Abdullah S., Lawton A. E., Davies L. A., Varathalingam A.,

- Nunez-Alonso G., Green A.-M., Bazzani R. P., Sumner-Jones S. G., Chan M., Li H., Yew N. S., Cheng S. H., Boyd A. C., Davies J. C., Griesenbach U., Porteous D. J., Sheppard D. N., Munkonge F. M., Alton E. W. F. W., and Gill D. R., 2008, "CpG-free plasmids confer reduced inflammation and sustained pulmonary gene expression.," *Nat Biotechnol*, **26**(5), pp. 549–551.
- [87] Cornélie S., Poulain-Godefroy O., Lund C., Vendeville C., Ban E., Capron M., and Riveau G., 2004, "Methylated CpG-containing plasmid activates the immune system.," *Scand. J. Immunol.*, **59**(2), pp. 143–151.
- [88] Ishii K. J., Coban C., Kato H., Takahashi K., Torii Y., Takeshita F., Ludwig H., Sutter G., Suzuki K., Hemmi H., Sato S., Yamamoto M., Uematsu S., Kawai T., Takeuchi O., and Akira S., 2006, "A Toll-like receptor-independent antiviral response induced by double-stranded B-form DNA.," *Nat. Immunol.*, **7**(1), pp. 40–48.
- [89] Takaoka A., Wang Z., Choi M. K., Yanai H., Negishi H., Ban T., Lu Y., Miyagishi M., Kodama T., Honda K., Ohba Y., and Taniguchi T., 2007, "DAI (DLM-1/ZBP1) is a cytosolic DNA sensor and an activator of innate immune response.," *Nature*, **448**(7152), pp. 501–505.
- [90] Tan Y., Liu F., Li Z., Li S., and Huang L., 2001, "Sequential injection of cationic liposome and plasmid DNA effectively transfects the lung with minimal inflammatory toxicity.," *Mol Ther*, **3**(5 Pt 1), pp. 673–682.
- [91] Suzuki M., Cerullo V., Bertin T. K., Cela R., Clarke C., Guenther M., Brunetti-Pierri N., and Lee B., 2010, "MyD88-dependent silencing of transgene expression during the innate and adaptive immune response to helper-dependent adenovirus.," *Hum Gene Ther*, **21**(3), pp. 325–336.
- [92] Sadler A. J., and Williams B. R. G., 2008, "Interferon-inducible antiviral effectors.," *Nature Reviews Immunology*, **8**(7), pp. 559–568.
- [93] Li S., Peters G. A., Ding K., Zhang X., Qin J., and Sen G. C., 2006, "Molecular basis for PKR activation by PACT or dsRNA.," *Proc Natl Acad Sci USA*, **103**(26), pp. 10005–10010.
- [94] Aguiar R. S., and Peterlin B. M., 2008, "APOBEC3 proteins and reverse transcription.," *Virus Res.*, **134**(1-2), pp. 74–85.

- [95] Fensterl V., and Sen G. C., 2009, "Interferons and viral infections.," *Biofactors*, **35**(1), pp. 14–20.
- [96] Riu E., Chen Z. Y., Xu H., He C.-Y., and Kay M. A., 2007, "Histone modifications are associated with the persistence or silencing of vector-mediated transgene expression in vivo.," *Mol Ther*, **15**(7), pp. 1348–1355.
- [97] Recillas-Targa F., 2006, "Multiple strategies for gene transfer, expression, knockdown, and chromatin influence in mammalian cell lines and transgenic animals.," *Mol Biotechnol*, **34**(3), pp. 337–354.
- [98] Chen Z. Y., He C.-Y., Ehrhardt A., and Kay M. A., 2003, "Minicircle DNA vectors devoid of bacterial DNA result in persistent and high-level transgene expression in vivo.," *Mol Ther*, **8**(3), pp. 495–500.
- [99] Yang J. P., and Huang L., 1998, "Time-dependent maturation of cationic liposome-DNA complex for serum resistance.," *Gene Ther*, **5**(3), pp. 380–387.
- [100] Li S., Tseng W. C., Stolz D. B., Wu S. P., Watkins S. C., and Huang L., 1999, "Dynamic changes in the characteristics of cationic lipidic vectors after exposure to mouse serum: implications for intravenous lipofection.," *Gene Ther*, **6**(4), pp. 585–594.
- [101] Wheeler J. J., Palmer L., Ossanlou M., MacLachlan I., Graham R. W., Zhang Y. P., Hope M. J., Scherrer P., and Cullis P. R., 1999, "Stabilized plasmid-lipid particles: construction and characterization.," *Gene Ther*, **6**(2), pp. 271–281.
- [102] Ikonen M., Murtomäki L., and Kontturi K., 2008, "Controlled complexation of plasmid DNA with cationic polymers: effect of surfactant on the complexation and stability of the complexes.," *Colloids and Surfaces B: Biointerfaces*, **66**(1), pp. 77–83.
- [103] Schaffert D., and Wagner E., 2008, "Gene therapy progress and prospects: synthetic polymer-based systems.," *Gene Ther*, **15**(16), p. 1131.
- [104] Yu J., and Anchordoquy T. J., 2009, "Synergistic effects of surfactants and sugars on lipoplex stability during freeze-drying and rehydration.," *J Pharm Sci*, **98**(9), pp. 3319–3328.

- [105] Marty R., N'soukpoé-Kossi C. N., Charbonneau D., Weinert C. M., Kreplak L., and Tajmir-Riahi H.-A., 2009, "Structural analysis of DNA complexation with cationic lipids," *Nucleic Acids Res*, **37**(3), pp. 849–857.
- [106] Harvie P., Dutzar B., Galbraith T., Cudmore S., O'Mahony D., Anklesaria P., and Paul R., 2003, "Targeting of lipid-protamine-DNA (LPD) lipopolyplexes using RGD motifs," *J Liposome Res*, **13**(3-4), pp. 231–247.
- [107] Sun X., and Zhang N., 2010, "Cationic polymer optimization for efficient gene delivery," *Mini Rev Med Chem*, **10**(2), pp. 108–125.
- [108] Chin-Ling Pai M.-J. S. P.-J. L. F.-H. H. T.-W. W. A. P.-S. L., 2010, "Characterization of the Uptake and Intracellular Trafficking of G4 Polyamidoamine Dendrimers," *Aust. J. Chem.*
- [109] Huang R., Liu S., Shao K., Han L., Ke W., Liu Y., Li J., Huang S., and Jiang C., 2010, "Evaluation and mechanism studies of PEGylated dendrigraft poly-L-lysines as novel gene delivery vectors," *Nanotechnology*, **21**(26), p. 265101.
- [110] Germershaus O., Mao S., Sitterberg J., Bakowsky U., and Kissel T., 2008, "Gene delivery using chitosan, trimethyl chitosan or polyethyleneglycol-graft-trimethyl chitosan block copolymers: establishment of structure-activity relationships in vitro," *J Control Release*, **125**(2), pp. 145–154.
- [111] Luo X., Pan S., Feng M., Wen Y., and Zhang W., 2010, "Stability of poly(ethylene glycol)-graft-polyethylenimine copolymer/DNA complexes: influences of PEG molecular weight and PEGylation degree," *J Mater Sci Mater Med*, **21**(2), pp. 597–607.
- [112] Glodde M., Sirsi S. R., and Lutz G. J., 2006, "Physicochemical properties of low and high molecular weight poly(ethylene glycol)-grafted poly(ethylene imine) copolymers and their complexes with oligonucleotides," *Biomacromolecules*, **7**(1), pp. 347–356.
- [113] Deshpande M. C., Davies M. C., Garnett M. C., Williams P. M., Armitage D., Bailey L., Vamvakaki M., Armes S. P., and Stolnik S., 2004, "The effect of poly(ethylene glycol) molecular architecture on cellular interaction and uptake of DNA complexes," *J Control Release*, **97**(1), pp. 143–156.

- [114] Remaut K., Lucas B., Braeckmans K., Demeester J., and De Smedt S. C., 2007, "Pegylation of liposomes favours the endosomal degradation of the delivered phosphodiester oligonucleotides," *J Control Release*, **117**(2), pp. 256–266.
- [115] Xu L., Huang C.-C., Huang W., Tang W.-H., Rait A., Yin Y. Z., Cruz I., Xiang L.-M., Pirollo K. F., and Chang E. H., 2002, "Systemic tumor-targeted gene delivery by anti-transferrin receptor scFv-immunoliposomes," *Mol. Cancer Ther.*, **1**(5), pp. 337–346.
- [116] Bruckheimer E., Harvie P., Orthel J., Dutzar B., Furstoss K., Mebel E., Anklesaria P., and Paul R., 2004, "In vivo efficacy of folate-targeted lipid-protamine-DNA (LPD-PEG-Folate) complexes in an immunocompetent syngeneic model for breast adenocarcinoma," *Cancer Gene Ther*, **11**(2), pp. 128–134.
- [117] Déas O., Angevin E., Cherbonnier C., Senik A., Charpentier B., Levillain J. P., Oosterwijk E., Hirsch F., and Dürrbach A., 2002, "In vivo-targeted gene delivery using antibody-based nonviral vector," *Hum Gene Ther*, **13**(9), pp. 1101–1114.
- [118] Mamot C., Drummond D. C., Noble C. O., Kallab V., Guo Z., Hong K., Kirpotin D. B., and Park J. W., 2005, "Epidermal growth factor receptor-targeted immunoliposomes significantly enhance the efficacy of multiple anticancer drugs in vivo," *Cancer Res.*, **65**(24), pp. 11631–11638.
- [119] Jiang H.-L., Kwon J.-T., Kim Y.-K., Kim E.-M., Arote R., Jeong H.-J., Nah J.-W., Choi Y.-J., Akaike T., Cho M.-H., and Cho C.-S., 2007, "Galactosylated chitosan-graft-polyethylenimine as a gene carrier for hepatocyte targeting," *Gene Ther*, **14**(19), pp. 1389–1398.
- [120] Diebold S. S., Kursu M., Wagner E., Cotten M., and Zenke M., 1999, "Mannose polyethylenimine conjugates for targeted DNA delivery into dendritic cells," *J Biol Chem*, **274**(27), pp. 19087–19094.
- [121] Meng Q., Yu M., Gu B., Li J., Liu Y., Zhan C., Xie C., Zhou J., and Lu W., 2010, "Myristic acid-conjugated polyethylenimine for brain-targeting delivery: in vivo and ex vivo imaging evaluation," *J Drug Target*, **18**(6), pp. 438–446.
- [122] Incani V., Lavasanifar A., and Uludağ H., 2010, "Lipid and hydrophobic modification of cationic carriers on route to superior gene vectors," *Soft Matter*,

6(10), pp. 2124–2138.

- [123] Tseng W. C., Haselton F. R., and Giorgio T. D., 1997, "Transfection by cationic liposomes using simultaneous single cell measurements of plasmid delivery and transgene expression.," *J Biol Chem*, **272**(41), pp. 25641–25647.
- [124] Xu L., and Anchordoquy T., 2011, "Drug delivery trends in clinical trials and translational medicine: challenges and opportunities in the delivery of nucleic acid-based therapeutics.," *J Pharm Sci*, **100**(1), pp. 38–52.
- [125] Hoekstra D., Rejman J., Wasungu L., Shi F., and Zuhorn I., 2007, "Gene delivery by cationic lipids: in and out of an endosome.," *Biochem. Soc. Trans.*, **35**(Pt 1), pp. 68–71.
- [126] Kichler A., Leborgne C., Danos O., and Bechinger B., 2007, "Characterization of the gene transfer process mediated by histidine-rich peptides.," *J. Mol. Med.*, **85**(2), pp. 191–201.
- [127] Akinc A., Thomas M., Klibanov A. M., and Langer R., 2005, "Exploring polyethylenimine-mediated DNA transfection and the proton sponge hypothesis.," *J Gene Med*, **7**(5), pp. 657–663.
- [128] Sonawane N. D., Szoka F. C., and Verkman A. S., 2003, "Chloride accumulation and swelling in endosomes enhances DNA transfer by polyamine-DNA polyplexes," *J Biol Chem*, **278**(45), pp. 44826–44831.
- [129] Jenssen H., Hamill P., and Hancock R. E. W., 2006, "Peptide antimicrobial agents.," *Clin. Microbiol. Rev.*, **19**(3), pp. 491–511.
- [130] Huang H. W., Chen F.-Y., and Lee M.-T., 2004, "Molecular mechanism of Peptide-induced pores in membranes.," *Phys. Rev. Lett.*, **92**(19), pp. 198304–.
- [131] Marsh M., and Helenius A., 1989, "Virus entry into animal cells.," *Adv. Virus Res.*, **36**, pp. 107–151.
- [132] Weis W. I., Cusack S. C., Brown J. H., Daniels R. S., Skehel J. J., and Wiley D. C., 1990, "The structure of a membrane fusion mutant of the influenza virus haemagglutinin.," *EMBO J.*, **9**(1), pp. 17–24.

- [133] Subramanian A., Ma H., Dahl K. N., Zhu J., and Diamond S. L., 2002, "Adenovirus or HA-2 fusogenic peptide-assisted lipofection increases cytoplasmic levels of plasmid in nondividing endothelium with little enhancement of transgene expression.," *J Gene Med*, **4**(1), pp. 75–83.
- [134] Wagner E., Plank C., Zatloukal K., Cotten M., and Birnstiel M. L., 1992, "Influenza virus hemagglutinin HA-2 N-terminal fusogenic peptides augment gene transfer by transferrin-polylysine-DNA complexes: toward a synthetic virus-like gene-transfer vehicle.," *Proc Natl Acad Sci USA*, **89**(17), pp. 7934–7938.
- [135] Lewin M., Carlesso N., Tung C. H., Tang X. W., Cory D., Scadden D. T., and Weissleder R., 2000, "Tat peptide-derivatized magnetic nanoparticles allow in vivo tracking and recovery of progenitor cells.," *Nat Biotechnol*, **18**(4), pp. 410–414.
- [136] Morris M. C., Chaloin L., Méry J., Heitz F., and Divita G., 1999, "A novel potent strategy for gene delivery using a single peptide vector as a carrier.," *Nucleic Acids Res*, **27**(17), pp. 3510–3517.
- [137] Lorenzi G. L., and Lee K.-D., 2005, "Enhanced plasmid DNA delivery using anionic LPDII by listeriolysin O incorporation.," *J Gene Med*, **7**(8), pp. 1077–1085.
- [138] Kullberg M., Owens J. L., and Mann K., 2010, "Listeriolysin O enhances cytoplasmic delivery by Her-2 targeting liposomes.," *J Drug Target*, **18**(4), pp. 313–320.
- [139] Walton C. M., Wu C. H., and Wu G. Y., 1999, "A DNA delivery system containing listeriolysin O results in enhanced hepatocyte-directed gene expression.," *World J. Gastroenterol.*, **5**(6), pp. 465–469.
- [140] Saito G., Amidon G. L., and Lee K.-D., 2003, "Enhanced cytosolic delivery of plasmid DNA by a sulfhydryl-activatable listeriolysin O/protamine conjugate utilizing cellular reducing potential.," *Gene Ther*, **10**(1), pp. 72–83.
- [141] Sun J., Pohl E. E., Krylova O. O., Krause E., Agapov I. I., Tonevitsky A. G., and Pohl P., 2004, "Membrane destabilization by ricin.," *Eur. Biophys. J.*, **33**(7), pp. 572–579.

- [142] Vago R., Marsden C. J., Lord J. M., Ippoliti R., Flavell D. J., Flavell S.-U., Ceriotti A., and Fabbrini M. S., 2005, "Saporin and ricin A chain follow different intracellular routes to enter the cytosol of intoxicated cells," *FEBS J.*, **272**(19), pp. 4983–4995.
- [143] Foerg C., Ziegler U., Fernandez-Carneado J., Giralt E., Rennert R., Beck-Sickinger A. G., and Merkle H. P., 2005, "Decoding the entry of two novel cell-penetrating peptides in HeLa cells: lipid raft-mediated endocytosis and endosomal escape.," *Biochemistry*, **44**(1), pp. 72–81.
- [144] Krauss U., Müller M., Stahl M., and Beck-Sickinger A. G., 2004, "In vitro gene delivery by a novel human calcitonin (hCT)-derived carrier peptide.," *Bioorg. Med. Chem. Lett.*, **14**(1), pp. 51–54.
- [145] Ogris M., Carlisle R. C., Bettinger T., and Seymour L. W., 2001, "Melittin enables efficient vesicular escape and enhanced nuclear access of nonviral gene delivery vectors.," *J Biol Chem*, **276**(50), pp. 47550–47555.
- [146] Dempsey C. E., 1990, "The actions of melittin on membranes.," *Biochim Biophys Acta*, **1031**(2), pp. 143–161.
- [147] Abes R., Arzumanov A., Moulton H., Abes S., Ivanova G., Gait M. J., Iversen P., and Lebleu B., 2008, "Arginine-rich cell penetrating peptides: design, structure-activity, and applications to alter pre-mRNA splicing by steric-block oligonucleotides.," *J. Pept. Sci.*, **14**(4), pp. 455–460.
- [148] Min S.-H., Lee D. C., Lim M. J., Park H. S., Kim D. M., Cho C. W., Yoon D. Y., and Yeom Y. I., 2006, "A composite gene delivery system consisting of polyethylenimine and an amphipathic peptide KALA.," *J Gene Med*, **8**(12), pp. 1425–1434.
- [149] Asayama S., Hamaya A., Sekine T., Kawakami H., and Nagaoka S., 2004, "Aminated poly(L-histidine) as new pH-sensitive DNA carrier.," *Nucleic Acids Symp Ser (Oxf)*, (48), pp. 229–230.
- [150] Hatefi A., Megeed Z., and Ghandehari H., 2006, "Recombinant polymer-protein fusion: a promising approach towards efficient and targeted gene delivery.," *J Gene Med*, **8**(4), pp. 468–476.

- [151] Fernandez-Carneado J., Kogan M. J., Castel S., and Giralt E., 2004, "Potential peptide carriers: amphipathic proline-rich peptides derived from the N-terminal domain of gamma-zein," *Angew. Chem. Int. Ed. Engl.*, **43**(14), pp. 1811–1814.
- [152] del Pozo-Rodríguez A., Pujals S., Delgado D., Solinís M. A., Gascón A. R., Giralt E., and Pedraz J. L., 2009, "A proline-rich peptide improves cell transfection of solid lipid nanoparticle-based non-viral vectors," *J Control Release*, **133**(1), pp. 52–59.
- [153] Caviston J. P., and Holzbaur E. L. F., 2006, "Microtubule motors at the intersection of trafficking and transport," *Trends Cell Biol.*, **16**(10), pp. 530–537.
- [154] Hasegawa S., Hirashima N., and Nakanishi M., 2001, "Microtubule involvement in the intracellular dynamics for gene transfection mediated by cationic liposomes," *Gene Ther*, **8**(21), pp. 1669–1673.
- [155] Suh J., Wirtz D., and Hanes J., 2003, "Efficient active transport of gene nanocarriers to the cell nucleus," *Proc Natl Acad Sci USA*, **100**(7), pp. 3878–3882.
- [156] Kulkarni R. P., Wu D. D., Davis M. E., and Fraser S. E., 2005, "Quantitating intracellular transport of polyplexes by spatio-temporal image correlation spectroscopy," *Proc Natl Acad Sci USA*, **102**(21), pp. 7523–7528.
- [157] Kural C., Kim H., Syed S., Goshima G., Gelfand V. I., and Selvin P. R., 2005, "Kinesin and dynein move a peroxisome in vivo: a tug-of-war or coordinated movement?," *Science*, **308**(5727), pp. 1469–1472.
- [158] Lukacs G. L., Haggie P., Seksek O., Lechardeur D., Freedman N., and Verkman A. S., 2000, "Size-dependent DNA mobility in cytoplasm and nucleus," *J Biol Chem*, **275**(3), pp. 1625–1629.
- [159] Pandey K. N., 2010, "Small peptide recognition sequence for intracellular sorting," *Curr. Opin. Biotechnol.*, **21**(5), pp. 611–620.
- [160] Fukata Y., and Fukata M., 2010, "Protein palmitoylation in neuronal development and synaptic plasticity," *Nat. Rev. Neurosci.*, **11**(3), pp. 161–175.

- [161] Rajendran L., Kn Ouml Lker H.-J., and Simons K., 2010, "Subcellular targeting strategies for drug design and delivery," *Nat Rev Drug Discov*, **9**(1), p. 29.
- [162] Döhner K., Nagel C.-H., and Sodeik B., 2005, "Viral stop-and-go along microtubules: taking a ride with dynein and kinesins.," *Trends Microbiol.*, **13**(7), pp. 320–327.
- [163] Radtke K., Döhner K., and Sodeik B., 2006, "Viral interactions with the cytoskeleton: a hitchhiker's guide to the cell.," *Cell. Microbiol.*, **8**(3), pp. 387–400.
- [164] Hébert E., 2003, "Improvement of exogenous DNA nuclear importation by nuclear localization signal-bearing vectors: a promising way for non-viral gene therapy?," *Biol. Cell*, **95**(2), pp. 59–68.
- [165] Cartier R., and Reszka R., 2002, "Utilization of synthetic peptides containing nuclear localization signals for nonviral gene transfer systems.," *Gene Ther*, **9**(3), pp. 157–167.
- [166] Nagasaki T., Myohoji T., Tachibana T., Futaki S., and Tamagaki S., 2003, "Can nuclear localization signals enhance nuclear localization of plasmid DNA?," *Bioconjug Chem*, **14**(2), pp. 282–286.
- [167] Wagstaff K. M., and Jans D. A., 2007, "Nucleocytoplasmic transport of DNA: enhancing non-viral gene transfer," *Biochem J*, **406**(2), pp. 185–202.

Chapter 3

A simple and rapid non-viral approach to efficiently transfect primary tissue-derived cells using polyethylenimine¹

¹A version of this chapter has been published in Hsu C. Y. M., and Uludağ H., 2012. "A simple and rapid non-viral approach to efficiently transfect primary tissue-derived cells using polyethylenimine," *Nat Protoc.* 7(5) 935-945.

3.1 Introduction

Exogenous nucleic acid molecules can be artificially introduced into mammalian cells using viral vectors, physical methods or biocompatible cationic materials. Viral vectors are the most efficient at transducing cells owing to their naturally evolved mechanism to evade cellular barriers. However, immunogenic components of viral vectors may limit their utility in sensitive applications. In addition, the construction and packaging of viral vectors can be technically demanding and require specialized lab equipment. Physical methods of delivery such as electroporation and microinjection provide safer alternatives to viral vectors, but the transfection window and efficiency are typically narrow and low, and the requirement for specialized equipment and devices can be expensive and limit accessibility. Non-specific damage to the cells is a further concern that limits the utility of physical transfection methods. Biocompatible cationic polymers and lipids have a wide transfection range and relatively low immunogenicity. They are readily available as off-the-shelf reagents; carrier-DNA complexes are formed by self-assembly through electrostatic interaction between the cationic reagents and the anionic nucleic acid. The complexes can then be added directly to the growth medium, without a need for specialized devices. Thus, non-viral gene carriers provide a more accessible option for routine genetic manipulation of cellular physiology in studies ranging from gene function to *ex vivo* therapeutics.

3.1.1 Cationic polymers

Among the first cationic polymers to be used in transfection was polyethyleneimine (PEI). PEI comes in linear and branched configurations, ranging in molecular weight from 800 Da to 1,000,000 Da [1]. Its ability to transfect is principally derived from the high density of positive charges attributed to amine groups, which interact electrostatically with the negative charged phosphate backbone of nucleic acid to condense both molecules into sub-micron particles that can bind to the cell surface

and be taken up via endocytosis. The abundance of amine groups further provides a “proton-sponge” effect in which absorption of protons (H^+) by the amine groups inside the endosome leads to osmotic swelling and eventual rupture of the endosome membrane to release the endocytosed cargo into the cytoplasm [2]. Transfection efficiency of PEI is closely tied in with nucleic acid binding and dissociation of the polymer as it relates to the packaging and release of nucleic acid cargo. Low molecular weight PEIs have fewer amine groups per molecule, which bind and condense DNA less efficiently, translating into lower overall transfection efficiencies. High molecular weight PEIs have stronger binding affinity, which can condense DNA more efficiently, but they have a less effective release, leading to reduced transfection efficiency. High MW PEIs are also more toxic, reducing the viability of cells for transgene expression. Therefore, mid-range molecular weight PEIs provide a balance between binding affinity and ease of dissociation. As such, 25 kDa branched PEI (bPEI25) and 22 kDa linear PEI are the most popular and most effective polymeric transfection agent cited to-date [3].

Despite the ability of PEI to transfect a wide range of cell types, achieving transfection efficiency suitable for the desired application remains a challenge. While the development of modified polymers is an ongoing area of research, the methods in which complexes are formed is often overlooked. The transfection utility of PEI polymers is highly dependent on the environment and conditions in which complexes are formed. In some cases, complexes formulated under one condition to transfect a particular cell line may not necessarily be optimal for another cell line. Thus, the transfection protocol should be specifically optimized for each polymer and each type of cell line. This is critical to ensure that the most utility can be derived from the transfection reagent as well as to ensure comparative evaluation of transfection efficiencies between existing polymers and novel gene carriers is achieved.

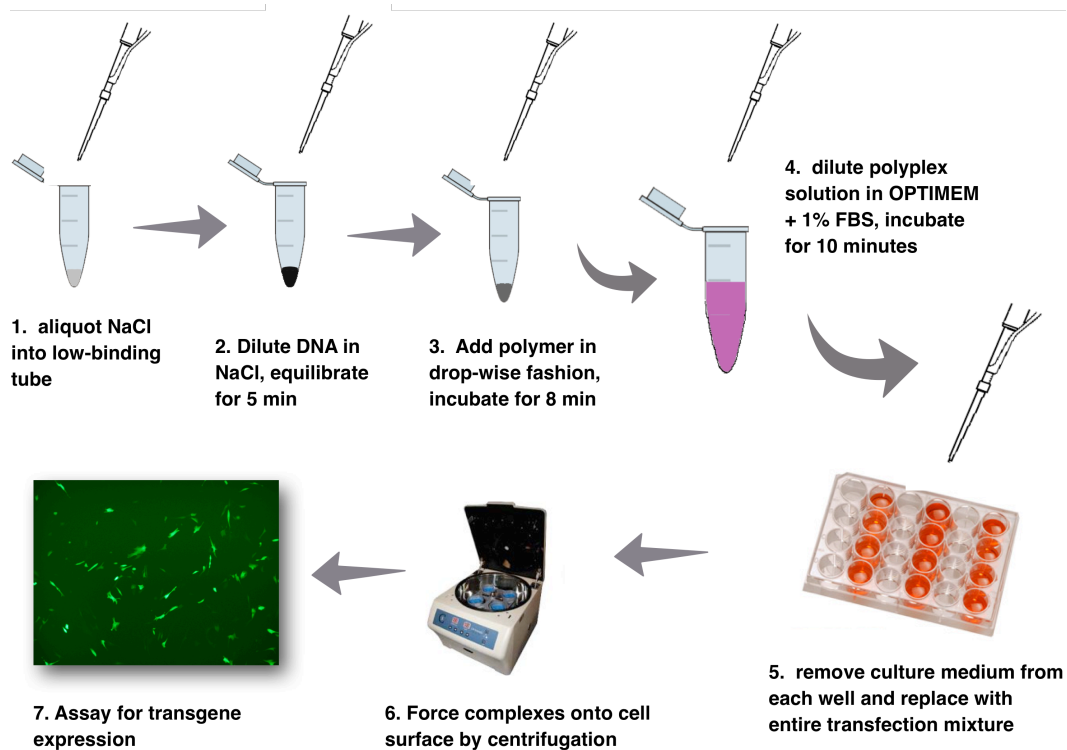


Figure 3.1
Schematic overview of suggested transfection protocol.

3.1.2 Experimental design

The overall procedure for transfection is outlined in **Figure 3.1** and can be envisioned as having two main parts. The first part involves the mixing of DNA and polymer in a smaller volume of aqueous solution followed by minutes of incubation to allow complexes to mature. The second part involves the addition of complexes to the cell in a larger volume of growth media and incubation for a few hours to allow adsorption and uptake of complexes. A number of parameters can affect the physicochemical properties of the complexes in both parts of the transfection process, including salt concentration, types of solute, volume of solution, pH, incubation time, viscosity, buffers, concentration of DNA, amount of polymer, polymer-to-DNA ratio, mixing order, mixing speed, temperature, presence of amphiphatic molecules (e.g.

surfactants), and ion species. Since transfection is typically done in minimum essential growth media, the condition in which complexes are formed needs to be compatible with the growth medium to preserve cell viability. As such, we focus our discussion on optimizing parameters that can be practically implemented under physiological conditions.

3.1.3 Cell line

Transfection efficiencies are known to vary greatly among mammalian cell lines. This is principally due to differences in cell physiology, which dictates metabolic requirement, and can affect the distribution of cell surface receptors and the uptake pathways utilized by the cell to internalize complexes [4,5]. Further, immortalized cultured cells such as COS-7, NIH/3T3, HeLa, HEK 293T, and CHO cells can be transfected much more readily to higher efficiency than tissue derived primary cells such as fibroblasts and bone marrow stromal cells [6,7]. The process of transforming cells to make them more amenable to culture conditions may have inadvertently altered some parts of the cellular processes, such as cell cycle and uptake pathways that made them more susceptible to transfection. In contrast, primary tissue-derived cells could be more selective towards the physicochemical properties of the complexes, which can define the predominant endocytic uptake pathway and ultimately how cargos are processed and transported within the intracellular domains. Thus, it is important to note that transfection procedures need to be optimized for individual cell line.

3.1.4 Complexation volume

Studies often report the amount of DNA used in transfection as a concentration of the final media volume, after complexes are added to the cell. This concentration is not the same as the concentration of DNA during complexation, which can drastically affect how complexes are formed. When complexes are formed at high concentrations

of DNA/polymer, the increased frequency of intermolecular interactions may not provide sufficient spacing to allow proper DNA condensation and maturation of individual particles, which can lead to partially formed particles and aggregation - features that are less desirable for efficient transfection. Therefore, dilution of DNA and polymers in a larger volume generally leads to smaller and more uniform particles that are more conducive to transfection. However, if the volume of the complexes becomes too large, it might dilute essential nutrients required to sustain metabolic activity in the growth media after addition of complexes. Thus, optimal volume for complexation will need to be empirically determined as a function of DNA concentration, NP ratio, and growth media volume.

3.1.5 Salt and solutes

The effect of solutes on particle stability varies with the structure and molecular weight of the PEIs. For example, 22 kDa linear PEI (LPEI22) and 25 kDa branched PEI (bPEI25) can both form complexes less than 100 nm in size under salt-free conditions. However, when physiological salt was added to the complexes, LPEI22 complexes grew into large aggregates whereas bPEI25 complexes remained small [3,5]. This suggests that complexes may undergo physicochemical changes when mixed with media of different solute concentrations. That is, when complexes are added to the growth media for transfection, the sizes and stability of the particles may change during mixing of the two solutions. Regardless of what the sizes of the complexes formed in salt-free or saline solution are, both should be tested as part of the optimization experiment to determine the best condition for transfection. In our experience, we have found that bPEI25 complexes formed in salt-free solution (20 mM HEPES, pH 7.4) lead to significantly higher transfection than complexes formed in buffered saline (150 mM NaCl, 20 mM HEPES, pH 7.4). However, the opposite is true for transfection in bone marrow stromal cells, in which complexes prepared in buffered

saline lead to better transfection. Thus, a universal complexation method may not yield optimal transfection protocol in every cell line.

3.1.6 DNA concentration, ratio of polymer-to-DNA, and polymer concentration

In general, the higher the concentration of DNA administered to the cells, the higher the level of transfection. However, the amount of DNA that can be applied in transfection is limited by the final concentration of polymer and the ratio of polymer-to-DNA. The optimal ratio of polymer-to-DNA (or nitrogen-to-phosphate ratio) is often in excess of the ratio at which full binding and full condensation occurs. This means that the solution of complexes often contains an excess of unbound polymers as well. PEI chains bound to DNA are mainly to condense and protect the cargo, but free PEI appears to be essential for intracellular trafficking and to overcome the inhibitory effect of the anionic cell-surface glycosaminoglycan (GAG) [8-10]. However, if the amount of PEI becomes too high, cell damage may ensue to reduce overall viability. Thus, optimal transfection conditions would occur at a polymer amount just enough to overcome the inhibitory effect of GAG, while providing robust complex uptake.

Optimizing the three parameters involves first determining the upper limit of polymer concentration the cells can withstand, then complexing with various amounts of DNA at the upper polymer concentration to test in transfection. The ratio of polymer-to-DNA that gives the highest level of transfection effectively determines the upper limit for DNA concentration. Since cell physiology can affect a range of metabolic activities, including uptake pathway and the expression of cell surface receptors, the amount of surface GAG will likely differ between cell lines. Thus, the optimal polymer concentration and polymer-to-DNA weight ratio needs to be empirically optimized for each cell line.

3.1.7 Effect of serum

Serum protein in growth media can interact with complexes to form large aggregates to reduce and inhibit transfection efficiency. The effect of serum on transfection varies between cell lines [11]. For example, HEK293T cells can be transfected in growth media supplemented with 10% FBS without significant reduction in reporter gene expression. In contrast, transfection of primary tissue-derived cells such as fibroblast and bone marrow stromal cells in the presence of serum nearly abolished reporter gene expression [12]. The amount of serum in the growth media during transfection will require optimization with respect to the polymer and the cell line. In our experience, the presence of any serum in the transfection media of fibroblasts significantly reduces transfection efficiency. However, low amounts of serum (1% FBS) for the transfection of bone marrow cells leads to better transfection in comparison to complete serum-free media. Since serum is required for metabolic activity and cell viability, the sensitivity of the cells to the absence of serum during the transfection incubation time may vary from cell line to cell line.

3.1.8 Complex stability and incubation time

Once complexes are formed, the utility time-frame for transfection is limited - complexes are unstable in solution and will gradually form large aggregates over time. Aggregation can arise due to heterologous intermolecular interaction with serum protein through charge-charge interaction, and/or homologous interaction with other PEI complexes as a result of hydrophobic shielding [13,14]. While the overall charge of the complex is positive, particles can exist as amphiphatic molecules with pockets of hydrophobic regions [14]; thus, particles may spontaneously bind to each other to shield these hydrophobic pockets from the aqueous solution, forming aggregates. Large aggregates are less efficiently taken up by the cell, are not as readily dissociated

and can lead to increased toxicity, resulting in dramatic reduction in transfection efficiency. Due to this time sensitivity, complexes are typically incubated with cells for a limited time frame (i.e. less than 24 h, typically between 2 and 24 h). However, one of the limiting factors in transfection is the diffusion barrier in the liquid media where particles need to sediment down by gravity to the bottom of the plate in order to bind to the cell surface. The time delay for this process ranges from 2 to 6 h. Due to the time-sensitivity nature of the particles stability, the diffusion barrier may effectively limit transfection efficiency. Methods to overcome this barrier include centrifugation to force the particle onto cell surface or magnetofection, in which magnetized PEI complexes are pulled down by a magnetic field [15].

3.1.9 Cell density

The density of cells during transfection is closely tied in with the polymer and DNA concentrations. If cell density is low, the concentration of polymer would be relatively great compared to transfection in a densely populated cell culture. Many transfection protocols cite a certain number of cells per well as the seeding density. However, it is important to keep in mind that seeding density does not necessary translate into attached cell density; attachment efficiency can vary from batch to batch, depending on culturing conditions, handling processes and age of culture. Thus, in a protocol where cell seeding is recommended 24 h before transfection, it is more critical to check that the cells have reached the desired density for transfection rather than follow a set time-frame for experiment.

3.1.10 Culturing condition

Cell physiology greatly influence transfection efficiency in carrier-assisted gene delivery [6,7,16]. While cell types remain an unchangeable factor in an experimental set up, their metabolic activity and growth rate can be maximized to enhance

transfection. Transfection efficiency is directly correlated to cell cycle; both the S-phase and the M-phase contribute to enhanced transgene expression as a result of elevated global transcriptional activity during DNA synthesis and pDNA nuclear import during transient disassembly of the nuclear envelope [17-19]. Thus, cells should be maintained in a highly active dividing mode to passively enhance transfection efficiency.

Cultures that are grown past the confluent stage generally start to exhibit lower metabolic activity; this slow-down of growth rate can be passed down to subsequent generations and may require a few additional passages before growth rate can resume. We advise sub-culturing cells when density reaches 80% or every 5-7 days to maintain cells in an actively dividing mode. However, cells with high passage number are generally less metabolically active and will eventually go into senescence. Thus, if experiments are not to be performed immediately, freeze cells in a cryogenic vial and store at -80C until needed.

Seeding density can also influence growth rate. Since adherent cells require attachment and presence of cells to some extent for growth (without excessive cell-to-cell contact that impede growth), cells grown at a low starting density (e.g. 20-30%) will grow slower than a culture with higher starting density (50-60%) and will reach the desired transfection density at different rates.

Contamination with mycoplasma can also pose severe challenges to transfection. Periodically monitor cultures for infection using a mycoplasma detection kit. If infection is found, either discard the culture or remove the intracellular microbe using a clean-up kit.

3.1.11 Choice of promoter and reporter gene construct

Regulatory and genetic elements on the plasmid DNA (pDNA) vector can have a significant impact on the level of transgene expression. It is widely observed that promoter activity can vary from cell line to cell line with respect to the amount of protein expressed and the duration of expression [20-24]. Constitutive promoters derived from viruses such as CMV and RSV are most commonly employed for high-level expression. However, viral promoters are subjected to epigenetic silencing over time and thus ubiquitous promoters from non-viral sources such as the human elongation factor 1 α (EF1 α), human polyubiquitin C (UbC), and chicken beta actin [20,22,25] are common alternatives. In our experience, the gWIZ series of vectors (Aldevron), which contain a recombinant CMV IE/Intron A promoter, were significantly more efficient at transfecting cells than the first generation of CMV-based vector such as the pEGFP-N2. Because promoter strength and activity is highly dependent on cell type, we recommend testing a series of expression pDNA under the control of different promoters, in order to optimize the level and duration of transfection that is ideal for your application.

Aside from positive regulatory elements, non-coding sequences found on the pDNA vector can have an inhibitory effect on overall transfection efficiency. Bacterially-derived vector backbone can induce strong innate immune response and lead to the production of proinflammatory cytokines [26-28]. Further, high abundance of unmethylated CpG dinucleotides that are characteristic of the bacterial sequences can induce heterochromatinization, rendering pDNA in a transcriptionally inactive state, and reducing both the level and duration of transgene expression [27-29]. As such, plasmid DNAs devoid of vector backbone, commonly termed minicircle DNA, have been shown to exhibit enhanced transgene expression and transgene persistence [30-32]. Replacement of expression construct with a CpG-depleted minicircle plasmid

DNA may be an option to provide enhanced transgene expression.

3.1.12 Limitations of the protocol

While this protocol optimizes the utility of off-the-shelf cationic polymers, the inherent limitations lie with the polymers and the cell lines. Transfection efficiency is highly dependent on the sizes of the polyplex particles. Polymers with lower binding affinity (e.g., 2 kDa PEI) tended to form less condensed and charged (ζ -potential) complexes, which result in larger particles that are less efficiently taken up in comparison to polymers that can condense pDNA into a more stable and compacted structure (e.g., bPEI25). Cell physiology dictates endocytic uptake pathway, growth rate and sensitivity to the polymer, which are critical factors in determining transfection outcome. That is, cells that take up complexes predominantly through a non-endosomolytic pathway (e.g., CHO and COS7 cell [7]) limit the capacity for PEI complexes to utilize the proton sponge effect to escape the endosome. As well, transfection efficiency is correlated with cell division, and slow dividing cells may limit nuclear import of pDNA for subsequent transgene expression. Further, sensitive cells impose a lower limit on the concentration of the polymer, which equates to lower concentration of pDNA, essentially limiting transfection efficiency.

Another inherent limitation is the duration of transfection, which is expected to be transient. Maximum transgene expression is expected to be between 1 to 3 d after complex addition but will gradually decline thereafter and only remain detectable up to 7 d. A mechanism to replicate and partition the pDNA throughout cell division is required to maintain a minimum intracellular copy number for transcription. Additional genetic elements are also needed for nuclear retention and to maintain the transgene in an open chromatin state for long-term expression. Typical mammalian expression constructs lack these epigenetic elements for transgene persistence and

thus can only provide transient transfection.

It is important to note that while this protocol may provide enhanced transfection utility of bPEI25, there remains a disparity between desired level of transfection and optimal transfection efficiency of the polymer. Desired level of transfection is highly dependent on the types of protein being expressed and the minimum concentration for bioactivity, and may not be achievable, despite optimal conditions. The development of novel biomaterials for gene delivery is an ongoing research area aimed to address this issues and is beyond the scope of this protocol.

3.1.13 Optimization required for NHFF and rat bone marrow and human stromal cells

In this procedure, we provide a step-by-step protocol optimized for the transfection of normal human foreskin fibroblast (NHFF, CRL2522), rat bone marrow stromal cells and human stromal cells using bPEI25 [33]. We note that a similar protocol is available for the transfection of epithelial cells [34]. The major difference between these two protocols lies in the preparation of complexes and the transfection conditions. We found that complexes formed by direct mixing in buffered saline works well in most cases whereas in some cells others have found mixing of two equal volumes of DNA and polymer solution in HEPES to be optimal. We believe that both methods work well, but the optimal method will depend on the cell lines. Transfection in 24-wells or larger format is recommended with the intention of adapting transfection for protein expression and *ex vivo* application, whereas 96-well format may be better suited for high-throughput screening. For transfection, we include a centrifugation step with incubation in the presence of reduced serum media, OPTI-MEM (instead of DMEM), to facilitate cell binding of complexes in a shorter time and to better preserve cell viability in the absence of serum.

While this protocol is written for transfection with pDNA for transgene expression, many of the concepts discussed so far (e.g. volume, buffer, solutes and ratios) can be applied to siRNA delivery as well. This protocol might be beneficial to researchers who are developing novel biomaterials for gene delivery as a guide to ensure carriers are evaluated at the optimal efficiency. Researchers requiring transfection reagent for routine biological studies might also find this guide useful in updating their transfection procedures, or as an alternative to commercial reagents such as Lipofectamine™ 2000, especially considering that bPEI25 provides a cost-effective reagent (>500-times cheaper per 'transfection') as compared to specialty reagents.

3.2 Materials

3.2.1 Reagents

- 📁 Cell line of interest, we use normal human foreskin fibroblast (NHFF, CRL2522), rat bone marrow stromal cells and human stromal cells
- 📁 Basic cell culture growth medium: Dulbecco's modified Eagle's medium DMEM, (low glucose) with L-glut & Na Pyruvate (see REAGENT SETUP)
- 📁 Fetal bovine albumin (Gibco, cat. no. 12483-020)
- 📁 Penicillin-Streptomycin Solution, Liquid 10000 U/ml Penicillin/10000 µg/ml Streptomycin (Invitrogen, cat. no. 15140-122)
- 📁 Trypsin EDTA Solution, 1x Liquid 0.05% Trypsin/0.53 mM EDTA
- 📁 Polyethyleneimine, branched, 25 kDa (Sigma-Aldrich, cat. no. 408727)
- 📁 OPTI-MEM® Reduced Serum Medium (Invitrogen, cat. no. 31985-070)
- 📁 HBS, 150 mM NaCl (see REAGENT SETUP)
- 📁 Hank's balanced salt solution, without Ca²⁺ and Mg²⁺
- 📁 Mammalian expression plasmid containing the reporter gene eGFP under

control of the hybrid CMV IE/Intron A promoter (Aldevron, cat. no. 5006).

3.2.2 Equipment

- 0.22- μ M stericup filtration system (Millipore)
- inverted phase contrast microscope
- 5% CO₂ water-jacketed incubator
- 75 cm² tissue culture flask with gas exchange ventilation cap
- 24-well flat bottom tissue culture treated plates
- 37 °C water bath
- low binding polypropylene microcentrifuge tubes
- 50-ml centrifuge tube with conical bottom (sterile)
- Multi-purpose centrifuge with swing bucket rotor and microplate adaptor rotors (e.g., Eppendorf 5810 or similar with A-4-62 and A-2-DWP rotors)

3.2 Reagent setup

Cell culture medium

DMEM with 100 U/ml of penicillin, 100 μ g/ml of streptomycin supplemented with 10% FBS (heat inactivate FBS at 56°C for 30 min prior to addition to DMEM).

Hepes buffer (20 mM HEPES, pH 7.4)

Make up 1 M stock solution by dissolving 2.383g of HEPES (N'-2-Hydroxyethylpiperazine-N'-2 ethanesulphonic acid) in 100 ml of ddH₂O, adjust to pH 7.4 with KOH. Mix 1 part 1 M HEPES to 49 parts ddH₂O to make the 20 mM HEPES solution. Solutions can be made in advance and store at room temperature (i.e. 21-23 °C).

HBS – Hepes buffered saline (150 mM NaCl, 20 mM HEPES pH 7.4)

Dissolve 0.8766 g of sodium chloride in 100 ml of 20 mM HEPES, pass through a 0.22- μ m filter to sterilize and remove any particulates.

Plasmid DNA solution

Dilute in RNase-free DNase-free water to a final concentration of 0.4 mg/ml DNA solution can be stored in 4 °C fridge for up to one week or in 20 °C freezer for long-term storage.

bPEI25 solution

Dissolve 10 mg of bPEI25 in 10 ml of de-ionized RNase-free, DNase-free water.

CRITICAL STEP

All PEI polymers are sticky viscous sap-like resins; when weighing the polymer, dispense directly into a low-binding polypropylene tube to ensure an accurate amount is weighed. Vortex rigorously and allow the solution to sit at room temperature (i.e. 21-23 °C) for at least 24 h prior to use to ensure complete dissolution. Store at 4 °C.

3.3 Procedure

3.3.1 Revive frozen cell stock for sub-culturing

TIMING - 10-min for seeding, 5-7 d before sub-culturing for transfection

1. Cover an empty sterile 75 cm² flask with 10 ml of pre-warmed cell culture medium. Roll flask gently to ensure even coverage of the bottom surface
 2. Remove frozen cell stock from -80 °C freezer and thaw the cells in 37 °C water bath.
- For the procedure on isolating tissue-derived fibroblast and bone marrow stromal cells, please refer to [35-37].

3. Check the vial every minute, once the vial has thawed, immediately aliquot $\sim 5 \times 10^6$ cells into the tissue culture flask.

CRITICAL STEP

The number of cells seeded into each flask is provided as a guideline since the actual number of cells attached to the surface will vary and depend on the storage, handling conditions, cell freezing medium, cell line, batch and passage number. Generally, an initial seeding density with 30-40% attachment should take about 5-7 days to reach 80-90% confluent.

4. Place flask in 37 °C incubator and allow cells to attach to surface. After 4 h, change medium. (See Table 3.2 for troubleshooting)

5. Return flask to incubator and allow 5-7 d for cells to become confluent. Check cells under the microscope daily to ensure there is an increase in density. Once cells have reached 80% density, proceed to step 6.

CRITICAL STEP

Cells will remain at the tail end of the log-phase at 80-90% confluent. Do not allow cells to grow for longer than 2 weeks as cells will start to die off and/or become senescent with reduced metabolic activity. This could significantly affect transfection efficiency in subsequent passages. Once cell density increases beyond 80%, fibroblasts begin to exhibit an elongated compacted morphology - an indication that they are no longer in the exponential growth phase.

3.3.2 Cell seeding for transfection (24-well plate)

TIMING - 30 to 40-min

6. Once cells are 80-90% confluent, aspirate cell culture medium with a sterile pasteur

pipette, and wash the cells twice with pre-warmed CMF-HBSS (Ca²⁺-free and Mg²⁺-free HBSS with phenol red) for 5 min per wash. (See Table 3.2 for troubleshooting)

CRITICAL STEP

Check to ensure that HBSS does not contain calcium and magnesium. The presence of the cations during the washes will prevent cells from detaching. Two or more washes may be necessary to sufficiently detach the cells. The first wash is to dilute and remove residual serum and traces of divalent cations from the surface; subsequent washes are to equilibrate the cells with the wash buffer.

7. Aspirate CMF-HBSS and detach the cells by adding 5 ml of 1x Liquid 0.05% Trypsin/ 0.53 mM EDTA, swirl to ensure even coverage across the flask surface. Leave in room temperature and let sit for 2 min.

8. After about 2 min contact with trypsin, gently tap the sides of the flask to agitate and loosen cells from the surface. (See Table 3.2 for troubleshooting)

CRITICAL STEP

Allow sufficient time for trypsin to equilibrate before tapping. Excess agitation may cause cells to aggregate, leading to patches of cells in each well after seeding. The ease at which cells can be detached with trypsin is dependent on the adhesion property of the cell and its sensitivity to trypsin, which vary among cell types. While detachment with trypsin can be enhanced by incubation at 37 °C, extending the incubation time (2 - 10 min), or using a more concentrated trypsin (0.25%), these changes may also increase the risk of cell damage. Detachment with a cell scraper or a cell lifter is NOT recommended.

9. Once cells have detached, stop trypsin activity by adding cell culture medium (FBS

contains trypsin inhibitor).

10. Transfer cell suspension into a 50 ml conical tube and pellet the cells by centrifugation at 600 rpm (72 x *g*) for 5 min

11. Following centrifugation, a cell pellet should be visible at the bottom of the tube. Aspirate the supernatant, being careful not to disturb the cell pellet.

12. Suspend cells in 48 ml of cell culture medium (1:4 split).

CRITICAL STEP

The re-suspension volume will depend on the split ratio or the desired seeding density. Typically, a 80% confluent flask is split 1:4 to obtain the ideal density of 40-50% confluence per-well for transfection. If the cell suspension requires dilution beyond this split ratio, it may be an indication that cells are overgrown.

13. Aliquot 500 µl of the suspended cells or approximately $60 - 70 \times 10^3$ cells into each well of the 24-well plate.

14. Gently shake the plate to ensure cells are uniformly distributed throughout the well surface. (See Table 3.2 for troubleshooting)

15. Place the seeded plates back in the incubator. Check under the microscope every 5 min to ensure cells are evenly distributed across the well.

CRITICAL STEP

Prior to attachment, cells tend to aggregate towards the center of the well. Visualize under a phase contrast microscope at low magnification (2.5x) and ensure cells are evenly distributed by gently shaking the plate. Cells will begin to attach once plate temperature has equilibrated back to 37 °C (or about 10 min after plate is placed back in the incubator), so check the plate for aggregation every 5 min prior. If not distributed evenly, cells concentrate at higher density in the center, creating a

topographical density gradient that can significantly affect reproducibility.

16. Check the cells under a microscope after 24 h, if the cells are at 40-50% density, proceed to transfection. If not, wait for an additional 1 - 2 d before transfection.

(See Table 3.2 for troubleshooting)

CRITICAL STEP

We emphasize the splitting ratio as a starting cell density over a particular number of cells since the latter does not always correlate to the number of cells attached to the surface. Attachment efficiency is highly dependent on the growth rate, passage number, and handling during the trypsin stage.

Table 3.1 Volume of individual components in transfection solution

Number expressed as μL per well

Components	48-well	24-well	12-well	6-well
150 mM NaCl	not recommended	45	90	180
pDNA (0.4 mg/ml)		2.5	5	10
bPEI (1 mg/ml)		2.5	5	10
OPTI-MEM (1% FBS)		450	900	1800

3.3.3 Preparation of bPEI25/pDNA polyplexes for transfection

TIMING 30-min

17. Make transfection complexes. Transfection efficiency among cell lines may be dependent on complexation methods. We provide two methods below – direct mixing in buffered saline (option A), and two-part mixing in salt-free buffer (option B). Both may need to be tested to determine the optimal condition. The following volumes and concentrations have been described for transfection per well in a 24-well plate. Maintain the same relative proportions when dispensing in replicates. Adjust the volume accordingly for 12- and 6-well plates (**Table 3.1**). Transfection in 48-well

plates is not recommended as the small volume generally results in unstable aggregates that can lead to sporadic toxicity.

CRITICAL STEP

The volume and incubation time listed in both (A) and (B) has been optimized for the concentrations of pDNA and polymer. If cells can withstand a higher concentration of polymer, then both the incubation time and volume may need to be adjusted proportionally to ensure stable complexes are formed.

CRITICAL STEP

We recommend transfecting in the absence of any antibiotics. Cell viability and membrane integrity may be compromised during interaction with polyplex and polymer, which may cause antibiotics to leak into the cell. While data on this for polyfection is limited, antibiotics had been shown to reduce transfection and increase cell death in lipofection [38].

(A) Direct mixing with buffered saline

- I. In 45 μ l of buffered saline (150 mM NaCl, 20 mM HEPES, pH 7.4) add 2.5 μ l of pDNA (0.4 mg/ml), mix and allow pDNA to equilibrate for 5 minutes at room temperature. (The final pDNA concentration per well in this set-up is 2 μ g/ml)

CRITICAL STEP

bPEI25 may precipitate out of solution during cold storage; allow all components to equilibrate to room temperature before proceeding with the preparation of complexes.

CRITICAL STEP

bPEI25 may bind to tube side walls [39] effectively lowering the concentration of the polymer upon prolonged storage; be sure to use low-binding polypropylene tubes in all steps.

- II. Add 2.5 μ l of bPEI25 (1 mg/ml) to the diluted DNA solution slowly, in a drop-wise fashion. The polymer-to-DNA weight ratio is 2.5, and the final polymer concentration per well is 5 μ g/ml.

CRITICAL STEP

It is critical that the sequence of addition is followed exactly as described. (i.e., aliquot buffered solution, add DNA to the solution, and then add PEI to mix). The volume of the initial polyplex solution should be at least 1/10 of the final transfection solution.

- III. Mix the solution by vortex for 5 sec, allow solution to sit at room temperature for 10 min.
- IV. Dilute the polyplex solution in 450 μ l of pre-warmed OPTI-MEM supplemented with 1% FBS. Let solution sit at room temperature for an additional 10 minutes.

CRITICAL STEP

The addition of 1% FBS here has been shown to enhance transfection efficiency in BMSC (**Figure 3.8** and **Figure 3.9**). If transfection is carried out on other primary cell line, the effect of low amounts of serum should be empirically determined first.

(B) Two-part mixing with salt-free buffer

- i. In 47.5 μ l of HEPES-buffer (20 mM HEPES, pH 7.4), add 2.5 μ l of pDNA (0.4 mg/ml). Mix, and allow pDNA to equilibrate for 5 minutes at room temperature.

(The final pDNA concentration per well in this set-up is 2 µg/ml)

- ii. In 47.5 µl of (HBS/HBG or Hepes-buffer) add 2.5 µl bPEI25 (1 mg/ml), pulse vortex to mix briefly. Let it sit for 5 min. The final polymer concentration per well is 5 µg/ml.
- iii. Form complex by adding the 50 µl of the diluted DNA solution in i) to the 50 µl of diluted polymer solution in ii), mix by vortexing for 5 sec.
- iv. Incubate at room temperature for 25 min.
- v. Dilute the polyplex solution in 400 µl of pre-warmed OPTI-MEM. Let solution sit at room temperature for an additional 5 min.

CRITICAL STEP

The final concentration of polymer listed above is 5 µg/ml, which may or may not be ideal every cell line. If cell viability is significantly reduced at this concentration (<60%), lower the amount of polymer, but maintain the same polymer-to-DNA weight ratio.

CRITICAL STEP

The polymer-to-DNA weight ratio listed above is 2.5, which we have found to work well for both fibroblast and bone marrow cells. However, the optimal weight ratio for other cell line may be different and need to be empirically determined by transfection with complexes formed at various weight ratios (i.e. weight ratios of 1.25, 2.5, 5, and 10, or NP range from 10-80). The upper limit to this range is effectively determined by toxicity of the polymer and sensitivity of the cells to the polymer.

18. Aspirate cell culture medium from each well and add the entire 500 µl of diluted polyplex transfection mixture to the cells directly. **(See Table 3.2 for troubleshooting)**

CRITICAL STEP

Steps 17 to 18 should not exceed 30 minutes.

19. Gently agitate the plates and allow the complexes to equilibrate for 5 min in the incubator

20. Force complexes onto cell surface, at the bottom of the plate, by centrifugation at $210 \times g$ for 5 min in a microplate adaptor rotor. Set acceleration and braking to 1.

(See Table 3.2 for troubleshooting)

CRITICAL STEP

Ensure plates are properly balanced before loading into the centrifuge. Some cells may be sensitive to sudden and excessive force, thus, gentle acceleration and deceleration is recommended to minimize *g*-force shock.

22. Gently remove plates from the centrifuge, being careful not to disturb the medium and return the plates to a 37°C incubator.

23. After 4 - 6 h, remove the transfection mixture by aspiration and replace with cell culture medium. If desired wash cells twice with cell culture medium to sufficiently remove complexes. (See Table 3.2 for troubleshooting)

CRITICAL STEP

The incubation time can vary between 2 and 8 h. Centrifugation forces complexes to the bottom of the plate, and onto the cell surface, thus, as little as 1 h can be allotted for transfection. If cells begin to exhibit toxicity after 2 h, remove complexes and replace with culture medium. It is not recommended to leave complexes in for more than 16 h as complexes will destabilize and aggregate, resulting in toxicity with lowered transfection efficiency (**Figure 3.4**).

3.4 Analysis of GFP Expression by FACS

23. After 24 – 48 h, quantify eGFP expression for transfection efficiency by FACS analysis. (See Table 3.2 for troubleshooting)
24. Aspirate culture medium from cells. Wash cells 3x with 500 μ l of clear CMF-HBSS.
25. Detach cells by adding 100 μ l of clear Trypsin/EDTA (0.05%, without phenol red) to each well
26. Allow trypsin to equilibrate across well surface for 2 min, then agitate loosely attached cells by tapping on all four sides of the plate. Visualize under microscope to monitor extent of detachment.
27. Once cells have detached from the surface, stop the trypsin activity and fix the cells by adding 100 - 150 μ l of 3.7% formalin in HBSS.
28. Analyze the cells on a flow cytometer. Excite GFP with an argon laser (488 nm) and detect in FL1 channel. Adjust voltage such that the distribution peak is between 10^0 and 10^1 .

PAUSE POINT: If samples are not to be assayed immediately, store the fixed cells in 4 $^{\circ}$ C fridge. Fixed cells may be stored for up to 1 week. Prolonged storage in the presence of formaldehyde is not recommended.

CRITICAL STEP

Be sure to set up a negative control by transfecting cells with a plasmid DNA that does not contain GFP (null). Toxicity can induce autofluorescence and result in overestimation of transfection efficiency.

TIMING

Step 1-5, Revive frozen cells cell stock for sub-culturing: 5-7 d

Step 6-16, Cell seeding for transfection: 30-40 min for seeding plus 1-2 d until cells are ready for transfection

Step 17-23, Preparation of bPEI25/pDNA polyplexes for transfection: 30 min, plus 1-2 d to allow reporter gene expression.

Step 24-28, FACS Analysis of GFP expression: 20 min to detach cells into suspension, plus 1-4 h to run samples through cytometer, depending on the number of samples.

Table 3.2 Transfection protocol troubleshooting table

Step	Problem	Possible reason	Possible solution
4, 14	cells are not attaching to surface	plate surface not conducive to attachment	make sure plates are tissue-culture treated. Alternatively, try plates treated with poly-L-lysine
	low percentage of cell attachment	prolonged handling of cells outside the incubator cells are thawed for too long	reduce the batch sizes to be workable within 30 min from start to finish equilibrate the surface of the culture substrate with cell culture medium for 2 - 4 h
8	Cells are difficult to detach	insufficient washing	Ensure wash buffer is free of divalent cations. Perform additional washes and extend wash time.
		wash buffer contains divalent cations	
		strongly adhering cells	Increase the strength of trypsin from 0.05% to 0.25% incubate at 37 °C for 2-5 minutes flush cells by GENTLY pipetting up and down
14	Cells aggregate in center of well	Failure to distribute cells evenly across the surface	monitor attachment closely by examining under the microscope. Agitate the plate frequently (every 5 min) to dislodge cells from collecting at the center of the well.
	cells aggregate in patches	cell damaged during treatment with trypsin	shorten the duration of trypsin treatment. dilute trypsin with HBSS Tap on all sides of the flask GENTLY. If unable to detach cells completely, it is best to minimize exposure to trypsin and seed healthy cells, albeit at lower density, than to have a higher density with patches of aggregated cells.

16	cells are slow growing	seeding density too low	cell-to-cell contact is required for efficient growth. If initial seeding density falls below 20%, growth rate may be compromised. Try lowering the split ratio to increase cell concentration.
19, 23	toxicity after exposure to complexes	complexes aggregate concentration of polymer too high complexes have destabilized	monitor the complex preparation time during each step closely. The time between step 16 and step 19 must not exceed 30 min. perform optimization by testing various concentration of polymer (as a function of NP ratio) to determine an acceptable range reduce incubation time with complexes toxicity is a function of cell density and polymer concentration. Try transfecting at a higher cell density supplement transfection media with 1% FBS
21	toxicity	centrifugation speed too high centrifugation not balanced pDNA is immunogenic	cells may be sensitive to excessive force Balance the centrifuge Reduce centrifugation force down to the 120 <i>g</i> - 180 <i>g</i> range. Typical mammalian expression plasmids contain unmethylated CpG dinucleotides, which are known to induce the innate immune response via TLR9 receptors. Try using a minicircle pDNA devoid of the bacterially derived sequences.
24	low transfection	cells are high passage	For fibroblasts, passages higher than 40 are less metabolically active and would start becoming senescent. Obtain a new batch of cells with a lower passage number.

	cells are slow dividing	previous passage may be overgrown. Sub-culture cells for another passage to re-establish log-phase growth
loss of transgene expression over time	pDNA lack replication and partitioning elements for maintenance in mammalian cells	try different vector constructs such as the pEPI-1, which contains S/MAR sequence. Replace expression vector with a minicircle DNA devoid of bacterial derived sequences.

3.4 Typical results

Two of the most critical parameters in complex formation that can be easily manipulated are volume of solution and incubation time for complexes. Smaller volume favors more frequent intermolecular interactions, effectively reducing the maturation time for complex formation – this may also accelerate the formation of aggregates, reducing overall transfection. A positive correlation can be seen between complexation volume and transfection efficiency in **Figure 3.2**. If toxicity is observed after complexes have been added to the cell, this could be the result of either destabilization of complexes/aggregates or excessively high dose of polymer. Resolve the first issue first by increasing the complexation volume or shortening the incubation time before attempting to lower the polymer concentration or the polymer-to-DNA weight ratio as the former effort will be more effective in optimizing transfection efficiency. Since time is a critical factor in the maturation and stability of complexes, assembled complexes left sitting for more than 30 min will gradually lose transfection efficiency.

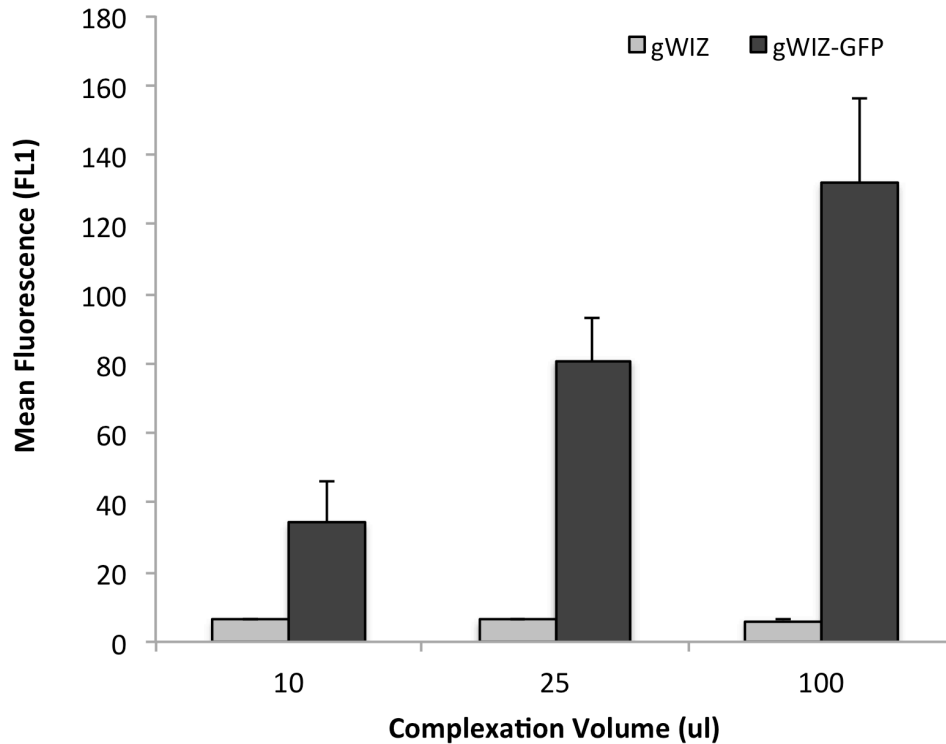


Figure 3.2

Effect of complexation volume on transfection efficiency.

Results were obtained from the transfection of NHFF in 12-well tissue culture plates where final transfection volume is 1000 μ l (complexes + media). gWIZ and gWIZ-GFP refer to complexes with a control (non-GFP expressing) plasmid and an eGFP expressing pDNA, respectively. A positive correlation can be seen between transgene expression (mean eGFP fluorescence) and volume of complexes. Results are mean \pm SD and is representative of two different experiments done in triplicates.

The optimal polymer-to-DNA ratio for transfection will be an equilibrium between protection, condensation, dissociation, and toxicity (for practical purpose, we refer the ratio in terms of weight of polymer-to-DNA). As described earlier in the introduction, the optimal ratio of polymer-to-DNA for transfection will be in excess of the ratio at which full condensation occurs. The presence of unbound free polymer is essential to overcome the inhibitory effect of cell-surface GAG. However, too much free polymer may lead to additional toxicity, to reduced uptake and transfection efficiency. **Figure 3.3** shows transfection of fibroblasts at different polymer-to-DNA weight ratio. The weight ratio of 2.5 (effectively NP ratio of \sim 19) is optimal for transfection in fibroblasts.

At a weight ratio of 5, the level of transgene expression is significantly reduced.

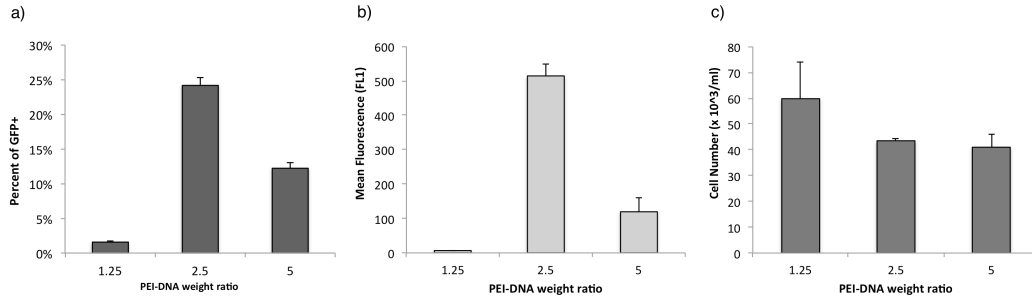


Figure 3.3

Effect of PEI-to-pDNA weight ratios used in complex formation on transfection efficiency.

Results show transfection of NHFF with bPEI25 complexes in a 24-well plate format. Transfection results are assayed by flow cytometry for eGFP expression and are summarized as the GFP-positive cell population (a) and mean GFP fluorescence per cell (b). At the final pDNA concentration of 2 $\mu\text{g}/\text{ml}$, the polymer-to-DNA weight ratio of 2.5 (approximate NP ratio of 19.4) was most efficient. Results are mean \pm SD from five different experiments done in triplicates.

Once complexes are added to the cells grown in aqueous media, a set incubation time is required to allow the complexes to settle down onto the bottom of the plate by gravity. **Figure 3.4** shows the level of transgene expression as a function of incubation time. Without centrifugation (0 g), transfection increases with incubation time and peaks at 6 h, but the mean eGFP fluorescence never reached the level achieved by centrifugation (210 g). Further, transfection efficiencies after centrifugation were comparable between 1 h and 6 h of incubation, suggesting the majority of the complexes have been effectively spun onto the cell surface. In short, transfection can be performed in as little as 1 h. Longer incubation (24 h) significantly reduced transfection efficiency presumably as a result of toxicity and loss of utility from the destabilized aggregates of complexes. Thus, centrifugation is a simple and easily

accessible step that works analogously to magnetofection in forcing the complexes onto cell surface quickly, bypassing the diffusion barrier to minimize the incubation time.

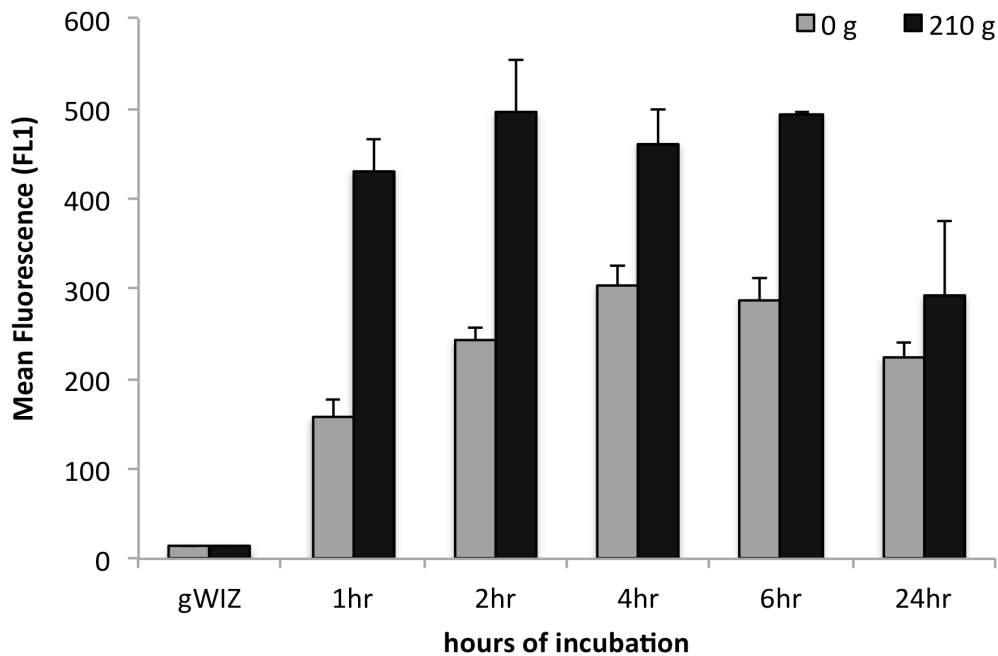


Figure 3.4

Effect of centrifugation and incubation time on transfection efficiency.

Results (mean eGFP fluorescence per cell from flow cytometry) are shown for transfection of NHFF with bPEI25 complexes in 24-well format. The control gWIZ polyplex is incubated for 6 h, whereas the gWIZ-GFP complexes were incubated for the indicated time periods. The cells were either incubated without centrifugation (0 x g) or with centrifugation (210 x g). The mean eGFP fluorescence of cells increased with incubation time in the absence of centrifugation. With centrifugation, the mean eGFP fluorescence was significantly higher across all incubation time frame with comparable levels from 1 h to 6 h, suggesting the majority of the complexes are effectively spun down onto the cell surface. Incubation with the complexes for 24 h dramatically reduced transfection efficiency, presumably due to toxicity from destabilized complex aggregates. Results are mean \pm SD and is representative of four different experiments done in triplicates.

Complex preparation using the direct mixing method in buffered saline followed by incubation in OPTI-MEM (with brief centrifugation) seemed to be the best method for transfection of NHFF and BMSC. We compared the updated procedure we have outlined here (HBS-OPTI) to some of the most common complex preparation methods in the literature [3,5,8,11,36,40], which involve either a) preparing complexes in a salt-free buffer by mixing two equal parts of diluted DNA and polymer (Buffer 2-part) or b) preparing complexes in buffered saline by mixing DNA and polymer in one volume (HBS Direct), then adding to the cell in DMEM, and incubating for 4 h. **Figure 3.5** and **Figure 3.6** shows transfection of NHFF with the 2 kDa bPEI (weight ratio of 10) and bPEI25 (weight ratio of 2.5) using the different complex preparation methods. In general, bPEI complexes prepared in salt-free buffer appeared to be better for transfection in NHFF. Transfection with PEI2 was significantly improved by the HBS-OPTI method (**Figure 3.5**). The presence of 1% serum was inhibitory to transfection. The use of OPTI-MEM in place of DMEM significantly preserved cell viability. Transfection of rat BMSC and human BMSC (**Figure 3.7** and **Figure 3.8**) however, seemed to exhibit a different trend. While complexes prepared in salt-free or saline buffer both yield transfection, mixing diluted DNA and polymer from two equal parts (2-part) appears to be ineffective in comparison to direct mixing in one volume (direct). As well, the addition of 1% FBS not only facilitated greater reporter gene expression, but also preserved cell viability. Overall, the HBS-OPTI method as outlined here seemed to provide the optimal procedure for transfection in both primary cell lines.

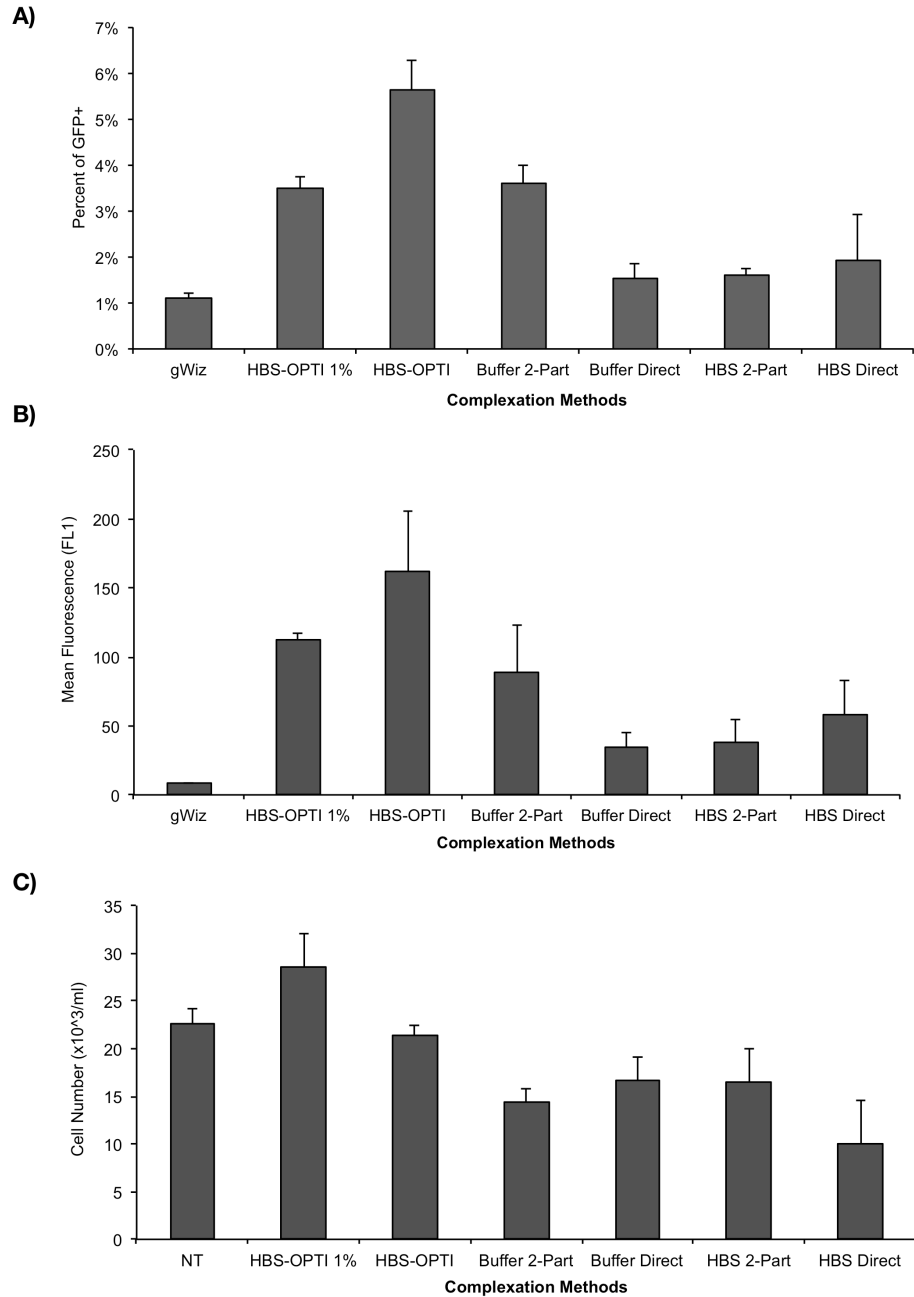


Figure 3.5

Comparison of transfection efficiency of PEI2 in NHFF using complexation methods outlined in this protocol and other conventional methods.

Cells are transfected as outlined in this protocol with or without serum (HBS-OPTI 1%; HBS-OPTI) or by conventional methods in which complexes are prepared by either mixing equal volumes of DNA and polymer (2-part) or by direct mixing of DNA and polymer in one volume (direct) in either salt-free buffer (buffer) or buffered saline (HBS), follow by transfection in DMEM for 4 h. Figure shows a) percent of GFP- positive cells, b) the mean fluorescence of the total cell population and c) cell number (viability). PEI2 prepared with the HBS-OPTI method was optimal for transfection.

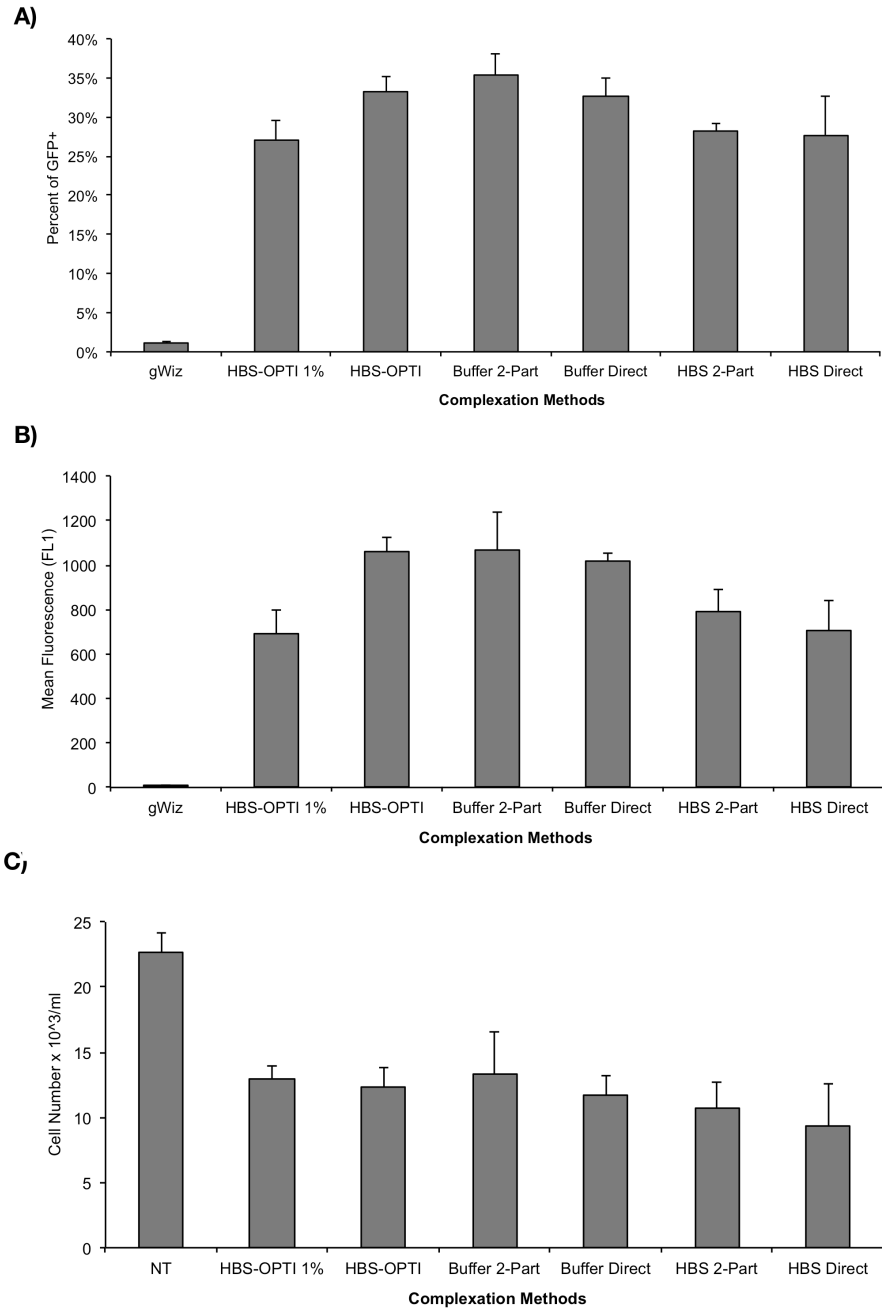


Figure 3.6
Comparison of transfection efficiency of bPEI25 in NHFF using complexation methods outlined in this protocol and other conventional methods.

Cells are transfected as outlined in this protocol with or without serum (HBS-OPTI 1%; HBS-OPTI) or by conventional methods in which complexes are prepared by either mixing equal volumes of DNA and polymer (2-part) or by direct mixing of DNA and polymer in one volume (direct) in either salt-free buffer (buffer) or buffered saline (HBS), follow by transfection in DMEM for 4 h. bPEI25 complexes prepared in salt-free buffer were more efficient for transfection. Figure shows a) percent of GFP-positive cells, b) the mean fluorescence of the total cell population and c) cell number (viability). Low amounts of serum (1%) in this case reduced transfection efficiency.

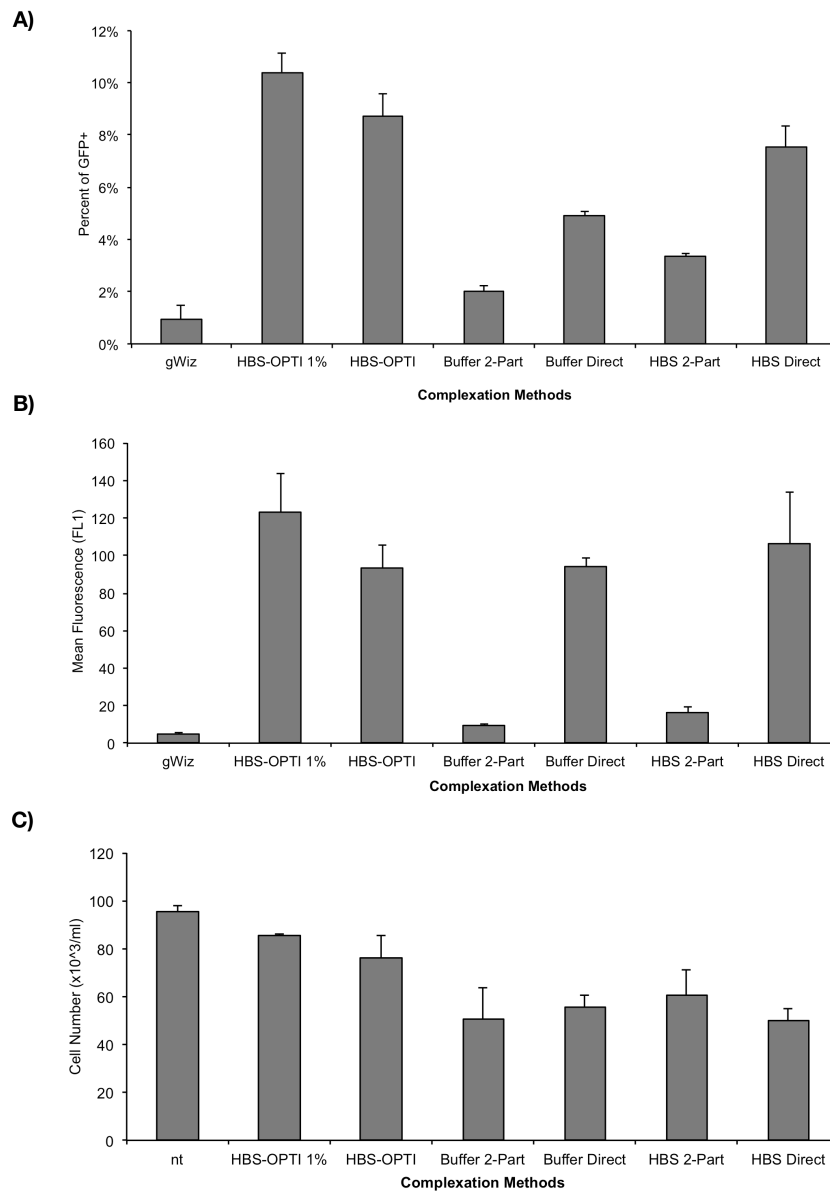


Figure 3.7

Comparison of transfection efficiency of bPEI25 in rBMSC using complexation methods outlined in this protocol and other conventional methods.

Cells are transfected as outlined in this protocol with or without serum (HBS-OPTI 1%; HBS-OPTI) or by conventional methods in which complexes are prepared by either mixing equal volumes of DNA and polymer (2-part) or by direct mixing of DNA and polymer in one volume (direct) in either salt-free buffer (buffer) or buffered saline (HBS), follow by transfection in DMEM for 4 h. Figure show a) percent of GFP-positive cells, b) the mean fluorescence of the total cell population and c) cell number (viability). Complexes prepared by mixing DNA and polymer from two equal parts was ineffective for transfection. The HBS-OPTI method adapted from the conventional methods was a significant improvement. The presence of 1% FBS in this case not only improved overall transfection efficiency, it also preserved cell viability.

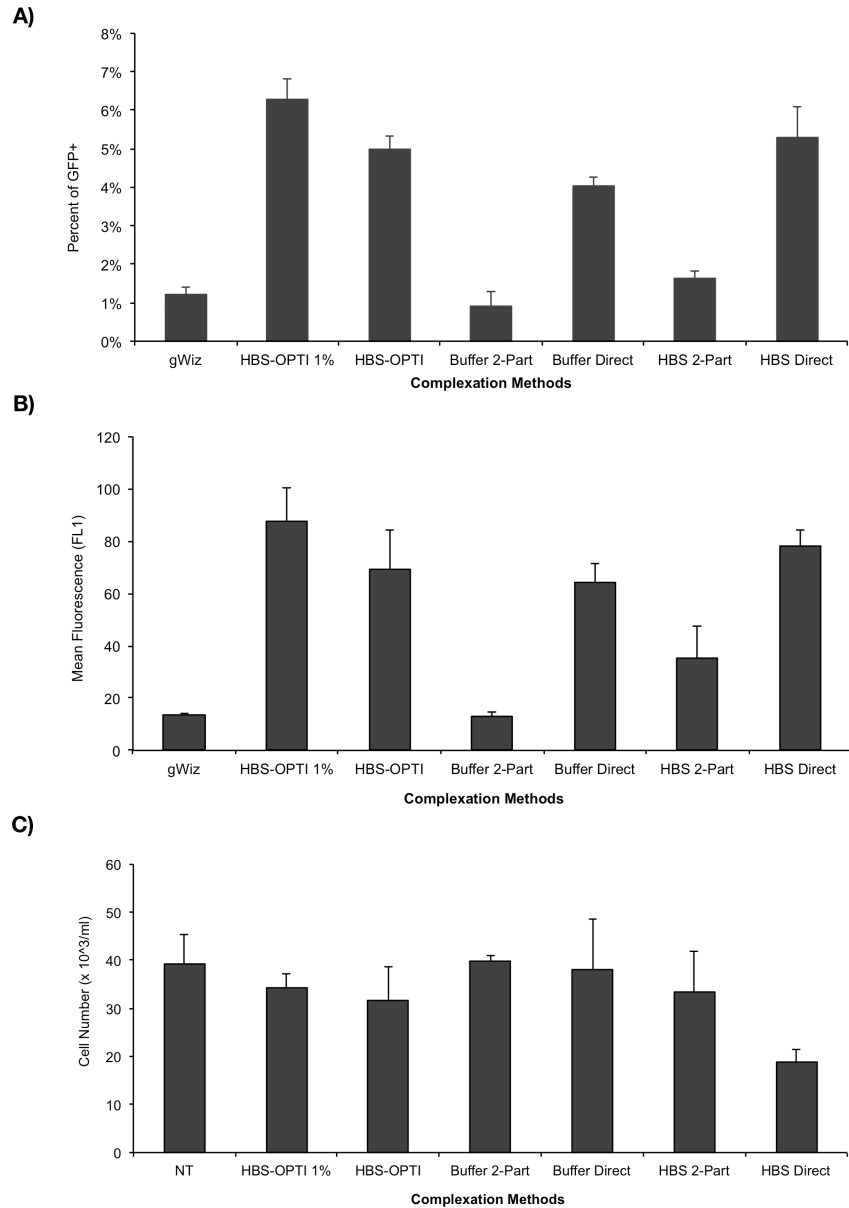


Figure 3.8

Comparison of transfection efficiency of bPEI25 in hBMSC using complexation methods outlined in this protocol and other conventional methods.

Cells are transfected as outlined in this protocol with or without serum (HBS-OPTI 1%; HBS-OPTI) or by conventional methods in which complexes are prepared by either mixing equal volumes of DNA and polymer (2-part) or by direct mixing of DNA and polymer in one volume (direct) in either salt-free buffer (buffer) or buffered saline (HBS), follow by transfection in DMEM for 4 h. Figure shows a) percent of GFP- positive cells, b) the mean fluorescence of the total cell population and c) cell number (viability). Similar to results obtained in rat BMSC, mixing complexes from two equal parts were generally less effective for transfection. In contrast, complexes prepared by direct mixing was much more conducive for transfection. The HBS-OPTI method outlined here was a significant improvement over conventional methods in both percent of GFP positive cells, the mean fluorescence of eGFP expression and cell number (viability).

Typical transfection efficiency in NHFF using the method outlined here is around 30-35%, but can range from 13% to 60%. The lower end of the spectrum is typically the result of slow growing cells, either due to low starting density, aging culture, or high passage. Typical transfection for bone marrow ranges from 8-12%, and up to 20% can be achieved with optimal culturing conditions.

Finally, we compared the relative transfection efficiencies of bPEI25, using the optimal protocol described here, to Lipofectamine-2000™ (LFN2000). **Figure 3.9 and Figure 3.10** shows transfection in NHFF and rat BMSC. Under optimized condition, bPEI25 can transfect up to 60% NHFF cells, which is comparable to transfection obtained by LFN2000 (~51%). In rat BMSC, the percent of GFP-expressing cells was comparable between bPEI25 and LFN2000 (15% vs 20%) but the mean fluorescence obtained by LFN2000 was significantly higher. However, this may be the result of high toxicity from LFN2000, which has a significantly lower percentage of viable cells, resulting in averaging of a smaller population of remaining cells. In summary, the utility of bPEI25 as a transfection agent can be enhanced by updating transfection methods with the optimization procedures outlined here, providing an inexpensive alternative to commercial reagent commonly employed as a method to genetically manipulate the physiology of cultured cells.

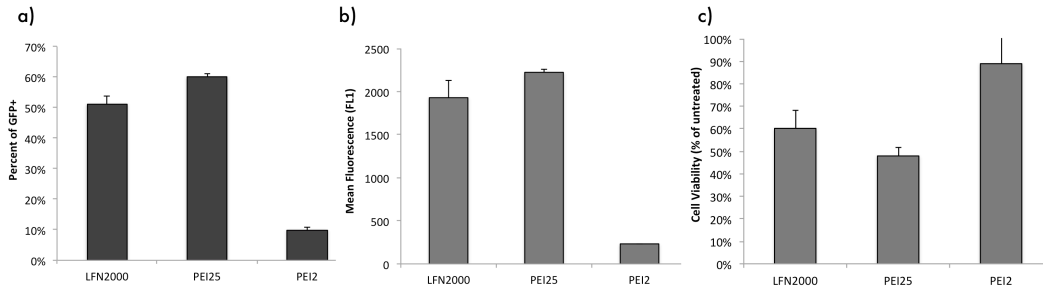


Figure 3.9

Comparison of transfection efficiency between bPEI25, PEI2 and Lipofectamine-2000™ in NHFF.

Figure shows a) percent of GFP-positive cells, b) the mean fluorescence of the total cell population and c) cell number (viability). Using methods outlined in this protocol to prepared bPEI25 complexes, transfection efficiency comparable to Lipofectamine-2000™ (LFN2000) can be achieved. PEI2 is presented for comparison as a relatively ineffective carrier. Despite its low efficiency, about 10% transfection efficiency can still be achieved using methods outlined here. Transfection with LFN2000 is carried out according to manufacturer's protocol.

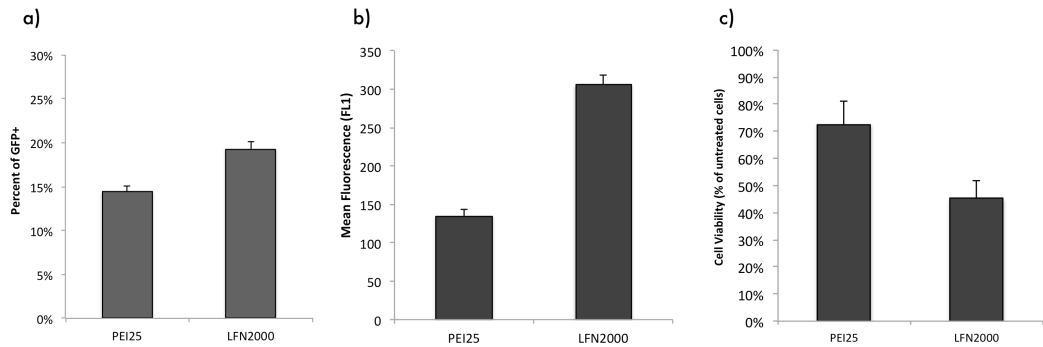


Figure 3.10

Comparison of transfection efficiency between bPEI25 and Lipofectamine-2000™ in rat bone marrow stromal cells.

Figure shows a) percent of GFP-positive cells, b) the mean fluorescence of the total cell population and c) cell number (viability). Using methods outlined in this protocol to prepared complexes, bPEI25 achieved comparable percentage of GFP positive cells to that obtained by LFN2000 (15% vs 20%). The mean eGFP fluorescence was significantly higher with LFN2000 transfected cells ($p < 0.05$). However, LFN2000 was significantly more toxic in rat BMSC than bPEI25 and the higher mean fluorescence may be a result of averaging values from a smaller population of viable cells.

3.5 References

- [1] Godbey W. T., Wu K. K., and Mikos A. G., 1999, "Poly(ethylenimine) and its role in gene delivery," *J Control Release*, **60**(2-3), pp. 149–160.
- [2] Akinc A., Thomas M., Klivanov A. M., and Langer R., 2005, "Exploring polyethylenimine-mediated DNA transfection and the proton sponge hypothesis," *J Gene Med*, **7**(5), pp. 657–663.
- [3] Wightman L., Kircheis R., Rössler V., Carotta S., Ruzicka R., Kursa M., and Wagner E., 2001, "Different behavior of branched and linear polyethylenimine for gene delivery in vitro and in vivo," *J Gene Med*, **3**(4), pp. 362–372.
- [4] Rejman J., Oberle V., Zuhorn I. S., and Hoekstra D., 2004, "Size-dependent internalization of particles via the pathways of clathrin- and caveolae-mediated endocytosis," *Biochem J*, **377**(Pt 1), pp. 159–169.
- [5] Gersdorff von K., Sanders N. N., Vandenbroucke R., De Smedt S. C., Wagner E., and Ogris M., 2006, "The internalization route resulting in successful gene expression depends on both cell line and polyethylenimine polyplex type," *Mol Ther*, **14**(5), pp. 745–753.
- [6] Izumisawa T., Hattori Y., Date M., Toma K., and Maitani Y., 2011, "Cell line-dependent internalization pathways determine DNA transfection efficiency of decaarginine-PEG-lipid," *Int J Pharm*, **404**(1-2), pp. 264–270.
- [7] Douglas K. L., Piccirillo C. A., and Tabrizian M., 2008, "Cell line-dependent internalization pathways and intracellular trafficking determine transfection efficiency of nanoparticle vectors," *Eur J Pharm Biopharm*, **68**(3), pp. 676–687.
- [8] Yue Y., Jin F., Deng R., Cai J., Chen Y., Lin M. C. M., Kung H.-F., and Wu C., 2011, "Revisit complexation between DNA and polyethylenimine - Effect of uncomplexed chains free in the solution mixture on gene transfection," *J Control Release*, **155**(1), pp. 67–76.
- [9] Deng R., Yue Y., Jin F., Chen Y., Kung H.-F., Lin M. C. M., and Wu C., 2009, "Revisit the complexation of PEI and DNA - how to make low cytotoxic and highly efficient PEI gene transfection non-viral vectors with a controllable chain

length and structure?," *J Control Release*, **140**(1), pp. 40–46.

- [10] Hanzlíková M., Ruponen M., Galli E., Raasmaja A., Aseyev V., Tenhu H., Urtti A., and Yliperttula M., 2011, "Mechanisms of polyethylenimine-mediated DNA delivery: free carrier helps to overcome the barrier of cell-surface glycosaminoglycans.," *J Gene Med*, **13**(7-8), pp. 402–409.
- [11] Liu Z., Zheng M., Meng F., and Zhong Z., 2011, "Non-viral gene transfection in vitro using endosomal pH-sensitive reversibly hydrophobilized polyethylenimine.," *Biomaterials*, **32**(34), pp. 9109–9119.
- [12] Neamark A., Suwantong O., Bahadur R. K. C., Hsu C. Y. M., Supaphol P., and Uludağ H., 2009, "Aliphatic lipid substitution on 2 kDa polyethylenimine improves plasmid delivery and transgene expression.," *Mol Pharm*, **6**(6), pp. 1798–1815.
- [13] Luo X.-H., Huang F.-W., Qin S.-Y., Wang H.-F., Feng J., Zhang X.-Z., and Zhuo R.-X., 2011, "A strategy to improve serum-tolerant transfection activity of polycation vectors by surface hydroxylation.," *Biomaterials*, **32**(36), pp. 9925–9939.
- [14] Ikonen M., Murtomäki L., and Kontturi K., 2008, "Controlled complexation of plasmid DNA with cationic polymers: effect of surfactant on the complexation and stability of the complexes.," *Colloids and Surfaces B: Biointerfaces*, **66**(1), pp. 77–83.
- [15] Mykhaylyk O., Antequera Y. S., Vlaskou D., and Plank C., 2007, "Generation of magnetic nonviral gene transfer agents and magnetofection in vitro.," *Nat Protoc*, **2**(10), pp. 2391–2411.
- [16] Laurie K. L., Blundell M. P., Baxendale H. E., Howe S. J., Sinclair J., Qasim W., Brunsberg U., Thrasher A. J., Holmdahl R., and Gustafsson K., 2007, "Cell-specific and efficient expression in mouse and human B cells by a novel hybrid immunoglobulin promoter in a lentiviral vector.," *Gene Ther*, **14**(23), pp. 1623–1631.
- [17] Brunner S., Sauer T., Carotta S., Cotten M., Saltik M., and Wagner E., 2000, "Cell cycle dependence of gene transfer by lipoplex, polyplex and recombinant adenovirus.," *Gene Ther*, **7**(5), pp. 401–407.

- [18] Akita H., Ito R., Kamiya H., Kogure K., and Harashima H., 2007, "Cell cycle dependent transcription, a determinant factor of heterogeneity in cationic lipid-mediated transgene expression.," *J Gene Med*, **9**(3), pp. 197–207.
- [19] Männistö M., Rönkkö S., Mättö M., Honkakoski P., Hyttinen M., Pelkonen J., and Urtti A., 2005, "The role of cell cycle on polyplex-mediated gene transfer into a retinal pigment epithelial cell line.," *J Gene Med*, **7**(4), pp. 466–476.
- [20] Walther W., and Stein U., 1996, "Cell type specific and inducible promoters for vectors in gene therapy as an approach for cell targeting.," *J. Mol. Med.*, **74**(7), pp. 379–392.
- [21] Londrigan S. L., Brady J. L., Sutherland R. M., Hawthorne W. J., Thomas H. E., Jhala G., Cowan P. J., Kay T. W. H., O'Connell P. J., and Lew A. M., 2007, "Evaluation of promoters for driving efficient transgene expression in neonatal porcine islets.," *Xenotransplantation*, **14**(2), pp. 119–125.
- [22] Nguyen A. T., Dow A. C., Kupiec-Weglinski J., Busuttill R. W., and Lipshutz G. S., 2008, "Evaluation of gene promoters for liver expression by hydrodynamic gene transfer.," *J. Surg. Res.*, **148**(1), pp. 60–66.
- [23] Zheng C., and Baum B. J., 2005, "Evaluation of viral and mammalian promoters for use in gene delivery to salivary glands.," *Mol Ther*, **12**(3), pp. 528–536.
- [24] Al-Dosari M., Zhang G., Knapp J. E., and Liu D., 2006, "Evaluation of viral and mammalian promoters for driving transgene expression in mouse liver.," *Biochem Biophys Res Commun*, **339**(2), pp. 673–678.
- [25] Pringle I. A., McLachlan G., Collie D. D. S., Sumner-Jones S. G., Lawton A. E., Tennant P., Baker A., Gordon C., Blundell R., Varathalingam A., Davies L. A., Schmid R. A., Cheng S. H., Porteous D. J., Gill D. R., and Hyde S. C., 2007, "Electroporation enhances reporter gene expression following delivery of naked plasmid DNA to the lung.," *J Gene Med*, **9**(5), pp. 369–380.
- [26] Zhao H., Hemmi H., Akira S., Cheng S. H., Scheule R. K., and Yew N. S., 2004, "Contribution of Toll-like receptor 9 signaling to the acute inflammatory response to nonviral vectors.," *Mol Ther*, **9**(2), pp. 241–248.

- [27] Reyes-Sandoval A., and Ertl H. C. J., 2004, "CpG methylation of a plasmid vector results in extended transgene product expression by circumventing induction of immune responses.," *Mol Ther*, **9**(2), pp. 249–261.
- [28] Hodges B. L., Taylor K. M., Joseph M. F., Bourgeois S. A., and Scheule R. K., 2004, "Long-term transgene expression from plasmid DNA gene therapy vectors is negatively affected by CpG dinucleotides.," *Mol Ther*, **10**(2), pp. 269–278.
- [29] Chen Z. Y., He C. Y., Meuse L., and Kay M. A., 2004, "Silencing of episomal transgene expression by plasmid bacterial DNA elements in vivo.," *Gene Ther*, **11**(10), pp. 856–864.
- [30] Chen Z. Y., He C.-Y., Ehrhardt A., and Kay M. A., 2003, "Minicircle DNA vectors devoid of bacterial DNA result in persistent and high-level transgene expression in vivo.," *Mol Ther*, **8**(3), pp. 495–500.
- [31] Huang M., Chen Z., Hu S., Jia F., Li Z., Hoyt G., Robbins R. C., Kay M. A., and Wu J. C., 2009, "Novel minicircle vector for gene therapy in murine myocardial infarction.," *Circulation*, **120**(11 Suppl), pp. S230–7.
- [32] Jia F., Wilson K. D., Sun N., Gupta D. M., Huang M., Li Z., Panetta N. J., Chen Z. Y., Robbins R. C., Kay M. A., Longaker M. T., and Wu J. C., 2010, "A nonviral minicircle vector for deriving human iPS cells.," *Nat. Methods*, **7**(3), pp. 197–199.
- [33] Hsu C. Y. M., Hendzel M., and Uludağ H., 2011, "Improved transfection efficiency of an aliphatic lipid substituted 2 kDa polyethylenimine is attributed to enhanced nuclear association and uptake in rat bone marrow stromal cell.," *J Gene Med*, **13**(1), pp. 46–59.
- [34] Subrizi A., Yliperttula M., Tibaldi L., Schacht E., Dubruel P., Joliot A., and Urtti A., 2009, "Optimized transfection protocol for efficient in vitro non-viral polymeric gene delivery to human retinal pigment epithelial cells (ARPE-19).," *Protocol Exchange*.
- [35] Farrell L.-L., Pepin J., Kucharski C., Lin X., Xu Z., and Uludağ H., 2007, "A comparison of the effectiveness of cationic polymers poly-L-lysine (PLL) and polyethylenimine (PEI) for non-viral delivery of plasmid DNA to bone marrow

stromal cells (BMSC).” *Eur J Pharm Biopharm*, **65**(3), pp. 388–397.

- [36] Hsu C. Y. M., and Uludağ H., 2008, “Effects of size and topology of DNA molecules on intracellular delivery with non-viral gene carriers,” *BMC Biotechnol.*, **8**, p. 23.
- [37] Wang J., Dodd C., Shankowsky H. A., Scott P. G., Tredget E. E., Wound Healing Research Group, 2008, “Deep dermal fibroblasts contribute to hypertrophic scarring,” *Lab. Invest.*, **88**(12), pp. 1278–1290.
- [38] Jacobsen L. B., Calvin S. A., Colvin K. E., and Wright M., 2004, “FuGENE 6 Transfection Reagent: the gentle power,” *Methods*, **33**(2), pp. 104–112.
- [39] Utsuno K., and Uludağ H., 2010, “Thermodynamics of polyethylenimine-DNA binding and DNA condensation,” *Biophys. J.*, **99**(1), pp. 201–207.
- [40] Palumbo R. N., Zhong X., and Wang C., 2011, “Polymer-mediated DNA vaccine delivery via bystander cells requires a proper balance between transfection efficiency and cytotoxicity,” *J Control Release*.

Chapter 4

Effects of size and topology of DNA molecules on intracellular delivery with non-viral gene carriers¹

¹A version of this chapter has been published in Hsu C. Y., and Uludağ H., 2008, "Effects of size and topology of DNA molecules on intracellular delivery with non-viral gene carriers," *BMC Biotechnol.* 8:23.

4.1 Introduction

Non-viral delivery systems are being pursued to facilitate therapeutic gene transfer in a clinical setting. Non-viral carriers, such as cationic lipids and polymers, typically interact with the anionic DNA through charged moieties, and condense the DNA molecules into compact, nano-sized particles that are suitable for cellular uptake [1,2]. A range of cationic lipids and polymers have been engineered to accomplish this function effectively, and intelligent carriers are being continually designed for the purpose of controlling the intracellular fate of DNA molecules. Most studies on non-viral gene transfer were conducted with circular plasmid DNA (c-DNA), which is known to be less susceptible to intracellular degradation. Linearized forms of c-DNA (l-DNA) with similar molecular weight, as well as shorter l-DNA that bears only the gene of interest and the promoter region have been used in some studies [3-8]. A c-DNA exhibits a higher intracellular diffusivity compared to its linearized forms [9], which facilitates its nuclear targeting for more effective expression. l-DNA is expected to be prone to nuclease attack intracellularly, but its stability could be increased by capping the 3' and 5' ends of the molecule with hairpin structures [8]. Smaller l-DNA molecules, on the other hand, display a better ability to traverse the nuclear membrane, potentially contributing to better translation of the transgene. Studies attempting to directly compare the efficiency of different DNA molecules yielded conflicting results. Whereas Cherng *et al.* observed better expression of *LacZ* gene when cells were transfected with c-DNA [9], Schakowski *et al.* observed a similar expression level (based on % transfected cells) for the two DNA topologies with both polymeric and lipid-based carriers [7]. A difference in the level of gene expression (based on IL-2 expression), however, was noted in the latter study, shorter l-DNA giving enhanced expression [7]. In direct nuclear injection studies, with no nuclear transport barriers to DNA molecules, l-DNA yielded more effective gene expression, suggesting an intrinsic superiority of l-DNA for transcription [6]. Shorter l-DNA molecules containing only the

transgene-expression sequences were even more effective, possibly due to better assembly of transcriptional factors and/ or reduced non-specific interactions of proteins with the non-coding regions of the DNA molecules. The nature of delivery vehicle appeared to influence the transfection efficiency, l-DNA being more sensitive to the choice of the carrier, unlike the c-DNA [8]. This was indicative of the differences in the transport efficiency among the carriers, but no studies directly compared the efficiency of cell delivery of different DNA molecules.

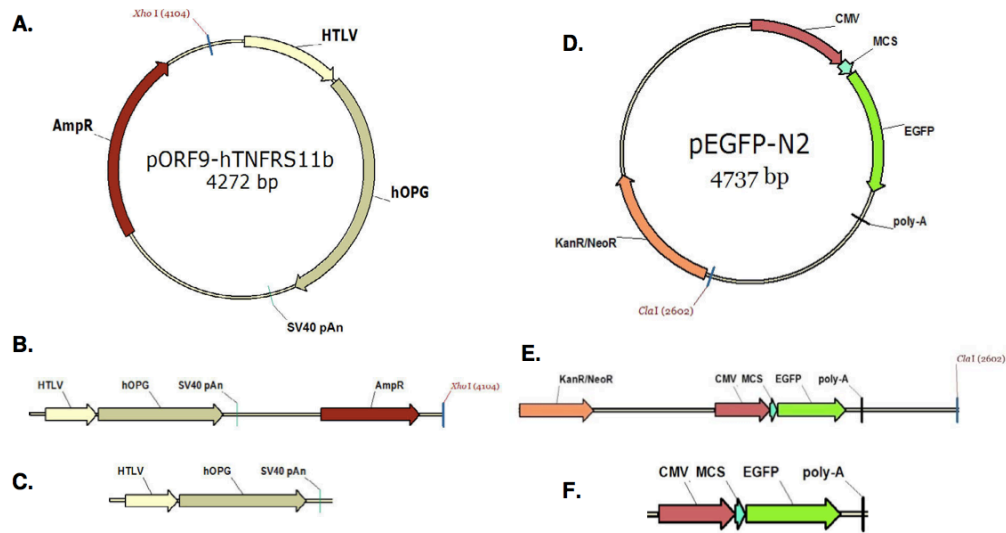


Figure 4.1

Structure of the DNA molecules used in this study.

A. Structure of the parent c-DNA. B. l-DNA formed by restriction digest of c-DNA with the enzyme XhoI. The size of the linearized plasmid was 4272 bp, C. pcr-DNA (2209 bp) generated by site-specific primers that amplified the region of the c-DNA containing the HTLV promoter, the hOPG open reading frame, and the SV40 Poly-A site. D. Structure of the parent c-DNA used in transfection. E. l-DNA formed by digest of pEGFP-N2 with the enzyme ClaI, which cuts in the vector backbone. F. pcr-DNA (1713 bp) generated by primers that are complementary to the sequence upstream of the CMV promoter and downstream of the polyA site.

This study investigated the non-viral delivery of 3 types of DNA molecules (**Figure 4.1**), namely a c-DNA representing a circular plasmid, a linearized version of the c-DNA after restriction digest at a single site, and a shorter version of the l-DNA amplified by a PCR reaction (pcr-DNA). Four different non-viral carriers were utilized, including 2 cationic

polymers commonly used for DNA delivery, polyethyleneimine (PEI) and poly-L-lysine (PLL), an in-house synthesized palmitic acid-grafted PLL (PLL-PA) [10], and the most commonly used commercial lipid Lipofectamine-2000™. By using combinations of different DNA molecules and carriers, the influences of DNA molecular weights and topologies on the delivery to bone marrow stromal cells were investigated. These cells, unlike commonly used immortal cells, are an important cell phenotype for clinical protocols. Finally, transgene expression by the three DNA forms were investigated by using the reporter gene Enhanced Green Fluorescent Protein (EGFP). Our results indicated the delivery of all three types of DNA molecules was equally effective for each carrier, with significant carrier-to-carrier differences in delivery rates, but c-DNA were more effective in yielding reporter gene expression as compared to the linearized DNA molecules.

4.2 Materials and methods

4.2.1 Chemicals and reagents

Branched 25-kDa PEI, PLL (25 kDa), Hank's Balanced Salt Solution (HBSS), trypsin/EDTA, and sodium salt of Ampicillin were obtained from SIGMA (St. Louis, MO). Lipofectamine2000™ was purchased from Life Technologies (Carlsbad, CA). Dulbecco's Modified Eagle Medium (DMEM; high glucose with L-glutamine), Penicillin (10,000 U/ml), and Streptomycin (10,000 µg/ml) were from GIBCO (Grand Island, NY). Dialysis tubing with a MW cut-off of 12-14 kDa was purchased from Spectrum Laboratories (Gardena, CA). Fetal Bovine Serum (FBS) was from Atlanta Biologicals (Lawrenceville, GA). A succinimide ester of Cy5.5 (Cy5.5-NHS) used for labeling DNA was purchased from Amersham (Baie d'Urfé, QC). PLL modified with palmitic acid was synthesized as previously described [10]. The plasmid gWiz-blank (5.1 kb), which lacks EGFP, was obtained from Aldevron (Fargo, ND).

4.2.2 Preparation of different DNA Molecules (Figure 4.1)

Circular Plasmid DNA (c-DNA)

The plasmid, pORF9-hTNFRS11b (4272 bp) encoding the human Osteoprotegerin gene, was purchased from Invivogen (San Diego, CA). The plasmid, pEGFP-N2 (4737 bp), incorporating an enhanced green fluorescent protein was obtained from BD Biosciences. Cells were revitalized and grown in 12 L of Luria-Bertani broth containing either 100 µg/mL of Ampicillin (pORF9-hTNFRS11b) or 50 µg/ml of Kanamycin (pEGFP-N2) for 16 hours at 37 °C with shaking at 125 rpm. Cells were harvested and plasmid was purified using QIAGEN Plasmid Giga Kit (QIAGEN; Mississauga, ON) as described in the manufacturer's handbook. The purified plasmid was dissolved in ddH₂O at a final concentration of ~1.8 mg/mL. Concentration and purity were determined by UV Spectroscopy using NanoDrop1000 instrumentation.

Linear DNA (l-DNA)

Purified c-DNA was linearized using the restriction enzyme, XhoI (New England Biolabs; Pickering, ON) for pORF9-hTNFRS11b or ClaI (Life Technologies; Burlington, ON) for pEGFP-N2, Restriction digestion were set up with 5 µg of DNA per 50 µL of reaction volume containing 3 units of enzyme and incubated at 37°C for 16 hours. The enzyme was then heat-inactivated by incubating the mixture at 65 °C for 10 min. Digested DNA was purified using QIAEX II Gel Extraction Kit (QIAGEN, Mississauga, ON). Purity of the isolated product was confirmed by spectrophotometry and gel electrophoresis was used to confirm the presence of a single band in the preparation.

Gene Cassette (pcr-DNA)

The primers, hOPG-F2 (5'-CGAAACAAAACAACTAGCAAAAT-3') and hOPG-R2 (5'-CCTTTTGCTCACATGTTCTTAATTA-3') was used to synthesize gene cassette from the plasmid pORF9-hTNFRS11b; GFP-F1 (5'-TCCTGCGTTATCCCCTGATT-3') and GFP-R1 (5'-

CGCTTACAATT- TACGCCTTAAG-3') was used to synthesis gene cassette from the plasmid pEGFP-N2. All primers were customarily designed and synthesized by IDT Technology (Toronto, ON). Synthesis of gene cassette was carried out using PCR in a 50 μ L reaction containing 0.6 μ M of each of the primers, 0.2 mM dNTP, 1 unit of Platinum[®] Taq DNA Polymerase High Fidelity (Life Technologies), 1 \times Hi Fi PCR buffer, 1.5 mM of MgSO₄, and 20 ng of c-DNA as the template. Reaction parameters were as follows: 2 min at 94 $^{\circ}$ C followed by 35 cycles of 30 s at 94 $^{\circ}$ C, 30 s at 60 $^{\circ}$ C, and 3 min at 68 $^{\circ}$ C, then an addition 5 min incubation at 68 $^{\circ}$ C. The PCR products so obtained were purified by QIAGEN PCR purification kit (QIAGEN, Mississauga, ON). Purity of the isolated product was confirmed by spectrophotometry, and gel electrophoresis was used to confirm the presence of a single band in the preparation. The resulting PCR product was approximately 2209 bp (pORF9- hTNFRS11b) or 1684 bp (pEGFP-N2).

4.2.3 Atomic force microscopy (AFM)

Prior to AFM measurements, carriers were added to the DNA solutions in 1:1 carrier-to-DNA weight ratios, and allowed to incubate for 20 min at room temperature. The solutions were diluted \times 100 with ddH₂O and 1.5 μ L of the resulting solution was deposited onto freshly cleaved mica surfaces. Samples were allowed to dry in air for 20 min or until water had visibly evaporated from the surfaces. Experiments were performed with MFP-3D-BIO (Asylum Research; Santa Barbara, CA) operating in tapping mode (AC) using standard silicon cantilever (AC240TS) with \sim 2 N/m spring constant and 70 KHz working frequency. All images were recorded in air at room temperature inside an acoustic enclosure, and on a vibration isolation table at a scan speed of 1 Hz.

4.2.4 Particle size measurement

The diameter of the particles formed by carrier/DNA complexes was measured by photon correlation spectroscopy (ZetaPALS, Brookhaven Instruments, Holtzville, NY). Four microgram of DNA was complexed with the appropriate volume of polymer solution at a carrier/DNA weight ratios of 5, 7.5 and 10 in a total volume of 50 μ L diluted with 150 mM NaCl. The complexes were left to stand at room temperature for 30 minutes, then diluted to 2 mL with DMEM and incubated for another 30 minutes before analysis. The measurement time was set at 30 seconds intervals and each run consisted of 10 consecutive measurements (SD among the measurements was typically ~1%). Particle sizes were measured at a wavelength of 660 nm and calculated by using a medium viscosity of 1.140 cP [11] and a refractive index of 1.333 (at 25°C).

4.2.5 Electrophoretic gel mobility assay (EMSA)

Electrophoretic mobility of carrier/DNA solutions was performed by loading the complexes (see preparation condition below) into a 0.7-0.8% agarose gel containing 1 μ g/mL of Ethidium Bromide in 1 \times Tris-Acetate/EDTA buffer. The agarose gel was run with 115 V of current for ~20 min and the DNA bands were visualized using the Alpha Imager (Alpha Innotech; San Leandro, CA). Mean fluorescent density (in arbitrary units) of each band was measured by the manufacturer-supplied software.

4.2.6 Analysis of carrier-DNA binding

200 ng of DNA was first suspended in 100 mM HEPES buffer (pH 5.2), carriers were then added to DNA solutions at DNA:carrier weight ratios of 2, 1, 0.5, 0.2, 0.1, and 0 in a final volume of 15 μ L, and the solutions were allowed to incubate at room temperature for 30 min. The samples were then loaded into the gel as described above. The amount of free DNA in each lane was quantitated by densitometric analysis. The percentage of DNA bound was calculated from the fluorescent density (F) values as: % DNA bound =

$[F(\text{DNA only}) - F(\text{specific DNA-polymer ratio})] \div [F(\text{DNA only}) - F(\text{background})] \cdot 100\%$. %DNA bound vs. carrier:DNA ratios were plotted, and used to obtain a carrier/DNA-specific IC₅₀ value, indicating the carrier:DNA ratio that gave binding to 50% of the DNA in the sample.

4.2.7 Analysis of carrier-DNA complex dissociation

350 ng of DNA molecules in 150 mM NaCl were complexed with 3 µg of polymer in a final volume of 10 µL for 30 min at room temperature. Then, 10 µL of either basic medium (with 10% FBS) or 10 µL of DMEM was added to the samples, and incubated at room temperature for an additional 1.5 hours. Heparin sulfate were then added at a final concentration range of 0.02 - 32 µg/mL and the samples were incubated for 30 min. The samples were then loaded onto the gel and visualized as described above. The percentage of DNA dissociated was calculated from the fluorescent density (F) values as: %DNA released = $[F(\text{specific heparin concentration}) - F(\text{background})] \div [F(\text{DNA only}) - F(\text{background})] \cdot 100\%$.

4.2.8 Cell culture and DNA uptake

Rat bone marrow stromal cells (rBMSC) were isolated and cultured as described previously [12]. Briefly, cells were isolated from both femurs of 8-week old female Sprague-Dawley rats and pooled to obtain a single suspension. The bone marrow was flushed out with 15 mL of DMEM containing 10% FBS, 50 µg/mL ascorbic acid, 100 U/mL Penicillin and 100 µg/L of Streptomycin (referred to hereon as basic medium). Cells were centrifuged for 6 min at 600 rpm, suspended in fresh basic medium and seeded in a single 75 cm² flask (Sarstedt; Montreal, QC). After medium change on day 3, the cells were trypsinized on day 7 and expanded in 75 cm² flasks (1:4 dilution). The rBMSC passaged between 2-4 generations were used in this study, and were grown in multi-well plates for DNA uptake studies.

To investigate DNA uptake, 20 μg of DNA was labeled with Cy5.5-NHS as suggested by manufacturer's protocol. Labeling reaction was stopped by the addition 100 mM Tris-Cl to quench the pre-activated succinimide ester moiety. Labeled DNA was dialyzed against 10 mM Tris-Cl (pH 7.4) then again with ddH₂O. The samples for uptake were prepared with 5 μL of the labeled DNA solution added to 2, 6 or 18 μg of the polymer (0.3, 1 and 3 μg for branched PEI) in a final volume of 40 μL . The samples were added directly to the rBMSC grown in 6-well plates with 2 mL of basic medium. Each polymer concentration was typically tested in duplicates. Cells are incubated for 24 hours at 37 °C (5% CO₂), after which they were washed with HBSS (x2), trypsinized for 5 min for detachment and suspended in HBSS with 4% formalin. Fluorescence was measured at $\lambda_{\text{em}} = 690 \text{ nm}$ and $\lambda_{\text{em}} = 705 \text{ nm}$. The results were expressed as the percentage of cells exhibiting significant fluorescence over that of control samples (i.e. cells exposed to DNA with no polymer), which was set to ~1% uptake. In some cases, the uptake was expressed as the average fluorescence exhibited in cells (in arbitrary units).

4.2.9 Transfection and assessment of GFP expression

Two cell types were used for assessment of transgene expression, primary rBMSC and immortalized HEK 293T cells. BMSC were cultured and maintained as described in the DNA uptake studies. HEK 293T cells were seeded in 12-well tissue culture plates supplemented with DMEM media containing 10% FBS. When cells reached ~80% confluence, they were transfected with PEI/DNA complexes prepared at a polymer/DNA weight ratio of 2.5 (PEI:DNA concentration of 5:2 $\mu\text{g}/\text{mL}$ in tissue culture medium). Complexes were incubated at room temperature for 25 minutes then added directly to cells covered in a basic medium. The cells were allowed to incubate at 37 °C in the presence of complexes for 24 h followed by replacement of 1 mL of DMEM containing 10% FBS. Transfected 293 cells were either processed for flow cytometry

following complex removal (24 hours), or incubated for another 72 hours before assessment of EGFP expression by flow cytometry. BMSC were processed 48 hours after complexes were removed. Flow cytometry was performed on a Cell Quanta SC with MPL Option (Beckman Coulter) where the EGFP fluorescence was detected in the FL1 channel. The instrument settings were calibrated for each run so as to obtain a background level of EGFP expression of ~1% for control cells. The latter included (i) cells treated with 2 µg/mL of c-DNA, l-DNA and pcr-DNA without any carriers, and (ii) cells treated with PEI/gWiz-blank plasmid that contained no functional genes (to ensure that internalized complexes do not provide a non-specific fluorescence in flow cytometry).

4.2.10 Statistical analysis

Where indicated, all results are summarized as mean \pm standard deviation, and statistical variations ($p < 0.05$) between the group means were analyzed by the Student's t-test.

4.3 Results

4.3.1 Particle formation

The three DNA molecules were mixed with various gene carriers in solution to examine particle formation and morphology (**Figure 4.2**). When the DNA molecules were examined using AFM in the absence of carriers, a network of interconnecting fibrous strands was observed, especially for c-DNA (**Figure 4.2a**) and l-DNA (**Figure 4.2f**), whereas pcr-DNA appeared as discontinuous strands (**Figure 4.2k**). When branched PEI was added to the DNA solutions (**Figure 4.2b, 4.2g, and 4.2l**), spherical particles were observed for all three types of DNA molecules with no evidence of string-like DNA molecules. The sizes of the particles ranged from ~40 nm to ~180 nm in diameter, and were independent of the type of DNA molecules used. Similar observation was noted for particles obtained with PLL (**Figure 4.2c, 4.2h, and 4.2m**) and PLL-PA (**Figure 4.2d, 4.2i and 4.2n**). The sizes of the particles formed by the PLL and PLL-PA were equivalent to those formed by the branched PEI. The cationic lipid, Lipofectamine-2000™, also bound and condensed c-DNA and l-DNA into spherical particles (**Figure 4.2e and 4.2j**). However, the sizes of some of the particles were significantly larger, with some particles being as large as ~450 nm. Some particles were observed when pcr-DNA were mixed with Lipofectamine-2000™ (**Figure 4.2o**), but isolated islands of presumably Lipofectamine-2000™ formed over the mica surface covering some of the DNA molecules. Although we followed the manufacturer's instructions for DNA condensation in the latter case, excess lipid was apparently present in these solutions. At the same time, some string-like structures, reminiscent of naked pcr-DNA, were also seen in these samples, suggesting incomplete condensation of pcr-DNA molecules with the Lipofectamine-2000™. Taken together, all of the gene carriers examined was able to condense the c-DNA, l-DNA and

pcr-DNA molecules into spherical particles, except the Lipofectamine-2000™/pcr-DNA combination, which gave incomplete condensation of the DNA molecules.

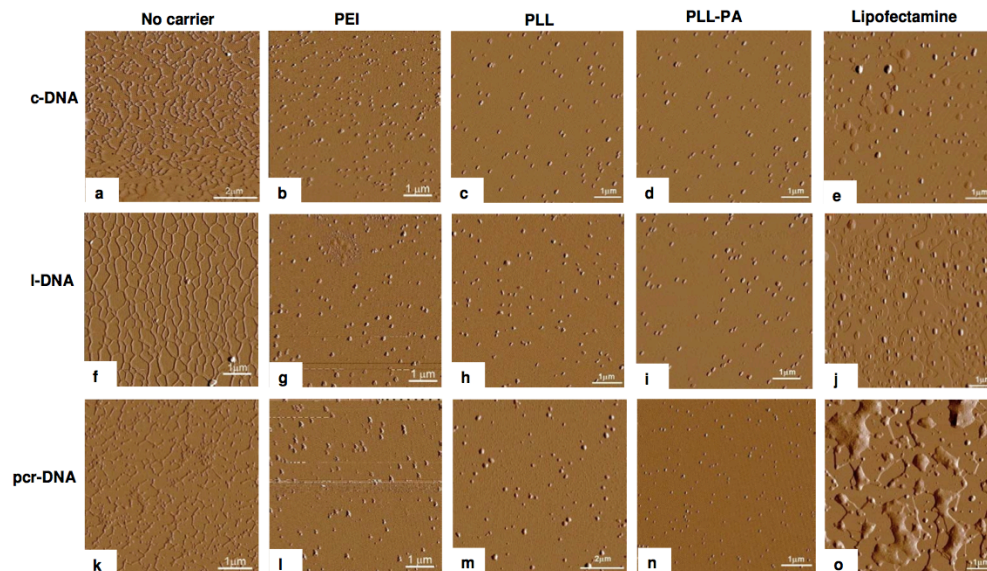


Figure 4.2

Tapping mode atomic force microscope amplitude topography of the three DNA molecules complexed with various gene carriers.

All images were captured at a scan size of $6 \times 6 \mu\text{m}$, except where noted. c-DNA without carriers [$8 \times 8 \mu\text{m}$] (a), with PEI (b), PLL (c), PLL-PA (d), and Lipofectamine-2000™ (e). I-DNA without carriers (f), with PEI (g), PLL (h), PLL-PA (i), and Lipofectamine2000™ (j). pcr-DNA without carriers [$5 \times 5 \mu\text{m}$] (k), with PEI (l), PLL (m), PLL-PA (n), and Lipofectamine- 2000™ (o).

	Circular DNA			Linear DNA			PCR DNA		
	5.0	7.5	10.0	5.0	7.5	10.0	5.0	7.5	10.0
PEI	337	188	159	735	710	772	518	414	273
PLL-PA	169	124	106	354	388	338	104	99	103
Lipo	758	964	1002	NS	1406	421	NS	NS	NS

Table 4.1 Mean particle sizes (nm) obtained for the DNA molecules

Complexes formed at at three (5.0, 7.5 and 10.0) carrier:DNA mass ratios. The values shown are usually derived from the average of 2 measurements, and SD between the measurements was <5% (not shown). NS: No stable measurements were taken for these samples. The zeta potential of the particles were >30 mV in all cases (not shown).

The particle sizes were additionally analyzed by dynamic light scattering (**Table 4.1**). Unlike AFM, this method characterizes the size of the particles in solution and it can be considered more representative of the state of the particles in contact with the cells. Three different carrier:DNA ratios were used to investigate its effect on particle sizes. Whereas some combinations (e.g., PLL-PA and PEI combined with c-DNA) gave the expected decrease in size with increasing carrier:DNA ratio, other combinations (e.g., ones involving l-DNA and Lipofectamine-2000™) did not give a predictable pattern. Particles from Lipofectamine-2000™ were generally larger for each DNA molecule, and in some cases, no stable measurements could be taken either due to visible precipitation of the complex solution or formation of large particle aggregates. This was consistent with the AFM observations on Lipofectamine-2000™ complexed DNA molecules. With PLL-PA, l-DNA gave relatively larger particles (~350 nm) as compared to c-DNA and pcr-DNA (100-160 nm). This was the case with PEI as well, except PEI complexes appeared to be significantly larger than the PLL-PA complexed particles for each type of DNA molecule.

4.3.2 DNA binding

Figure 4.3 shows the results of the densitometric analysis from the EMSA assay intended for semi-quantitative analysis of DNA-carrier interactions. For each carrier examined, there was no significant difference in the binding interaction among the DNA molecules; i.e., the curve indicating percent bound vs. carrier:DNA ratio overlapped for all three DNA molecules. However, the carrier:DNA ratios necessary for complete (100%) binding and for IC_{50} were different among the carriers. Complete binding was achieved at ~ 0.5 , ~ 1.0 , ~ 1.0 , and ~ 3.0 carrier:DNA ratios for branched PEI, PLL, PLL-PA, and Lipofectamine-2000TM, respectively (**Figure 4.3a, 4.3b, 4.3c, and 4.3d**). The IC_{50} values were ~ 0.15 , ~ 0.45 , ~ 0.3 , and ~ 1.2 for branched PEI, PLL, PLL-PA, and Lipofectamine-2000TM, respectively.

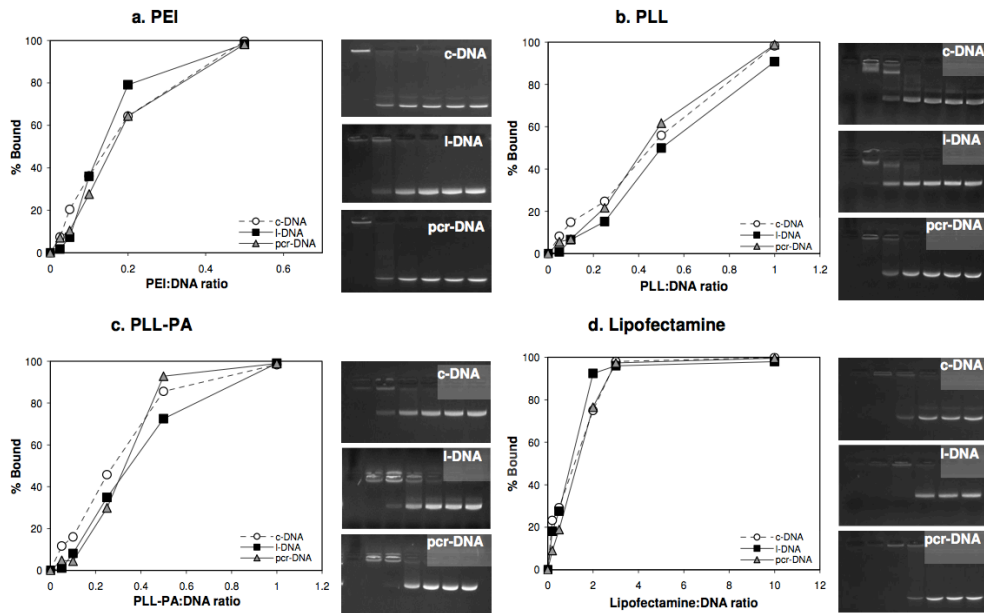


Figure 4.3

Analysis of DNA binding to the gene carriers

PEI (a), PLL (b), PLL-PA (c), and Lipofectamine-2000TM (d). Densitometric analyses of the binding results in the form of percent DNA bound were summarized as a function of increasing carrier:DNA weight ratio. The corresponding gel pictures of DNA-carrier complex were also shown.

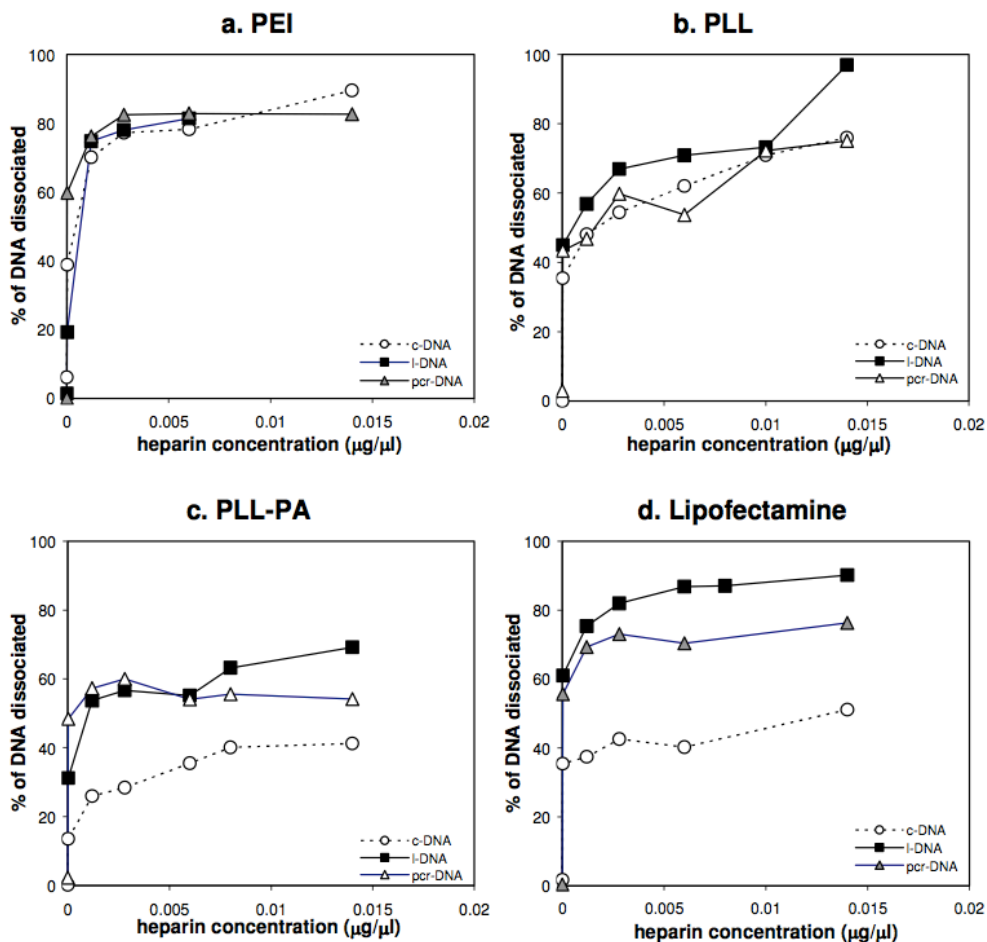


Figure 4.4
Dissociation kinetics of DNA-carrier complexes using heparin sulfate as the competitive polyanion.
 Results are displayed as a function of the concentration of heparin added and the percent of DNA released. Shown here are dissociation of the complexes with PEI (a), PLL (b), PLL-PA (c), and Lipofectamine-2000™ (d).

4.3.3 Complex dissociation

The dissociation of DNA/carrier complexes was investigated by incubating heparin sulfate with the complexes. The dissociation was conducted in complete culture medium to mimic the conditions while the complexes are incubated with the cells. Heparin was able to dissociate the complexes for all carriers (**Figure 4.4**), based on the liberation of free DNA molecules upon incubation with the highest heparin concentration. With branched PEI, the dissociation of the complexes as a function of

heparin concentration was similar for all three DNA molecules (**Figure 4.4a**), where >80% dissociation of the complexes was observed at the highest heparin concentrations. This was the case for PLL as well (Figure 4b), except the extent of dissociation was generally less than 80%. With PLL-PA and Lipofectamine-2000™, c-DNA gave a relatively lower heparin-induced dissociation as compared to l-DNA and pcr-DNA (**Figure 4.4c and 4.4d**, respectively) and, in both cases, it was not possible to release more than 50% of the c-DNA.

4.3.4 DNA delivery to rBMSC

The intracellular DNA delivery was investigated by using DNA molecules fluorescently labeled with Cy5.5 fluorophore, as outlined in materials and methods. **Figure 4.5** shows the results of Cy5.5-labeled DNA uptake by BMSC grown in basic medium, which were carried out with a fixed concentration of DNA and varying concentrations of the carriers. In all cases, the cellular delivery increased with increasing carrier concentration in the formulations. The percentages of Cy5.5-positive cells were generally highest when branched PEI and PLL-PA were used as the carriers. Branched PEI was able to deliver all three types of DNA molecules up to ~80% of the cells at a lower polymer concentration as compared to the PLL-PA (~1.5 µg/mL vs. ~3.0 µg/mL; **Figure 4.5a and 4.5c**, respectively). PLL did not give any elevated level of DNA uptake in comparison to cells exposed to their respective DNA controls (**Figure 4.5b**). Lipofectamine-2000™ had a maximum of ~20% of Cy5.5-positive cells at the highest concentration tested (9 µg/mL; **Figure 4.5d**). For each carrier, there were no apparent differences in the delivery efficiency among the three DNA molecules.

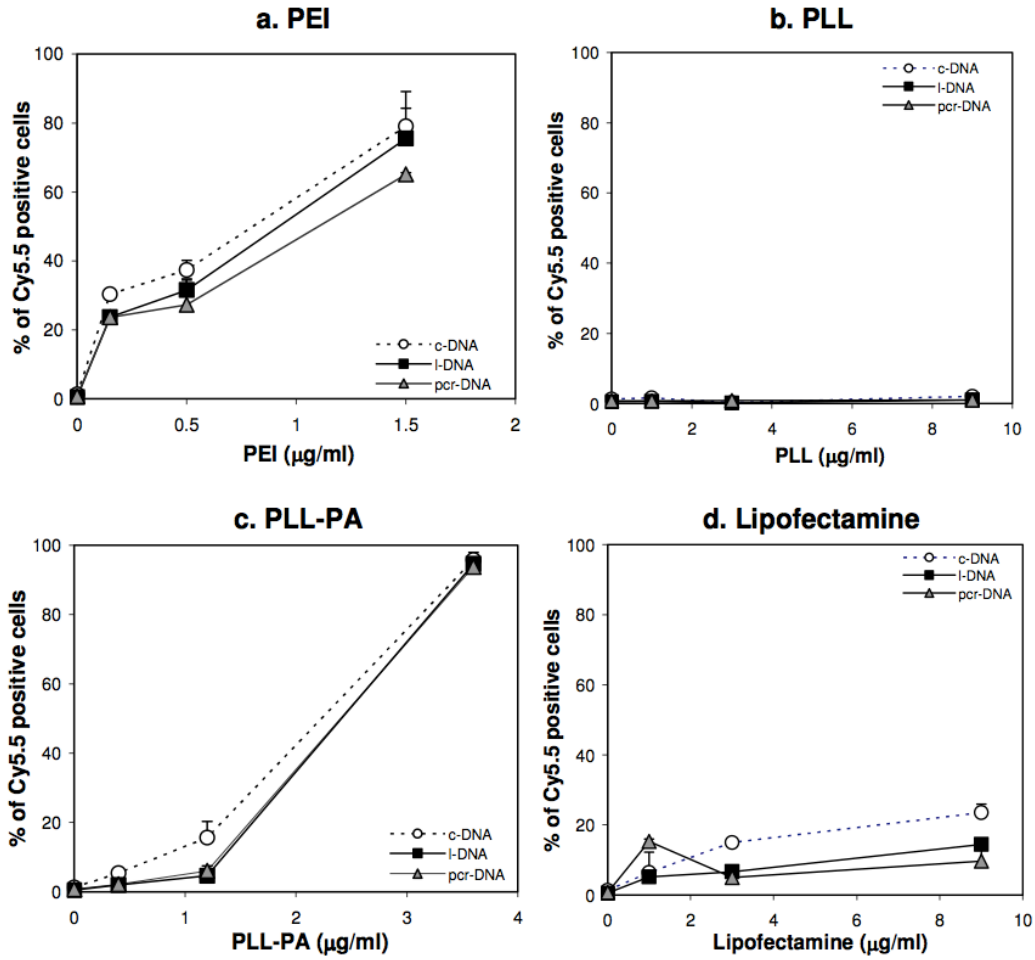


Figure 4.5

Delivery of c-DNA, I-DNA and pcr-DNA into rBMSC

With PEI (a), PLL (b), PLL-PA (c), and Lipofectamine-2000™ (d) at various concentrations of carriers. The cells were grown in 6-well plates for 24 hours, and incubated with carrier/DNA complexes for an additional 24 hours. Results from the flow cytometry were expressed as percentages of cells positive for Cy5.5- fluorescence, where the cells incubated with DNA alone (i.e., without any carrier) was calibrated at ~1%.

4.3.5 Effect of serum on DNA delivery

Several studies have shown serum in culture medium to influence gene delivery by non-viral gene carriers [13,14]. To investigate whether serum had an effect on delivery of different DNA molecules, complexes were incubated with the cells for 4 and 24 hours in the presence (10% serum) and absence of serum. Branched PEI and PLL-PA again gave the highest extend of DNA delivery (**Figure 4.6a** and **4.6c**, respectively), with PLL giving the lowest delivery of DNA to the cells (**Figure 4.6b**), similar to the results shown in **Figure 4.5**. With branched PEI (**Figure 4.6a**), the extent of DNA delivery among the three DNA molecules was similar (70- 90%). The presence of serum did not have a major effect on DNA delivery, except at the early time point (4 hour) for pcr-DNA, where the uptake appeared to increase by ~31% in the absence of serum. With PLL-PA as the carrier (**Figure 6c**), the extent of DNA delivery reached saturation (~100% of rBMSC) for the three types of DNA molecules in the absence of serum. However, l-DNA and pcr-DNA gave lower delivery at earlier time point (4 hour) in the presence of serum (~64% and ~37% reduction, respectively). With Lipofectamine-2000™ as the carrier (**Figure 4.6d**), the extent of delivery was low in the presence of serum (~20%) for all DNA molecules. In the absence of serum, DNA uptake after 24 hours was ~2-fold higher for all three DNA molecules.

The average fluorescence of Cy5.5-positive cells after incubation with complexes is also shown in **Figure 4.6**. These fluorescent values were used as a quantitative measure of the amount of DNA internalized by the rBMSC. Consistent with the percent uptake results, the highest DNA delivery was obtained with the branched PEI and PLL-PA as the carriers. With branched PEI, there was a ~2-fold increase ($p < 0.01$) in DNA delivery from 4 to 24 hour time point (**Figure 4.6a**). Neither serum nor the type of DNA molecules had an effect on the amount of Cy5.5-labeled DNA being internalized by the cells. When PLL was used as the carrier, the amount of internalized Cy5.5-labeled

DNA was low; there was no effect of the serum or the type of DNA molecules on the DNA delivery (**Figure 4.6b**). With PLL-PA as the carrier, ~2-fold increase in the DNA uptake was again observed upon incubation of the complexes with the cells from 4 to 24 hours (**Figure 4.6c**). In this case, approximately 2.3-3.7 fold increase in DNA delivery was observed in the absence of serum with all three types of DNA molecules. With Lipofectamine-2000™, an increase in DNA delivery was also observed under longer incubation time (4 vs. 24 hours; **Figure 4.6d**). Eliminating serum gave a significant increase in DNA delivery for all three types of DNA molecules at the 24-hour time point.

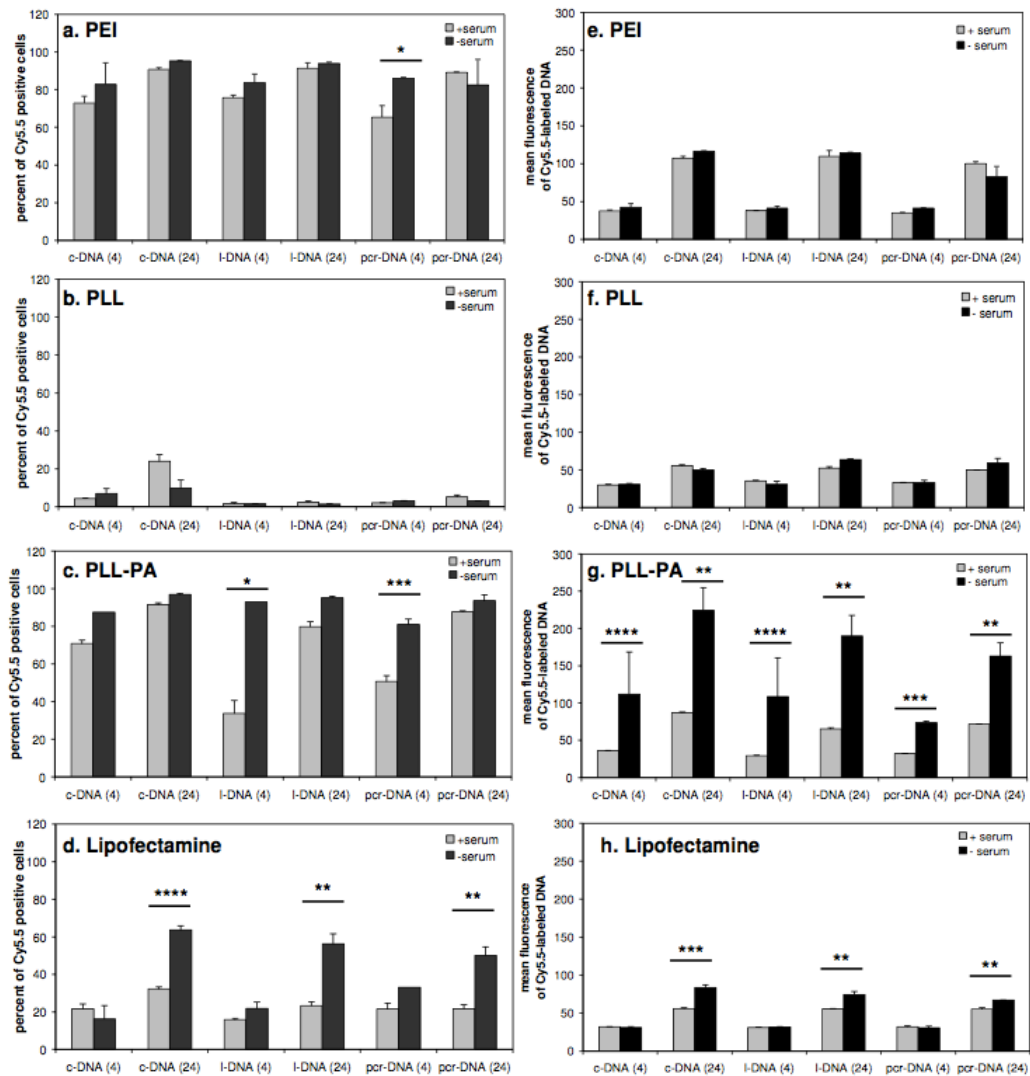


Figure 4.6

DNA delivery various cationic reagents in the presence and absence of serum.

PEI (a and e), PLL (b and f), PLL-PA (c and g), and Lipofectamine-2000™ (d and h) The cells were grown in 24-well plates for 24 hours, and incubated with carrier/DNA complexes for an additional 4 and 24 hours. Results from the flow cytometry were expressed either as percentages of cells positive for Cy5.5- fluorescence (a, b, c and d) or mean fluorescence for Cy5.5-positive cells (e, f, g and h). Statistical differences between the medium with and without serum are indicated above: *p < 0.05, **<0.025, ***p < 0.01 and ****p < 0.001.

4.3.6 Transgene expression

Assessment of gene expression was carried out by using the reporter gene EGFP, rather than the OPG plasmid previously used, since quantitating the extent of gene expression could be readily assessed by flow cytometry. Preliminary studies using pEGFP-N2 with PLL, PLL-PA, Lipofectamine-2000™ and PEI indicated the PEI to be the most effective carrier in our set up (data not shown). Therefore, subsequent expression studies were performed by using PEI as the sole carrier and the three types of DNA molecules to specifically focus on the relative effectiveness of each DNA molecule for the expression of reporter gene (rather than focusing on the effectiveness of each carrier). To determine if the enzymatic manipulations used to generate the l-DNA and pcr-DNA yielded functional gene constructs, transfections were initially carried out in HEK 293T cells since they are considered to be a readily-transfectable cell phenotype. The results obtained from these cells are summarized in **Figure 4.7**. The c-DNA was the most effective form of DNA based on percentage of EGFP-positive cells (**Figure 4.7a**), giving ~90% cells with EGFP expression on Day 1. Transfection efficiency using l-DNA and pcr-DNA were significantly lower: ~61% and ~48% EGFP- positive cells, respectively. On Day 4, the percentage of EGFP-positive cells was reduced for c-DNA and l-DNA (but not pcr-DNA) transfected cells as compared to Day 1. The relative mean fluorescence values of the EGFP-positive cells (**Figure 4.7b**) were used as a measure of extent of EGFP expression; the c-DNA transfected cells displayed ~3.5 and ~2.5 fold increase in mean fluorescence over l- DNA and pcr-DNA transfected cells, respectively (Day 4). Non-treated cells, as well as the cells exposed to the three forms of DNA alone (i.e., without any carrier) gave results similar to the cells treated with PEI/gWiz complexes (not shown).

Using complexes similar to the ones used on 293 cells, transfection efficiency of rBMSC was found to be much lower; control cells exposed to PEI/gWiz complexes with- out an

EGFP gene gave ~1.5% EGFP-positive cells as a background (**Figure 4.7c**), which was similar to values obtained with non-treated cells, and cells exposed to the three DNA molecules without any carrier (~1%; not shown). rBMSC transfected with complexes containing a functional EGFP gene afforded only 2-3% EGFP-positive cells (**Figure 4.7c**). There was no significant difference in the percent of GFP-positive cells between c-DNA and l-DNA; however, both forms of DNA were significantly more effective than pcr-DNA ($p < 0.05$). Among the EGFP-positive cells, the mean fluorescence values for all three DNA molecules were significantly greater than the control cells (Figure 7d). The cell treated with c-DNA had a greater mean fluorescence than the cells treated with l-DNA ($p < 0.05$), and both c-DNA and l-DNA gave a significantly ($p < 0.05$) greater mean fluorescence values than the pcr-DNA.

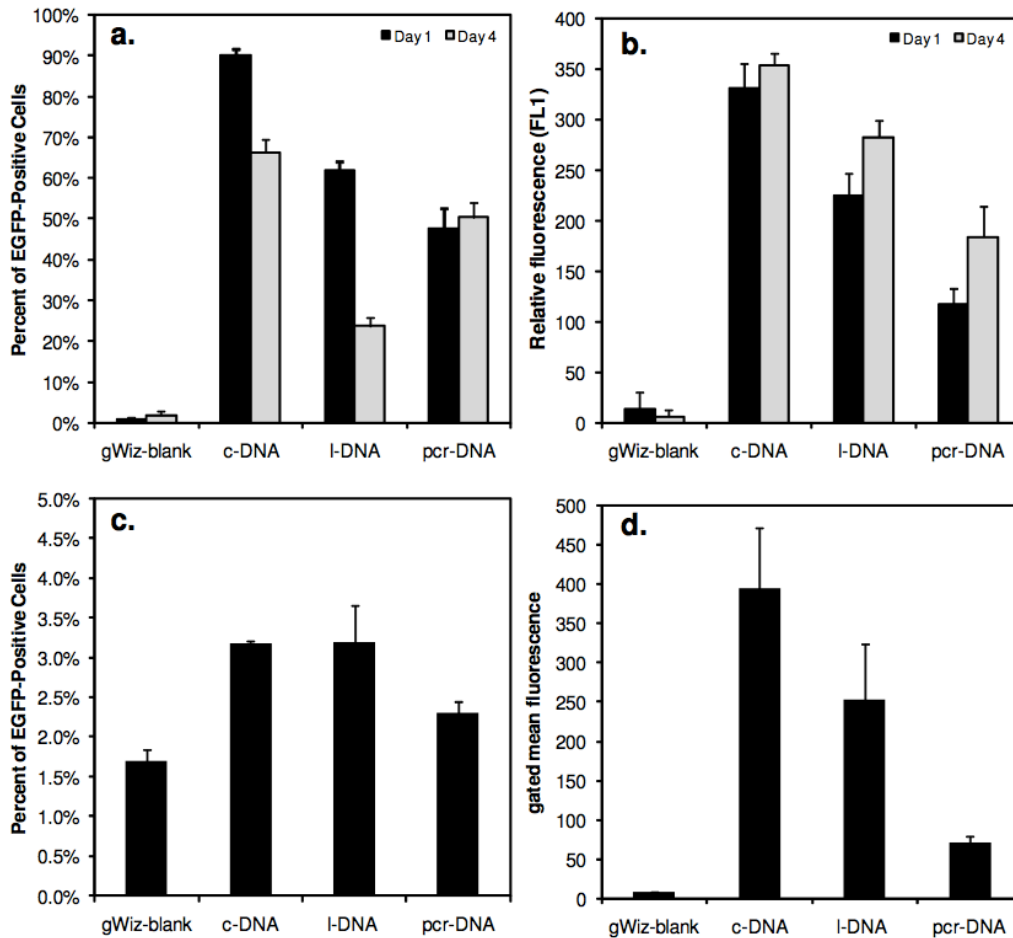


Figure 4.7

Transfection efficiency of c-DNA, l-DNA, and pcr-DNA using PEI as the gene carrier

in HEK 293T Cells (A and B) and rBMSC (C and D). Cells were grown in 12-well plates and incubated with the complexes for 24 hours. EGFP expression was assessed on Day 1 and 4 for 293 cells, and on Day 3 for rBMSC. Results from the flow cytometry were expressed as either (i) percent- age of EGFP-positive cells, when control cells were assigned to ~1% EGFP-positive cells (A and C), or (ii) the relative fluorescence values for EGFP-positive cells (B and D). The control cells in both cases were the cells exposed to PEI/gWiz-blank complexes without the EGFP gene. In the case of 293 cells, the relative fluorescence for the EGFP-positive cells was normalized with the fluorescence values for control cells to account for the day-to-day differences. For rBMSC, the mean fluorescence values were shown without normalization.

4.4 Discussion

Non-viral gene delivery systems employ cationic polymers or lipids as vectors for delivery of therapeutic genes into pertinent cells. Previous studies have examined the effects of DNA molecular weight and topology on transfection efficiency [7,8,15] but failed to study the intracellular delivery of different DNA molecules *per se*. We employed three types of cationic polymers and one cationic lipid to determine if common non-viral gene carriers would have the same delivery efficacy using different physical forms of DNA. To compare the effects of physical properties alone on cellular uptake, all DNA molecules were manipulated from a single source of circular plasmid DNA extracted from bacteria. I-DNA and pcr-DNA were prepared by restriction digest and PCR, respectively, using c-DNA as the source or the template. The procedures were optimized to obtain homogenous products without gel electrophoresis. It is known that EtBr/UV light combination damages DNA by inducing strand breakage and oxidation [16,17]. To avoid this potential artifact, all DNA preparations have been performed in the absence of EtBr.

The ability of gene carriers to bind DNA and condense the molecule into particles is assessed qualitatively by AFM and quantitatively by photon correlation spectroscopy. AFM assessment indicated that the cationic polymers were able to condense all three types of DNA molecules into spherical particles with no discernible morphological differences. A variation in particle sizes was evident for individual carriers in AFM measurements, but size ranges appeared to overlap between the types of DNA molecules. Photon correlation spectroscopy indicated the PEI complexed DNA to be larger than the PLL-PA particles. The smaller size of the particles obtained from AFM is not surprising, considering that they were obtained under 'dry' condition which is likely to represent a collapsed state of the particles. The type of DNA molecule was a determining factor in the sizes of particles formed with the polymeric carriers (**Table**

4.1). Lipofectamine-2000TM also condensed DNA into spherical particles for both c-DNA and l-DNA, and the particles were similar in size to those observed elsewhere [18]. However, full condensation did not occur for the pcr-DNA at the weight ratios used in this experimental set-up. This was also the case for these particles from photon correlation spectroscopy measurements. Based on semi-quantitative EMSA analysis [19], no significant differences in the binding interaction among the three types of DNA molecules was evident for each carrier. Branched PEI was able to completely condense DNA at lower polymer-to-DNA weight ratio compared to other carriers. Both PLL and PLL-PA were able to completely condense DNA at the same ratio, however, the modification of PLL with palmitic acid led to an increase in binding affinity, contrary to the observation reported earlier [10]. The combination of AFM and EMSA results pointed to no apparent differences between the DNA molecules and their interaction with the carriers. It was interesting to note that EMSA results (indicating 100% binding at carrier:DNA ratios of ≤ 1), were mostly consistent with the AFM results, which indicated no free DNA at the carrier:DNA ratio of 1. The only exception was the results from Lipofectamine-2000TM, where complete binding was seen at the carrier:DNA ratios of ~ 3 , whereas AFM indicated no free DNA (for c-DNA and l-DNA) at the ratio of 1. It was possible that Lipofectamine-2000TM complexation led to more fragile particles that did not withstand the electrophoretic forces under EMSA assay conditions.

Dissociation of DNA from gene carriers is essential for efficient gene expression because access by the transcription machinery requires free and intact DNA [20,21]. The dissociation characteristics of the complexes were studied using heparin sulfate as a competitive polyanion to disrupt the interaction between the carriers and DNA molecules. Heparin sulfate is an anionic polysaccharide known to be a major component of extracellular matrix, and have been shown to inhibit DNA delivery [22-24]. It was used here to mimic the conditions that particles encounter under cell

culture conditions. For DNA complexes formed with PEI and PLL, there was no significant difference in the dissociation profile among the three types of DNA molecules. With both vectors, however, DNA could not be fully dissociated from the complex. This may be due to a rate-dependent reorganization process that takes place after the initial complexes were formed, leading to a 'mature' complex with stronger electrostatic interaction that cannot be easily disrupted [20]. Complexes of PLL-PA and Lipofectamine-2000™ showed a different dissociation profile among the three types of DNA, where linear forms of DNA molecules were dissociated to a greater extent than the c-DNA. This suggested that a similar maturation process exist for the lipoplexes [[25], and the extent of maturation varied among the different topologies of DNA. Grafting of the fatty acid palmitic acid on PLL renders a partial lipophilic characteristic to the cationic polymer, and is likely to account for the similarity in the dissociation profile to that of Lipofectamine-2000™, that is, with c-DNA being the least dissociated. Overall, our results suggested a similar efficiency in the unpacking of vector (dissociation) among the three DNA molecules for the polymeric carriers, but not for the lipid-based carriers whose dissociation was stronger with l-DNA molecules. Since expression of the transgene (OPG) was not explored in this study, it remains to be determined whether such a difference in dissociation would ultimately lead to differences in expression efficiency for different DNA isoforms.

With respect to DNA delivery to the cells, we observed no major difference in the level of DNA uptake among the three physical forms of DNA molecules. This was the case despite the fact that average particle sizes were found to depend on the nature of the DNA molecule. It is possible that significant variations in particle sizes in each complex preparation might have masked such a possible effect. Different routes of entry (i.e., clathrin- vs. caveolae-mediated) could also have been utilized by different complexes [26], but our studies were not designed to probe these differences. It must be pointed

out that serum could not be used during photon correlation spectroscopy due to unstable readings obtained. Any changes in particle sizes in the presence of serum might complicate our understanding of size effects on the DNA delivery [27,28]. However, there was a difference in the delivery efficiency of DNA among the carriers. PEI was able to deliver DNA to cells at much lower concentrations and was the most effective carrier of the four examined. PLL was the least effective carrier for DNA uptake and its performance was comparable to when no carrier was used. In previous studies, PLL was shown to be readily taken up by the cells [29], but it appeared that its ability to carry a DNA cargo was relatively low. This is in contrast to the results obtained in other studies when fluorescent microscopy was used to detect DNA uptake [29]. The low level of uptake observed in this study may be attributed to the low sensitivity of the flow cytometer or a high cut-off level set up with the control samples (i.e. no carrier). There was no apparent correlation between particle formation, polymer-DNA interaction, complex dissociation and the DNA uptake. For example, PLL, despite showing typical DNA binding and dissociation activity, did not enable an equivalent DNA level of delivery into cells when compared to other carriers. This conclusion was valid for all three DNA molecules used in this study.

The presence of serum during cellular internalization of complexes did not influence the uptake of complexes of pure cationic carriers PEI and PLL, but did influence delivery by the lipophilic Lipofectamine-2000™ and PLL-PA. This may be due to serum inhibition of the complex maturation process, resulting in reduced uptake [26]. The fact that 24-hour uptake was still influenced by the presence of serum suggested the maturation process to last through- out this time period. Serum has previously been described to inhibit lipofection as well as DNA uptake of lipoplexes [30-32]. For PLL-PA, only the linear forms of the DNA were affected by the serum. Given its partial lipophilic characteristic, the difference in the level of uptake may be directly related to the rate of

complex maturation mentioned earlier. The observation that I-DNA is affected to a greater extent than pcr-DNA may be attributed to size differences between the molecules. Larger I-DNA was expected to take longer to reorganize itself into the matured complex; this may cause it to become more susceptible to binding by serum proteins than smaller I-DNA. All polymers resulted in an increase in absolute amount of DNA delivery from 4 to 24 hours, suggesting that the uptake pathway is a rate-limiting process for these carriers. Furthermore, PLL-PA showed a significant increase in absolute amount of DNA delivery in the absence of serum, where a similar increase was absent in Lipofectamine-2000™. Serum thereby affected PLL-PA differently than the Lipofectamine-2000™. The difference in the degree of sensitivity to serum can be accounted for by the nature of the lipid groups (monovalent vs. multivalent; [25], in addition to the polymeric nature of PLL-PA, which contributed to the continued uptake of complexes in the absence of serum.

The transfection results from both 293 cells and rBMSC showed that the supercoiled circular plasmid DNA was more effective topology for transfection than its linearized equivalent of the same molecular weight. This observation was consistent with previous reports [5,33]. Remaut *et al.* attributed better translocation of c-DNA to perinuclear regions for better transgene expression by the c-DNA [33]. We have further investigated the effectiveness of a gene cassette, which is approximately half the size of the linearized plasmid DNA; pcr-DNA was even less effective than I-DNA, even though the number of gene-encoding templates was expected to be twice that of I-DNA or c-DNA (per unit mass basis exposed to the cells). The carrier-DNA interactions (either binding or dissociation) were not expected to be different between the I-DNA and pcr-DNA at a given carrier:DNA ratio, as well as the uptake into the cells (data from Figures 3, 4 and 5). Thus, the difference in transfection efficiency between I-DNA and pcr-DNA cannot be explained from these considerations. The only difference between

these two DNA molecules was in the hydrodynamic diameter of the complexes, where pcr-DNA gave smaller particles compared to l-DNA, but our data on this issue is too limited to probe a correlation between transfection and complex size. The difference observed in transfection could be attributed to intracellular response to the DNA itself. Several factors might come into play, including; (i) different rates of intracellular degradation of the DNAs (the smaller pcr-DNA could be more sensitive to degradation due to lower content of ectopic sites), and (ii) ease of accessibility of the template to transcription factors (the promoter of the smaller pcr-DNA might be more effectively blocked with the carrier as compared to the longer l-DNA). It is also possible that different types of DNA molecules would elicit different metabolic responses. For example, double-stranded l-DNA and pcr-DNA have exposed 5'-phosphate groups on their ends, which resemble damaged DNA. When introduced into cells, these DNA molecules might cause an inhibition of overall gene expression as a protection mechanism against aberrant expression, effectively reducing transgene efficiency. Still other factors may come into play, but this study was not intended to explore the intracellular fate and consequences of exogenous DNA delivery. Further studies on these issues will be conducted in the future to explain the difference in transfection efficiency among different DNA molecules.

4.5 References

- [1] Park T. G., Jeong J. H., and Kim S. W., 2006, "Current status of polymeric gene delivery systems," *Adv Drug Deliv Rev*, **58**(4), pp. 467–486.
- [2] Tiera M. J., Winnik F. O. M., and Fernandes J. C., 2006, "Synthetic and natural polycations for gene therapy: state of the art and new perspectives," *Curr Gene Ther*, **6**(1), pp. 59–71.
- [3] Anada T., Karinaga R., Koumoto K., Mizu M., Nagasaki T., Kato Y., Taira K., Shinkai S., and Sakurai K., 2005, "Linear double-stranded DNA that mimics an infective tail of virus genome to enhance transfection," *J Control Release*, **108**(2-3), pp. 529–539.
- [4] Chen Z. Y., Yant S. R., He C. Y., Meuse L., Shen S., and Kay M. A., 2001, "Linear DNAs concatemerize in vivo and result in sustained transgene expression in mouse liver," *Mol Ther*, **3**(3), pp. 403–410.
- [5] Cherng J. Y., Schuurmans-Nieuwenbroek N. M. E., Jiskoot W., Talsma H., Zuidam N. J., Hennink W. E., and Crommelin D. J. A., 1999, "Effect of DNA topology on the transfection efficiency of poly((2-dimethylamino)ethyl methacrylate)–plasmid complexes," *Journal of Controlled Release*, **60**(2-3), pp. 343–353.
- [6] Kamiya H., Yamazaki J., and Harashima H., 2002, "Size and topology of exogenous DNA as determinant factors of transgene transcription in mammalian cells," *Gene Ther*, **9**(22), pp. 1500–1507.
- [7] Schakowski F., Gorschlüter M., Junghans C., Schroff M., Buttgereit P., Ziske C., Schöttker B., König-Merediz S. A., Sauerbruch T., Wittig B., and Schmidt-Wolf I. G., 2001, "A novel minimal-size vector (MIDGE) improves transgene expression in colon carcinoma cells and avoids transfection of undesired DNA," *Mol Ther*, **3**(5 Pt 1), pp. 793–800.
- [8] van der Aa M. A. E. M., Koning G. A., d'Oliveira C., Oosting R. S., Wilschut K. J., Hennink W. E., and Crommelin D. J. A., 2005, "An NLS peptide covalently linked to linear DNA does not enhance transfection efficiency of cationic polymer based gene delivery systems," *J Gene Med*, **7**(2), pp. 208–217.

- [9] Robertson R. M., Laib S., and Smith D. E., 2006, "Diffusion of isolated DNA molecules: dependence on length and topology," *Proc Natl Acad Sci USA*, **103**(19), pp. 7310–7314.
- [10] Incani V., Tunis E., Clements B. A., Olson C., Kucharski C., Lavasanifar A., and Uludağ H., 2007, "Palmitic acid substitution on cationic polymers for effective delivery of plasmid DNA to bone marrow stromal cells," *J Biomed Mater Res A*, **81**(2), pp. 493–504.
- [11] Rudolph C., Miller R. H., and Rosenecker J., 2002, "Jet nebulization of PEI/DNA polyplexes: physical stability and in vitro gene delivery efficiency," *J Gene Med*, **4**(1), pp. 66–74.
- [12] Varkey M., Kucharski C., Haque T., Sebald W., and Uludağ H., 2006, "In vitro osteogenic response of rat bone marrow cells to bFGF and BMP-2 treatments," *Clin. Orthop. Relat. Res.*, **443**, pp. 113–123.
- [13] Cheng J. Y., van de Wetering P., Talsma H., Crommelin D. J., and Hennink W. E., 1996, "Effect of size and serum proteins on transfection efficiency of poly ((2-dimethylamino)ethyl methacrylate)-plasmid nanoparticles," *Pharmaceutical research*, **13**(7), pp. 1038–1042.
- [14] Escriou V., Carrière M., Scherman D., and Wils P., 2003, "NLS bioconjugates for targeting therapeutic genes to the nucleus," *Adv Drug Deliv Rev*, **55**(2), pp. 295–306.
- [15] Kamiya H., Fukunaga S., Ohyama T., and Harashima H., 2009, "Effects of carriers on transgene expression from plasmids containing a DNA sequence with high histone affinity," *Int J Pharm*, **376**(1-2), pp. 99–103.
- [16] Deniss I. S., and Morgan A. R., 1976, "Studies on the mechanism of DNA cleavage by ethidium," *Nucleic Acids Res*, **3**(2), pp. 315–323.
- [17] Krishnamurthy G., Polte T., Rooney T., and Hogan M. E., 1990, "A photochemical method to map ethidium bromide binding sites on DNA: application to a bent DNA fragment," *Biochemistry*, **29**(4), pp. 981–988.
- [18] Kawaura C., Noguchi A., Furuno T., and Nakanishi M., 1998, "Atomic force

microscopy for studying gene transfection mediated by cationic liposomes with a cationic cholesterol derivative.," FEBS Lett., **421**(1), pp. 69–72.

- [19] Kabanov A. V., and Kabanov V. A., 1995, "DNA complexes with polycations for the delivery of genetic material into cells.," *Bioconjug Chem*, **6**(1), pp. 7–20.
- [20] Arigita C., Zuidam N. J., Crommelin D. J. A., and Hennink W. E., 1999, "Association and dissociation characteristics of polymer/DNA complexes used for gene delivery," *Pharmaceutical research*, **16**(10), pp. 1534–1541.
- [21] Schaffer D. V., Fidelman N. A., Dan N., and Lauffenburger D. A., 2000, "Vector unpacking as a potential barrier for receptor-mediated polyplex gene delivery.," *Biotechnol Bioeng*, **67**(5), pp. 598–606.
- [22] Hawley P., and Gibson I., 1996, "Interaction of oligodeoxynucleotides with mammalian cells.," *Antisense Nucleic Acid Drug Dev.*, **6**(3), pp. 185–195.
- [23] Mislick K. A., and Baldeschwieler J. D., 1996, "Evidence for the role of proteoglycans in cation-mediated gene transfer.," *Proc Natl Acad Sci USA*, **93**(22), pp. 12349–12354.
- [24] Ruponen M., Rönkkö S., Honkakoski P., Pelkonen J., Tammi M., and Urtti A., 2001, "Extracellular glycosaminoglycans modify cellular trafficking of lipoplexes and polyplexes.," *J Biol Chem*, **276**(36), pp. 33875–33880.
- [25] Yang J. P., and Huang L., 1998, "Time-dependent maturation of cationic liposome-DNA complex for serum resistance.," *Gene Ther*, **5**(3), pp. 380–387.
- [26] Rejman J., Conese M., and Hoekstra D., 2006, "Gene transfer by means of lipo- and polyplexes: role of clathrin and caveolae-mediated endocytosis.," *J Liposome Res*, **16**(3), pp. 237–247.
- [27] Medberry P., Dennis S., Van Hecke T., and DeLong R. K., 2004, "pDNA bioparticles: comparative heterogeneity, surface, binding, and activity analyses," *Biochem Biophys Res Commun*, **319**(2), pp. 426–432.
- [28] Rosenecker J., Naundorf S., Gersting S. W., Hauck R. W., Gessner A., Nicklaus P., Müller R. H., and Rudolph C., 2003, "Interaction of bronchoalveolar lavage fluid

with polyplexes and lipoplexes: analysing the role of proteins and glycoproteins," *J Gene Med*, **5**(1), pp. 49–60.

- [29] Farrell L.-L., Pepin J., Kucharski C., Lin X., Xu Z., and Uludağ H., 2007, "A comparison of the effectiveness of cationic polymers poly-L-lysine (PLL) and polyethylenimine (PEI) for non-viral delivery of plasmid DNA to bone marrow stromal cells (BMSC).," *Eur J Pharm Biopharm*, **65**(3), pp. 388–397.
- [30] Vitiello L., Chonn A., Wasserman J. D., Duff C., and Worton R. G., 1996, "Condensation of plasmid DNA with polylysine improves liposome-mediated gene transfer into established and primary muscle cells.," *Gene Ther*, **3**(5), pp. 396–404.
- [31] Escriou V., Ciolina C., Lacroix F., Byk G., Scherman D., and Wils P., 1998, "Cationic lipid-mediated gene transfer: effect of serum on cellular uptake and intracellular fate of lipopolyamine/DNA complexes," *Biochimica et Biophysica Acta (BBA) - Biomembranes*, **1368**(2), pp. 276–288.
- [32] Sakurai F., Inoue R., Nishino Y., Okuda A., Matsumoto O., Taga T., Yamashita F., Takakura Y., and Hashida M., 2000, "Effect of DNA/liposome mixing ratio on the physicochemical characteristics, cellular uptake and intracellular trafficking of plasmid DNA/cationic liposome complexes and subsequent gene expression," *Journal of Controlled Release*, **66**(2-3), pp. 255–269.
- [33] Remaut K., Sanders N. N., Fayazpour F., Demeester J., and De Smedt S. C., 2006, "Influence of plasmid DNA topology on the transfection properties of DOTAP/DOPE lipoplexes," *Journal of Controlled Release*, **115**(3), pp. 335–343.

Chapter 5

Improved transfection efficiency of an aliphatic lipid substituted 2 kDa polyethylenimine is attributed to enhanced nuclear association and uptake in rat bone marrow stromal cell¹

¹A version of this chapter has been published in Hsu C. Y. M., Hendzel M., and Uludağ H., 2011, "Improved transfection efficiency of an aliphatic lipid substituted 2 kDa polyethylenimine is attributed to enhanced nuclear association and uptake in rat bone marrow stromal cell.," *J Gene Med*, 13(1), pp. 46–59.

5.1 Introduction

Gene therapy is a promising therapeutic approach for a wide range of chronic and infectious diseases. The treatment is based on the accurate delivery of nucleic acids to the pertinent cells to correct the physiological abnormalities at the genetic level. Successful gene therapy relies on the development of efficient gene carriers to facilitate the entry of nucleic acid across the plasma membrane. Disarmed viral particles were initially employed for this purpose, but mutagenic and immunogenic concerns prompted the development of safer alternative nonviral gene delivery systems [1]. Cationic polymers such as polyethyleneimine (PEI) have been one of the most promising polymers for nonviral gene delivery as an alternative for viral vectors. The high density of cationic charges on PEI facilitates efficient binding to the anionic phosphate groups on nucleic acids while the abundance of amine groups provides a suitable mean for further functionalization [2]. The latter feature allows various cell compatible ligands to be chemically conjugated to enhance the gene delivery efficiency of the carrier [3-8].

Among the ligands used to functionalize the cationic polymers, grafting lipid moieties such as cholesterol and aliphatic fatty acid to low molecular weight PEI have been shown to be an effective approach to improving the gene delivery and transfection efficiency of the polymer [9-11]. Our lab has pursued this approach to develop a novel water soluble amphiphatic polymer by grafting a series of aliphatic lipids (from C8 to C18) to a low molecular weight (2 kDa) PEI [12]. Among the lipids, the linoleic acid (LA) substitution was found to be particularly advantageous; the resulting polymer, PEI2LA, displayed significant improvement in transfection efficiency in the transformed human embryonic kidney cell line, HEK 293T, over the unmodified PEI2 [12]. Hydrophobic modification through lipid substitution may enhance polymer compatibility with cells by increasing affinity to lipid-based cellular membrane such as the plasma

membranes, to promote subsequent cellular uptake. This was shown to be the case with PEI2LA, where the degree of lipid substitution correlated directly with the uptake efficiency of the polyplexes [12].

Increased affinity to cellular membrane in lipid substituted polymers could also facilitate nuclear uptake of the DNA cargo through association with the nuclear envelope. The nuclear envelope acts as a physical barrier, separating the cytoplasm from the nucleoplasm. The double membrane structure permits passive entry of low molecular weight macromolecules (< 40 nm; [13]) while larger molecules need to be actively transported. Polyplexes with a size range of >100 nm are inherently too large to traverse through the nuclear pore complex embedded in the nuclear envelope and typically do not contain signal elements required to be actively imported. It has been suggested that entry may be opportunistically permitted during mitosis when the nuclear envelope disintegrates [14-17]. That is, the transient removal of the membrane barrier during cell division allows plasmid DNA (pDNA) to be transported into the nucleoplasm. This form of "nuclear uptake" would favor pDNA that are physically close to the nucleus prior to cell division. Thus, lipid-substituted polymer may increase nuclear uptake by maintaining the proximity of pDNA to the nucleus prior to cell division through polyplex association with the membrane. This issue has not been explored with previous lipid-substituted polymers.

A previous study was performed to screen a lipid-modified polymer library, which included PEI2LA polymers, in order to identify effective pDNA carriers. While PEI2LA appeared to be the best carrier to support transgene expression in HEK293T cells, little to no transfection was evident in BMSC in that preliminary study. Thus, PEI2LA was chosen for this study to further explore transfection parameters and enhance its utility for gene delivery to BMSC. Further, we aimed to characterize the intracellular

distribution of the polyplex in order to gain better understanding of the role of lipid substitution in cytoplasmic trafficking and nuclear routing. The pDNA was fluorescently labeled to track the amount of intracellular pDNA and the level of transgene expression simultaneously, which enabled us to directly correlate transfection efficiency with pDNA distribution. We further measured the amount of nuclear associated pDNA using both flow cytometry and confocal laser scanning microscopy to characterize the nuclear trafficking capability of PEI2LA in relation to its unmodified parental molecule PEI2, and branched 25 kDa PEI. We demonstrated here that PEI2LA displayed greater transfection efficiency over PEI2 via enhanced association with the nuclear periphery.

5.2 Materials and methods

5.2.1 Materials

The 2 kDa branched PEI (PEI2; Mn = 1.8 kDa, Mw = 2.0 kDa), 25 kDa branched PEI (PEI25; Mn = 10 kDa; Mw = 25 kDa), Hanks' Balanced Salt Solution (HBSS, with phenol red) and trypsin/EDTA were obtained from SIGMA (St. Louis, MO). The PEI2LA was synthesized according to the synthetic scheme outlined in [12], with LA:PEI2 feed ratio of 0.1. The PEI2LA with an average substitution of 1.2 linoleic acids per polymer was obtained and used for these studies. Opti-MEM® I Reduced Serum Media, Dulbecco's Modified Eagle Medium (DMEM; high and low glucose with L-glutamine), penicillin (10000 U/mL), and streptomycin (10 mg/mL) were from Invitrogen (Grand Island, NY). Fetal bovine serum (FBS) was from PAA Laboratories (Etobicoke, Ontario). The blank plasmid gWIZ (i.e., no functional gene product) and gWIZ-GFP (i.e., Green Fluorescent Protein mammalian expression plasmid) were purchased from Aldevron (Fargo, ND).

5.2.2 Plasmid labeling

The gWIZ-GFP plasmid is a 5757 bp mammalian expression plasmid which contains a modified promoter from the human cytomegalovirus (CMV) immediate early (IE) genes. gWiz-GFP was labeled with the fluorophore Cy5 using the Label IT[®] Tracker[™] Intracellular Nucleic Acid Localization Kit (Mirus Bio, WI) as per manufacturer's instructions. Briefly, a 1:5 (v/w) ratio of dye to nucleic acid reaction mix was prepared and incubated at 37 °C for 1 h. Unbound and free Cy5 molecules were removed by ethanol precipitation after adding 0.1 vol of 5 M NaCl and 2 vol of 100% ethanol. Purified labeled pDNA was then suspended in ddH₂O. Labeling efficiency was determined by calculating the ratio of base to dye using the equation $(A_{\text{base}} * \epsilon_{\text{dye}}) / (A_{\text{dye}} * \epsilon_{\text{base}})$ by measuring absorbance at 260 nm (base) and 649 nm (dye) using the values $\epsilon_{\text{Cy5}} = 250,000$; $\epsilon_{\text{base}} = 6,600$ and $CF_{260} = 0.05$. The contribution of dye to the A_{260} reading was corrected by using the equation $A_{\text{base}} = A_{260} - (A_{\text{dye}} * CF_{260})$. Plasmid DNA labeled using the concentration outlined yielded approximately 300 Cy5 labels per pDNA.

5.2.3 Cell culture and transfection

Rat bone marrow stromal cells (rBMSC) were isolated and cultured as described previously [18,19]. Briefly, cells were isolated from both femurs of 8-week old female Sprague-Dawley rats and pooled to obtain a single suspension. The bone marrow was flushed out with 15 mL of DMEM containing 10% FBS, 50 µg/mL ascorbic acid, 100 U/mL Penicillin and 100 µg/L of Streptomycin (referred to hereon as basic medium). Cells were centrifuged for 6 min at 600 rpm, suspended in fresh basic medium and seeded in a single 75 cm² flask (Sarstedt; Montreal, QC). After medium change on day 3, the cells were trypsinized on day 7 and expanded in 75 cm² flasks (1:4 dilution). The rBMSC passaged between 2-4 generations were used in this study, and were grown in multi-well plates for transfection studies.

5.2.4 Complex preparation

Self-assembled polymer/pDNA polyplexes were formed by first diluting the desired pDNA in 150 mM NaCl; cationic polymers were then added at a polymer-to-pDNA weight ratio of 5 (PEI25; N/P = ~38.7) or 10 (PEI2 and PEI2LA; N/P = ~75.5, assuming a similar MW for these two polymers), mixed using a Vortex mixer and incubated at room temperature for 25 min. The polyplex solution were then diluted with 9 vol of OptiMEM (+ 1% FBS) to bring the final pDNA concentration to 3 µg/mL and incubated for an additional 20 min at room temperature. The diluted polyplex solutions were then added directly to the cells. For multiplexed flow cytometry and confocal laser scanning microscopy, labeled pDNA was mixed with unlabeled pDNA at a ratio of 1:2 before complexation.

5.2.5 Particle size measurement

The hydrodynamic size range of the polymer/pDNA complexes was measured by photon correlation spectroscopy (Zetasizer Nano, Malvern Instruments Ltd, Worcestershire, UK). Polyplexes were prepared at various polymer-to-pDNA weight ratios in 150 mM NaCl with a final volume of 100 µL and incubated for 25 min. The polyplex solutions were then diluted to 1 mL by adding 900 µL of OptiMEM (+ 1% FBS) to bring a final pDNA concentration of 2 µg/mL or a final polymer concentration of 10 µg/mL. Measurements was taken in a heated chamber set at 37 °C, at a wavelength of 660 nm and calculated by using a medium viscosity of 1.140 cP and a refractive index of 1.333 (at 37 °C). Values reported were an average of 12 measurements with 10 seconds interval between each measurement.

5.2.6 Polyplex uptake and transfection efficiency

The polyplexes were prepared as above and then added to rBMSC grown in 6-well plates at a cell density of 70-80%. After 4 hour incubation with the polyplexes, the transfection medium (OptiMEM + 1% FBS) was replaced with the basic medium (DMEM + 10% FBS) and incubated at 37°C until analysis. Processing for flow cytometry were done by first washing the cells twice with $\text{Ca}^{2+}/\text{Mg}^{2+}$ HBSS (without phenol red), then detached from tissue culture plates with 1x Trypsin-EDTA (GIBCO) and subsequently fixed in 3.7% formaldehyde in HBSS. Quantification of pDNA uptake and GFP expression were performed using a FACSCalibur (BD Biosciences); Cy5-labeled plasmid DNA uptake was measured in the FL4 channel using the red diode laser (633nm); GFP fluorescence from the expression of the plasmid DNA was measured in the FL1 channel using the 488 nm blue laser. Analysis was performed by calibrating gating to the negative control (i.e. polymer complexes prepared with gWIZ) such that the auto-fluorescent cell population represented 1-2% of total cell population.

5.2.7 Nuclei isolation and quantification of nuclear-associated pDNA

To release nuclei from the cells, cells were detached from the tissue culture plates using 1x Trypsin-EDTA as described above. Trypsin reaction was stopped by adding a basic medium with 10% FBS. Cells were then pelleted by spinning at 150 x *g* for 5 min, re-suspended in a hypotonic solution (5 mM NaCl, 10 mM Tris-Cl pH 7.4) and incubated on ice for 15 min to allow the cells to swell. Cells were subsequently lysed by adding a Cell Lysis Buffer (10 mM NaCl, 5 mM MgCl_2 , 10 mM Tris-Cl pH 7.4, and 0.33% NP-40) to release nuclei from the cytoplasm. Purity and integrity of the nuclei were confirmed under light microscope.

5.2.8 Confocal microscopy and image quantification

Rat BMSC were seeded onto No. 1 ½ glass coverslip measuring 18 mm x 18 mm (Fischer Scientific) in 6-well plates and transfected as described above. At designated time point, cells were fixed in 3.7% formalin in HBSS for 15 min and washed with HBSS. 12-bit images were acquired using an inverted Zeiss LSM 710 Laser Scanning Confocal Microscope through a 1.3 N.A. 40x Plan Fluor oil-immersion objective with a field view of 103.7 nm/pixel x 103.7 nm/pixel. Cy5-labeled pDNA was excited by the 5 mW HeNe-laser (633 nm); GFP was excited by the 25 mW Ar-laser (488 nm). Nuclei were stained with Hoechst 33528 (300 ng/mL) for 15 minute and excited by the 405 nm laser. Quantification of images acquired by CLSM were performed using NIH ImageJ with a collection of plugins for microscopy analysis downloaded from the McMaster Biphotonics Facility (MBF_ImageJ, <http://www.macbiophotonics.ca/>). The stained nuclei were used to define the region of interest (ROI) to derive fluorescent intensity values from the Cy5 channel and used to calculate the percent of nuclei with pDNA associated as well as the distribution of pDNA, after a threshold value was defined to take into account auto fluorescence and background noise from the images.

5.2.9 Statistical analysis

Where indicated, the data is summarized as the mean \pm standard deviation of triplicate measurements. Unpaired Student's t-test was used to assess statistical differences ($p < 0.05$) between the group means.

5.3 Results

5.3.1 Polyplex sizes in transfection medium

The hydrodynamic sizes of the polyplexes were measured to determine any functional relationship between particles sizes and the level of transgene expression.

Measurements were taken in conditions that were representative of those carried out in transfection. That is, complexes were first prepared in 150 mM NaCl then subsequently diluted in OptiMEM supplemented with 1% FBS at 37 °C to give the same final DNA concentration as those applied in tissue culture. In the absence of complexes, OptiMEM + 1% FBS gave two peaks in the intensity histogram at mean sizes 60 and 10 nm (**Figure 5.1A**). No stable measurements can be taken with OptiMEM only, and hence, these two peaks were likely due to serum protein from FBS. When polyplexes were added to the media, three peaks were observed in the intensity histogram (**Figure 5.1B**). Two of the peaks are below 100 nm, similar to the sizes of the two peaks observed in OptiMEM 1% FBS only and thus were presumed to be the serum protein. The additional third peak had a much larger size distribution (>200 nm) and is taken as the peak corresponding to the polyplexes. We noted that the peaks corresponding to the serum protein shifted in sizes in the presence of polyplexes, depending on the polymer-to-pDNA weight ratios used to prepare the polyplexes. This suggests that interaction between proteins in the serum and the polyplexes may take place in the media, altering the overall sizes of the polyplexes during transfection.

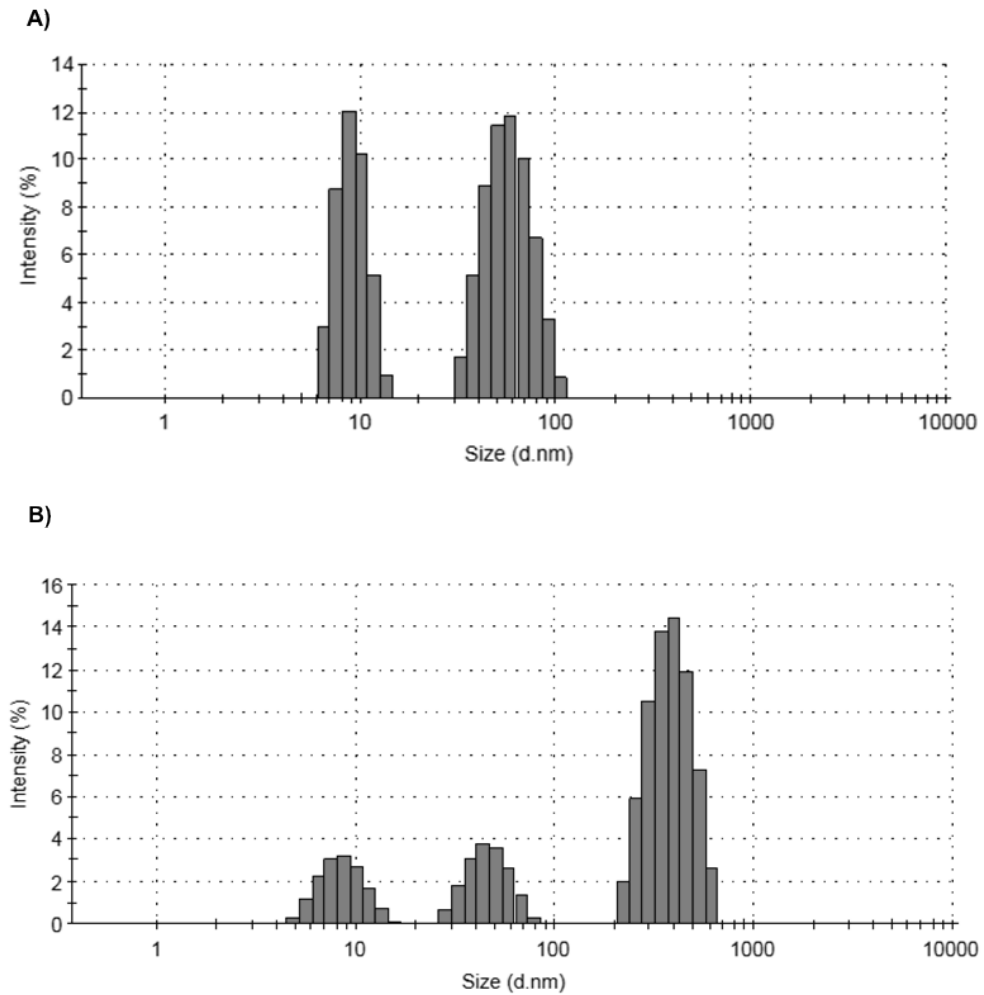


Figure 5.1

Typical intensity histogram of particle sizes.

(A) OptiMEM with 1% FBS with no particles. **(B)** PEI25/pDNA polyplex at polymer-to-pDNA weight ratio of 2.5 at a pDNA concentration of 2 $\mu\text{g/ml}$, in OptiMEM + 1% FBS. Note the third peak with the highest intensity and a mean size of 210 nm. This peak was not present in the previous figure and is taken as the peak corresponding to the PEI25 polyplexes.

Complexes were prepared at different polymer-to-pDNA weight ratios by adjusting either the concentration of pDNA or the concentration of the polymers. The hydrodynamic sizes of the resulting polyplexes are summarized in Table 1. The particle sizes for PEI2LA (10) were not significantly different from PEI2 (10) at the weight ratio used for transfection. Polyplexes of PEI25 (5) were, however, approximately 4 times smaller than polyplexes of PEI2LA (10) and PEI2 (10) (210 nm vs. 947 nm and 834 nm, respectively). The same size differences were observed when the amount of DNA was reduced, while maintaining the same relative polymer-to-pDNA weight ratio, where PEI25 polyplexes particles were again approximately 4 times smaller than PEI2 and PEI2LA particles (146.2 nm vs. 626 nm and 634 nm respectively). Thus, the relative polyplexes sizes between PEI2, PEI2LA and PEI25 did not appear to be affected by the concentrations of the polymers or the pDNA. When the concentration of pDNA was reduced, the particle sizes were comparatively smaller, suggesting that the size of the polyplexes may reflect the amount of DNA packed per particle. This trend was only observed at the highest weight ratios tested. At lower ratios, polyplexes tended to form clusters of aggregates that ranged in sizes with varying degree of aggregation. The aggregation would affect accurate calculation of individual particles sizes and may account for the lack of correlation between particle sizes and DNA concentrations at the lower weight ratios. Increasing the polymer:pDNA ratio, however, generally reduced the particle sizes for all complexes, indicating a stabilizing effect of the excess polymer on particle sizes.

5.3.2 Correlation between pDNA uptake and transgene expression

To evaluate the relationship between pDNA uptake and transgene expression, multiplexed flow cytometry were carried out to measure the amount of Cy5-labeled pDNA internalized by the cell and the subsequent GFP fluorescence expressed. To

compare the efficacy among PEI2, PEI2LA and PEI25, each polyplex was prepared at the polymer-to-pDNA weight ratio that were previously determined to be the most effective for transfection. The weight ratios used for each polymer are indicated in parenthesis in each figure legend.

Transfection efficiency is summarized by the level of transgene expression (**Figure 5.2**, mean fluorescence of GFP-positive cells) and the percentage of transfected cell (percentage of GFP-positive cells). The highest level of transgene expression was observed 24 hours after polyplexes were applied to the cell (**Figure 5.2A**). The highest percentage of transfected cells was observed on Day 3 for PEI2 and PEI2LA and on Day 7 for PEI25 (**Figure 5.2B**). The levels of transgene expression from PEI2LA and PEI2 transfected rBMSC were significantly higher than PEI25 ($p < 0.05$). PEI25 and PEI2LA were able to transfect significantly higher percentages of cells than PEI2.

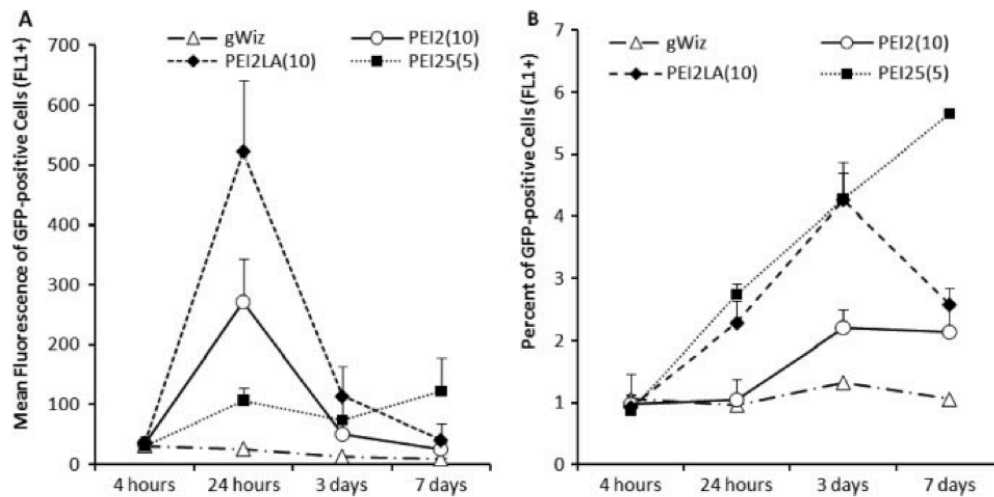


Figure 5.2

Transfection efficiency with PEI2, PEI2LA and PEI25 polyplexes in rBMSC

collectively represented by **(A)** the mean fluorescence of GFP-positive cells and **(B)** the percentage of transfected cells (FL1+) over a 7-day experimental period. Analysis was carried out by calibrating the auto-fluorescent value against rBMSC treated with gWIZ polyplexes, which had no reporter gene in the expression plasmid. Maximum GFP fluorescence intensity was observed on day 1, although the percentage of GFP-positive cells was gradually increased over the study period

The amount of pDNA uptake for each carrier is summarized in **Figure 5.3A**. The mean fluorescence of Cy5-positive cells declined over the one-week experimental period. The drop in pDNA content may be a result of cell division, decrease in fluorescent intensity over the fluorophore half-life time and/or pDNA degradation by intracellular nucleases. There was no significant difference in the amount of pDNA uptake between PEI2 and PEI2LA or between PEI2 and PEI25. By Day 3, the amount of pDNA in cells was ~2-fold lower with PEI2LA complexes when compared to PEI2 and PEI25 (2.2-fold and 2.1-fold, respectively). The percentage of cells with pDNA uptake were greater than 90% for all carriers from Day 1 to Day 3 and showed no significant difference between carriers (data not shown).

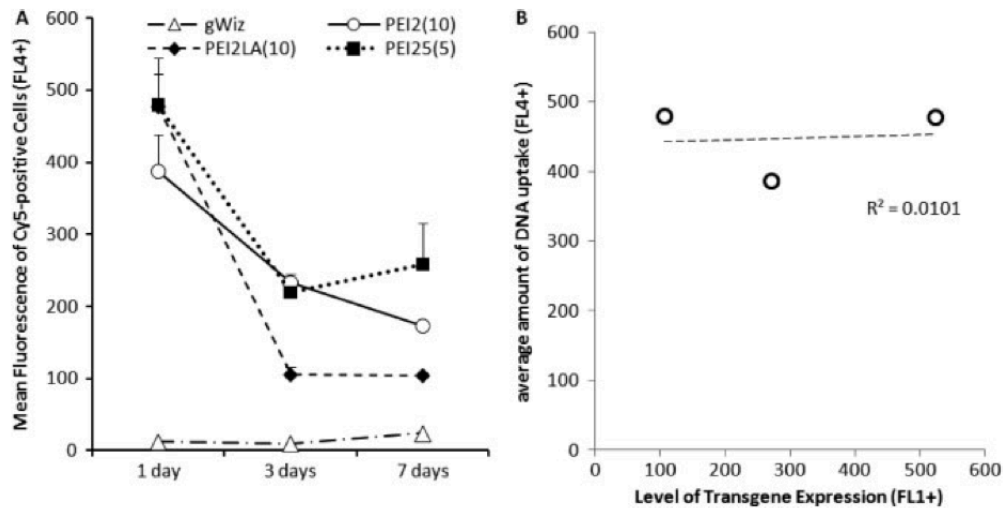


Figure 5.3

The amount of cellular uptake of Cy5-fluorophore labeled pDNA polyplexes

in rBMSC on days 1, 3 and 7. **(A)** The amount of pDNA uptake in Cy5-positive cells (FL4+) and **(B)** the correlation between the amount of pDNA (FL4+) and the level of transgene expression (FL1+) on day 1. There was a gradual reduction of pDNA from day 1 and a lack of correlation between the pDNA uptake and GFP expression

The relationship between the level of transgene expression and the amount of pDNA internalized on day 1 is shown in **Figure 5.3B**. An R^2 value of 0.0101 was obtained, suggesting there was no correlation between GFP expression and pDNA uptake at this time point. We did not perform the analysis for the other time points since the mean GFP fluorescence declined after day 1 to background levels, which might be associated with large errors. A correlation between the GFP fluorescence and pDNA uptake at the single cell level was also analyzed based on a scatter plot of fluorescent intensity from the FL1 (GFP expression) and FL4 (pDNA uptake). Representative plots for each of the carrier are shown in **Figure 5.4**. All GFP-expressing cells had pDNA uptake and were found in the top-right quadrant of the 2D plot. However, there was no apparent relationship between the intensity of GFP fluorescence and the amount of Cy5-labeled pDNA uptake. This further suggests that while DNA uptake is a pre-requisite for transfection, the amount of DNA uptake was not correlated with the level of transgene expression.

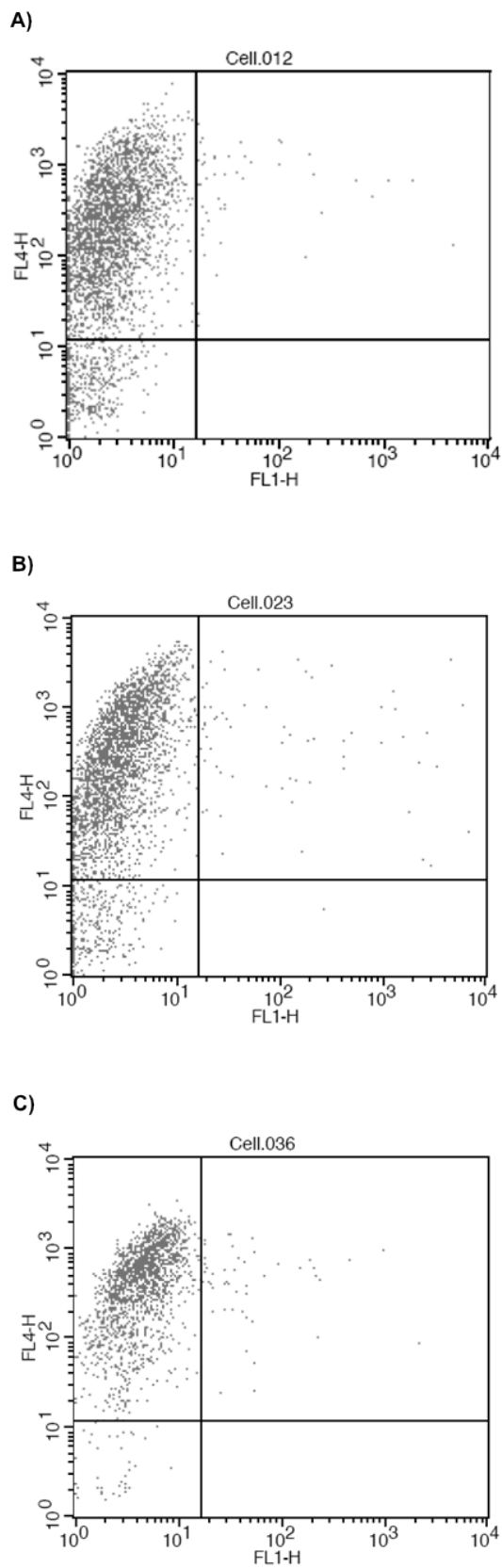


Figure 5.4
Two-dimensional histogram plotted with fluorescent intensity values
 from the FL1-H (GFP) and FL4-H (Cy5-labeled pDNA) channels of rBMSC treated with polyplexes of (A) PEI2 (B) PEI2LA and (C) PEI25 as measured by flow cytometry. The horizontal-vertical perpendicular lines in the graph divides cells into populations, which represents cells with no pDNA uptake and no GFP expression (bottom left), cells with GFP-expression but no pDNA uptake (bottom right), cells with pDNA uptake but no GFP-expression (top left) and cells with pDNA uptake and GFP-expression (top right). Note the scatter distribution of dots in the top right quadrant, which indicates no strong correlation between GFP fluorescence and pDNA uptake.

5.3.3 Nuclear-associated pDNA and transgene expression

The conditions used to release nuclei from whole cells were optimized to obtain intact nuclei that were free of cytoplasmic debris, as visualized inspected under phase contrast microscope, and robust enough to be analyzed with a flow cytometer. The rBMSC were on average significantly larger in size compared to typical cultured cell lines such as HEK 293T (19 microns vs. 13 microns). The relatively higher volume ratio of cytoplasm-to-nuclei makes purifying nuclei technically challenging. We employed a hypertonic shock treatment prior to cell lysis in order to loosen and dilute the cytoplasm, followed by treatment with low concentration of non-ionic detergent in the presence of a divalent cation. A typical nucleus released into suspension using this protocol is shown **Figure 5.5**. While this treatment worked to significantly improve the purity of nuclei, a small percentage of nuclei might still have had cytoplasmic debris associated. Additional measures to counter these contaminants were done through selective gating following FACS. Nuclei associated with cytoplasmic debris were presumably larger than free nuclei, which would translate into a rightward shift on the forward scatter histogram (FSC-H). A typical scatter plot for nuclei is shown in **Figure 5.6**. Free nuclei produced a distinct population concentrated around the lower end of the FSC, enabling the larger cytoplasm associated contaminating nuclei to be excluded from the gated population.



Figure 5.5
Representative images of isolated intact nuclei from rBMSC viewed under a phase contrast microscope.

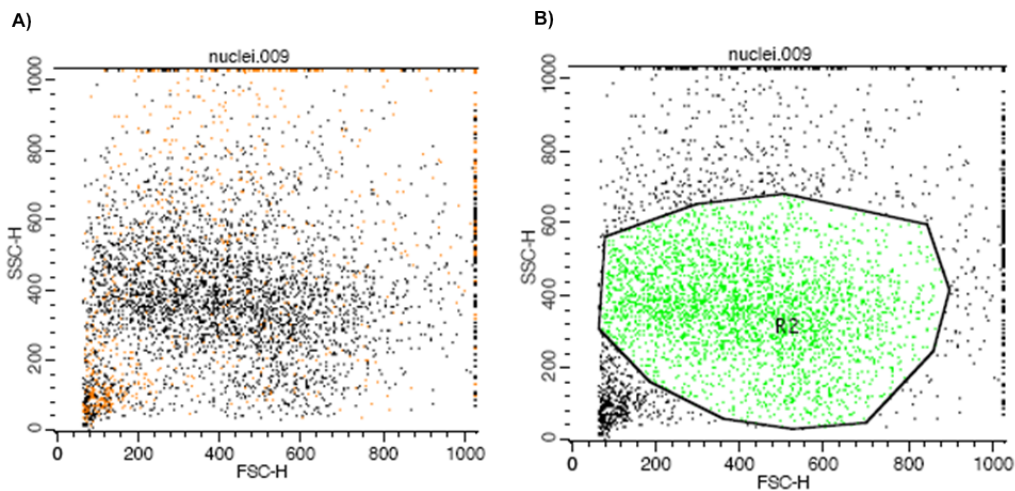


Figure 5.6
Typical forward scatter (FSC-H) and side scatter (SSC-H) flow cytometry analysis of intact nuclei from rBMSC treated with PEI2LA complexes; cells were treated with 0.33% NP-40 to release nuclei from the cell. **(A)** raw nuclei scatter. The dense black dot region represents the majority of the nuclei, whereas orange dots near the border lines represent nuclei with cytoplasmic debris contamination. **(B)** R2 (in green) shows the gate applied to final analysis of pDNA-associated nuclei. In general, singlet of intact nuclei had similar SSC and FSC profile and was found concentric in the lower left region of the graph. By contrast, multipliants and contaminated nuclei were irregular in shapes and sizes and were found scattered near the borders of the graph.

To evaluate the correlation between nuclear-associated pDNA and transgene expression, a portion of the cells used for multiplexed flow cytometry described above were processed for nuclei extraction. The amount of pDNA associated with nucleus is summarized in **Figure 5.7A**. In general, nuclear-associated pDNA declined rapidly over a one week period and was near background level by Day 7. The amount of pDNA associated with the nucleus was highest in PEI2LA polyplexes at 24 hours and was significantly greater than either PEI2 or PEI25 polyplexes ($p < 0.05$). The relationship between the amount of nuclear-associated pDNA and the level of transgene expression was shown in **Figure 5.7B**. An R^2 value of 0.8362 was obtained, suggesting a high correlation between the two parameters.

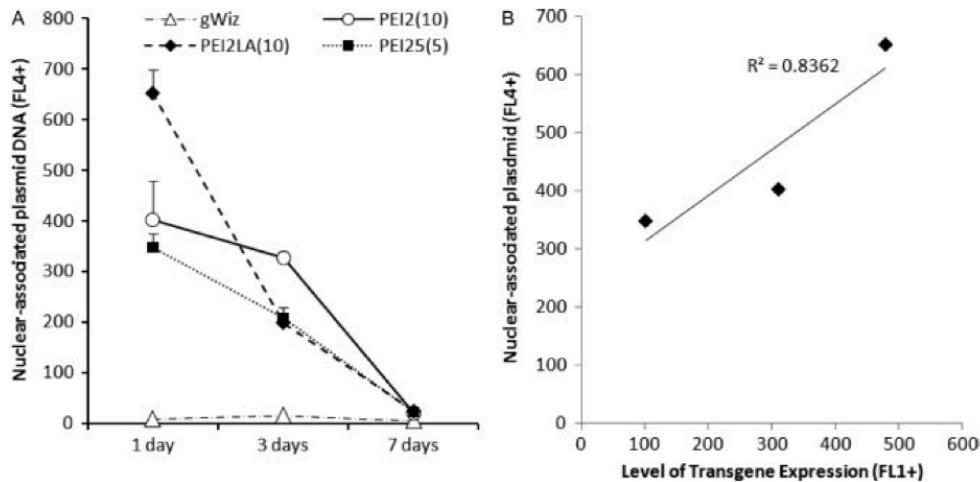


Figure 5.7

The amount of nuclear-associated Cy5-labeled pDNA in rBMSC

The percentage of nuclear-associated pDNA at days 1, 3 and 7 (**A**) and the correlation between the amount of nuclear-associated pDNA (FL4+) and level of transgene expression (FL1+) on day 1 (**B**). Similar to cellular uptake (Figure 5.2A), there was a gradual reduction in nuclear associated pDNA but a good correlation between the nuclear associated pDNA and the GFP expression

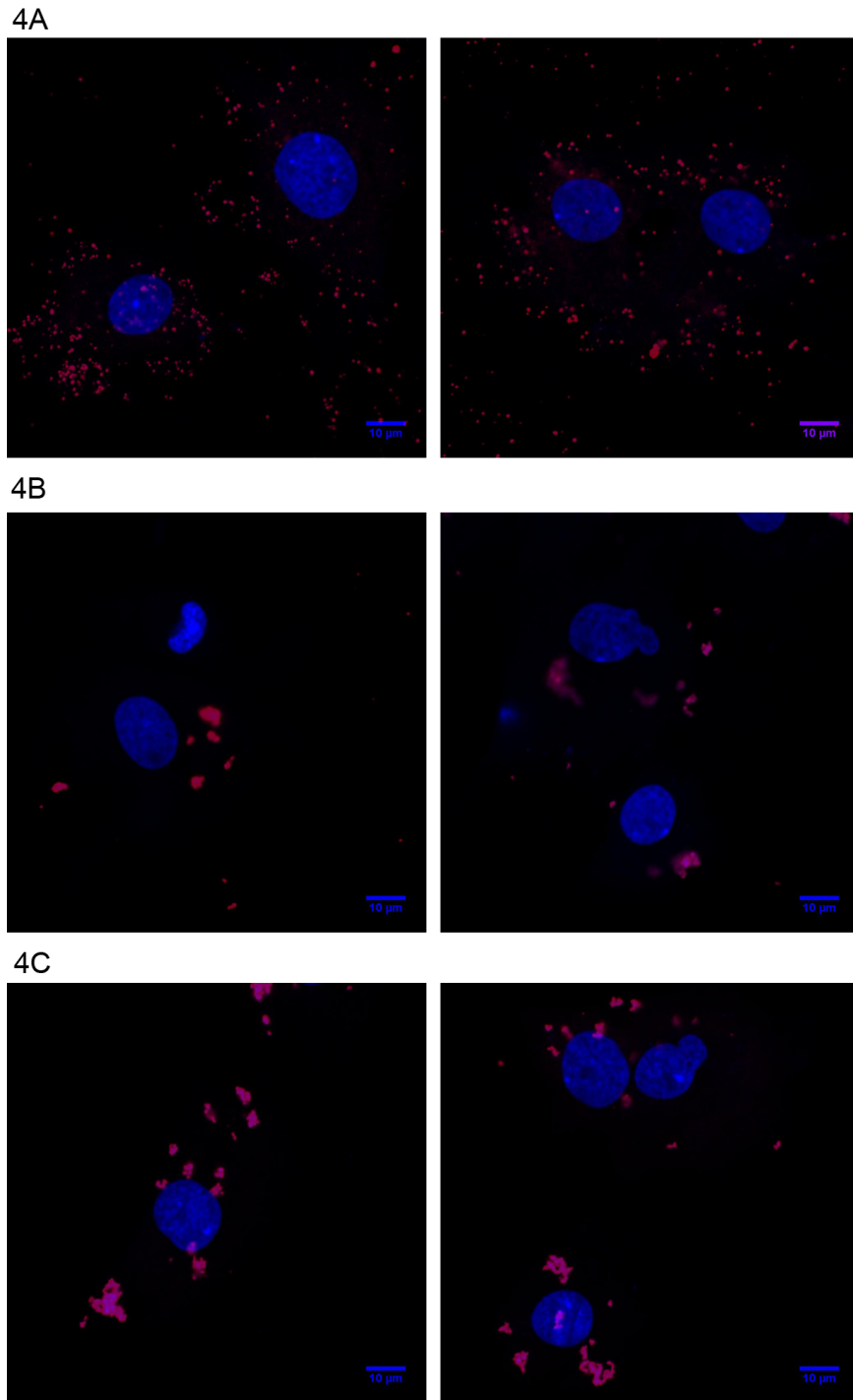


Figure 5.8
 CLSM showing typical images of rBMSC nuclear-associated pDNA at 4 h after incubation with polyplexes of **(A)** PEI25 **(B)** PEI2 and **(C)** PEI2LA. Nuclei are stained with Hoechst 33258. Post image processing was applied to display the nuclei in blue and Cy5-labeled pDNA clusters in red–purple. Note the dispersed distribution of PEI25 polyplexes, unlike the clustered distribution of PEI2 and PEI2LA polyplexes (scale bar = 10 μm)

5.3.4 CSLM image quantification of nuclear-associated plasmid DNA

To further support the data obtained from flow cytometry, we examined the nuclear association of pDNA using CLSM. Representative images of the sub cellular distribution of the polyplexes relative to nuclei are shown in **Figure 5.8**. With PEI25 polyplex, the particles were relatively small and densely distributed throughout the cell; many of the particles could be seen in and around the nuclear periphery and inside the nucleus (**Figure 5.8A**). In contrast, PEI2 polyplexes displayed aggregate-like pDNA clusters with only a few large particles sparsely distributed in the cytosol (**Figure 5.8B**). PEI2LA polyplexes exhibited similar clustered like pDNA aggregates as PEI2 polyplexes, however, the morphology of the fluorescent particles had a bundled filamentous appearance (**Figure 5.8C**). The relative sizes of the particles were consistent with the particle sizes obtained from the photon correlation spectroscopy.

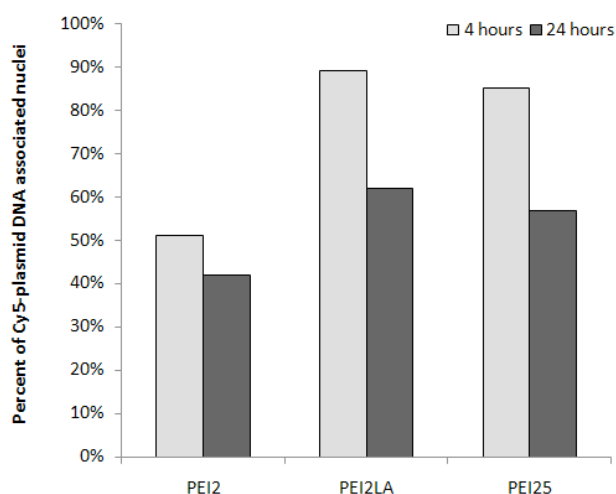


Figure 5.9

Percentage of nuclei with pDNA associated

at 4 and 24 h after initial incubation with the PEI2, PEI2LA or PEI25 polyplexes as quantified by image analysis. Images were optically sliced using CLSM to obtain the section with the thickest nuclei density. pDNA-positive nuclei were identified by defining the nucleus as the region of interest (ROI); nuclei which had a fluorescent value above the arbitrary defined background was scored as positive (n = 34–66). Note the better nuclear association of pDNA as a result of delivery with PEI25 and PEI2LA

To systematically evaluate the extent of nuclear uptake of pDNA, images acquired from random regions on the glass slide were quantified for percent of nuclei positive for pDNA and the amount of pDNA associated to each positive nucleus. The number of cells sampled for quantification ranged from $n = 40$ to 55. The percentage of nuclei with pDNA association (pDNA+ nuclei) is summarized in **Figure 5.9** for 2 incubation periods (4 and 24 hours). Both PEI2LA and PEI25 treated cells had significantly higher percentage of nuclei with pDNA associated compared to PEI2 at 4 hours (89%, 85% and 51%, respectively). The amount of pDNA associated with each nucleus for each polymer was further calculated and tabulated into a box plot histogram (**Figure 5.10**). At 4 hours, the average fluorescent intensity of PEI25 complexed pDNA clusters was 61.9, which was significantly lower than PEI2 and PEI2LA, each with an average intensity value of 92.5 and 148.0, respectively. A similar trend was observed at 24 hours as well, where the average fluorescent intensity of PEI25 complexed pDNA was lower than both PEI2 and PEI2LA (75.8 versus 116.9 and 184.5, respectively). In terms of distribution, PEI25 had an approximately symmetrical interquartile range with a median of 58.4 at 4 hours, whereas both PEI2 and PEI2LA had larger inter-quartile region with median values of 62.6 and 105.3, respectively and displayed positively skewed distributions. For PEI25, the third quartile fell in the range 58.8 to 70.9, a much lower and narrower range than PEI2LA, which ranges from 105.3 to 203.1. At 24 hours, a similar trend continued, but the interquartile range for each polymer was narrower than at 4 hours. PEI2LA still has the highest mean value (186.3) follow by PEI2 (117.3), with the lowest being PEI25 (75.9). Taken together, these data showed that while PEI25 polyplexes were able to associate with more nuclei than PEI2, each nucleus had low amounts of pDNA associated. The majority of nuclei associated with PEI2LA polyplexes had a significantly greater amount of pDNA than PEI25 polyplexes.

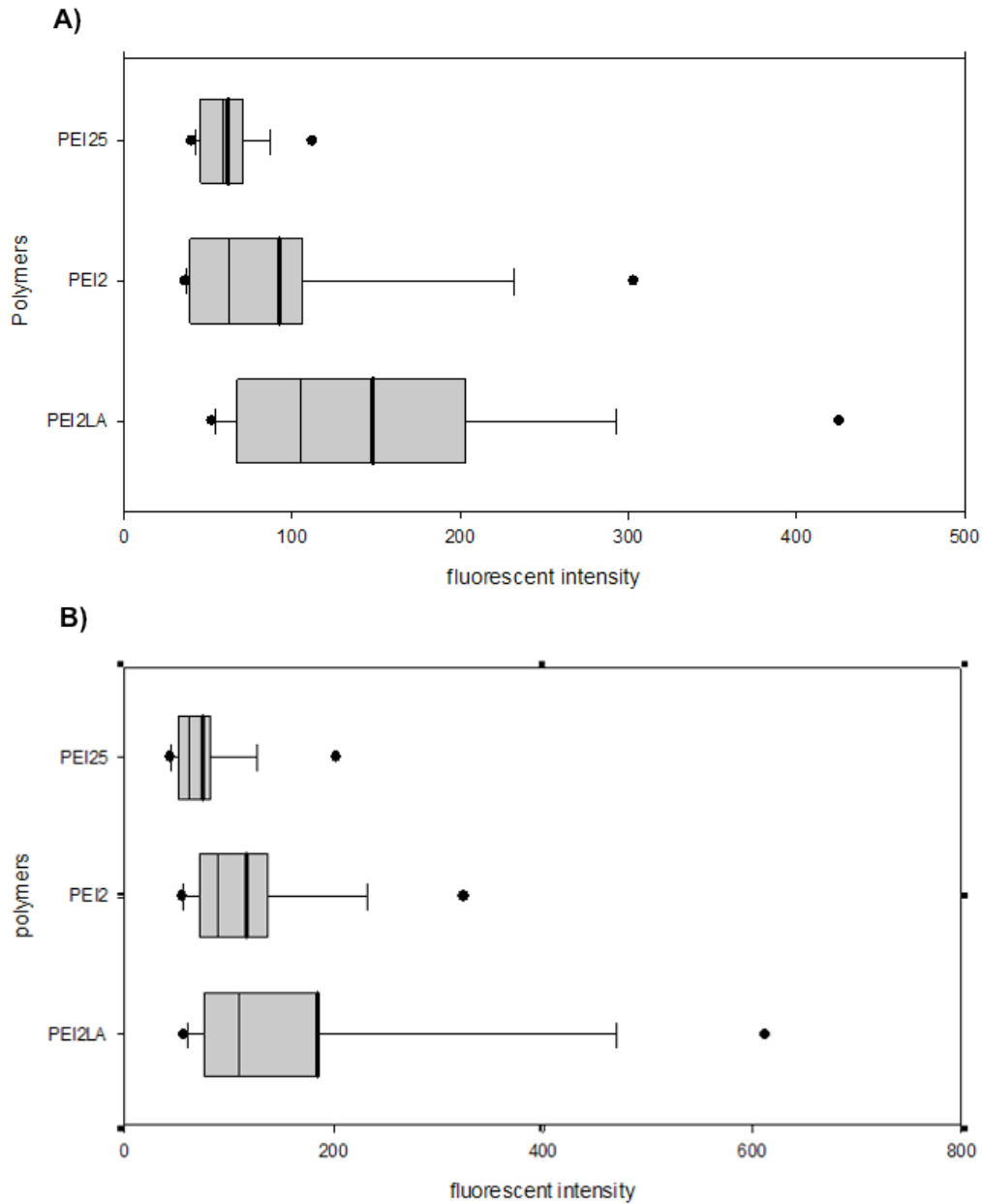


Figure 5.10
Box plot histogram distribution in fluorescent intensity of pDNA associated with nuclei from rBMSC

at 4 h (A) and 24 h (B) after initial exposure with polyplexes of PEI2, PEI2LA and PEI25. The data were derived by quantitating images acquired by CLSM. Grey shaded boxes represent the middle 50% of the data range, and the thick solid line in the box denotes the mean fluorescent value; black solid circle-dots denote the minimum and maximum values and define the range. Note that PEI2LA had the highest mean value and the largest range, whereas PEI25 had the lowest mean and the smallest range at both 4 h and 24 h

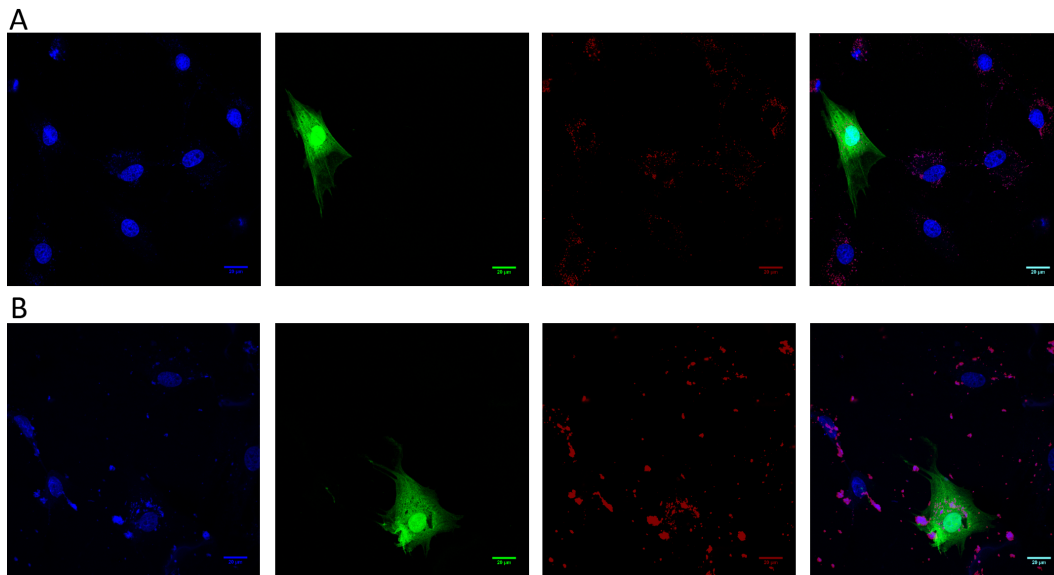


Figure 5.11

Representative CLSM images of GFP-positive (GFP+) cells transected

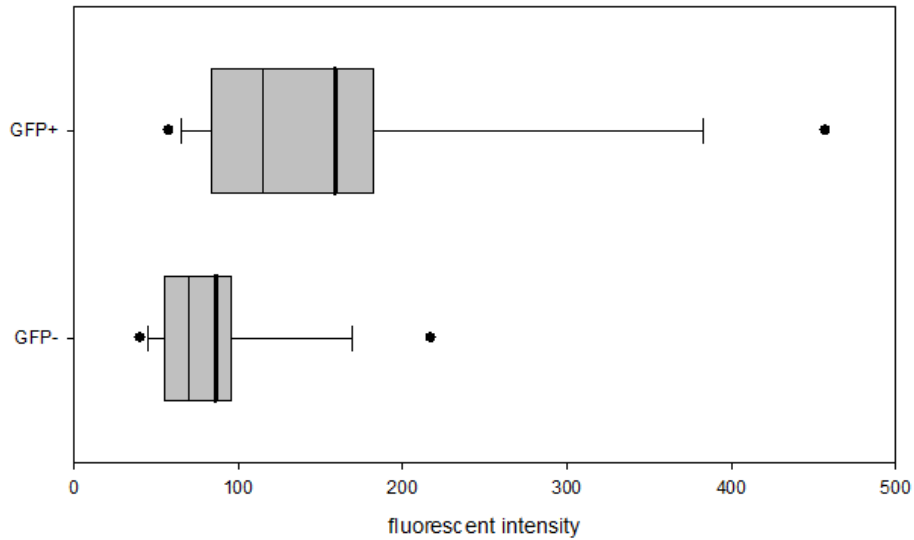
with **(A)** PEI25 and **(B)** PEI2LA. Nuclei were stained with Hoechst 33258 and the pDNA were labeled with Cy5. Post image processing was performed to show the nuclei in blue (left column), GFP in green (second column from left) and pDNA cluster in red (third column from left). Composite images are shown on the right column. (scale bar = 20 μ m). Note the dispersed PEI25 polyplexes in contrast to the aggregated, cluster-like appearance of PEI2LA polyplexes

5.3.5 Sub-cellular distribution of pDNA in GFP Positive and Negative Cells

Using the Cy5-labeled pDNA, we were able to perform multiplexed confocal microscopy to visualize both GFP expression and pDNA localization simultaneously. Using this dual labeled technique, we wanted to see if there was a difference in the nuclear distribution of pDNA between GFP positive cells (GFP+) and GFP-negative (GFP-) cells. Representative confocal images of GFP-expressing cells on Day 1 from the regions sampled are shown in **Figure 5.11**. Similar to particles observed on Day 1, PEI25 polyplexes were smaller and more uniformly distributed throughout the cell (**Figure 5.11A**) than PEI2LA, whose complexed pDNA clusters were aggregated, string-like and punctate in distribution (**Figure 5.11B**). The number of cells sampled for quantification ranged from $n = 34$ to 61 for PEI2LA and PEI25. It had been demonstrated elsewhere that 30 cells are sufficient to draw a general conclusion from

the statistical point of view [20]. However, we were not able to perform statistically significant distribution comparison for PEI2 because there were not enough transfected cells. The fluorescent intensity distribution box plot histogram for PEI25 and PEI2LA are shown in **Figure 5.12**. In general, the distributions of nuclear-associated pDNA in GFP+ cells were positively skewed and had a much larger range than GFP- cells. Further, in both polymers, the mean fluorescence values of the GFP+ distributions were higher than GFP- (marked bold lines in each box plot). These data suggest that the majority of the GFP+ cells had higher pDNA associated with their nuclei as compared to GFP- cells.

A)



B)

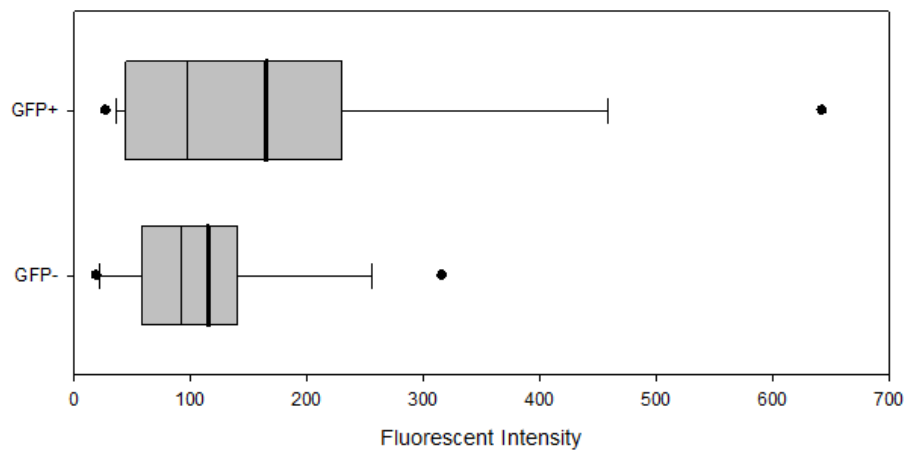


Figure 5.12

Box plot histogram distribution in fluorescent intensity of pDNA associated with nuclei between transfected cells (GFP+) and non-transfected cells (GFP-)

at 24 h after exposure to polyplexes of (A) PEI25 and (B) PEI2LA. Grey shaded boxes represent the middle 50% of the data range and the thick solid line in the box denotes the mean fluorescent value; black solid circle-dots represent the minimum and maximum values, which together define the range of the distribution. Note in both PEI25 and PEI2LA, the GFP+ population had greater mean values and a larger range than GFP-. In addition, the GFP+ distribution was positively skewed

5.4 Discussion

We previously demonstrated that the ineffective cationic polymeric gene carrier PEI2 can be modified into an effective transfection agent through lipid substitution with linoleic acid [12]. In this study, we provided a mechanistic look at the intracellular kinetics of the lipid modified polyplexes with respect to trafficking to the nuclear periphery. We employed a dual modality approach using a combination of high-throughput flow cytometry and CLSM to characterize the intracellular trafficking of polyplexes. A key aspect of this approach was the multiplexed fluorescent labeling, which allowed us to quantitatively correlate pDNA with transgene expression directly. We demonstrated that improved transfection efficiency seen in PEI2LA was due to enhanced trafficking and association with the nuclear periphery, which is thought to reflect nuclear uptake of the transgene during the transient breakdown of nuclear envelope in mitosis. Further, transgene expression was correlated with nuclear-associated pDNA, and not cellular pDNA uptake, consistent with findings reported previously for other nonviral gene carriers in the immortalized HeLa cells [21,22]. The differences in the level of transgene expression between PEI2LA and PEI25 appeared to be correlated with the size of the polyplexes, which may reflect the amount of pDNA packed per particle, and thus the amount of template available for expression. The distribution in the fluorescent intensity of pDNA associated nuclei among GFP-expressing transfected cells was positively skewed with a concurrent rightward shift towards higher average than those apparent non-expressing or low expressing cells, suggesting a transgene expression dependency on template copy number.

Post-translational modifications of endogenous proteins are crucial for protein trafficking to various sub-cellular compartments. Lipid modification is one of the strategies employed by the cell to provide additional functional and regulatory control beyond genomic information to maintain intracellular homeostasis. For example,

proteins modified with the lipid palmitate, allows targeting to specialized membrane microdomains involved in synaptic scaffolding, signaling and cytoskeletal proteins [23]. Palmitoylation may act as a replacement for membrane spanning protein domains by serving as the interface to the hydrocarbon core of the lipid bilayer. Thus, lipid moieties may act as a membrane anchor to enhance the hydrophobicity of proteins and contributes to their membrane association [24]. In a similar fashion as lipid-modified proteins, lipid-modified cationic polymers may facilitate association of polyplexes to various membrane bound sub-cellular compartments, including the nucleus. Indeed, we have observed an increase in the amount of nuclear-associated pDNA with PEI2LA complexes compared to its unmodified parental molecules, PEI2. However, it is reasonable to infer that the hydrophobic interaction is a non-specific event and that the positively-charged polyplexes may also interact with other negatively-charged lipid moieties on other membrane-bound organelles such as the endoplasmic reticulum, Golgi complex, and mitochondria [25]. Therefore, the nuclear association of the polyplexes may be limited by non-specific binding to other intracellular compartments. This issue needs to be further explored and, if significant, strategies to improve specific binding of polyplexes with the nuclear membrane may further increase transfection efficiency.

It is generally held that the strong correlation between nuclear associated pDNA and transfection efficiency is due to the spatial proximity of the transgene to the nucleoplasm, which increases the probability of pDNA nuclear translocation during mitosis. That is, during prophase when the nuclear envelope is transiently broken down, the absence of the physical barrier grants pDNA access to nucleoplasm for it to bind to chromatin and/or nuclear proteins. This allows pDNA to be tethered onto nuclear materials and be incorporated into the nucleus following telophase, when the nuclear envelope reassembles. However, recent evidence suggests that the

breakdown of nuclear envelope may not be necessary for nuclear translocation. Kamiya et al. investigated the nuclear uptake of lipoplexes in the presence of intact nuclear membrane and observed that some pDNA appeared to extend through the nuclear membrane in the aggregated form, which were much larger than the nuclear pore complex, similar to our observation of PEI2LA polyplexes in CSLM. The author reasoned that lipoplexes with the nuclear membrane and the electrostatic interaction between the complex and the membrane releases pDNA into the nucleus [26]. Such a fusion and dissociation event may also take place with lipopolyplexes employed in this study.

The intensity of GFP fluorescence from cells transfected with low molecular weight PEIs (PEI2LA and PEI2) was consistently higher than those transfected with PEI25, indicative of higher transgene expression activity from the former two carriers. This may be accounted by the differences in the binding affinity to pDNA. The level of transgene expression has been shown to be directly correlated with vector unpacking of DNA; Itaka et al., (2004) found that the disparity in transfection efficiency between linear PEI and branched PEI was directly correlated with their pDNA dissociation kinetics [27]. Similarly, higher transfection efficiencies seen in low molecular weight polyplexes was attributed to their ability to dissociate and decondensed DNA more readily than high molecular weight polyplexes [28,29]. While we did not observe any difference in the dissociation kinetics between PEI2 and PEI25 previously, we did see a stronger pDNA binding with PEI25 [12] and could explain the lower level of transgene expression observed with PEI25 complexes.

A second explanation for the difference in transgene expression among carriers is the amount of pDNA packed per particle. With both DLS and CLSM, we observed significantly larger clusters of pDNA in low molecular weight PEI polyplexes when

compared to PEI25 polyplexes. Because the pDNA used in this study was covalently labeled with a fluorophore, the intensity of the fluorescence was presumed to be proportional to the amount of pDNA present. The observation that PEI2 and PEI2LA complexes had larger pDNA clusters suggests that there are more molecules of pDNA per cluster. The relationship between particle size and pDNA content was also verified under DLS; at a given polymer-to-pDNA weight ratio, when the pDNA concentration was reduced, the hydrodynamic sizes of the complexes became smaller, suggesting fewer pDNA molecules was packed per polyplex on average. Thus, the higher level of transgene expression seen in low molecular PEIs may be due to more copies of pDNA packed per particle available for transgene expression than PEI25 with smaller, fewer templates.

A third explanation supplementary to the pDNA cluster size is the distribution in the amount of pDNA associated with each nucleus. Nuclei from cells treated with PEI25 polyplexes had much lower fluorescent intensity than either PEI2 or PEI2LA. In fact, even though PEI2LA and PEI25 treated cells had approximately same percent of nuclei with plasmid DNA, the intensity of fluorescently labeled DNA were much higher with PEI2LA. In other words, there was more DNA associated with each nucleus from cells treated with PEI2LA polyplexes than PEI25. This suggests that more DNA is available for subsequent nuclear translocation and transgene expression, leading to higher transfection efficiency.

We further examined the nuclear association of pDNA between GFP+ and GFP- cells to determine if the heterogeneity in transgene expression is attributed to the amount of pDNA associated with the nucleus. We found with both PEI2LA and PEI25 polyplexes that GFP+ cells had higher amounts of pDNA associated with the nuclei than those non-expressing ones. On a population scale, this is consistent with those reported

previously [21,30] and supports the data derived from the flow cytometry, that nuclear-association is correlated with transgene expression. However, at the single cell level, the pDNA/nuclear distributions does not explain why some cells with apparent low pDNA/nuclear association expresses GFP while some with high pDNA association show no transgene expression. This further highlights the intrinsic cell-to-cell differences that appear to be of greater importance than the intracellular trafficking and physical interaction of polyplexes. The heterogeneity in transgene expression may be due to cells in different cell cycle stages. Many reports have demonstrated that cells undergoing the S to M phase of the cell cycle tend to exhibit enhancement in transgene expression [14-17]. Given that ~20% of the cells in the population were likely to be in the G2/M, and that the percent of nuclei with plasmid associated had dropped to 50-60% by Day 1, this leaves only about 10-12% of the cells primed for transgene expression. Presumably, the dependency on the M phase is due to the breakdown of the nuclear membrane and entry of the transgene into the nucleus. However, a recent study has shown that the heterogeneity and cell cycle dependency may be attributed to the events associated with the S and M phases [20]. During the S phase, histones are actively synthesized to prepare for the daughter genome following mitosis. The increase in intranuclear concentration of histone may induce decondensation of polyplexes by competitive dissociation and may even form a nucleosome structure with the pDNA, which is primed for efficient transcription. In addition, following decondensation, the released polymeric gene carrier may continue to interact with other nucleic acids, even the newly synthesized transgene mRNA, thereby inhibiting the translation [31]. Thus, transgene expression efficiency may involve a dynamic equilibrium between the gene carrier, pDNA and nuclear materials, which is closely associated with the homeostasis of the cell. Irrespective of the specific factors, intranuclear trafficking appears to play a vital role in determining transgene expression. Pharmacokinetics studies of nonviral gene carriers have so far being

limited to cytoplasmic trafficking; with no emphasis on the fate of polyplexes in various sub-nuclear domains. Investigation into intranuclear trafficking of nonviral pDNA polyplexes may provide significant insight on barriers to transfection.

The eventual goal of this study is to develop a BMSC-based therapy for bone regeneration by directing osteogenic differentiation in vitro using nonviral gene carriers as transfection agent and subsequently transplant the modified cells back to the patient. Intracellular mechanistic studies and carrier optimization of nonviral gene carrier are often done in transformed immortalized cell line such as HEK293T, HeLa, and COS-7 cells with the aim that information derived will be applicable to a clinical model. However, data derived in this setting is limited in clinical relevance since i) immortalized cell lines cannot be used for clinical application due to tumorigenicity concerns, and ii) transfection efficiency varies greatly between cell types - a transfection agent effective in one may not be effective at all in another and relative efficiency between carriers seemed to lack concordance in this regard [21,32-34]. This difference seemed to arise due to cellular physiology, which affects the uptake and intracellular trafficking pathway. For example, a recombinant Ad5 penton based protein, which has been incorporated as molecular conjugates for its cell binding and endosomolytic activity, was reportedly internalized efficiently by HeLa cells [35,36] but remained on the surface of primary acinar epithelial cells even after prolonged incubation, with no evidence of internalization [37]. More importantly, transformed cell lines are "too" easily transfected, indicating that the relevant biological barriers present in patient cells have been removed in transformed cells. Thus, mechanistic studies are ideally conducted in the primary cell type that is ultimately going to be used for clinical application such that strategy towards carrier optimization can be directly applied.

5.5 References

- [1] Thomas C. E., Ehrhardt A., and Kay M. A., 2003, "Progress and problems with the use of viral vectors for gene therapy," *Nat Rev Genet*, **4**(5), pp. 346–358.
- [2] Lungwitz U., Breunig M., Blunk T., and Göpferich A., 2005, "Polyethylenimine-based non-viral gene delivery systems," *Eur J Pharm Biopharm*, **60**(2), pp. 247–266.
- [3] Kakudo T., Chaki S., Futaki S., Nakase I., Akaji K., Kawakami T., Maruyama K., Kamiya H., and Harashima H., 2004, "Transferrin-modified liposomes equipped with a pH-sensitive fusogenic peptide: an artificial viral-like delivery system," *Biochemistry*, **43**(19), pp. 5618–5628.
- [4] Hyndman L., Lemoine J. L., Huang L., Porteous D. J., Boyd A. C., and Nan X., 2004, "HIV-1 Tat protein transduction domain peptide facilitates gene transfer in combination with cationic liposomes," *J Control Release*, **99**(3), pp. 435–444.
- [5] Kunath K., Merdan T., Hegener O., Häberlein H., and Kissel T., 2003, "Integrin targeting using RGD-PEI conjugates for in vitro gene transfer," *J Gene Med*, **5**(7), pp. 588–599.
- [6] Opanasopit P., Rojanarata T., Apirakaramwong A., Ngawhirunpat T., and Ruktanonchai U., 2009, "Nuclear localization signal peptides enhance transfection efficiency of chitosan/DNA complexes," *Int J Pharm*, **382**(1-2), pp. 291–295.
- [7] Yamada Y., Nomura T., Harashima H., Yamashita A., Katoono R., and Yui N., 2010, "Intranuclear DNA release is a determinant of transfection activity for a non-viral vector: biocleavable polyrotaxane as a supramolecularly dissociative condenser for efficient intranuclear DNA release," *Biol Pharm Bull*, **33**(7), pp. 1218–1222.
- [8] Jeong J. H., Kim S. H., Christensen L. V., Feijen J., and Kim S. W., 2010, "Reducible poly(amido ethylenimine)-based gene delivery system for improved nucleus trafficking of plasmid DNA," *Bioconjug Chem*, **21**(2), pp. 296–301.
- [9] Chen T.-H. H., Bae Y., and Furgeson D. Y., 2008, "Intelligent biosynthetic

- nanobiomaterials (IBNs) for hyperthermic gene delivery,” *Pharmaceutical research*, **25**(3), pp. 683–691.
- [10] Lee M., Rentz J., Han S.-O., Bull D. A., and Kim S. W., 2003, “Water-soluble lipopolymer as an efficient carrier for gene delivery to myocardium,” *Gene Ther*, **10**(7), pp. 585–593.
- [11] Mi Bae Y., Choi H., Lee S., Ho Kang S., Tae Kim Y., Nam K., Sang Park J., Lee M., and Sig Choi J., 2007, “Dexamethasone-conjugated low molecular weight polyethylenimine as a nucleus-targeting lipopolymer gene carrier,” *Bioconjug Chem*, **18**(6), pp. 2029–2036.
- [12] Neamark A., Suwanton O., Bahadur R. K. C., Hsu C. Y. M., Supaphol P., and Uludağ H., 2009, “Aliphatic lipid substitution on 2 kDa polyethylenimine improves plasmid delivery and transgene expression,” *Mol Pharm*, **6**(6), pp. 1798–1815.
- [13] Khalil I. A., Kogure K., Akita H., and Harashima H., 2006, “Uptake pathways and subsequent intracellular trafficking in nonviral gene delivery,” *Pharmacol. Rev.*, **58**(1), pp. 32–45.
- [14] Brunner S., Fürtbauer E., Sauer T., Kursa M., and Wagner E., 2002, “Overcoming the nuclear barrier: cell cycle independent nonviral gene transfer with linear polyethylenimine or electroporation,” *Mol Ther*, **5**(1), pp. 80–86.
- [15] Brunner S., Sauer T., Carotta S., Cotten M., Saltik M., and Wagner E., 2000, “Cell cycle dependence of gene transfer by lipoplex, polyplex and recombinant adenovirus,” *Gene Ther*, **7**(5), pp. 401–407.
- [16] Mortimer I., Tam P., MacLachlan I., Graham R. W., Saravolac E. G., and Joshi P. B., 1999, “Cationic lipid-mediated transfection of cells in culture requires mitotic activity,” *Gene Ther*, **6**(3), pp. 403–411.
- [17] Tseng W. C., Haselton F. R., and Giorgio T. D., 1999, “Mitosis enhances transgene expression of plasmid delivered by cationic liposomes,” *Biochim Biophys Acta*, **1445**(1), pp. 53–64.
- [18] Hsu C. Y. M., and Uludağ H., 2008, “Effects of size and topology of DNA

molecules on intracellular delivery with non-viral gene carriers,” *BMC Biotechnol.*, **8**, p. 23.

- [19] Clements B. A., Hsu C. Y. M., Kucharski C., Lin X., Rose L., and Uludağ H., 2009, “Nonviral delivery of basic fibroblast growth factor gene to bone marrow stromal cells,” *Clin. Orthop. Relat. Res.*, **467**(12), pp. 3129–3137.
- [20] Akita H., Ito R., Kamiya H., Kogure K., and Harashima H., 2007, “Cell cycle dependent transcription, a determinant factor of heterogeneity in cationic lipid-mediated transgene expression,” *J Gene Med*, **9**(3), pp. 197–207.
- [21] James M., and Giorgio T., 2000, “Nuclear-associated plasmid, but not cell-associated plasmid, is correlated with transgene expression in cultured mammalian cells,” *Mol Ther.*
- [22] Glover D. J., Leyton D. L., Moseley G. W., and Jans D. A., 2010, “The efficiency of nuclear plasmid DNA delivery is a critical determinant of transgene expression at the single cell level,” *J Gene Med*, **12**(1), pp. 77–85.
- [23] Fukata Y., and Fukata M., 2010, “Protein palmitoylation in neuronal development and synaptic plasticity,” *Nat. Rev. Neurosci.*, **11**(3), pp. 161–175.
- [24] Levental I., Grzybek M., and Simons K., 2010, “Greasing their way: lipid modifications determine protein association with membrane rafts,” *Biochemistry*, **49**(30), pp. 6305–6316.
- [25] Daum G., 1985, “Lipids of mitochondria,” *Biochim Biophys Acta*, **822**(1), pp. 1–42.
- [26] Kamiya H., Fujimura Y., Matsuoka I., and Harashima H., 2002, “Visualization of intracellular trafficking of exogenous DNA delivered by cationic liposomes,” *Biochem Biophys Res Commun*, **298**(4), pp. 591–597.
- [27] Itaka K., Harada A., Yamasaki Y., Nakamura K., Kawaguchi H., and Kataoka K., 2004, “In situ single cell observation by fluorescence resonance energy transfer reveals fast intra-cytoplasmic delivery and easy release of plasmid DNA complexed with linear polyethylenimine,” *J Gene Med*, **6**(1), pp. 76–84.

- [28] Huang M., Fong C.-W., Khor E., and Lim L.-Y., 2005, "Transfection efficiency of chitosan vectors: effect of polymer molecular weight and degree of deacetylation.," *J Control Release*, **106**(3), pp. 391–406.
- [29] Cho Y. W., Kim J.-D., and Park K., 2003, "Polycation gene delivery systems: escape from endosomes to cytosol.," *J. Pharm. Pharmacol.*, **55**(6), pp. 721–734.
- [30] Bengali Z., Rea J. C., Gibly R. F., and Shea L. D., 2009, "Efficacy of immobilized polyplexes and lipoplexes for substrate-mediated gene delivery.," *Biotechnol Bioeng*, **102**(6), pp. 1679–1691.
- [31] Hama S., Akita H., Iida S., Mizuguchi H., and Harashima H., 2007, "Quantitative and mechanism-based investigation of post-nuclear delivery events between adenovirus and lipoplex.," *Nucleic Acids Res*, **35**(5), pp. 1533–1543.
- [32] Douglas K. L., Piccirillo C. A., and Tabrizian M., 2006, "Effects of alginate inclusion on the vector properties of chitosan-based nanoparticles.," *J Control Release*, **115**(3), pp. 354–361.
- [33] Dastan T., and Turan K., 2004, "In vitro characterization and delivery of chitosan-DNA microparticles into mammalian cells.," *J Pharm Pharm Sci*, **7**(2), pp. 205–214.
- [34] Rejman J., Conese M., and Hoekstra D., 2006, "Gene transfer by means of lipopolyplexes: role of clathrin and caveolae-mediated endocytosis.," *J Liposome Res*, **16**(3), pp. 237–247.
- [35] Medina-Kauwe L. K., 2003, "Endocytosis of adenovirus and adenovirus capsid proteins.," *Adv Drug Deliv Rev*, **55**(11), pp. 1485–1496.
- [36] Rentsendorj A., Agadjanian H., Chen X., Cirivello M., Macveigh M., Kedes L., Hamm-Alvarez S., and Medina-Kauwe L. K., 2005, "The Ad5 fiber mediates nonviral gene transfer in the absence of the whole virus, utilizing a novel cell entry pathway.," *Gene Ther*, **12**(3), pp. 225–237.
- [37] Hamm-Alvarez S. F., Xie J., Wang Y., and Medina-Kauwe L. K., 2003, "Modulation of secretory functions in epithelia by adenovirus capsid proteins.," *J Control Release*, **93**(2), pp. 129–140.

Chapter 6

Cellular uptake pathways of lipid-modified cationic polymers in gene delivery to primary cells¹

¹A version of this chapter has been published in Hsu C.Y., and Uludag H., (2013) Cellular Uptake Pathways of Lipid-Modified Cationic Polymers in Gene Delivery to Primary Cells. *Biomaterials*. In Press

6.1 Introduction

Cellular delivery of exogenous DNA molecules to manipulate physiological functions at the genetic level has been an indispensable tool in both molecular biology studies and biotechnology applications. Clinical translation of gene delivery as a form of molecular therapy has been slow to progress largely due to the absence of gene delivery vectors (GDVs) that can satisfy both efficiency and safety requirements. Disarmed recombinant viral vectors remain as the most efficient method of gene delivery at present. However, the risk of immunogenicity, residual infectivity and insertional mutagenesis currently precludes their wide spread use [1]. Ongoing efforts into the development of non-viral GDVs have yielded a large library of biocompatible materials capable with sufficient DNA packaging and delivery ability in pre-clinical models, but they have yet to achieve the efficacy that viral vectors are able to incite. Strategies to improve the efficiency and biocompatibility of cationic reagents for gene delivery typically involve grafting functional ligands such as peptides, lipids, sugars, or a combination thereof, to improve stability, targeting, uptake and sub-cellular trafficking capabilities of the vectors [2]. In that regard, hydrophobic modification of cationic reagents with lipid moieties was shown to improve membrane binding and enhance gene delivery efficiency [3]. Our group has demonstrated the feasibility of this approach by grafting several endogenous lipids to the low molecular weight (2 kDa) polyethylenimine (PEI2). The most effective polymer, namely linoleic acid substituted PEI2 (PEI2LA), displayed markedly enhanced transfection efficiency over its relatively ineffective precursor molecule in both cultured cell lines and tissue-derived primary cells [4,5]. We previously showed that the enhanced efficiency of PEI2LA was partly due to stronger association with the nuclear membrane, which was correlated with better nuclear uptake and subsequent transgene expression [5]. However, the specific

uptake pathway employed as well as the subsequent intracellular trafficking events mediated by the PEI2LA remain to be elucidated.

Lipid substitution is expected to enhance gene delivery by promoting stronger binding of the polymer/DNA complexes to hydrophobic domains of the plasma membrane to increase uptake. Hydrophobic modifications can also alter the physicochemical properties of the complexes, leading to a change in the uptake pathways. Uptake pathways are vitally important in determining the efficiency of GDVs as it relates to the intracellular processing, trafficking and recycling of the internalized complexes. Uptake of assembled complexes are widely regarded to proceed via endocytosis [6,7]. Endocytosis is broadly defined into two categories, pinocytosis and phagocytosis, the latter of which is restricted to specialized cell types such as lymphocytes and macrophages. Pinocytosis is further sub-divided into clathrin-dependent endocytosis (CME), caveolin-mediated endocytosis (CvME), macropinocytosis, and clathrin-/caveolin-independent pathway. CvME was thought to be the uptake pathway most conducive to transfection owing to its non-acidic, non-degradative environment, which maintains the intracellular integrity of the nucleic acid cargo. CvME was shown to be the endocytic pathway leading to efficient transgene expression in COS-7 and HeLa cells for PEI-mediated transfection [8-10]. However, others suggested the CME as the most efficient uptake pathway, as it not only provide an acidic environment for PEI complexes to facilitate endosome disruption via the proton-sponge effect, but also facilitate movement of the transgene cargo proximal to the perinuclear region, which subsequently increases the propensity for nuclear import [11]. Yet, recent studies have also suggested that uptake via macropinocytosis is the most efficient route of entry leading to transfection in PEI25 [12]. Regardless of which endocytic pathway is the most effective route for transfection, the notion that a single pathway can be optimal for all GDVs may not be

realistic. Transfection pathways vary among different cell types [13,14] and are likely to depend on the biochemical nature of the GDVs and the physicochemical properties of resulting complexes [15]. In that regard, mechanistic studies and further design optimizations for non-viral GDVs should be ideally investigated in clinically relevant primary cell lines so that clinical translation to both ex vivo and in vivo delivery settings can be streamlined. That was not the case for previous studies exploring the role of endocytic pathways on the efficiency of non-viral GDVs, where transformed cell lines were routinely used [8,9,13,14,16-18]

In this study, we employed normal human foreskin fibroblast (NHFF) cells to elucidate the mechanism of cell entry and trafficking of polymeric GDVs. NHFF cells is a versatile platform in this regard since it has clinical relevance in both cell-based therapy for the induction of pluripotent cells and in cutaneous gene therapy for skin regeneration and wound repair [19-22]. We aimed to identify the predominant endocytic pathway involved in the uptake of PEI2LA complexes in NHFF cells as compared to native PEIs (PEI2 and PEI25). We applied a series of pharmacological inhibitors that selectively inhibited CME, CvME and macropinocytosis to determine the uptake pathway by reduction. The specific activities of the inhibitors were defined by titrating the concentrations of the drug against cell viability and transfection efficiency. We further examined the intracellular distribution of the complexes and the role of endosome release as a rate-limiting step in the overall transfection. Conclusions derived from this study would not only provide mechanistic insight into the impact of lipid-moieties in GDV trafficking but would also have direct implication on the future design of polymeric GDVs for therapeutic delivery to NHFF cells.

6.2 Materials and Methods

6.2.1 Materials

The 2 kDa branched PEI (PEI2; Mn = 1.8 kDa, Mw = 2.0 kDa), 25 kDa branched PEI (PEI25; Mn = 10 kDa; Mw = 25 kDa), Hanks' Balanced Salt Solution (HBSS, with phenol red), (3-(4,5-dimethylthiazol-2-yl)-2,5-diphenyltetrazolium bromide (MTT), spectrophotometric-grade dimethylsulfoxide (DMSO), sucrose, chloroquine diphosphate salt, chlorpromazine hydrochloride, methyl- β -cyclodextrin (m β CD), genistein and trypsin/EDTA were obtained from SIGMA (St. Louis, MO). The PEI2LA was prepared according to the synthetic scheme outlined in [4], with LA:PEI2 feed ratio of 0.1, that gave a polymer with an average substitution of 1.2 linoleic acids per polymer. Opti-MEM® I Reduced Serum Media, Dulbecco's Modified Eagle Medium (DMEM; high and low glucose with L-glutamine), penicillin (10000 U/mL), streptomycin (10 mg/mL) and non-essential amino acids (100x) were from Invitrogen (Grand Island, NY). Fetal bovine serum (FBS) was from PAA Laboratories (Etobicoke, Ontario). The blank plasmid gWIZ (i.e., no functional gene product) and gWIZ-GFP (i.e., Green Fluorescent Protein mammalian expression plasmid) were purchased from Aldevron (Fargo, ND). The photosensitizer aluminium phthalocyanine disulfonate (AlPcS2a) was purchased from Frontier Scientific (Logan, UT, USA). Wortmannin and amiloride hydrochloride were obtained from Santa Cruz Biotechnology (Santa Cruz, CA). Hoechst 33258, Pentahydrate (bis-Benzimide) and Alexa Fluor® 488 labeled Dextran (10 kDa) were from Life Technologies (Burlington, ON).

6.2.2 Cell culture

NHFF cells were isolated from patients as described previously [23] and cultured in a basic growth medium comprised of DMEM containing 4.5 g/ml D-glucose,

supplemented with 10% heat inactivated fetal bovine serum (FBS), 2 mM L-glutamine, 0.1 mM MEM non-essential amino acids, 100 U/mL penicillin, and 100 µg/L of streptomycin. Cells were maintained in a humidified 37 °C incubator with 5% CO₂. NHFF cells passaged between 14-24 generations were used in this study, and were grown in multi-well plates for transfection studies. For both uptake and transfection studies, cells were seeded in 24-well plates at an initial seeding density of 3 x 10⁵ cells/well.

6.2.3 Plasmid DNA (pDNA) labeling

The gWIZ-GFP plasmid is a 5757 bp mammalian expression plasmid, which contains a modified promoter from the human cytomegalovirus (CMV) immediate early (IE) genes. gWIZ-GFP was labeled with the fluorophore Cy3 using the Label IT[®] Tracker[™] Intracellular Nucleic Acid Localization Kit (Mirus Bio, WI) as per manufacturer's instructions. Briefly, a 0.2 (v/w) ratio of dye to nucleic acid reaction mix was prepared and incubated at 37 °C for 90 min. Unbound free Cy3 molecules were removed by ethanol precipitation after adding 0.1 vol of 5 M NaCl and 2 vol of 100% ethanol and incubated at -20 °C for 2 h. Purified labeled pDNA was then suspended in ddH₂O. Labeling efficiency was determined by calculating the ratio of base to dye using the equation $(A_{\text{base}} * \epsilon_{\text{dye}}) / (A_{\text{dye}} * \epsilon_{\text{base}})$ by measuring absorbance at 260 nm (base) and 550 nm (dye) using the values $\epsilon_{\text{Cy3}} = 250,000$; $\epsilon_{\text{base}} = 6,600$ and $CF_{260} = 0.05$. The contribution of dye to the A_{260} reading was corrected by using the equation $A_{\text{base}} = A_{260} - (A_{\text{dye}} * CF_{260})$. Plasmid DNA labeled using the concentration outlined yielded approximately 300 Cy3 labels per pDNA.

6.2.4 Cytotoxicity assessment of endocytosis inhibitors by MTT assay

The cytotoxic effects of the uptake inhibitors were assessed using the MTT cell viability assay, in which the yellow tetrazolium salt (MTT) is reduced in metabolically active

cells to form insoluble purple formazan crystals, which are solubilized by the addition of DMSO. Briefly, NHFF cells were seeded in 48-well plates at a concentration of 1×10^5 cells/well. Once the cells reached a density of 50-60% or after 1-2 days, inhibitors were added and incubated in OPTI-MEM. After 4 h incubation, inhibitors were removed and cells were further incubated for an additional 20 h in fresh growth medium. To process cells for assay, MTT was added directly to the medium to a final concentration of 1 mg/ml, and incubated at 37 °C for 2 h. Afterwards, the supernatant was removed by inverting the plates to decant the liquid. Crystals remaining at the bottom of the plate were dissolved in DMSO at 200 μ l/well. The absorbance was measured at 570 nm using a ELx800 absorbance microplate reader (Bio-Tek, Winooski, VT). Cell viability was expressed as a percentage relative to untreated cells, which served as the control.

6.2.5 Preparation of complexes for transfection

Self-assembled polymer/pDNA complexes were formed by diluting pDNA and polymer solutions separately in equal volumes of salt-free buffer (20 mM HEPES, pH 7.4) for PEI25 and PEI2 or OPTI-MEM for PEI2LA. After 5 min of equilibration, the pDNA and polymer solutions were mixed together, vortexed for 5 sec, and incubated at room temperature for 25 min. The volume of the complexes at this stage was 1/5 of the final transfection media volume (i.e., 100 μ l complex volume in a total of 500 μ l tissue culture medium per 24-well). The polyplex solutions were then diluted 1:5 in OPTI-MEM to bring the final pDNA concentration to 2 μ g/mL per well and added directly to each well; plates were then centrifuged at 210 x g for 5 min (acceleration and deceleration set to lowest setting) to force the complexes onto the cell surface. All transfection and uptake studies included this centrifugation step following the addition of complexes.

6.2.6 Transfection efficiency and gene expression kinetics

For gene expression kinetics, complexes were prepared for transfection as described above. After 4 h incubation, complexes were removed and replaced with growth medium. At the designated time point, cells were processed for flow cytometry; cells were first washed and equilibrated with $\text{Ca}^{2+}/\text{Mg}^{2+}$ free HBSS (without phenol red; CMF-HBSS) for ~5 min to remove residual divalent cations and detached by enzymatic treatment with clear 0.01% Trypsin/EDTA for 1 - 2 min. The detached cells were fixed in 3.7% formalin in HBSS.

For transfection studies involving the inhibitors, cells were pre-treated with the inhibitors diluted in OPTI-MEM to the concentrations outlined in the figures (400 μl were dispensed into each well in a 24-well plate). After 2 h incubation, 100 μl of complexes were added directly to each well (final DNA concentration at 2 $\mu\text{g}/\text{ml}$), then centrifuged as described above and incubated in the presence of the inhibitors for an additional 4 h; transfection complexes were subsequently removed and replaced with growth media. GFP expression was assayed 20 h later by processing cells for flow cytometry analysis on a Beckman Coulter Cell Lab Quanta with MPL Option (Mississauga, ON) equipped with a 488 nm laser diode and standard filter (460BP, 525BP, 575BP and 670 LP).

To investigate the effect of chloroquine on transfection, cells were pre-treated with 40 μM chloroquine for 2 h prior to transfection. This concentration was empirically determined to give the overall highest increase in mean fluorescence without significant reduction in cell viability (data not shown). For light-induced endosome disruption, cells were pre-loaded with the photosensitizer (PS) by incubating cells with 5 $\mu\text{g}/\text{ml}$ of ALPcS2a in growth media for 16 h. Then cells were washed (x3) with growth media and chased for 2 h in PS-free media to remove surface-bound PS before

transfection. After incubation with transfection complexes for 3 h, cells were exposed to light emitted by a bank of six T5 wide-spectrum high output fluorescent lamps (F54T5/841) placed at 30 cm directly above the plate for 45 seconds, then placed back in the incubator for an additional 3 h before complexes were removed and replaced with growth media. Expression of GFP was assayed 24 h later by flow cytometry. The utilized concentration of AIPcS2a and light dose were empirically determined by titrating a range of concentrations (1, 2, 5, and 10 µg/ml) and exposure time (30, 45, 60, 90, 120 sec) against transfection efficiencies (data not shown).

Analysis for transfection efficiency was performed by calibrating the gated regions such that the negative control (i.e., polymer complexes prepared with gWIZ) had 1% auto-fluorescent cells. Transfection efficiency was expressed in terms of the mean fluorescent intensity value captured in the FL1 channel. The relative transfection efficiency was expressed as a percentage of untreated cells.

6.2.7 Uptake kinetics and inhibition of endocytosis

For measurement of uptake kinetics, Cy3-labeled pDNA (Cy3-pDNA) was used to quantitate the amount of intracellular pDNA. Cells were seeded in 24-well plates and transfected as above, except Cy3-pDNA were mixed with unlabeled pDNA at a 1:1 ratio. Prior to the prescribed time point for analysis, complexes were removed, and cells were washed twice with growth media, then chased for 30 min in label-free media to allow residual complexes to be internalized. Cells were then detached by trypsin and suspended in 3.7% formalin for flow cytometry. Quantification of Cy3-pDNA uptake was performed by taking the mean fluorescent values from the FL2 channel, calibrated to 1% auto-fluorescence in cells transfected with unlabeled gWIZ complexes.

For uptake studies in the presence of endocytosis inhibitors, cells were pre-treated for 2 h with the inhibitors diluted in OPTI-MEM to the concentrations outlined in the results section (400 μ l were dispensed into each well in a 24-well plate). Then, complexes were prepared as described above, with labeled and unlabeled DNA mixed in a 1:1 ratio and 100 μ l of complexes were added directly to each well (final concentration of pDNA was 2 μ g/ml), then centrifuged as described above and incubated in the presence of the inhibitors for an additional 4 h. Afterwards, complexes were removed, cells were washed with growth media (x2) and further chased in dye-free growth media for an additional 2 h to allow cells to recover. Removal of surface-bound complexes was verified by microscopy (data not shown). Relative percentage of uptake was expressed in terms of transfected cells that were not exposed to the inhibitors (buffers only).

6.2.8 Laser scanning confocal fluorescent microscopy

NHFF cells were seeded onto a 12-well tissue culture plates at 3×10^6 /well. Once attached and cell density has reached ~60-70%, endosomes were labeled by incubating the cells for 16 h in the presence of 500 μ g/ml of Dextran-Alexa Fluor[®] 488, diluted in cell media. Cells were then washed twice in dye-free media then transfected as described above. After 4 h incubation, complexes were removed, washed twice with basic medium and chased in dye-free medium for 30 minutes. Cells were then washed with CMF-HBSS (x2) and fixed in 3.7% formalin for 15 minutes. Nuclei were stained with Hoechst 33258 (300 nm/ml in HBSS). Prior to imaging, CMF-HBSS was replaced with a glycerol mixture containing 9:1 glycerol-to-HBSS (v/v). 16-bit images were acquired using an inverted Zeiss LSM 710 Laser Scanning Confocal Microscope (Carl Zeiss, Oberkochen, Germany) through a 10x 0.45NA EC Plan-Neofluar objective lens with a field view of 125.03 μ m x 125.03 μ m at 0.08 μ m/pixel. Nuclei stained with

Hoechst were visualized by excitation at 405 nm, while Dextran-Alexa Fluor[®] 488 and Cy3-pDNA were excited at 488 nm and at 561 nm, respectively.

For live-cell imaging, cells were seeded onto a glass bottom dish with a No. 1.5 cover glass (0.16-0.19 mm; MatTek Corporation, Ashland, MA). Cells were incubated with AIPcS2a (5 µg/ml) diluted in growth media for 16 h, then washed twice with growth media and transfected with Cy3-pDNA complexes as before. After 4 h incubation, transfection complexes were replaced with cell media, and the cells directly imaged on a Quorum WaveFX-X1 Spinning Disc Confocal System (Quorum Technologies Inc., Guelph, ON). Cells were staged in an environmentally controlled Chamlide TC-A Live Cell Chamber (37 °C incubator + 5% CO₂ atmosphere) fitted with a 35 mm micro-dish adaptor. Images were acquired through a 20X/0.75 dry lens and detected on a Hamamatsu EMCCD (C9100-13) with a voxel size of 0.499 µm/pixel (x, y). AIPcS2a was excited by a 45 mW 642 nm pumped diode laser while Cy3-DNA were visualized with 50 mW 561 nm pumped diode laser.

Wide-field fluorescent microscopy was performed on an Olympus FSX100 equipped with a metal halide lamp. Live-cell imaging of cells seeded in plastic tissue culture plates were acquired through the LCACHN40xPHP lens (NA0.55) at 20x magnification. Cy3-pDNA was visualized in the TRITC channel (BP530-550, BA575IF, DM570).

6.2.9 Particle size measurements

The hydrodynamic size range of the polymer/pDNA complexes was measured by photon correlation spectroscopy (Zetasizer Nano, Malvern Instruments Ltd, Worcestershire, UK). Polyplexes were prepared as above and diluted to 1 ml in OPTI-MEM at a final DNA concentration of 2 µg/ml prior to measurement. Measurements was taken in a heated chamber at 37 °C and 660 nm wavelength, and particle sizes

were calculated by using a medium viscosity of 1.140 cP and a refractive index of 1.333 (at 37 °C). Values reported were from an average of 12 measurements with 10 seconds interval between each measurement.

6.2.10 Statistical analysis

Where indicated, the data is summarized as the mean \pm standard deviation of triplicate measurements. Unpaired Student's t-test was used to assess statistical differences ($p < 0.05$) between the group means. All experiments were done in triplicate with a minimum of three independent experiments.

6.3 Results

6.3.1 Particle sizes and transfection efficiencies in NHFF cells

We initially sought out to optimize the complexation conditions for each polymer so that subsequent uptake and trafficking studies were investigated under optimal conditions that accurately reflected the transfection capability of each polymer. Based on an optimization procedure outlined [24], we found that PEI2LA complexes prepared in OPTI-MEM transfected more efficiently than those prepared in salt-free buffers (**Figure 6.1**). The opposite trend was observed for PEI25 and PEI2 complexes, in which salt-free buffers favored formation of more effective complexes. The mean hydrodynamic sizes of PEI2LA complexes were 570 nm with >75% in the 530 to 615 nm range (**Figure 6.2**); PEI2 complexes were smaller and exhibited a broader size distribution compared to PEI2LA, where most complexes were in the 295 to 531 nm range. PEI25 complexes were the smallest, with ~80% falling within the 164 to 255 nm range.

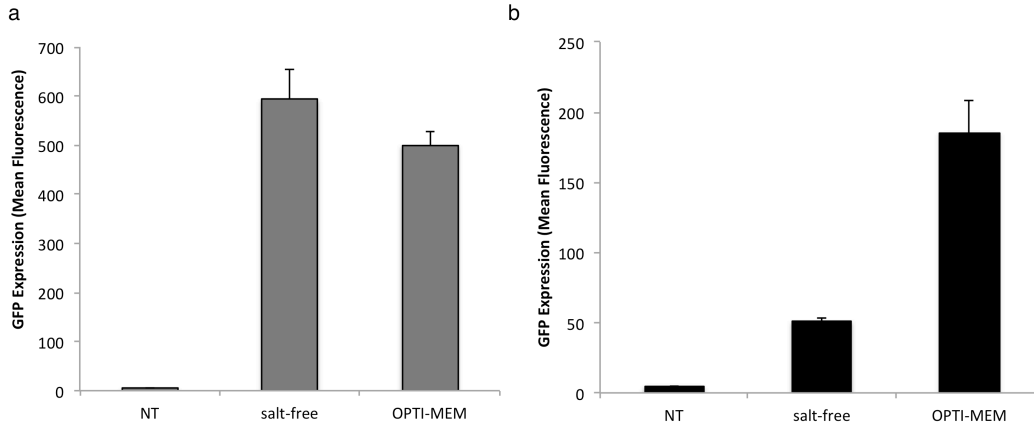


Figure 6.1

Comparison of transfection efficiency between complexes in different buffers.

In salt-free buffer (20 mM HEPES, pH 7.4) and in OPTI-MEM for a) PEI25 and b) PEI2LA. Bar height depicts the mean fluorescence (FL1) of transfected cells.

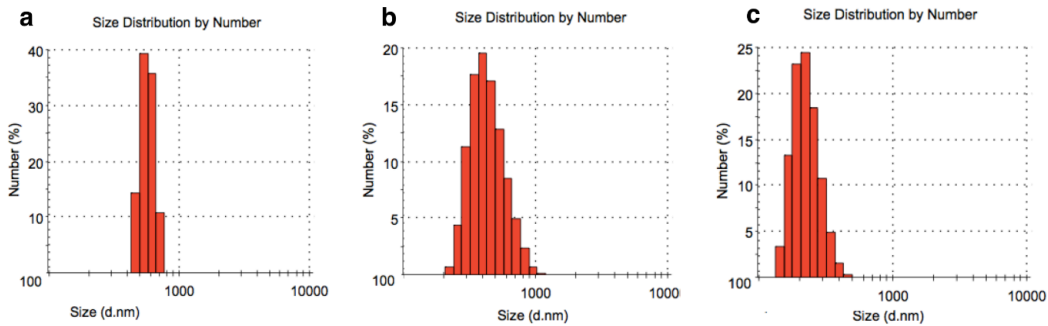


Figure 6.2

Hydrodynamic size ranges of complexes

formulated with **PEI2LA in OPTI-MEM (A)**. The sizes of the particles in terms of proportional make up is as follows (in nm): 458.7, 14.3%; 531.2, 39.3%; 615.1, 35.7%; 712.4, 10.7%). Hydrodynamic size ranges of complexes formulated with **PEI2 in salt-free buffer (B)**. Size distribution (nm): 220.2, 0.7%; 255, 4.3%; 295.3, 11.3%; 342, 17.6%; 396.1, 19.5%; 458.7, 17.1%; 531.2, 12.8%; 615.1, 8.5%; 712.4, 5.0%; 825.0, 2.3%; 955.4, 0.7%; 1106, 0.1%). Hydrodynamic size ranges of complexes formulated with **PEI25 in salt-free buffer (C)**. Size distribution (nm): 141.8, 3.3%; 164.2, 13.3%; 190.1, 23.2%; 220.2, 24.5%; 255, 18.4%; 295.3, 10.7%; 342, 4.8%; 396.1, 1.5%; 458.7, 0.2%.

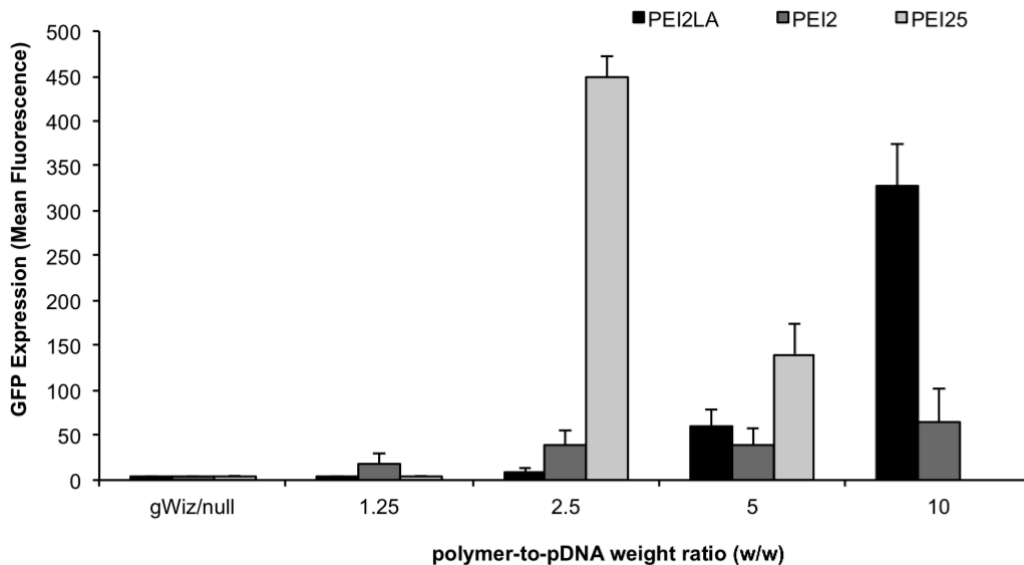


Figure 6.3

Transfection efficiency of PEI2LA, PEI25 and PEI2 in NHFF cells at various polymer-to-pDNA weight ratios.

Bar height depicts the mean cellular fluorescence in the FL1 channel. The efficiency of PEI25 was optimal at a weight ratio of 2.5 while the efficiency of PEI2 and PEI2LA was optimal at a weight ratio of 10. GFP expression in PEI2LA-transfected cells was 5-fold higher than those transfected by PEI2. PEI25 at a ratio of 10 was toxic and no data could be collected.

Using the optimized conditions, transfection efficiencies obtained in NHFF cells are summarized in **Figure 6.3**. At the polymer-to-DNA weight ratio of 10, the mean GFP fluorescence of PEI2LA transfected cells was 5-fold higher than those transfected by PEI2. PEI25 was the most effective GDV yielding 1.4-fold and 7-fold higher reporter gene expression than PEI2LA and PEI2, respectively. Transfection efficiencies were dependent on the ratio of polymer-to-DNA (w/w); a ratio of 2.5 was most effective for PEI25, which is equivalent to a nitrogen-to-phosphate (NP) ratio of 19.35, while a ratio of 10 (NP = ~75.5, assuming a similar MW for these two polymers) was optimal for both PEI2 and PEI2LA. These weight ratios were employed for the subsequent studies.

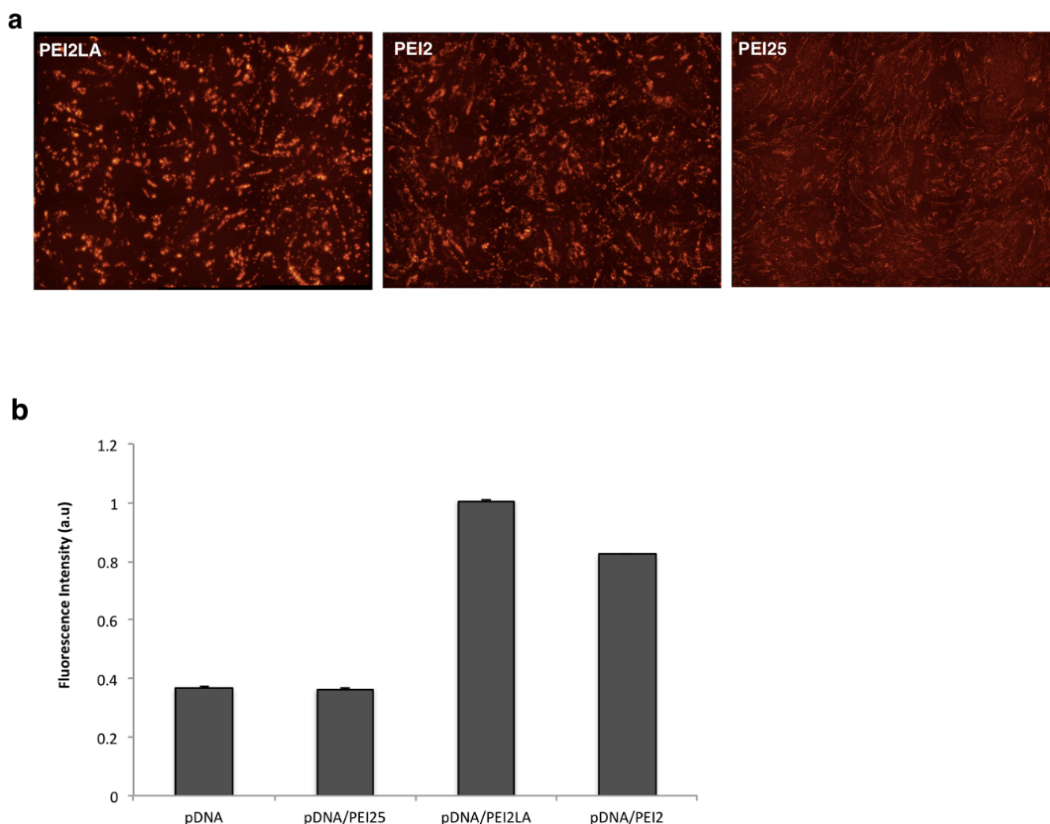


Figure 6.4

Fluorescent intensity of PEI2LA, PEI2 and PEI25 complexes.

a) PEI2LA complexes (left pane) were brighter under fluorescent microscope as judged by the difference between the signal and background. The fluorescent intensity of PEI2 complexes (middle pane) and PEI25 (right pane) was noticeably dimmer than PEI2LA. **b)** Quantitative measurement of the fluorescence of pDNA/polymer particles by a plate reader using the 544/590 nm filter pair.

6.3.2 Uptake kinetics of pDNA

The pDNA uptake studies was conducted by using Cy3 as the fluorophore for pDNA labeling since its fluorescence is relatively insensitive to pH changes that occur in the endosomes. Visual assessment of cellular uptake under wide-field fluorescent microscope showed differences in fluorescent intensities among the three complexes (**Figure 6.4a**), where PEI2LA was much brighter than PEI2 and PEI25 complexes. Quantification of fluorescence of the complexes showed that PEI25 complexes had intensity similar to free pDNA whereas PEI2 and PEI2LA complexes were 2 and 2.5

times brighter (**Figure 6.4b**). Accordingly, we did not use fluorescence intensity as a measure of relative uptake efficiency. The relative sizes of the complexes as seen under microscopy (**Figure 6.4a**) was also consistent with sizes measured by DLS (**Figure 6.2**), in which PEI2LA complexes were noticeably larger than the complexes seen in PEI25.

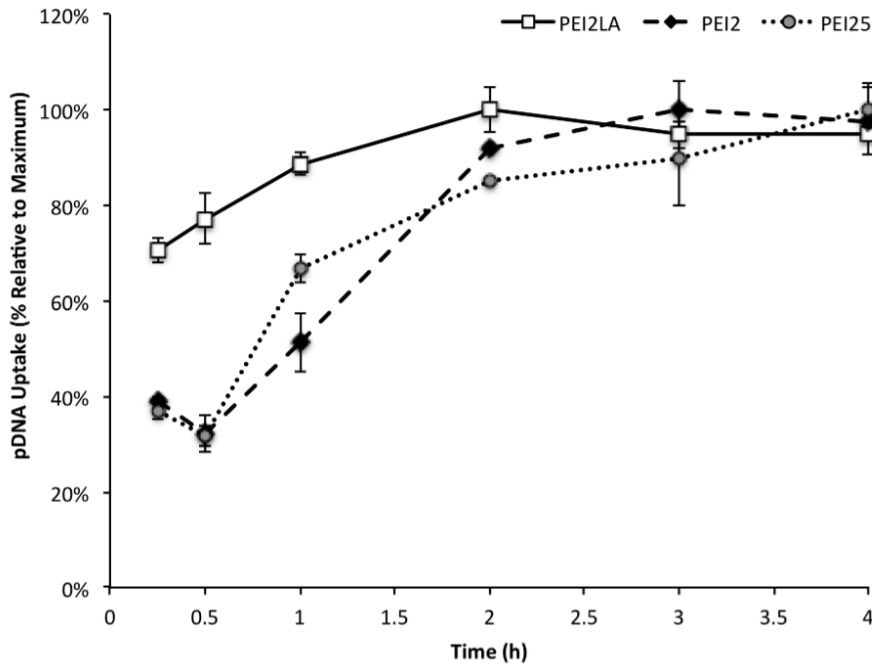


Figure 6.5
Uptake kinetics of PEI2LA, PEI25 and PEI2 complexes in NHFF cells.

Prior to the designated time point, transfection complexes were removed and cells were chased in dye-free for 30 min before processing for flow cytometry. Values are represented as a percent of maximum, which took place at 2, 3, and 4 hours for PEI2LA, PEI25 and PEI2 complexes, respectively. The level of uptake for PEI2LA reached 70% of maximum at 0.25 h, while PEI25 and PEI2 exhibited slower uptake kinetics, starting at 37% and 40%, respectively.

The kinetics of complex uptake was determined to provide insights into the uptake pathways, since the rate of internalization is pathway dependent. CME is considered to be a rapid process (<10 min), whereas uptake via CvME or macropinocytosis tended to exhibit slower kinetics (>20 min; [25]). **Figure 6.5** shows the uptake of the Cy3-pDNA/complexes over time, expressed as a percentage of the highest uptake, which was reached at different time points for each of the polymer. Uptake of PEI2LA complexes

reached a saturation maximum at 2 h, followed by PEI25 and PEI2 complexes at 3 and 4 h, respectively. Furthermore, within 15 min of incubation, uptake of PEI2LA complexes was already at 70% of maximum, compared to 37% and 40% for PEI25 and PEI2 complexes. Therefore, we infer that PEI2LA exhibited a faster rate of internalization than PEI2 and PEI25, which may suggest a greater involvement of CME during the uptake.

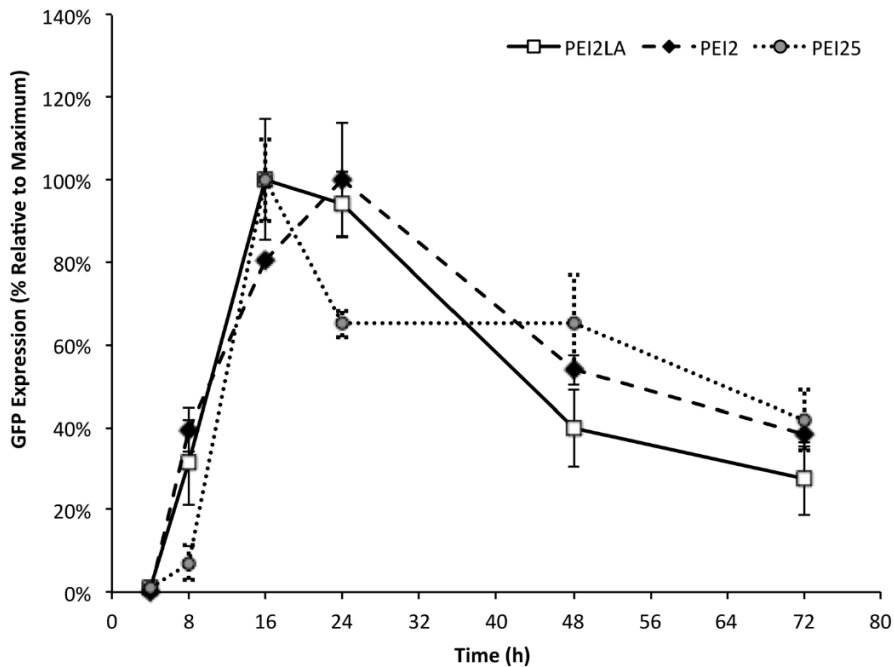


Figure 6.6
Kinetics of GFP expression during the first 72 h following the transfection with complexes.
 Values are expressed as a percentage of the maximum, which was achieved at 16 h for PEI2LA and PEI2, and at 24 h for PEI25. GFP expression in transfected cells for the three GDVs gradually diminished after 24 h.

6.3.3 Transgene expression kinetics

The kinetics of transgene expression was determined to establish a time frame for intracellular trafficking events leading to gene expression. **Figure 6.6** shows the relative GFP expression over a 72 h period in which transgene expression was expressed as a percentage of the highest mean fluorescence for each polymer. Highest

transgene expression for PEI2LA and PEI25 were observed at 16 h while PEI2 had maximal expression at 24 h. By 48 h, transgene expression had dropped to 66%, 54% and 40% for PEI25, PEI2 and PE2LA, respectively. Hence, the majority of intracellular processes leading to transgene expression took place within the first 16 to 24 h. The gradual decline in GFP fluorescence suggested there was no additional transgene expression beyond the first 24 h, indicating a coupling between the transfection and uptake processes.

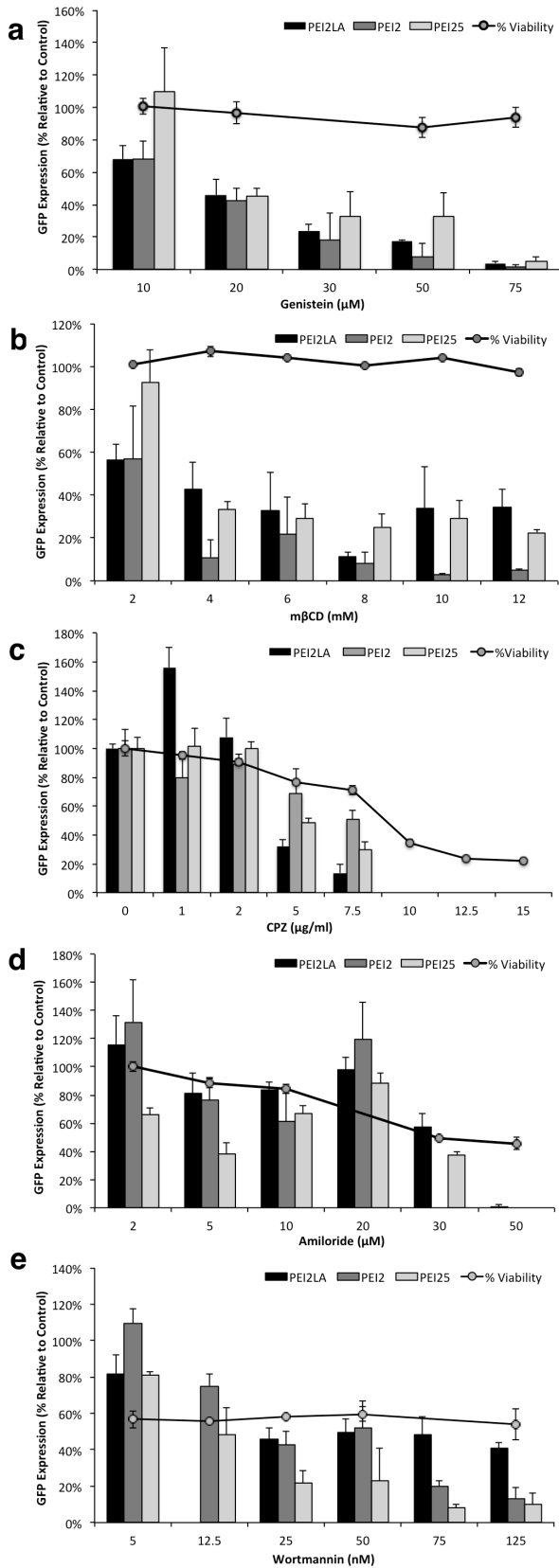


Figure 6.7

The effect of the endocytic inhibitors on transfection efficiency

Genistein (a), mβCD (b), CPZ (c), amiloride (d), and wortmannin (e) on transfection efficiency. Bar graph denotes the relative mean fluorescent (FL1) of transfected cells treated with the indicated inhibitor as a percentage of control cells (without treatment with inhibitors). Line graphs denote the cell viability with inhibitor treatment at indicated concentrations as a percentage of untreated cells (no inhibitors).

6.3.4 Effect of endocytosis inhibitors on transfection efficiency

To elucidate the endocytic pathways involved in the uptake of complexes, we employed a number of inhibitors that are specific to CME, CvM, and macropinocytosis (**Table 6.1**). Since the activity of the inhibitors is highly dependent on the cell type and the administered concentrations [26], the effects of inhibitors were investigated over a practical range of concentrations to draw our conclusions. **Figure 6.7a** and **6.7b** show the effect of CvME inhibitors genistein and m β CD on transfection efficiency. Transfections by all three polymers were strongly inhibited by genistein, with 50% reduction at 20 μ M, reaching complete inhibition at 75 μ M (**Figure 6.7a**). A dose-dependent effect on transfection was evident for genistein, where increasing concentrations resulted in corresponding reductions in transgene expression. The effect of genistein did not appear to differ significantly among the polymers and suggested an equal dependence on tyrosine phosphorylation for transfection. m β CD also had a dose-dependent effect on transfection (**Figure 6.7b**), in which transfections were reduced by 50% above 4 μ M. The effect of m β CD was heterogeneous on the cell population; even with >90% reduction in the number of transfected cells, there remained a few GFP-positive cells that displayed high fluorescence (data not shown). This accounts for the relatively large error bars in the figures, in which the overall fluorescence is represented by a few highly GFP-expressing cells. m β CD inhibited transfection by PEI2 (5% of control) to a greater extent than transfections by PEI2LA and PEI25 (34% and 23% of control, respectively), suggesting PEI2 complexes have higher dependence on lipid-raft mediated endocytosis for transfection. However, we note that transfection efficiency of PEI2 was low to begin with, which may not provide the same quantitative resolution as PEI2LA and PEI25 when calculating relative transfection efficiency.

Figure 6.7c shows the effect of CPZ on transfection efficiency. The inhibitory effect of CPZ on transfection starts at 5 µg/ml; 7.5 µg/ml was the highest concentration that can be administered without causing significant toxicity (80% viability). CPZ reduced transfection by PEI2LA significantly more than PEI2 and PEI25 (86% vs. 50% and 70%, respectively), suggesting a proportionally greater involvement of CME in the uptake of PEI2LA complexes

The effects of the macropinocytosis inhibitors amiloride and wortmannin on transfection efficiency are shown in **Figure 6.7d and 6.7e**. The inhibitory effect of amiloride was greatest on PEI2-mediated transfection, which completely abolished transgene expression at 30 µM. In contrast, PEI2LA was least affected, with 42% reduction in GFP fluorescence. Similarly, wortmannin strongly reduced transfection by PEI2 and PEI25 to 20% and 8% of the control groups at 75 nM, respectively (**Figure 6.7e**). The PEI2LA again were least affected by the macropinocytosis inhibitor wortmannin (50% reduction).

Table 6.1 List of inhibitors and endosome disruptors used in this study.

Drug	Mechanism of Activity	Pathway	Concentration	Reference
Methyl- β -cyclodextrin (m β CD)	A cyclic oligomer of glucopyranoside, extracts cholesterol from the plasma membrane	CvME	8 μ M	[58]
Genistein	tyrosine kinase inhibitor, blocks the phosphorylation of caveolin-1	CvME	75 nM	[59]
Chlorpromazine (CPZ)	a cationic amphiphilic drug, inhibits clathrin-coated pit formation by relocating clathrin and its adapter proteins from the plasma membrane to the endosomes	CME	7.5 μ g/ml	[60]
Amiloride	Interferes with membrane ATPase required for ruffling.	Na ⁺ /H ⁺ macro-pinocytosis	30 μ M	[61]
Wortmannin	Inhibitor of phosphatidylinositol-3-phosphate (PI3K)	macro-pinocytosis	75 nM	[62]
AlPcS2a	Taken up via endocytosis and localized in endosome. Light irradiation induced oxidative damage to rupture endosomes	Endosome release	5 μ g/ml; 45 seconds of light exposure	[27,63]
Chloroquine	weak hydrophobic base, buffers acidification in early endosomes to prevent DNA degradation and promoting endosomal release of the cargo	endosome release	40 μ M	[7]
Sucrose	Hypertonic media, induces lysosomal swelling by increasing osmotic pressure within endosomes	lysosome	0.45 M	[64] [28]

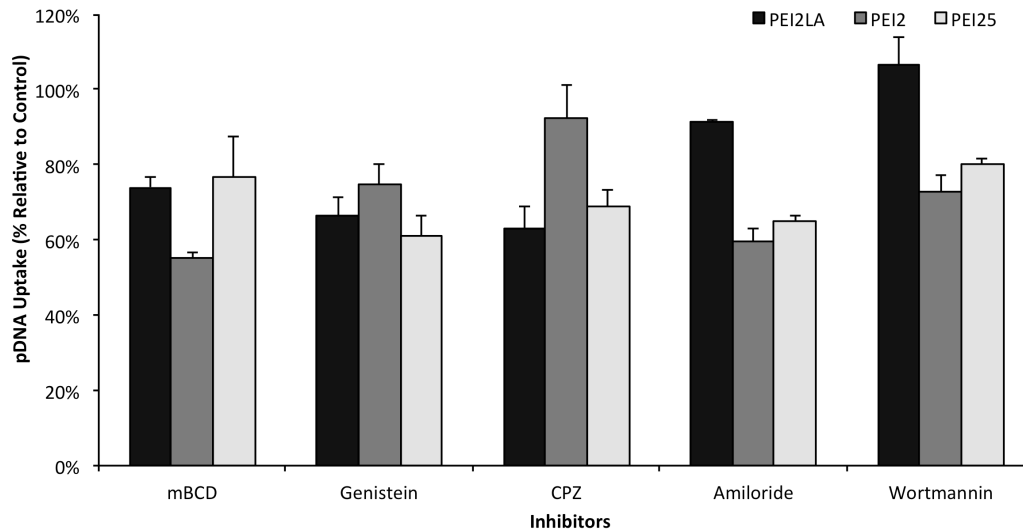


Figure 6.8
The effect of endocytic inhibitors on the level Cy3-pDNA uptake of PEI2LA, PEI2 and PEI25 complexes.

Cells were pre-treated with the inhibitors for 2 h before transfection and the pDNA uptake was determined 6 h after transfection. The concentrations employed for each inhibitor were noted in the results section. Bar height depicts the relative Cy3-pDNA fluorescent intensity as a percentage of untreated cells.

6.3.5 Effect of endocytosis inhibitors on pDNA Uptake

Since the effect of the endocytosis inhibitors is dose-dependent, vital cellular processes may be compromised at high concentrations, leading to reduced cell viability and changes in uptake pathways in a non-specific manner. We assessed the cytotoxic effect of the inhibitors over a concentration range. The line graph overlay in Figures 6 depicts the percentage of viable cells at the same concentrations as those administered in the transfection studies. There was no significant toxicity from genistein or mβCD on NHFF cells for all concentrations tested. CPZ and amiloride had a dose-dependent effect on cell viability; 7.5 μg/ml and 30 μM of the drugs resulted in >50% reduction in cell number, respectively. Wortmannin also reduced cell number by 40% without a dose dependence. In addition to decrease in viability, toxicity can be seen in the form of altered and irregular cell morphology for cells treated with

amiloride and CPZ (not shown). Rather than the elongated shape typical of fibroblasts, treatment with these drugs resulted in shriveling and detachment from the surface, suggestive of necrosis. In light of recent work by Vercauteran et al. on the proper use of inhibitors to study endocytic pathways [26], concentrations for specific inhibitor were chosen based on securing a significant effect on transfection without an equivalent effect on cell viability. The chosen concentrations for subsequent uptake studies were 75 μ M for genistein, 10 μ M for m β CD, 7.5 μ g/ml for CPZ, 30 μ M for amiloride, and 75 nM for wortmannin.

The effect of inhibitors on pDNA uptake was measured 6 h after transfection and expressed as a percentage of untreated cells (**Figure 6.8**). Treatment with m β CD significantly inhibited the uptake of all three complexes ($p < 0.05$); the extent of blockage was greatest in PEI2 (45% vs. 26% and 24% for PEI2, PEI2LA and PEI25, respectively). Genistein interfered with the uptake of all three complexes as well, but the differences in uptake among the three GDVs were negligible. Wortmannin reduced the uptake of PEI2 and PEI25 complexes by 27% and 20%, respectively, but otherwise had no effect on PEI2LA complexes. Similarly, amiloride partially blocked the uptake of PEI2 and PEI25 by 35-40%, but had minimal effect on PEI2LA uptake. The CME-inhibitor CPZ significantly reduced the uptake of PEI2LA (38%) and PEI25 (31%) complexes, but not those of the PEI2 complexes (7%). Taken together, we infer that PEI25 complexes utilized a wide range of uptake pathway involving macropinocytosis, CME and CvME. In contrast, PEI2 was taken up predominantly through macropinocytosis and CvME-mediated endocytosis. Linoleic acid substitution on PEI2 re-routed the entry pathways to predominantly CME, while engaging the CvME to some extent.

6.3.6 Effect of endosome disruption on transfection

We investigated the role of endosome entrapment on transfection efficiency using a number of complementary endosome disruptive methods. Chloroquine is a weak hydrophobic base that buffers acidification in endolysosomal compartments to promote endosomal release of pDNA [7]. Following 2 h pre-treatment with chloroquine, transfection by PEI2LA was increased by 50% (based on mean GFP fluorescence), but transfection of PEI2 and PEI25 complexes was reduced by 36% and 31%, respectively (**Figure 6.9**).

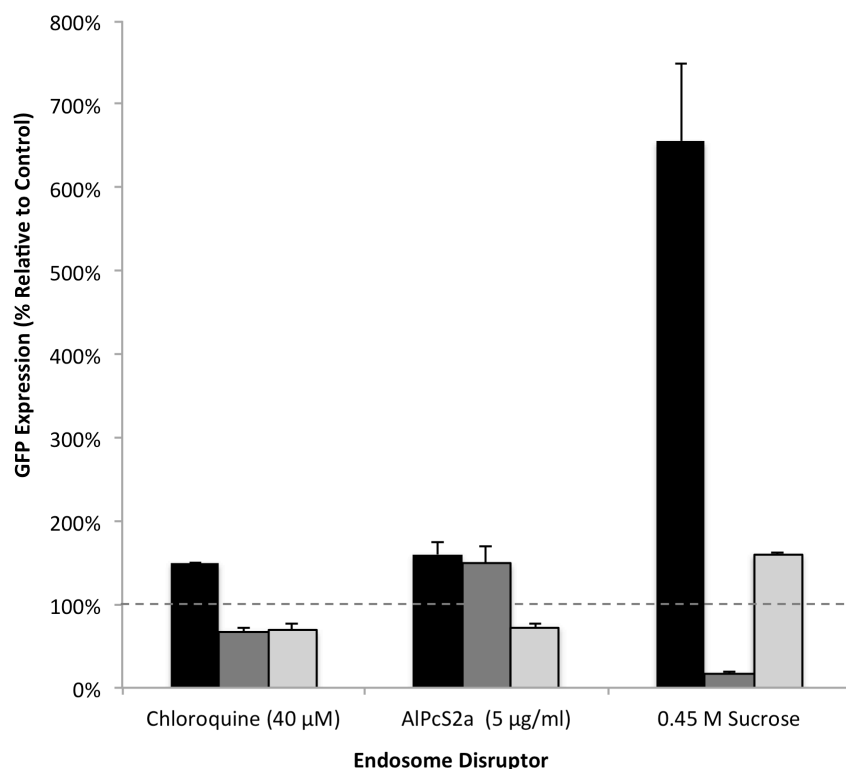


Figure 6.9

Effects of the lysosomotropic agent chloroquine, the photosensitizer AIPcS2a and 0.45 M sucrose on the transfection efficiency of PEI2LA, PEI2, and PEI25 complexes.

Bar height depicts the relative fluorescent intensity of transfected cells with the indicated treatment as a percentage of untreated cells. Transfection by PEI2LA was increased by 50% following treatment with chloroquine, by 60% following light irradiation of AIPcS2a-loaded cells and by 655% after 0.45 M sucrose treatment.

We then employed the photosensitizer (PS), ALPcS2a to facilitate light-induced endosome disruption [27]. Endosomes were loaded with the PS by incubating cells with 5 µg/ml of ALPcS2a for 16 h prior to transfection. Transfected cells were then irradiated with a wide-spectrum light at 3 h after the addition of complexes; this time frame was empirically determined to give most significant changes in transgene expression (data not shown). ALPcS2a-induced endosome release had a positive effect on transfection by PEI2LA and PEI2 complexes, increasing transgene expression by 60% and 49%, respectively (Figure 8), but reduced the efficiency of PEI25 by 27%.

We further transfected the cells in 0.45 M sucrose, which is a hypertonic media that can cause intracellular cytoplasmic swelling within endosomes [28] to promote cytosolic release of endocytosed materials. The hypertonic media enhanced the transfection of PEI2LA complexes by 655% (based on mean GFP fluorescence), while PEI25 complexes displayed 60% increase and PEI2 complexes displayed 85% decrease.

Since endosomal transport is most commonly associated with CME, the effects of these endosome disruptive methods on the transfection efficiency of PEI2LA further suggest that uptake of PEI2LA proceeds predominantly through CME, and that endosome escape is a rate-limiting step in the transfection pathway of PEI2LA.

6.3.7 Intracellular distribution of complexes

To complement the quantitative results from flow cytometry, qualitative information on the intracellular distribution of complexes was generated using fluorescent microscopy. **Figure 6.10** shows CLSM images of cells transfected with Cy3-pDNA (red) complexes, with the nuclei and late endosomes/lysosomes stained with Hoechst 33528 (blue) and AF488-Dextran (green), respectively. The patterns of distribution in PEI2 resemble that of dextran-labeled endosomes, which coalesced into regions

surrounding the nuclei (Figure 9a). The shared pattern between AF488-Dextran and PEI2 complexes, however, did not appear to indicate co-localization, as the red and green punctates were distinctly separated. The distribution pattern of PEI2LA noticeably differed from PEI2 and appeared throughout the cell as large string-like aggregates (**Figure 6.10b**). PEI25 complexes were much smaller, uniform in size and morphology, and were generally distributed randomly throughout the cell (**Figure 6.10c**). Neither PEI2LA nor PEI25 appeared to be co-localized with AF488-Dextran. We also noted that the DNA-intercalating Hoechst dye bound to PEI2LA complexes more than PEI2 complexes (some binding) or PEI25 complexes (no binding), as evident by the purple colors in the composite image. This may suggest that DNA complexed with PEI2LA were more accessible to tertiary binding - a feature that may be beneficial for transgene expression, which require binding by transcription factors.

We further carried out confocal microscopy on transfected cells loaded with the photosensitizer AIPcS2a to gain insights into the observed transfection effects. Because AIPcS2a is extremely sensitive to light and is non-fixable, we employed spinning disk confocal microscopy to carry out live-cell imaging. **Figure 6.11** shows confocal images of transfected cells with AIPcS2a (cyan) and Cy3-pDNA (orange). Consistent with the fixed cell images acquired with CLSM above, PEI2 complexes tended to concentrate into defined regions, whereas PEI2LA and PEI25 complexes appeared more randomly distributed. AIPcS2a displayed a defined distribution pattern in which a hollow circular region can be negatively traced out by the exclusion of AIPcS2a from the area, suggestive of a perinuclear localization. The superimposed images indicated a low degree of co-localization between AIPcS2a and PEI2LA or PEI25 complexes, as evident by the exclusivity between the two colors. PEI2, appeared to share similar distribution pattern as AIPcS2a, but we were not able to collect z-stacks required for quantitative co-localization analysis, since AIPcS2a destabilized after just

20 sec of laser exposure. Regardless, we can conclude by qualitative visual assessment that AlPcS2a had low degree of co-localization with the complexes, suggestive of distinct sets of uptake pathways for the molecules,

Given the significant increase in the transfection of PEI2LA under hypertonic conditions, we next examined the intracellular distribution of Cy3-pDNA in transfected cells treated with 0.45 M sucrose (**Figure 6.12**). Untreated cells showed complexes in discrete regions of bright punctates and appeared more concentrated around the perinuclear region where a negative outline of the nucleus can be seen. In contrast, under hypertonic media, both PEI2 and PEI25 complexes appeared diffused, with lower signal-to-background ratio, which may be indicative of partially decondensed or dissociated complexes since free DNA showed lower fluorescence than complexes, as Figure 3b indicated. Further, PEI2 and PEI25 complexes and were more evenly distributed in sucrose treated cells, hinting a disruption to the endolysosomal trafficking, whereby released complexes were free to move within the cytoplasmic space. Despite the contrasting patterns noted in PEI2 and PEI25, we did not see a discernible difference among cells transfected with PEI2LA. The lack of an observable effect on the intracellular distribution of PEI2LA complexes in hypertonic media may further suggest that PEI2LA adopts a different mode of intracellular transport than the unmodified PEIs.

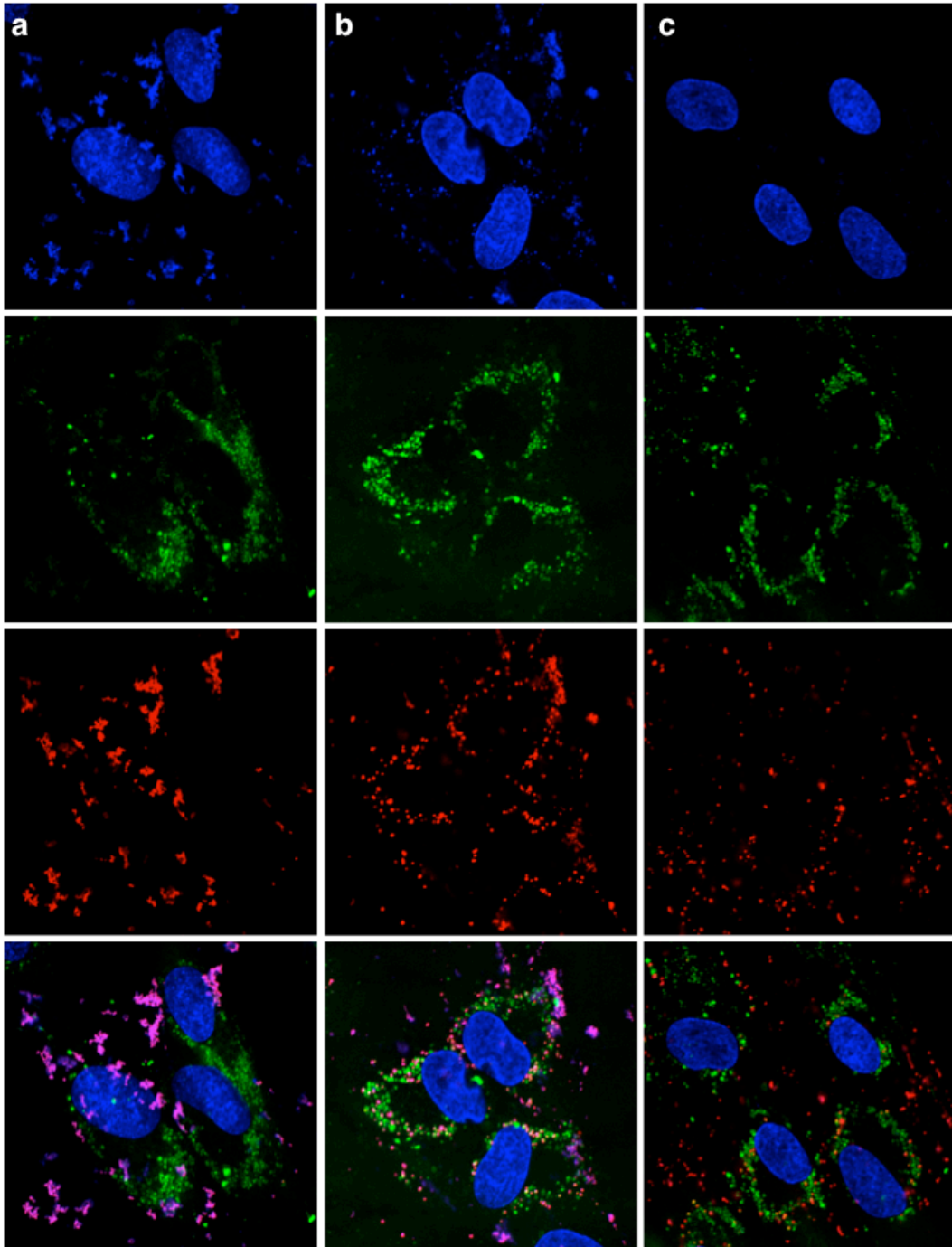


Figure 6.10

Fixed-cell confocal microscopy images showing the intracellular distribution of Cy3-pDNA (red) complexes of PEI2LA (a), PEI2 (b) and PEI25 (c). Each image shown on the optical section was representative of the transfected cell population. Cells were stained with Hoechst 33528 and 10 kDa AF488-Dextran conjugate to visualize the nucleus (blue) and the endosomes (green). Purple images are indicative of both Hoechst 33528 and Cy3 stained pDNA.

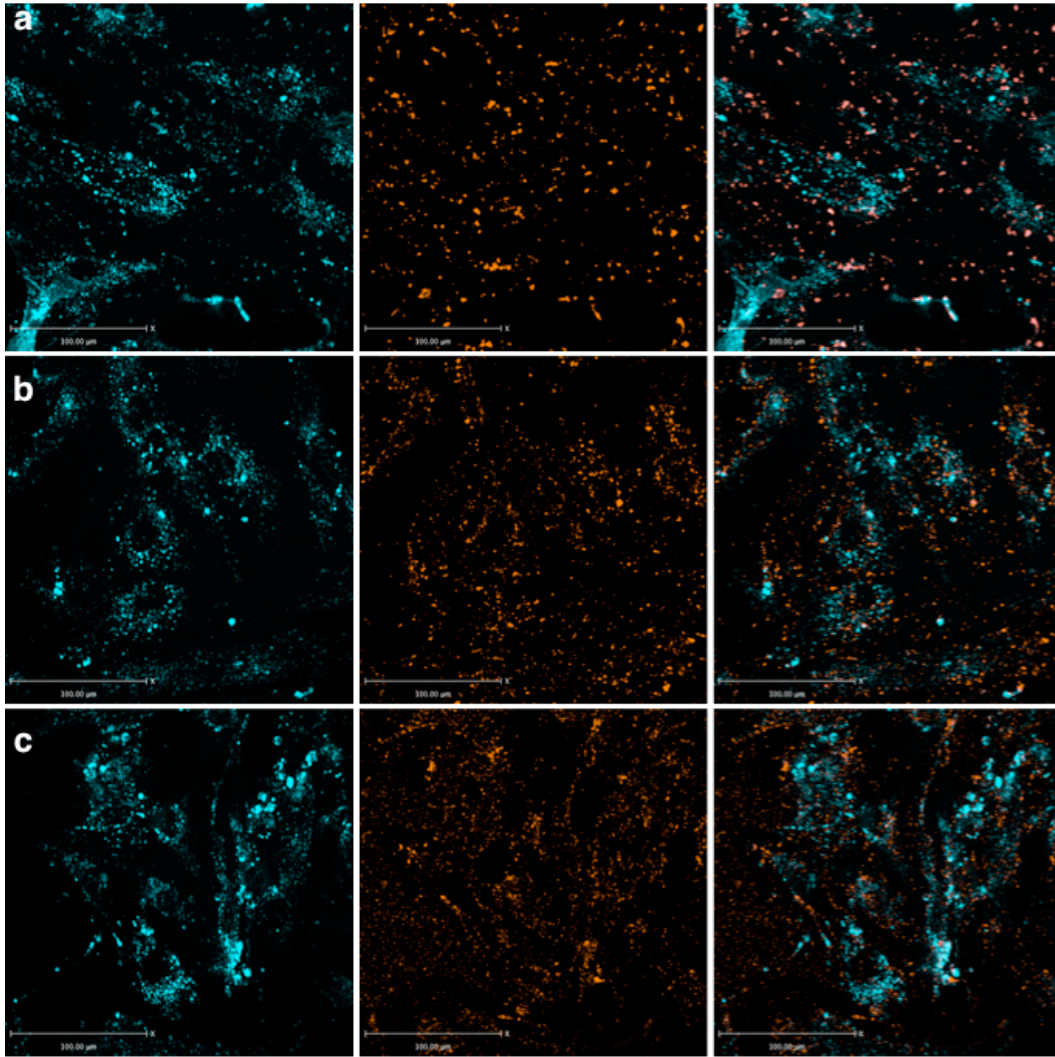


Figure 6.11

Live-cell images acquired with a spinning disk confocal microscope of cells transfected with PEI2LA (a), PEI2 (b), and PEI25 (c) complexes. Cells were pre-loaded with the photosensitizer, ALPcS2a (cyan) for 16 h, then transfected with Cy3-pDNA (orange).

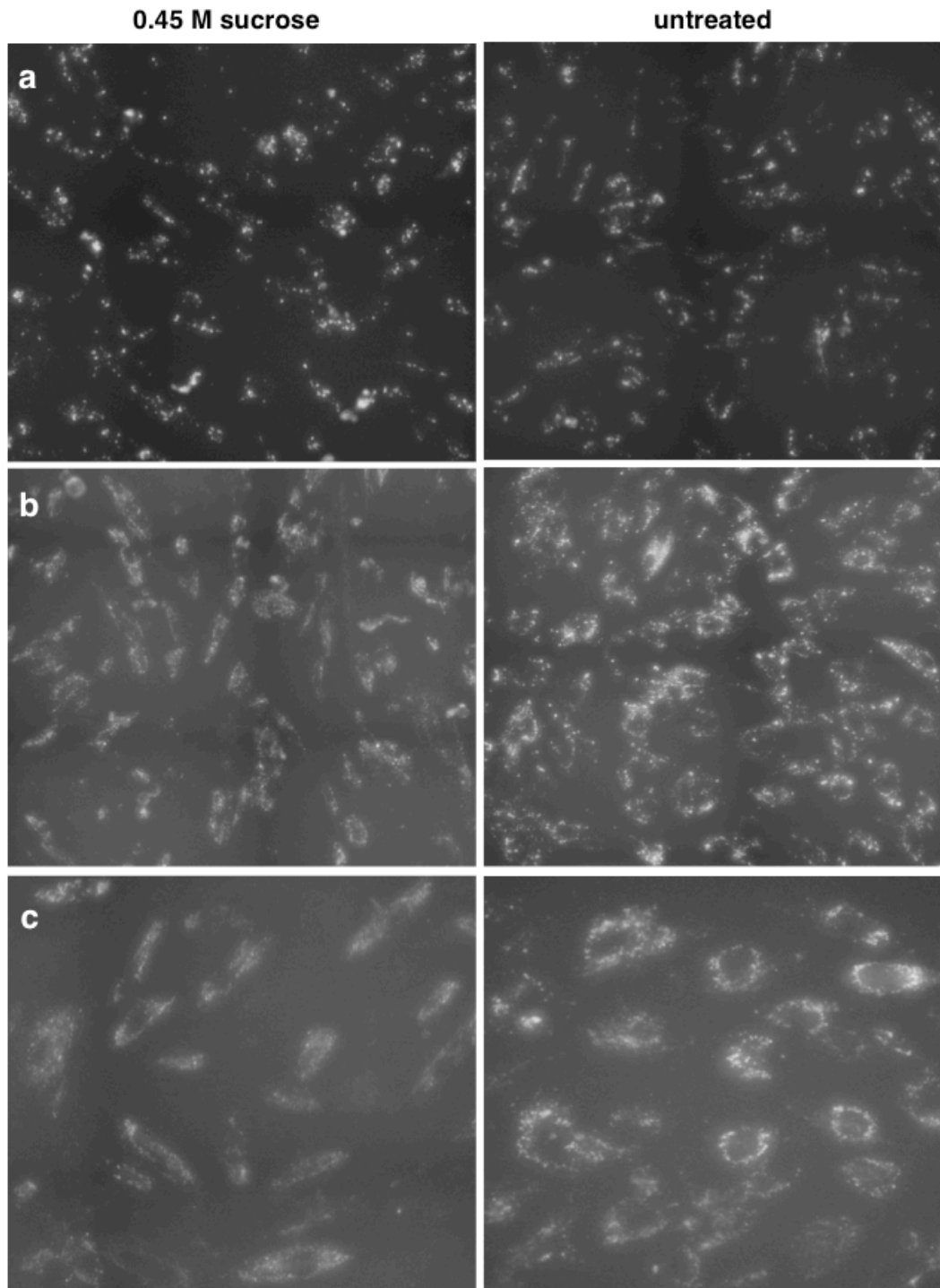


Figure 6.12

Wide-field microscopy images of cells pre-treated for 2 h with hypertonic media

(0.45 M sucrose in OPTI-MEM, left column) and in OPTI-MEM only (right column), then transfected with PEI2LA (a), PEI2 (b), and PEI25 (c) complexes. Images were captured on live cells grown in a plastic tissue culture plate.

6.4 Discussion

Cellular uptake of complexes can be processed via a number of endocytic pathways; the precise pathways to be utilized is expected to be largely determined by physicochemical properties of the complexes such as the size, charge, surface features, hydrophobicity or shape [7,29]. Grafting of linoleic acid moieties to the low molecular weight PEI2 renders new physicochemical features to the assembled polymer/DNA complexes, which may alter the uptake pathway in comparison to its unmodified precursor. Indeed, the results presented herein suggest that uptake of the PEI2 complexes depended largely on CvME and macropinocytosis, as pharmacological compounds that either extracted plasma membrane cholesterol, inhibited the activities of tyrosine kinase, phosphoinositide-3-kinase, or membrane Na⁺/H⁺-ATPase, resulted in significant reduction in both uptake and transfection. In contrast, hydrophobically-modified PEI2LA complexes were taken up primarily through the CME pathway, as evident by the faster rate of uptake, a stronger inhibitory effect by CPZ, and enhanced transfection from endosome disruptions, while CvME continued to be involved in the uptake process, albeit to a lesser extent. On the other hand, the uptake profile of PEI25 complexes was different from PEI2 and PEI2LA complexes, and appeared to involve all three endocytic pathways to the same extent since no single pathway stood out as being strongly inhibited. It should be noted that the involvement of the lesser-known clathrin-/caveolin independent pathways in the uptake of these complexes remains to be clarified. In all cases, uptake was not exclusive to a particular pathway, but multiple routes of entry were utilized to varying degrees. Size data obtained by DLS showed bell-shaped distributions in complex sizes, and further suggest that more than one pathways would be required to sufficiently accommodate the uptake of a heterogeneous population of complexes. Microscopy images showed PEI2 complexes to be concentrated around regions

excluded from the nucleus, while PEI2LA aggregates were found in and around the nucleus, which stood to be unique from the whole-cell distribution pattern in PEI25. Taken together, the intracellular distribution of complexes complemented the finding from the inhibitor studies, whereby PEI2, PEI2LA and PEI25 each exhibited a distinct profile of uptake pathways.

There are several technical aspects of this study that we consider important to highlight. First, because transfection efficiencies are dependent on the complexation conditions, a single complexation method may not accurately portray the relative efficiencies among the GDVs since this will invariably favor one GDV over another [30]. We therefore formulated the complexes in different optimal conditions to ensure the results best reflect the transfection capability of the GDV. Second, there is an inherent delay between the point when complexes are added to the media and the point when complexes reach the cells for internalization. Since complexes formed with different GDVs display different properties, this may translate into different sedimentation rates. Aggregation or destabilization of complexes at different rates [31,32] may further distort the uptake rates. We compensated for these variabilities by applying a centrifugation step immediately following the addition of the complexes to ensure sedimentation rate and complex stability are not limiting the uptake process. Finally, some fluorophore, such as FITC or its derivatives, are sensitive to pH and may diminish at low pHs [33,34]. Since endosomes and macropinosomes involved in CME and macropinocytosis are known to undergo acidification [7,35], in which the luminal pH of these compartments can drop to 4.3-4.7, we employed a pH-insensitive fluorophore to ensure complexes that are localized in acidic compartments do not result in diminished signal intensity. This is particularly important for studies involving comparative evaluation of novel biomaterials for gene delivery where prior knowledge

of the uptake pathways are largely unknown. Overall, we believe these steps should improve the design of future studies on complex uptake and trafficking.

Our results from PS-induced endosome disruption showed improved transfection efficiency for PEI2LA and PEI2. However, the enhancement observed was minimal compared to other studies [36-39]. It should be noted that, in cases of sub-optimal complexation conditions (e.g., low N/P ratio), PSs are expected to be more beneficial in transfection [40,41]. Considering that we optimized transfection conditions for each polymer, it is not surprising that PS did not make a great impact in transfection efficiency. Further, the effectiveness of PS-induced endosome disruption is dependent on the extent of co-localization between the complexes and the PS. [42]. The images captures by confocal microscope in this study revealed a lack of spatial coordination between the PSs and complexes, confirming that PSs did not promote efficient release of complexes from the endosome. A method to synchronize the intracellular location of PS and complexes may lead to a greater margin of enhancement in transfection.

It is surprising that PEI2LA complexes, despite being the largest, were nevertheless taken up predominantly through CME rather than macropinocytosis, even though CME and CvME are often associated with smaller complexes (up to 200 nm) while macropinocytosis is typically involved with larger complexes up to 1 μm [13,25,43,44]. We did not find a correlation between the sizes of our complexes and the reported sizes associated with each endocytic pathways [15,43]. Since uptake pathway should be largely dependent on complex composition and cell type [14,15,45], direct comparison of results with previous studies may not be applicable. The LA moiety may very well serve as a ligand to facilitate receptor-mediated endocytosis via CME. Size measurements in aqueous environment could be an over-estimation of actual complex size owing to the hydrophobic nature of the complexes, which has a higher

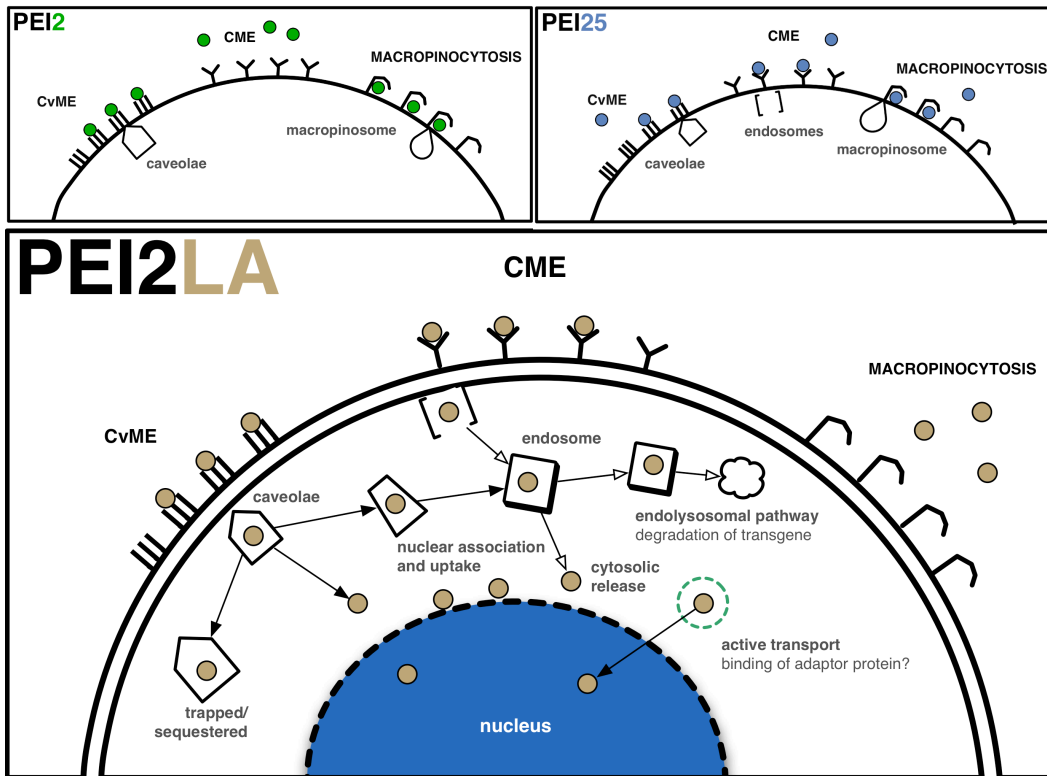
tendency towards aggregation, leading measurement to the aggregates of the complexes, rather than individual complex. It is still conceivable that size does impose certain restriction on the uptake pathway, but in a way that permit smaller complexes to have more flexibility in terms of which route to use, whereas larger complexes are restricted to a few specific routes. This notion came from the observation that PEI25 complexes, being the smallest of the three, were sufficiently taken up by all of the pathways examined in this work, whereas the larger PEI2 and PEI2LA, showed a preference for CvME and CME, respectively. Still, the notion that LA moiety could be involved in facilitating receptor-ligand mediated endocytosis cannot be ruled out here; further investigation is needed to reveal additional mechanistic role of LA in uptake

The fact that CPZ had the greatest impact on the transfection efficiency of PEI2LA may simply imply that a larger proportion of the complexes are taken up through CME. This does not suggest that CME is the most efficient pathway or that this route is responsible for the increase in transfection efficiency of PEI2LA per se since the shift to CME may be a mere consequence of the change in complex properties induced by LA substitution. The most efficient pathway would need to be determined by actively targeting the complexes to each of the endocytic pathways, in which the pathway with the highest ratio of transgene expression-to-pDNA would be deemed the most efficient. It is conceivable that CME in this case is not the most conducive transfection pathway for PEI2LA and that the enhancement in transfection is principally derived from the small proportion of the complexes released into the cytosolic domain, which were able to mediate highly efficient trafficking for transfection. In other words, the role of lipid-moieties might not be limited to increasing binding affinity to cellular membranes, but to further act as signaling ligand to mediate active intracellular transport.

Mechanistic studies on the effect of hydrophobic modification are currently limited and the few studies that have been published so far focused primarily on chitosan conjugates. In one instance, the substitution of chitosan with palmitic acid progressively shifted dependence towards lipid-raft mediated endocytosis, as degree of substitution increased [16]. In another instance, glycol chitosan modified with 5 β -cholanic acid were found to be taken up by all endocytic pathways and were distributed evenly throughout the cell [46]. Though the cell type and GDV used in those studies are significantly different from ours, two aspects were consistent with our data; (i) biochemical modification alters the surface properties of the complexes and changes the uptake pathways, and; (ii) complex uptake was not exclusive to one pathway, but employed multiple pathways to varying degrees.

Our work presented here provides the first mechanistic view into the transfection pathway of lipid modified PEIs. **Scheme 6** shows a proposed model for the uptake and intracellular trafficking of PEI2LA in NHFF cells. We believe that LA-substituted complexes are taken up predominantly via CME, and to a lesser extent by CvME; macropinocytosis is either not involved or play a minor role in the uptake. Following release into the cytosol, the LA moieties mediate nuclear import either through association with hydrophobic domain of the nuclear membrane or through fusion to gain direct entry [5]. What remains to be determined is the fate of the complexes within vesicular compartments and the mechanism by which the portion of complexes manage to get released into the cytosol. Existing literature on the uptake pathways of cationic GDVs employed transformed cell lines such as HEK293, CHO, COS-7, and HeLa cells [8-10,18,47]. To the best of our knowledge, this study is the first study to probe transfection pathways of polymeric GDVs in the context of a clinically-relevant primary tissue derived human foreskin fibroblast cells. The results from this

study should further facilitate the rational design of non-viral gene delivery systems for clinical applications.



Scheme 6

A proposed model for the uptake and subsequent intracellular trafficking pathway of PEI2LA complexes in NHFF cells.

PEI2LA complexes were predominantly taken up through CME, and to some extent by the CvME. Macropinocytosis is either not involved or play a minor role in the uptake of PEI2LA. PEI2 complexes are internalized mainly through CvME and macropinocytosis while PEI25 are taken up by all endocytic pathways to some extent. Following uptake, endosomes undergo gradual acidification and are trafficked to the endolysosomal pathway, where the ingested pDNA may become degraded. A portion of the complexes nevertheless is released into the cytosol by yet unknown mechanism(s) and nucleocytoplasmic transport leads to lipid-moieties associating with the lipophilic domains of nuclear membrane. Subsequent nuclear entry is gained by a flip-flop mechanism or passively during cell division when the nuclear membrane breaks down [5].

6.5 References

- [1] Demeneix B., Hassani Z., and Behr J.-P., 2004, "Towards multifunctional synthetic vectors," *Curr Gene Ther*, **4**(4), pp. 445–455.
- [2] Mintzer M. A., and Simanek E. E., 2009, "Nonviral vectors for gene delivery," *Chem. Rev.*, **109**(2), pp. 259–302.
- [3] Incani V., Lavasanifar A., and Uludağ H., 2010, "Lipid and hydrophobic modification of cationic carriers on route to superior gene vectors," *Soft Matter*, **6**(10), pp. 2124–2138.
- [4] Neamark A., Suwantong O., Bahadur R. K. C., Hsu C. Y. M., Supaphol P., and Uludağ H., 2009, "Aliphatic lipid substitution on 2 kDa polyethylenimine improves plasmid delivery and transgene expression.," *Mol Pharm*, **6**(6), pp. 1798–1815.
- [5] Hsu C. Y. M., Hendzel M., and Uludağ H., 2011, "Improved transfection efficiency of an aliphatic lipid substituted 2 kDa polyethylenimine is attributed to enhanced nuclear association and uptake in rat bone marrow stromal cell.," *J Gene Med*, **13**(1), pp. 46–59.
- [6] Medina-Kauwe L. K., Xie J., and Hamm-Alvarez S., 2005, "Intracellular trafficking of nonviral vectors.," *Gene Ther*, **12**(24), pp. 1734–1751.
- [7] Khalil I. A., Kogure K., Akita H., and Harashima H., 2006, "Uptake pathways and subsequent intracellular trafficking in nonviral gene delivery.," *Pharmacol. Rev.*, **58**(1), pp. 32–45.
- [8] Rejman J., Bragonzi A., and Conese M., 2005, "Role of clathrin- and caveolae-mediated endocytosis in gene transfer mediated by lipo- and polyplexes.," *Mol Ther*, **12**(3), pp. 468–474.
- [9] van der Aa M. A. E. M., Huth U. S., Häfele S. Y., Schubert R., Oosting R. S., Mastrobattista E., Hennink W. E., Peschka-Süss R., Koning G. A., and Crommelin D. J. A., 2007, "Cellular uptake of cationic polymer-DNA complexes via caveolae plays a pivotal role in gene transfection in COS-7 cells.," *Pharmaceutical research*, **24**(8), pp. 1590–1598.

- [10] Gabrielson N. P., and Pack D. W., 2009, "Efficient polyethylenimine-mediated gene delivery proceeds via a caveolar pathway in HeLa cells," *J Control Release*, **136**(1), pp. 54–61.
- [11] Douglas K. L., 2008, "Toward development of artificial viruses for gene therapy: A comparative evaluation of viral and non-viral transfection," *Biotechnology Progress*, pp. 871–883.
- [12] Hufnagel H., Hakim P., Lima A., and Hollfelder F., 2009, "Fluid phase endocytosis contributes to transfection of DNA by PEI-25," *Mol Ther*, **17**(8), pp. 1411–1417.
- [13] Izumisawa T., Hattori Y., Date M., Toma K., and Maitani Y., 2011, "Cell line-dependent internalization pathways determine DNA transfection efficiency of decaarginine-PEG-lipid," *Int J Pharm*, **404**(1-2), pp. 264–270.
- [14] Douglas K. L., Piccirillo C. A., and Tabrizian M., 2008, "Cell line-dependent internalization pathways and intracellular trafficking determine transfection efficiency of nanoparticle vectors," *Eur J Pharm Biopharm*, **68**(3), pp. 676–687.
- [15] Gersdorff von K., Sanders N. N., Vandenbroucke R., De Smedt S. C., Wagner E., and Ogris M., 2006, "The internalization route resulting in successful gene expression depends on both cell line and polyethylenimine polyplex type," *Mol Ther*, **14**(5), pp. 745–753.
- [16] Chiu Y.-L., Ho Y.-C., Chen Y.-M., Peng S.-F., Ke C.-J., Chen K.-J., Mi F.-L., and Sung H.-W., 2010, "The characteristics, cellular uptake and intracellular trafficking of nanoparticles made of hydrophobically-modified chitosan," *J Control Release*, **146**(1), pp. 152–159.
- [17] Wang B., He C., Tang C., and Yin C., 2011, "Effects of hydrophobic and hydrophilic modifications on gene delivery of amphiphilic chitosan based nanocarriers," *Biomaterials*, **32**(20), pp. 4630–4638.
- [18] Olton D. Y. E., Close J. M., Sfeir C. S., and Kumta P. N., 2011, "Intracellular trafficking pathways involved in the gene transfer of nano-structured calcium phosphate-DNA particles," *Biomaterials*, **32**(30), pp. 7662–7670.

- [19] Yu J., Vodyanik M. A., Smuga-Otto K., Antosiewicz-Bourget J., Frane J. L., Tian S., Nie J., Jonsdottir G. A., Ruotti V., Stewart R., Slukvin I. I., and Thomson J. A., 2007, "Induced pluripotent stem cell lines derived from human somatic cells," *Science*, **318**(5858), pp. 1917–1920.
- [20] Maherali N., Sridharan R., Xie W., Utikal J., Eminli S., Arnold K., Stadtfeld M., Yachechko R., Tchieu J., Jaenisch R., Plath K., and Hochedlinger K., 2007, "Directly reprogrammed fibroblasts show global epigenetic remodeling and widespread tissue contribution," *Cell Stem Cell*, **1**(1), pp. 55–70.
- [21] Jensen T. G., 2007, "Cutaneous gene therapy," *Ann. Med.*, **39**(2), pp. 108–115.
- [22] Wernig M., Meissner A., Foreman R., Brambrink T., Ku M., Hochedlinger K., Bernstein B. E., and Jaenisch R., 2007, "In vitro reprogramming of fibroblasts into a pluripotent ES-cell-like state," *Nature*, **448**(7151), pp. 318–324.
- [23] Wang J., Dodd C., Shankowsky H. A., Scott P. G., Tredget E. E., Wound Healing Research Group, 2008, "Deep dermal fibroblasts contribute to hypertrophic scarring," *Lab. Invest.*, **88**(12), pp. 1278–1290.
- [24] Hsu C. Y. M., and Uludağ H., "A simple and rapid non-viral approach to efficiently transfect primary tissue-derived cells using polyethylenimine," *Nat Protoc.*
- [25] Conner S. D., and Schmid S. L., 2003, "Regulated portals of entry into the cell," *Nature*, **422**(6927), pp. 37–44.
- [26] Vercauteren D., Vandenbroucke R. E., Jones A. T., Rejman J., Demeester J., De Smedt S. C., Sanders N. N., and Braeckmans K., 2010, "The use of inhibitors to study endocytic pathways of gene carriers: optimization and pitfalls," *Mol Ther*, **18**(3), pp. 561–569.
- [27] Prasmickaite L., Høgset A., Engesaeter B. B. Ø., Bonsted A., and Berg K., 2004, "Light-directed gene delivery by photochemical internalisation," *Expert Opin Biol Ther*, **4**(9), pp. 1403–1412.
- [28] Kato T., Okada S., Yutaka T., and Yabuuchi H., 1984, "The effects of sucrose loading on lysosomal hydrolases," *Mol. Cell. Biochem.*, **60**(1), pp. 83–98.

- [29] Chavanpatil M. D., Khdair A., and Panyam J., 2006, "Nanoparticles for cellular drug delivery: mechanisms and factors influencing delivery.," *J Nanosci Nanotechnol*, **6**(9-10), pp. 2651–2663.
- [30] van Gaal E. V. B., van Eijk R., Oosting R. S., Kok R. J., Hennink W. E., Crommelin D. J. A., and Mastrobattista E., 2011, "How to screen non-viral gene delivery systems in vitro?," *J Control Release*, **154**(3), pp. 218–232.
- [31] Sharma V. K., Thomas M., and Klibanov A. M., 2005, "Mechanistic studies on aggregation of polyethylenimine-DNA complexes and its prevention.," *Biotechnol Bioeng*, **90**(5), pp. 614–620.
- [32] Ikonen M., Murtomäki L., and Kontturi K., 2008, "Controlled complexation of plasmid DNA with cationic polymers: effect of surfactant on the complexation and stability of the complexes.," *Colloids and Surfaces B: Biointerfaces*, **66**(1), pp. 77–83.
- [33] Klonis N., and Sawyer W. H., 1996, "Spectral properties of the prototropic forms of fluorescein in aqueous solution," *J Fluoresc*, **6**(3), pp. 147–157.
- [34] Sjöback R., Nygren J., and Kubista M., 1995, "Absorption and fluorescence properties of fluorescein," *Spectrochimica Acta Part A: Molecular and Biomolecular Spectroscopy*, **51**(6), pp. L7–L21.
- [35] Xiang S., Tong H., Shi Q., Fernandes J. C., Jin T., Dai K., and Zhang X., 2011, "Uptake mechanisms of non-viral gene delivery," *Journal of Controlled Release*.
- [36] Prasmickaite L., Høgset A., Tjelle T. E., Olsen V. M., and Berg K., 2000, "Role of endosomes in gene transfection mediated by photochemical internalisation (PCI).," *J Gene Med*, **2**(6), pp. 477–488.
- [37] Bøe S., Saebøe-Larssen S., and Hovig E., 2010, "Light-induced gene expression using messenger RNA molecules," *Oligonucleotides*, **20**(1), pp. 1–6.
- [38] Varkouhi A. K., Lammers T., Schiffelers R. M., van Steenbergen M. J., Hennink W. E., and Storm G., 2011, "Gene silencing activity of siRNA polyplexes based on biodegradable polymers," *Eur J Pharm Biopharm*, **77**(3), pp. 450–457.

- [39] Nishiyama N., Arnida, Jang W.-D., Date K., Miyata K., and Kataoka K., 2006, "Photochemical enhancement of transgene expression by polymeric micelles incorporating plasmid DNA and dendrimer-based photosensitizer," *J Drug Target*, **14**(6), pp. 413–424.
- [40] Bøe S., Longva A. S., and Hovig E., 2008, "Evaluation of various polyethylenimine formulations for light-controlled gene silencing using small interfering RNA molecules," *Oligonucleotides*, **18**(2), pp. 123–132.
- [41] Gargouri M., Sapin A., Arica-Yegin B., Merlin J. L., Becuwe P., and Maincent P., 2011, "Photochemical internalization for pDNA transfection: evaluation of poly(d,l-lactide-co-glycolide) and poly(ethylenimine) nanoparticles," *Int J Pharm*, **403**(1-2), pp. 276–284.
- [42] Bonneau S., Morlière P., and Brault D., 2004, "Dynamics of interactions of photosensitizers with lipoproteins and membrane-models: correlation with cellular incorporation and subcellular distribution," *Biochem Pharmacol*, **68**(7), pp. 1443–1452.
- [43] Rejman J., Oberle V., Zuhorn I. S., and Hoekstra D., 2004, "Size-dependent internalization of particles via the pathways of clathrin- and caveolae-mediated endocytosis," *Biochem J*, **377**(Pt 1), pp. 159–169.
- [44] Grosse S., Aron Y., Thévenot G., François D., Monsigny M., and Fajac I., 2005, "Potocytosis and cellular exit of complexes as cellular pathways for gene delivery by polycations," *J Gene Med*, **7**(10), pp. 1275–1286.
- [45] Hsu C. Y. M. C., and Uludağ H. H., 2012, "Nucleic-acid based gene therapeutics: delivery challenges and modular design of nonviral gene carriers and expression cassettes to overcome intracellular barriers for sustained targeted expression," *J Drug Targeting*, **20**(4), pp. 301–328.
- [46] Nam H. Y., Kwon S. M., Chung H., Lee S.-Y., Kwon S.-H., Jeon H., Kim Y., Park J. H., Kim J., Her S., Oh Y.-K., Kwon I. C., Kim K., and Jeong S. Y., 2009, "Cellular uptake mechanism and intracellular fate of hydrophobically modified glycol chitosan nanoparticles," *Journal of Controlled Release*, **135**(3), pp. 259–267.

- [47] Mäger I., Langel K., Lehto T., Eiríksdóttir E., and Langel U., 2011, "The role of endocytosis on the uptake kinetics of luciferin-conjugated cell-penetrating peptides.," *Biochim Biophys Acta*, **1818**(3), pp. 502–511.

Chapter 7

General discussion, conclusions, future directions and perspectives

7.1 General discussion

Biocompatible cationic materials are promising alternative to viral vectors for gene therapy. Despite demonstrating efficient transfection capability *in vitro*, clinical translation of these non-viral gene carriers is currently hampered by poor efficacy *in vivo*. While evolving efforts continue with the rational design of novel bio-conjugates, two areas of research are needed to overcome design impediments to more effective carriers. One area involves mapping the intracellular fate of non-viral gene complexes to gain insights into the rate-limiting steps. The other area should be focused on developing a clinically-relevant model for validating carrier efficiencies. The use of established cultured cells lines such as HEK293T, COS-7, HeLa or CHO cells have become a common practice owing to their availability and ease of handling. But the process of transformation to make them more amenable to culturing conditions also render an abnormal physiology, limiting the direct clinical translation and account for the lack of concordance between *in vitro* and *in vivo* models.

The focus of this thesis is on developing a mechanistic view of the intracellular fate of lipid modified cationic polymers within the context of clinically-relevant tissue-derived primary cells. Primary cell lines are the ideal pre-clinical models for *in vitro* studies, but one of the technical challenge that precludes their widespread use is their hard-to-transfect nature; transfection efficiency is significantly lower compared to established cultured cell lines, which limits the quantitative resolution necessary to generate statistically significant data. We addressed this technical shortfall and developed an optimized protocol for the transfection of rat bone marrow stromal cells and normal human foreskin fibroblast cells using polyethyleneimine [1]. The main tenet behind this modified transfection protocol is in maximizing the utility time-frame of the assembled complexes. Complexes of cationic polymer and DNA are unstable in solution, aggregates can form spontaneously over time, which is attributed to reduced

transfection efficiency and cell viability [2,3]. The optimized protocol incorporates several workaround procedural changes to minimize aggregate formation, including 1) increasing the complexation volume to reduce intermolecular interactions, 2) removal of serum to prevent the formation of protein-complex aggregates, and 3) inclusion of a centrifugation step to minimize the time required for complexes to reach cell surfaces. It is important to note that the transfection conditions described in the protocol do not mimic *in vivo* delivery conditions. The intention here is to be able to differentiate rate-limiting steps within intracellular domains from those extracellular factors to obtain an accurate view of the transfection capability of the non-viral gene carriers.

One of the unique aspect of non-viral carriers that sets itself apart from viral vectors is the way genetic materials are packaged for delivery. Non-viral gene complexes are self-assembled through electrostatic interaction between the cationic reagent and the anionic nucleic acid molecules. Thus, there is no restriction on the molecular weights and topologies of DNA for packaging. Indeed, we have shown that there were no discernible differences in either the *in vitro* binding interaction to the gene carriers or the efficiency of uptake between either the circular and linear forms or between large and small DNA molecules. Circular DNA (c-DNA) was found to be more effective than the linearized DNA molecules for transgene expression. Better cellular uptake of c-DNA into the cells was not the reason for its better performance, since all carriers were able to efficiently deliver all DNA molecules into the cells regardless of their sizes and topologies [4]. Intracellular processing of the DNA molecules was more likely to be the underlying reason for better efficiency of c-DNA. The implication of this study suggest that non-viral gene carriers are more flexible in the types of nucleic acid cargo they can carry and are not restricted by particular vector constructs or sequence elements, as is the case for viral vectors. This suggest the types of genetic modifications that can be

facilitated by non-viral gene carriers extend beyond those typically mediated by viral vector and may position non-viral gene delivery systems as more than just a safer alternative to viruses.

The transfection capability of a carrier-DNA complex is closely tied to its uptake pathway, which dictates subsequent intracellular routing and processing. To better understand the mechanistic role of lipid moieties in gene delivery, we set out to define the transfection pathway of DNA delivered by hydrophobically modified cationic polymers. We focused on three events along the transfection pathway: 1) endocytic pathways, 2) endosome escape, and 3) nuclear import. We found that lipid modification renders a new set of the physicochemical properties to the assembled complexes, and changed the uptake pathway profile as a result; complex uptake was not exclusive to singular route of entry, but employed multiple pathways to varying degrees. Endosome entrapment continues to be a road block in transfection, suggesting either the altered uptake pathways exerted additional rate-limiting pressure on the lipid-conjugates or lipid moieties were ineffective at promoting endosome escape. Despite insufficient endosome escape, we did find that enhanced transfection efficiency in lipid-modified carriers was partly due to increased association of lipophilic complexes with the nuclear periphery [5]. Further, transgene-positive cells had, on average, a greater amount of pDNA associated with their nuclei than non-expressing cells, reinforcing the notion that trafficking to the nucleus is critical for transfection. However, nuclear uptake alone cannot predict transfection at the individual cell level since cells that display high pDNA nuclear disposition did not always express transgene, suggesting epigenetic regulation and intranuclear disposition are additional factors to consider in the transfection pathway.

7.1 Future directions

Our work presented herein described the correlation between several physicochemical aspects of the DNA molecule, gene carrier and transfection efficiency. However, several additional questions have now naturally arisen that require further resolution. In **Chapter 4**, we showed that circularized DNA was the most effective topology for transfection. But, it was not clear why the linearized version, with identical DNA sequences, were significantly less effective in transfection. It is plausible that linearized DNA with uncapped ends are more susceptible to intracellular nuclease degradation and can further act as stress response stimuli since double stranded breaks are signs of compromised genomic integrity [6]. This might lead to increased degradation of linearized DNAs, making it unavailable for transcription. Assays probing the extent of DNA degradation and markers for DNA repair pathways should address this issue. Moreover, it is widely regarded that the unmethylated CpG dinucleotide sequences found in the plasmid vector backbone are immunogenic and can activate innate immune responses that effectively attenuate transgene expression [7]. This may explain why the PCR generated DNA used in our study, which had the bacterial vector sequence removed, performed better than its full-length counterpart [4]. Minicircle DNA devoid of the vector sequences have been shown to provide greater and longer transgene expression both *in vitro* and *in vivo* [8-10]. Methods to circularize the PCR generated DNA for use in transfection and subsequently assay for the cytokine profile may provide clarification on this front.

In **Chapter 6**, we attributed additional uptake and intracellular trafficking roles to the lipid-moieties in transfection. More specifically, we speculated the possibility of specific receptors that mediate binding to lipids, and affecting both uptake and intracellular transport. The question surrounding the role of lipids in promoting cell surface binding for better uptake has yet to be fully resolved. The studies that we

typically conduct measure both binding and uptake as one event. While it shows that lipid-substitution provided more efficient complex uptake, it does not directly show if this is the result of better cell binding. Methods to dissociate cell surface complexes or quench extracellular signal of labeled complexes as well as inhibiting endocytosis would help to resolve this issue.

We also reinforced the notion that the amount of pDNA associated with the nucleus is positively correlated with transfection efficiency and that lipid-moieties are able to facilitate this process to enhance transfection (**Chapter 5**). Future studies on this front can be expanded into two avenues. One of which could be directed towards understanding the mechanism of nuclear import of lipid-substituted gene carriers, specifically, whether the lipid ligands are able to facilitate transport across the nuclear membrane through fusion/flip-flop, promoting nuclear uptake in a cell-cycle independent fashion; methods to attenuated or accelerate cell proliferation rate may be necessary to conduct these studies. It should be noted that nanoparticles are structures larger than the nuclear pore complexes and whether such pores expand to accommodate the DNA/polymer particles is one area that requires clarification. The second avenue could be directed towards understanding the role of lipid moieties as intracellular transport signal molecule. Endogenous proteins are known to be post-translationally modified for further sorting to sub-cellular compartments during organelle biosynthesis [11]. For example, palmitoylation allow protein to be targeted to specialized membrane microdomains involved in synaptic scaffolding, signaling and cytoskeletal proteins [12] as well as in retrograde transport during lysosome trafficking [13]. The possibility that lipid moieties can act as signaling ligands in gene delivery has never been considered. Gaining insight into additional mechanistic role of aliphatic acid moieties in sub-cellular trafficking should further enhance its utility as a functional ligand in gene delivery.

In **Chapter 6**, we described the uptake pathways taken by lipid-substituted gene carriers as predominantly CME. However, since the results are principally derived from the effects of pharmacological inhibitors, which are known to exhibit pleiotropic activities, the conclusions from the chapter may require additional studies for further validation. The ideal approach would be to conduct the study in endocytic pathway mutants that either over-express a dominant-negative protein or are devoid of pathway regulators for a particular pathway [14]. However, such methods may not be technically feasible for primary cells at the moment due to a lack of an efficient method to manipulate primary cells for this reason. Complementary techniques such as confocal microscopy is a necessary follow-up in this regard; uptake pathways of DNA complexes could be mapped by quantitative co-localization analysis using pathway markers such as Transferrin and Cholera Toxin, which are commonly used to indicate CME and CvME, respectively [15-17]. However, the exact uptake pathway by which complexes are taken up is beginning to become less important in recent years as exceptions to their intracellular fate emerge. For example, CvME has often been regarded as the ideal uptake pathway since caveolae are generally non-acidic and non-degradative [18]. However, recent evidence demonstrated that caveolae not only undergo acidification but can also merge with endosome and become destined for the endolysosomal pathway [19,20]. Even macropinocytosis, which is not known to be a degradative path, were recently shown to harbor acidic pH inside macropinosomes and trafficked to the lysosomal pathway [21,22]. Regardless of the pH or the type of degradative environment the complexes end up in, it can be agreed upon that disruption of the vesicular compartment is a priority to enhance carrier performance in transfection. Thus, subsequent focus in non-viral gene carrier design should be on promoting efficient release into the cytoplasm, rather than on defining a specific endocytic pathway as target.

For non-viral gene carriers to be successfully translated into the clinics, more long-term studies regarding the fate of complexes and the ensuing cellular responses to transfection are needed to fully understand its safety profile. In **Appendix A** and **Appendix B**, we showed that plasmid DNA persisted inside the cell for as long as 37 days after transfection, yet transgene expression rapidly declined to background level after just 7 days. It is not known which sub-cellular compartments the transgene DNA resided in during this period and whether the plasmid DNA is capable of genomic integration, which can impose significant mutagenic risks. Further, in **Appendix C**, we demonstrated that transgene expression can be sustained when inhibitors of the NF- κ B pathway is applied, suggesting the innate immune response is activated and acting negatively on transfection. The prospective safety profile driving the development of non-viral gene delivery systems have so far stand uncontested due to insufficient clinical evidence. While cationic reagents are potentially safer than viral vectors, several studies have reported immunogenic properties in cationic lipids [23-27]. In light of the amphipathic nature of these lipid-modified cationic polymers, future studies would need to monitor for signs of immune responses in order to fully understand the safety risks associated with its clinical use.

7.2 Concluding remarks and perspectives

Current design of gene carriers and expression cassettes has been limited to a few functional elements, tackling one or two rate-limiting steps at a time, which may not provide as significant gain in efficiency since other inhibitory factors may continue to act negatively on the process. The advancement of non-viral gene delivery systems would need to be complemented by genetic approaches to design better DNA vectors that incorporate functional epigenetic elements. Nucleic acid molecules are different from conventional pharmaceutical compounds in that, in addition to serving as the therapeutic molecules, it can also act as a vector to provide both supplementary and

complementary delivery and trafficking capabilities to work in concert with the gene carrier. For example, tissue-specific targeting can be mediated by the carrier through ligand-cell surface receptor binding, then enhanced by genetic elements to delimit expression to specific cell type while suppressing activity in non-targeted cells. In terms of supplementary activity, the carrier can circumnavigate the endolysosomal pathway using its membrane-disruptive components, then subsequent trafficking through the nucleocytoplasmic pathway can be supplemented by nuclear targeting DNA sequences recombined into the vector [28]. Where the two components work exclusively from each other is at either ends of the transfection pathway, namely extracellular and intra-nuclear domains. Carriers are required to package and condense the nucleic acid in order to protect it from degradation and promote its uptake, which the nucleic acid does poorly on its own. On the other hand, sub-nuclear events such as transcriptional activity, replicative distribution, nuclear retention, and chromatin positioning are beyond the capabilities of the carrier. Thus, incorporating genetic and epigenetic elements into the DNA vector may overcome some of the hurdles currently limiting the advancement of non-viral carrier-assisted gene delivery systems. A hypothetical construct of such a DNA vector for long-term targeted transgene expression is show in **Figure 7.1**; detailed discussion on the principle of each genetic elements is continued in **Appendix D**.

Nucleic acid therapeutics can access biological pathways that are far more extensive than traditional protein or drug-based therapies. The types of physiological response can be easily tweaked by changing the type of genetic cargo for delivery to target alternative pathways that may be more efficiently manipulated. In that sense, gene augmentation or gene knockdown is not limited to supplementing deficient products or removing 'toxic' mediators, but as control elements that can work in parallel or in conjunction for a desired therapeutic outcome. The process of identifying alternative

interventions, however, is not a trivial one and will require a basic understanding of the cellular and molecular processes involved. Understanding the molecular mechanism of pathogenesis would be key to designing a gene therapy protocol with high therapeutic potential while limiting ectopic effects. Ultimately, gene delivery systems may need to be optimized on a disease-by-disease basis, where both the activity and specificity of the gene carriers/nucleic acid molecules are adapted towards the target cell type as well as the modality of genetic modifications.

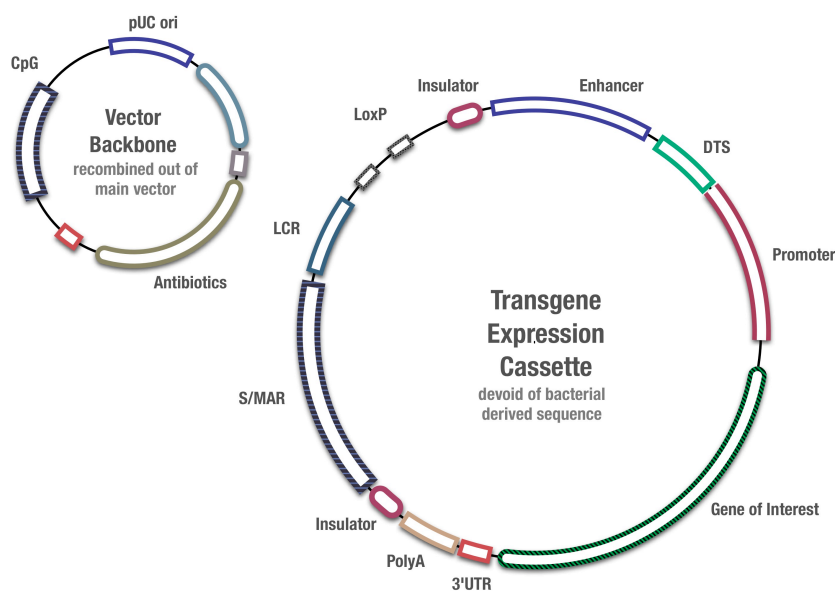


Figure 4.

Figure 7.1

A hypothetical map of DNA vector for the long-term targeted expression of transgene in mammalian cells.

In this construct, expression of the gene of interest is driven by a tissue-specific promoter with the activity complemented by an enhancer element. The promoter contains transcription factor binding sites, which can double as nuclear DNA targeting sequence (DTS) for nuclear import. Noncoding elements such as 3'-UTR and polyadenylation sites further enhance the stability of mRNA, prolonging its cytoplasmic half-life during translation. S/MAR sequences promote the replication and nuclear retention of the plasmid throughout cell division while insulator and LCR shield the transgene from heterochromatin domains. Finally, loxP/ or similar repeat sequences mediate the removal of bacterial derived vector backbone through site-specific recombination to minimize immune reactivity to the vector.

7.3 References

- [1] Hsu C. Y. M., and Uludağ H., "A simple and rapid non-viral approach to efficiently transfect primary tissue-derived cells using polyethylenimine," *Nat Protoc.*
- [2] Ikonen M., Murtomäki L., and Kontturi K., 2008, "Controlled complexation of plasmid DNA with cationic polymers: effect of surfactant on the complexation and stability of the complexes," *Colloids and Surfaces B: Biointerfaces*, **66**(1), pp. 77–83.
- [3] Sharma V. K., Thomas M., and Klibanov A. M., 2005, "Mechanistic studies on aggregation of polyethylenimine-DNA complexes and its prevention," *Biotechnol Bioeng*, **90**(5), pp. 614–620.
- [4] Hsu C. Y. M., and Uludağ H., 2008, "Effects of size and topology of DNA molecules on intracellular delivery with non-viral gene carriers," *BMC Biotechnol.*, **8**, p. 23.
- [5] Hsu C. Y. M., Hendzel M., and Uludağ H., 2011, "Improved transfection efficiency of an aliphatic lipid substituted 2 kDa polyethylenimine is attributed to enhanced nuclear association and uptake in rat bone marrow stromal cell," *J Gene Med*, **13**(1), pp. 46–59.
- [6] Jackson S. P., 2002, "Sensing and repairing DNA double-strand breaks," *Carcinogenesis*, **23**(5), pp. 687–696.
- [7] Hyde S. C., Pringle I. A., Abdullah S., Lawton A. E., Davies L. A., Varathalingam A., Nunez-Alonso G., Green A.-M., Bazzani R. P., Sumner-Jones S. G., Chan M., Li H., Yew N. S., Cheng S. H., Boyd A. C., Davies J. C., Griesenbach U., Porteous D. J., Sheppard D. N., Munkonge F. M., Alton E. W. F. W., and Gill D. R., 2008, "CpG-free plasmids confer reduced inflammation and sustained pulmonary gene expression," *Nat Biotechnol*, **26**(5), pp. 549–551.
- [8] Osborn M. J., McElmurry R. T., Lees C. J., Defeo A. P., Chen Z. Y., Kay M. A., Naldini L., Freeman G., Tolar J., and Blazar B. R., 2011, "Minicircle DNA-based gene therapy coupled with immune modulation permits long-term expression of α -

- L-iduronidase in mice with mucopolysaccharidosis type I," *Mol Ther*, **19**(3), pp. 450–460.
- [9] Chen Z. Y., He C.-Y., Ehrhardt A., and Kay M. A., 2003, "Minicircle DNA vectors devoid of bacterial DNA result in persistent and high-level transgene expression in vivo.," *Mol Ther*, **8**(3), pp. 495–500.
- [10] Huang M., Chen Z., Hu S., Jia F., Li Z., Hoyt G., Robbins R. C., Kay M. A., and Wu J. C., 2009, "Novel minicircle vector for gene therapy in murine myocardial infarction.," *Circulation*, **120**(11 Suppl), pp. S230–7.
- [11] Rajendran L., Kn Ouml Lker H.-J., and Simons K., 2010, "Subcellular targeting strategies for drug design and delivery," *Nat Rev Drug Discov*, **9**(1), p. 29.
- [12] Fukata Y., and Fukata M., 2010, "Protein palmitoylation in neuronal development and synaptic plasticity.," *Nat. Rev. Neurosci.*, **11**(3), pp. 161–175.
- [13] McCormick P. J., Dumaresq-Doiron K., Pluiose A.-S., Pichette V., Tosato G., and Lefrancois S., 2008, "Palmitoylation Controls Recycling in Lysosomal Sorting and Trafficking," *Traffic*, **9**(11), pp. 1984–1997.
- [14] Vercauteren D., Vandenbroucke R. E., Jones A. T., Rejman J., Demeester J., De Smedt S. C., Sanders N. N., and Braeckmans K., 2010, "The use of inhibitors to study endocytic pathways of gene carriers: optimization and pitfalls.," *Mol Ther*, **18**(3), pp. 561–569.
- [15] van der Aa M. A. E. M., Huth U. S., Häfele S. Y., Schubert R., Oosting R. S., Mastrobattista E., Hennink W. E., Peschka-Süss R., Koning G. A., and Crommelin D. J. A., 2007, "Cellular uptake of cationic polymer-DNA complexes via caveolae plays a pivotal role in gene transfection in COS-7 cells.," *Pharmaceutical research*, **24**(8), pp. 1590–1598.
- [16] Gersdorff von K., Sanders N. N., Vandenbroucke R., De Smedt S. C., Wagner E., and Ogris M., 2006, "The internalization route resulting in successful gene expression depends on both cell line and polyethylenimine polyplex type.," *Mol Ther*, **14**(5), pp. 745–753.

- [17] Olton D. Y. E., Close J. M., Sfeir C. S., and Kumta P. N., 2011, "Intracellular trafficking pathways involved in the gene transfer of nano-structured calcium phosphate-DNA particles," *Biomaterials*, **32**(30), pp. 7662–7670.
- [18] Razani B., Woodman S. E., and Lisanti M. P., 2002, "Caveolae: from cell biology to animal physiology," *Pharmacol. Rev.*, **54**(3), pp. 431–467.
- [19] Chiu Y.-L., Ho Y.-C., Chen Y.-M., Peng S.-F., Ke C.-J., Chen K.-J., Mi F.-L., and Sung H.-W., 2010, "The characteristics, cellular uptake and intracellular trafficking of nanoparticles made of hydrophobically-modified chitosan," *J Control Release*, **146**(1), pp. 152–159.
- [20] Kiss A. L., and Botos E., 2009, "Endocytosis via caveolae: alternative pathway with distinct cellular compartments to avoid lysosomal degradation?" *J. Cell. Mol. Med.*, **13**(7), pp. 1228–1237.
- [21] Falcone S., Cocucci E., Podini P., Kirchhausen T., Clementi E., and Meldolesi J., 2006, "Macropinocytosis: regulated coordination of endocytic and exocytic membrane traffic events," *J. Cell. Sci.*, **119**(Pt 22), pp. 4758–4769.
- [22] Racoosin E. L., and Swanson J. A., 1993, "Macropinosome maturation and fusion with tubular lysosomes in macrophages," *J. Cell Biol.*, **121**(5), pp. 1011–1020.
- [23] Sakurai H., Sakurai F., Kawabata K., Sasaki T., Koizumi N., Huang H., Tashiro K., Kurachi S., Nakagawa S., and Mizuguchi H., 2007, "Comparison of gene expression efficiency and innate immune response induced by Ad vector and lipoplex," *J Control Release*, **117**(3), pp. 430–437.
- [24] Sakurai H., Kawabata K., Sakurai F., Nakagawa S., and Mizuguchi H., 2008, "Innate immune response induced by gene delivery vectors," *Int J Pharm*, **354**(1-2), pp. 9–15.
- [25] Zhang J.-S., Liu F., and Huang L., 2005, "Implications of pharmacokinetic behavior of lipoplex for its inflammatory toxicity," *Adv Drug Deliv Rev*, **57**(5), pp. 689–698.

- [26] Sakurai F., Terada T., Yasuda K., Yamashita F., Takakura Y., and Hashida M., 2002, "The role of tissue macrophages in the induction of proinflammatory cytokine production following intravenous injection of lipoplexes.," *Gene Ther*, **9**(16), pp. 1120–1126.
- [27] Li S., Wu S. P., Whitmore M., Loeffert E. J., Wang L., Watkins S. C., Pitt B. R., and Huang L., 1999, "Effect of immune response on gene transfer to the lung via systemic administration of cationic lipidic vectors.," *Am. J. Physiol.*, **276**(5 Pt 1), pp. L796–804.
- [28] Vacik J., Dean B. S., Zimmer W. E., and Dean D. A., 1999, "Cell-specific nuclear import of plasmid DNA.," *Gene Ther*, **6**(6), pp. 1006–1014.

Appendix A

Delivering plasmid DNA with a non-viral polymeric carrier: plasmid persistence does not necessarily lead to transgene expression¹

¹A version of this appendix has been presented as an abstract at the 8th World Biomaterials Congress in Amsterdam, NL. (2008). Hsu, C., Zylstra, A., and Uludag, H.

A.1 Introduction

Non-viral gene carriers formulated with cationic polymers offer a safe alternative to viral vectors, but remain limited in use in clinical settings due to low transfection efficiency and a lack of sustained transgene expression. Understanding the mechanism behind transient transgene expression is critical to developing rational designs towards a sustained gene delivery system.

Previously, we observed good transfection of bone marrow stromal cells (BMSC) with an in-house modified polymer, poly-L-lysine grafted with palmitic acid (PLL-PA). However, the transgene expression declined over a 10-14 day period. It was not known if the reduction in transgene expression was due to loss of exogenous plasmid, or to silencing of the transgene. This study was conducted to clarify this issue.

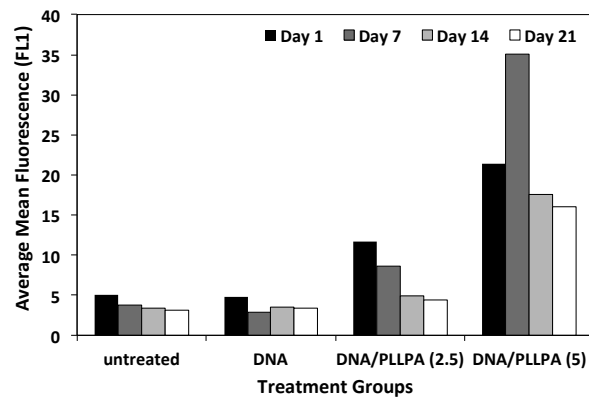
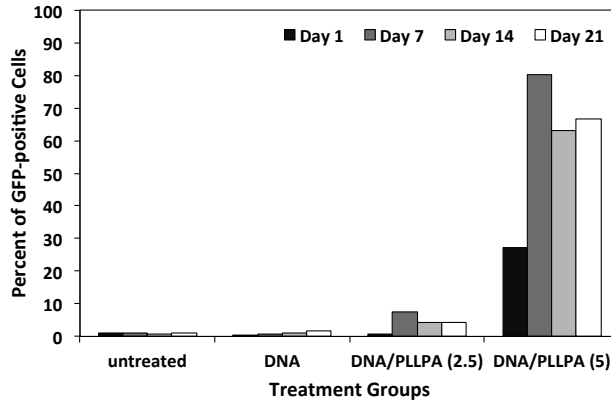
A.2 Materials and methods

An in-house constructed plasmid, pIRES2-bFGF-AcGFP1, which co-expresses the reporter gene *AcGFP* and basic Fibroblast Growth Factor (bFGF), were used in this study. The plasmid was complexed with PLL-PA for 30 min at a polymer/DNA weight ratio of 2.5 and 5, then added directly to BMSC cultured in OptiMEM+1% FBS at a final DNA concentration of 2 µg/mL. The BMSC was derived from the femurs of Sprague-Dawley rats. After incubating the cells with the complexes for 24 hours, the cells were washed, and fresh medium was added for prolonged culture (14 days). Cells were processed at the specified time point for the analysis of reporter gene expression using flow cytometry; total genomic DNA and total RNA were extracted using the QIAGEN AllPrep DNA/RNA Mini Kit. First strand cDNA was synthesized from total RNA using MMLV Reverse Transcriptase according to the manufacturer's instruction. PCR was performed on total genomic DNA and cDNA using customarily designed primer

specific to the plasmid DNA sequence (F:TCCTGCGTTATCCCCTGATT; R:CGCTTACAATT-TACGCCTTAAG) and the GFP cDNA sequence (F: TGTTGAATGTCGTGAAGGAAG; R: CTC-CATCTTATTGCCAGG), respectively.

A.3 Results and discussion

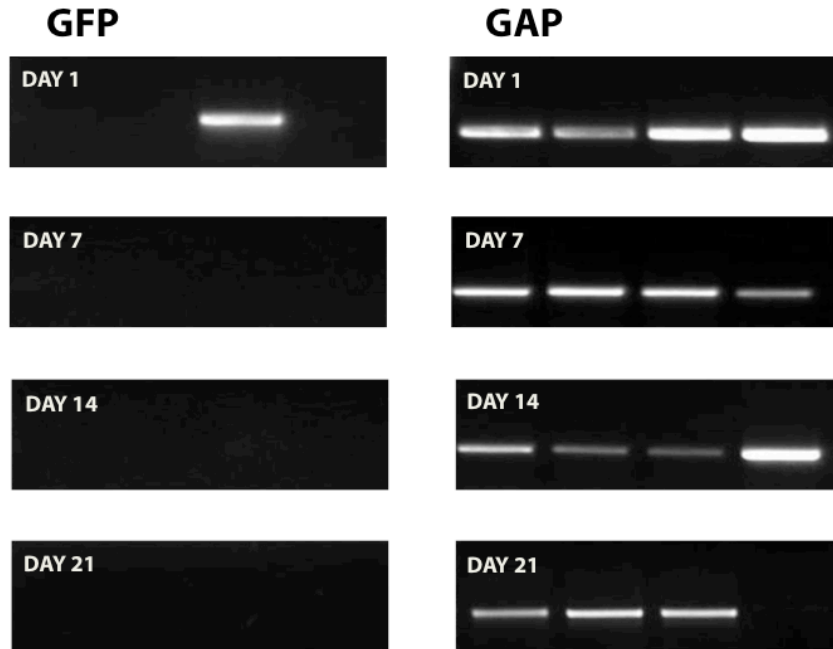
Transfection of BMSC with pDNA/PLL-PA complexes led to detectable GFP expression by flow cytometry. The higher polymer-to-pDNA weight ratio (5) gave better transfection efficiency than the lower ratio (2.5). Maximal GFP expression was seen on day 7 and declined to less than 50% thereafter (**Figure A-1**). Total RNA was purified and reverse transcribed to cDNA for RT-PCR to detect GFP-specific mRNA. **Figure A-2** showed that GFP mRNA was amplifiable only on Day 1, suggesting no additional transcription took place. However, when PCR was performed on total DNA to detect pDNA, PCR product could be amplified from samples that have been in culture for 21 days, suggesting DNA remained in the cell and did not appear to be degraded. We conclude that the lack of sustained transgene expression is not immediately attributed to the loss of exogenous plasmid DNA, but rather, a lack of transgene-specific transcription. Understanding the mechanism behind this silencing effect will be paramount to enhance the effectiveness of polymeric carriers for gene delivery.



Appendix Figure A-1

Transfection efficiency of PLL-PA in rBMSC over a 21 day period.

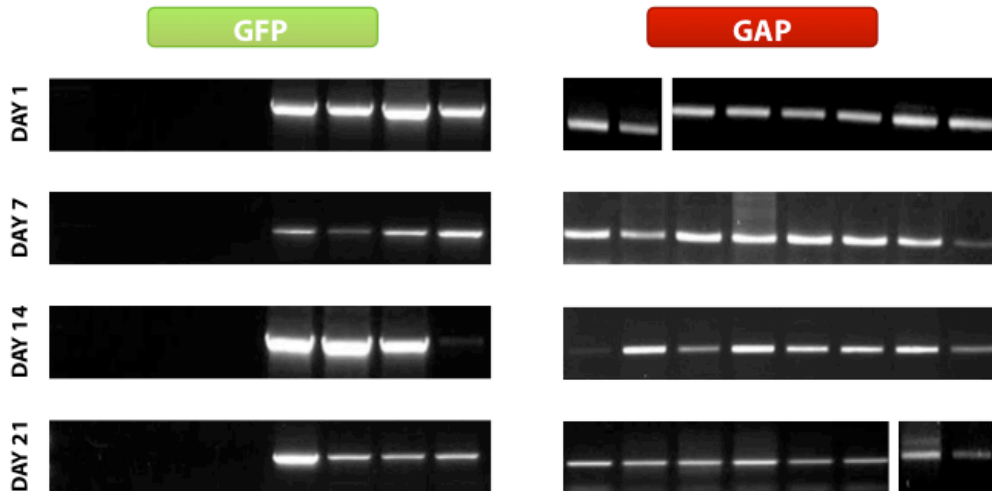
The percent of GFP-positive cells as a function of treatment applied to BMSC (top); The mean fluorescence values (FL1) of gated cells from the treatment groups collected on day 1, 7, 14 and 21 (bottom). Untreated: cells treated with buffer. DNA: cells treated with DNA only. DNA/PLLPA: cells treated with the polyplex; value in parenthesis denotes the DNA-polymer weight ratio. A final polymer concentration of 5 $\mu\text{g}/\text{ml}$ and 10 $\mu\text{g}/\text{ml}$ were used for (2.5) and (5), respectively.



Appendix Figure A-2

Analysis of total RNA for the presence of AcGFP-specific mRNA transcript and GAPDH

The analysis was conducted after pooling the total RNA isolated on days 1, 7, 14 and 21 for cells treated with buffer (lane 1), plasmid (lane 2), plasmid/PLL-PA (1:2.5; lane 3) and plasmid/PLL-PA (1:5; lane 4). Lanes are numbered from left to right



Appendix Figure A-3

Analysis of total DNA for the plasmid pIRES2-bFGF-AcGFP1 and GAPDH.

The analysis was conducted in duplicate on days 1, 7, 14 and 21 for cells treated with buffer (lanes 1 and 2), plasmid (lanes 3 and 4), plasmid/PLL-PA (1:2.5; lanes 5 and 6) and plasmid/PLL-PA (1:5; lanes 7 and 8). Lanes are numbered from left to right

Appendix B

Persistence of Plasmid DNA does not lead to sustained transgene expression in PEI mediated transfection *in vitro*: implication of transcriptional and post-transcriptional silencing¹

¹version of this appendix has been presented as an abstract at The Twelfth Annual Meeting of the American Society of Gene Therapy, San Diego, California. 9th American Society of Gene Therapy in San Diego. (2009). Hsu, C.Y., and Uludag, H.

B.1 Introduction

Non-viral gene delivery systems are currently limited in clinical use due to the lack of sustained expression from the exogenous DNA in clinically relevant cells. Plasmid DNA typically used with non-viral gene carriers lack sequence elements required to faithfully propagate inside the host. Thus, through rounds to cell division, the transgene copy number per cell is expected to decrease, effectively lowering the delivery efficiency [1]. In addition, unprotected episomal DNAs are prone to degradation by intracellular nucleases, further reducing the transgene concentration among transfection cells. These factors contribute to the loss of template copy number and may account for the short duration of transfection. However, copy number alone do not account for the rapid decline in transgene expression. Several studies have demonstrated that transgene expression was “attenuated” at a much earlier time point than the gradual loss of plasmid, suggesting other mechanisms may be involved in diminished transgene expression [2,3]. While much of the characterizations on transgene silencing have been done in vivo, little is known regarding the fate of transgene expression in vitro and the mechanism of silencing. Here we profile transfection over a period of 37 days by examining the presence of the reporter gene with respect to DNA, RNA and protein. We then applied the histone deacetylase inhibitor, TSA to determine if histone modification is involved in transfection under tissue culture setting.

B.2 Material and methods

Cell culture and transfection

Rat bone marrow stromal cells (rBMSC) isolated from the femur of Sprague-Dawley rats were grown in tissue culture supplemented with DMEM (+10%FBS) except during transfection where OptiMEM (1% FBS) was used instead. Transfection was carried out using complex of PEI (25kDa, branched) and gWiz-GFP at a polymer-to-DNA ratio of 2.5 (wt/wt). Polyplex was added directly to the media, incubated for 24 hours and replaced with growth media thereafter until processing for analysis.

Reverse-transcribed PCR

Total DNA and total RNA was extracted and purified from rBMSC using QIAGEN's DNeasy mini kit and RNeasy mini kit, respectively, accordingly to manufacturer suggested protocol. Nucleic acid was quantified using Nanovue spectrophotometer. Reverse transcription of RNA to cDNA was performed using MMLV reverse transcriptase with oligo(dT) primers.

Each PCR reaction was carried out with the following conditions: 1x PCR buffer, 1.5 mM MgCl₂, 0.3 μM of each forward and reverse primers, 200 μM dNTP, and 2.5 U of Taq polymerase. Cycling condition was as follows: [94°C for 5:00; 28 cycles x (94°C for 0:30 sec, Primer T_m for 0:30, 72°C for 0:30); 72°C for 5:00]. Note that elongation time for plasmid detection is extended to 2:30 to account for the larger PCR product size. Primers used for PCR are as follow

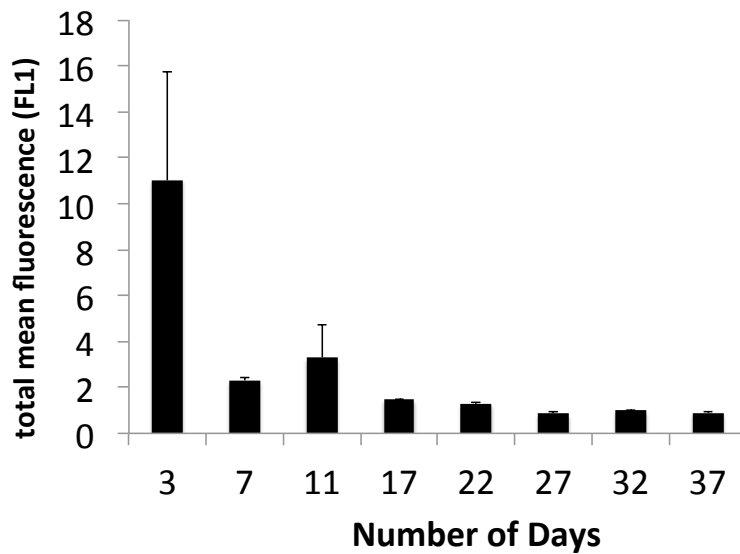
Plasmid DNA (PCR)	Forward: AGATGCGTAAGGAGAAAATACCG	Tm= 55°C
	Reverse: TGGCAACTAGAAAGGCACAG	Tm = 55°C
GFP (RT-PCR)	Forward: AACGGCCACAGGTTCTCTGTC	Tm= 58°C
	Reverse: GTGTCCCAGAATGTTGCCATCT	Tm = 58°C
GAPDH	Forward: ACCACAGTCCATGCCATCAC	Tm = 58°C
	Reverse: TCCACCACCCTGTTGCTGTA	Tm = 59°C

B.3 Results and discussion

BMSCs were transfected with PEI25 complexes then assayed for reporter gene expression over a course of 37 days. Highest transgene expression was observed on Day 3, and declined to background level after 7 days; no transgene expression were detected beyond this period (**Figure B-1**). GFP transcript could be detected by RT-PCR throughout the 37 day time frame, however, the amount of GFP mRNA declined over time, as evident by the decrease in fluorescent intensity of the amplified product (**Figure B-2**). PCR performed on total DNA showed detectable amount of gWIZ-GFP, but the amount of pDNA decreased with over time as well (**Figure B-3**).

The decrease in transgene expression could also be attributed to epigenetic mechanisms such as histone deacetylation, which renders histone-bound DNA in a compressed structure, thereby silencing gene expression by limiting transcriptional access. To determine if histone deacetylation is involved in the decline of transgene expression, we applied the histone deacetylase inhibitor, Trichostatin A (TSA), to transfected cells. **Figure B-4** shows that TSA has a positive effect on transgene expression when applied on Day 8, but not on Day 3. The magnitude of difference in GFP fluorescence between Day 3 and Day 8 increased as the concentration of TSA increases.

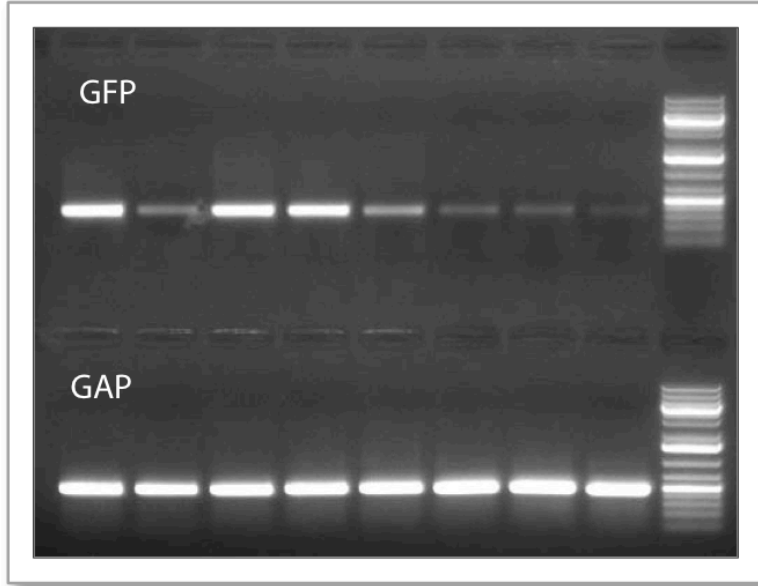
Taken together, these results suggest the lack of sustained transgene expression is attributed to the gradual decline in the amount of intracellular pDNA, which effectively reduced the transcription of transgene mRNA. Histone deacetylation exerts silencing pressure on transgene expression at a later time point, further limiting transgene persistence. Methods to facilitate the replication of transgene DNA as well as to prevent its heterochromatinization will be necessary to extend the duration of transfection.



Appendix Figure B-1

Mean fluorescence (FL1) of total cell population from Day 3 to Day 37.

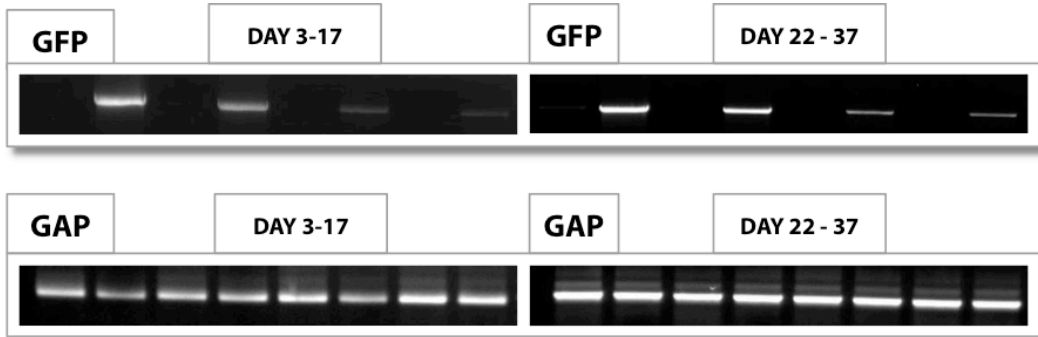
Fluorescent values for each of the days have been normalized to cells transfected with a null vector (gWIZ). GFP fluorescence dropped to background level after just 7 days.



Appendix Figure B-2

RT-PCR on reverse transcribed cDNA to detect transgene expression

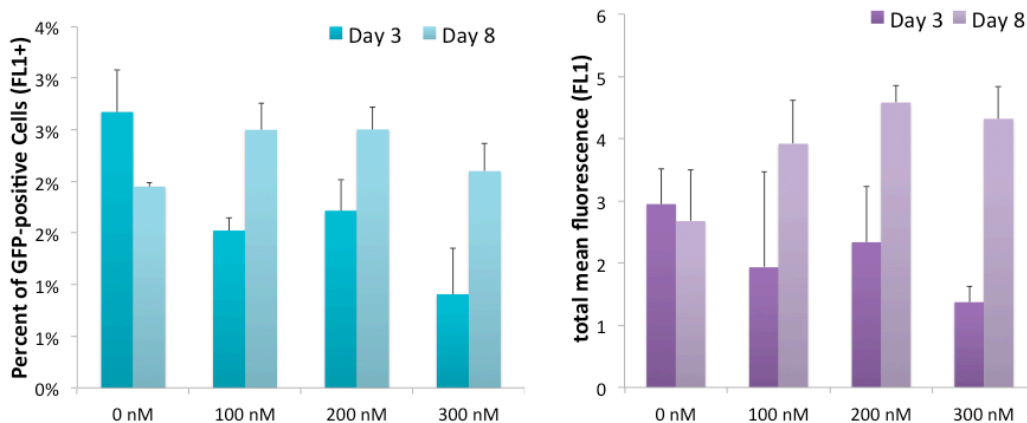
GFP-specific transcript (top half) and GAPDH (bottom half) from Days 3-37 (lanes left to right). Negative control RT control using RNA as template show no GFP product (not shown).



Appendix Figure B-3

PCR on total DNA showing the presence of plasmid DNA

from day 3-17 (left) and 22-37 (right). Each lane is separated by a non-transfected sample (no plasmid). The amount of DNA template loaded in PCR have been increased for samples from Day 22-37, to account for the anticipated decrease in intracellular pDNA.



Appendix Figure B-4

Transfection Efficiency in the presence of trichostatin A

Percent of GFP-positive cells (left) and mean fluorescence of total cell population (right) from transfected cells treated with increasing concentration of TSA.

B.4 References

- [1] Hsu C. Y. M. C., and Uludağ H. H., 2012, "Nucleic-acid based gene therapeutics: delivery challenges and modular design of nonviral gene carriers and expression cassettes to overcome intracellular barriers for sustained targeted expression.," *J Drug Targeting*, **20**(4), pp. 301–328.
- [2] Zaldumbide A., and Hoeben R. C., 2008, "How not to be seen: immune-evasion strategies in gene therapy.," *Gene Ther*, **15**(4), pp. 239–246.
- [3] Bartoli A., Fettucciari K., Fettriconi I., Rosati E., Di Ianni M., Tabilio A., Delfino D. V., Rossi R., and Marconi P., 2003, "Effect of trichostatin a and 5'-azacytidine on transgene reactivation in U937 transduced cells.," *Pharmacol. Res.*, **48**(1), pp. 111–118.

Appendix C

Transfection mediated by cationic polymer in vitro is enhanced by blocking NF- κ B activation: involvement of the intracellular innate immune response in non-viral gene delivery¹

¹A version of this appendix has been presented as an abstract at The Twelfth Annual Meeting of the American Society of Gene Therapy, San Diego, California. 9th American Society of Gene Therapy in San Diego. (2009). Hsu, C.Y., and Uludag, H.

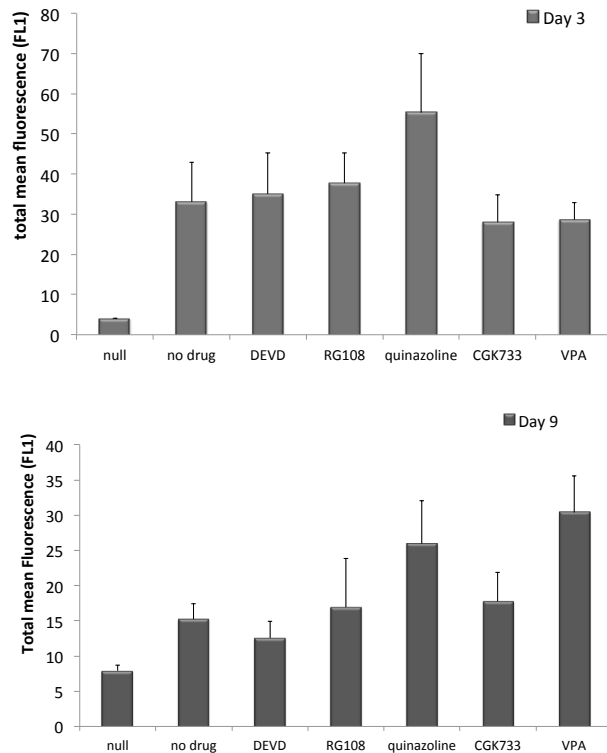
C.1 Introduction

Intracellular nucleases can nick or digest plasmid DNA into smaller fragments. Fragmented DNA can act as stress stimuli to trigger the DNA repair pathway, apoptosis, cell cycle arrest and abolish global transcription altogether as a self-regulating mechanism to prevent production of aberrant genes [1,2]. The net result of these cascade of events is accelerated decline in transgene expression. In addition to degradation, sequence elements found on the plasmid DNA can further activate pathways aimed at reversing transfection as part of the naturally evolved cellular defense mechanism against non-native transforming processes. In particular, the bacterial derived vector sequences, characterized by the high abundance of unmethylated CpG dinucleotide, which are needed for the cloning and propagation of the expression vector from a bacterial host, can attenuate transgene expression via methylation, heterochromatinization and induction of the innate immune response [3,4]. Transgene silencing via nucleotide methylation is a well documented process in viral vectors [5]. The presence of CMV promoters in non-viral expression cassettes are expected to evoke similar nucleotide modifications to inactive transcriptional competence. CpG dinucleotides can further attract binding from heterochromatin-associated histone proteins and position pDNA in a transcriptionally-inactive part of the nucleus to reduce overall transgene expression [6]. Finally, unmethylated CpG sequences are known to interact with the toll-like receptor 9 found in the endosome, where upon binding, can trigger the innate immune response, which include activation of the interferons and render the cell in an anti-viral state as well as secretion of cytokines to recruit macrophages and lymphocytes towards the destruction of transfected cells [7,8]. In short, non-mammalian sequences found on pDNA can severely limit the persistence of transgene expression by epigenetic silencing and activated immune responses.

In this study, we applied a number of pharmacological inhibitor to determine which stress-inducible pathways, apoptosis, NF- κ B activation, DNA repair, histone deacetylase inhibitor and DNA methylation inhibitor negatively affects transgene expression. The pathways blocked are: were also applied to determine if epigenetic regulation is involved.

C.2 Materials and methods

Bone marrow stromal cells from femur of Sprague-Dawley rat (rBMSC) were seeded on 12-well tissue culture plates. Transfection were carried out by incubating polyplex of branched PEI (25kDa) and the plasmid DNA gWiz-GFP for 24 hours in OptiMEM (1% FBS), then replaced with a basic medium. Drugs were added 1 day or 7 days after transfection, and incubated for 48 hours thereafter, then processed for analysis via flow cytometry. Effective drug concentrations were determined by MTT assays and cell number. The drugs used are: CGK733 (ATM/ATR kinase inhibitor), RG108 (DNA methyltransferase inhibitor), 6-Amino-4-(4-phenoxyphenethylamino)quinazoline (quinazolines, NF- κ B inhibitor), and a polypeptide Z-DEVD-FMK (Caspase-3 inhibitor), Valporic Acid (Histone Deacetylase Inhibitor).



Appendix Figure C-1

Effect of various pathway inhibitors on transgene expression

Average fluorescence (FL1) of total cell population 3 days (a) and 9 days (b) after transfection and treatment with drugs.

C.3 Results and discussion

Among the drug administered, only transfected cells exposed to quinazolines showed significant increase in both the percent of transfected cells and total mean fluorescence on Day 3 (**Figure C-1**). No other drug was able to enhance transgene expression significantly. After 9 days, the percent and mean fluorescence of transfected cells dropped to 50% of those observed from the previous time point; addition of quinazolines resulted in a significant increase in total mean fluorescence of the green fluorescent protein. Valporic acid, a histone deacetylase (HDAC) inhibitor, also lead to significant increase in transgene expression, similar to what we have observed previously with trichostatin A, another HDAC inhibitor.

Quinazolines, a NF- κ B activation inhibitor, were able to induce a higher level of transgene expression, suggesting the NF- κ B pathway may be activated during transfection and result in the gradual reduction in transgene expression.

C. 4 References

- [1] Habraken Y., and Piette J., 2006, "NF-kappaB activation by double-strand breaks," *Biochem Pharmacol*, **72**(9), pp. 1132–1141.
- [2] Meyn M. S., 1995, "Ataxia-telangiectasia and cellular responses to DNA damage," *Cancer Res.*, **55**(24), pp. 5991–6001.
- [3] Chen Z. Y., He C. Y., Meuse L., and Kay M. A., 2004, "Silencing of episomal transgene expression by plasmid bacterial DNA elements in vivo," *Gene Ther*, **11**(10), pp. 856–864.
- [4] Chen Z. Y., Riu E., He C.-Y., Xu H., and Kay M. A., 2008, "Silencing of episomal transgene expression in liver by plasmid bacterial backbone DNA is independent of CpG methylation," *Mol Ther*, **16**(3), pp. 548–556.
- [5] Brooks A. R., Harkins R. N., Wang P., Qian H. S., Liu P., and Rubanyi G. M., 2004, "Transcriptional silencing is associated with extensive methylation of the CMV promoter following adenoviral gene delivery to muscle," *J Gene Med*, **6**(4), pp. 395–404.
- [6] Riu E., Chen Z. Y., Xu H., He C.-Y., and Kay M. A., 2007, "Histone modifications are associated with the persistence or silencing of vector-mediated transgene expression in vivo," *Mol Ther*, **15**(7), pp. 1348–1355.
- [7] Sakurai H., Kawabata K., Sakurai F., Nakagawa S., and Mizuguchi H., 2008, "Innate immune response induced by gene delivery vectors," *Int J Pharm*, **354**(1-2), pp. 9–15.
- [8] Kumar H., Kawai T., and Akira S., 2009, "Pathogen recognition in the innate immune response," *Biochem J*, **420**(1), pp. 1–16.

Appendix D

Modular genetic and epigenetic elements for targeted and sustained transgene expression in non-viral gene delivery system¹

¹This section of the thesis was part of a review paper published in: Hsu C. Y., and Uludağ H., 2012, "Nucleic-acid based gene therapeutics: delivery challenges and modular design of nonviral gene carriers and expression cassettes to overcome intracellular barriers for sustained targeted expression.," *J Drug Targeting*, 20(4), pp. 301–328.

D.1 Trafficking and modulating targeting specificity through DNA sequences

Nucleocytoplasmic transport of pDNA can be indirectly facilitated by the NLS/Importin pathway through specific sequence elements called the DNA nuclear targeting sequences (DTS), which contain binding sites for ubiquitous transcription factors (e.g. AP1, AP2, NF- κ B, Oct1, TEF-1 [1]. While the activity of transcription factors are located in the nucleus, most reside in the cytoplasm, either as a conclusion of protein synthesis or as a mean to regulate their activities (e.g. NF- κ B, NFAT, Glucocorticoid receptors). The cytosolic location of the transcription factors allows them to bind to DTS on the pDNA. Upon stimuli triggered activation of metabolic events, the associated transcription factors undergo conformation changes, exposing buried NLS peptide, allowing nuclear transport receptors to bind and shuttle the protein/pDNA complex into the nucleus [2,3].

DTS-mediated pDNA nuclear import can be further refined to drive tissue- or physiology-specific transgene expression. Rather than DTS that are bound by ubiquitous transcription factors, tissue-specific DTS can be employed to limit binding to tissue-specific transcription factors. Non-targeted cells devoid of tissue-specific transcription factor would not be able to co-import pDNA for subsequent transcription. Indeed, DTS isolated from smooth muscle gamma actin (SMGA) promoter and surfactant promoter C (SP-C) have been shown to direct expression specifically to smooth muscle cells and type II pneumonocytes, respectively [4]. However, tissue- or physiologically-specific pDNA import may be limited to certain cell types or physiological conditions since it requires that DNA-binding transcription factor or co-factors bearing the NLS to be regulated via cytosol sequestration prior to activation. In addition, some transcription factors may not be able to display NLS when

bound to DNA, either due to steric hindrance or conformational changes and thus may not be suited to binding both DNA and the nuclear import machinery at the same time [5]. Nevertheless, DTS provides a practical mean to shuttle pDNA into the nucleus without the aid of a gene carrier.

Perhaps the most widely used approach to limit expression in target cells is through tissue-specific promoters. Incorporating tissue-derived regulatory elements limit transcriptional activity to only targeted cells that harbor compatible transcription factors, similar to tissue-specific DTS. These tissue-specific promoters contain both proximal promoters elements and distal regulatory DNA sequences (e.g. locus control regions, enhancers, and introns) to drive targeting by enhancing tissue-specific expression and/or repressing non-tissue-specific expression [6]. Naturally derived promoters from albumin, human 1 antitrypsin (hAAT), creatine kinase, insulin, [7-10] as well as synthetic promoters have been constructed to enhance specificity and transgene expression in liver, muscle, and epithelium [11,12].

Tissue-specific or physiologically-regulated promoters also provide levels of transgene expression that are closely matched to wild type phenotypes. This is critical for some diseases, which not only require delivery and expression of the therapeutic product in specific target cell type but also the correct pattern and the level of expression. An example of this requirement is in the Wiskott–Aldrich syndrome, an X-linked genetic disorder caused by mutation in the WAS gene. Gene therapy for WAS require precisely modulated expression of the WAS protein in the whole heamatopoietic lineage. Ectopic delivery to non-heamatopoietic cells combined with WASP over-expression can interfere with cytoskeleton function, reducing cell viability and contribute to cancer cell invasion [13,14]. DNA fragments isolated from the WAS gene proximal promoter in hematopoietic cells was shown to be sufficient to drive strong

hematopoietic-restricted expression with a concurrent reduction in deleterious effects associated with ectopic expression [15,16]. Thus, tissue-derived promoters not only promote spatially restricted expression, but concurrently provide physiologically relevant level of expression in sensitive targets. While utility of tissue- and physiological-specific promoters is preferred over constitutive viral promoters, progress in this area has been slow due to the fact the promoter must be isolated from the gene of interest, and therefore needs to be custom tailored to a particular disease. But more critically, the expression pattern of the gene of interest may be regulated by epigenetic mechanisms (i.e. chromatin positioning, post-transcriptional silencing) and thus cannot simply be isolated from the genome. Regardless, this example illustrates a method of fine-tuning transgene expression using genetic elements that is more precise than conventional pharmacokinetic measures.

In addition to tissue-specific promoter, targeted expression can be indirectly enforced by suppressing expression in non-targeted cells using miRNA-mediated gene knockdown. Given the population and distribution of endogenous miRNA varies between tissues and differentiated cell lineage, the expression of transgene can be selectively regulated by harnessing the differential pattern of miRNA profile [6]. This strategy has been implemented by incorporating a miRNA recognition elements (MREs) to the pDNA construct [17]; non-targeted cells which express miRNA specific to the MREs would inhibit the expression of the transgene mRNA, while targeted cells lacking the miRNA would allow transgene mRNA to be translated [18,19]. Papapetrou et al., applied this approach to construct a lentiviral vector encoding a chimeric antigen receptor tagged with MRE for mirR-181a. mirR181a expression is elevated in developing thymocytes but suppressed in post-thymic T cells. Utilizing this difference in intracellular mirR181a concentration, the construct was able to selectively transfect

post-thymic resting and activated T cells, but not of developing T cells, to restore self-reactive TCR, which could confer anti-tumor activity for cancer immunotherapy [20].

These strategies focus on targeted expression rather than targeted delivery, whereby selectivity in transfection is controlled by genetic elements. However, this approach still involves system wide delivery to all cell lines, and it could lead to nonspecific reactivity to carriers and nucleic acids. A combinatorial approach incorporating both receptor-ligand assisted delivery and tissue-delimited genetic elements in expression cassettes could work in concert to exponentially enhance the specificity of targeted gene therapy.

D.2 Enhancing the level and duration of transgene expression

Pharmacokinetics approach to enhancing transgene expression is typically achieved by increasing the intranuclear concentration of exogenous nucleic acid through optimization of delivery system, to increase the number of templates available for transcription. This approach can be technically limiting when a saturation point is reached and more intranuclear DNA does not equate to a linear return in expression. Modulating transgene expression through genetic elements provides a viable option to enhancing expression while concurrently reducing the need for high concentration of carrier/pDNA complexes. Methods to enhance transfection efficiency through genetic control elements involve the addition of positive regulators, as well as removal of inhibitory elements. Genetic elements employed in this regard include promoters [21], enhancers [22], locus control region (LCR; [23]), scaffold/matrix attachment regions (S/MAR; [24]), insulators ([25,26] and removal of non-mammalian sequences.

Promoter strengths are dependent on two factors, namely, (i) consensus binding motif and (ii) activity and concentration of endogenous transcription factors, which can

depend on the cell type as well. Promoters with a higher percentage of homology to the consensus sequences are more efficient at recruiting RNA polymerase that has a faster rate of elongation, which clears the binding sites for the next cycle of transcription complex [27]. The most common constitutive promoters for mammalian expression are derived from viruses, such as cytomegalovirus (CMV), Rous Sarcoma virus (RSV) and simian virus (SV40). However, viral sequences can induce immune response and become attenuated in the long term [28]. Nonviral promoters derived from human elongation factor 1 α (EF1 α), human polyubiquitin C (UbC), and chicken β actin/CMV enhancer, phosphoglycerolkinase (PGK) promoter [29,30] are common alternatives used in mammalian expression systems. It should be noted that the activity of the promoters is largely dependent on the cell type, which dictates the abundance of transcription factors that are compatible with those promoters [31,32]. Thus, the optimal promoter would depend on the cell line and the application need (i.e. high expression vs. sustained expression) and may need to be determined empirically through screening and comparative evaluation of several types of promoters.

Enhancers are cis-acting regulatory elements typically incorporated into an expression construct either downstream or upstream of the promoter to increase expression by facilitating efficient recruitment of co-factors for the transcription complex. The most widely cited enhancer is derived from the CMV immediate early genes (CMV IE; [33]) as a hybrid cassette combined with a mammalian promoter [34]. But mammalian derived enhancers such as the Apolipoprotein (ApoE), [8], immunoglobulin [35], microglobulin, and prothrombin [36] have all demonstrated enhancement in transgene expression. The overall performance output of an enhancer-promoter pair will likely depend on the cassette combination and the cell type [37].

Enhancement of post-transcriptional processing of newly synthesized transgene mRNA is another way to improve expression without modifying the carriers. The 3'-end of the expression cassette typically contains three functional sequence elements: polyadenylation (polyA) site, cleavage signal and transcription termination. The polyA tail is functionally critical for nuclear export and translation [38] as well as stability of mRNA [39]. Stable transcripts have a slower turnover rate and accumulate to a higher concentration, allowing more protein to be synthesized. Several polyA sites derived from bovine growth hormone [40], mouse β -globin [41], HSV thymidine kinase gene [42], woodchuck post regulatory element [43], and SV40 early transcription unit [44] have been used in mammalian expression vector. Similarly, transcription termination site is critical for termination of transcription and the dissociation of RNA polymerase (RNAP) from the DNA, minimizing promoter occlusion ([45] and enhance the rate of transcription cycle to allow RNAP to become available for a new round of transcription [46].

These cis-acting regulatory elements described above rely on the recruitment of endogenous trans-acting factors for enhanced expression; the latter may ultimately become limiting factor since it depends on cell physiology. Alternatively, both cis and trans components can be provided exogenously to create a two-step transcriptional amplification system (TSTA). TSTA utilize an expression vector containing a tissue-specific or physiologically-regulated promoter to drive the expression of a transcriptional activator, which then binds to the upstream regulatory region of a second expression construct to enhance the promoter-driven expression of the therapeutic gene [47]. The regulatory elements in the therapeutic gene construct can also be inserted into the activator construct to create a positive feedback loop where the transcriptional activator enhances its own expression [48]. The transcriptional activator in this system is typically a recombinant fusion protein between the DNA

binding domain of a transcription factor from one source and the transcriptional activation domain from another source [48]. This allows the recombinant transcriptional activator to be modularized for adaptation to a wide range of promoters and activation level. TSTA has been shown to greatly enhance tissue-specific expression over the standalone use of tissue-specific promoter ([49-51]).

D.3 Plasmid retention for sustained transgene expression

In order for exogenous nucleic acids to be mitotically stable through cell division, expression cassettes need to be capable of both replicating autonomously as an extra-chromosomal element as well as harboring a mechanism for nuclear retention. Non-integrating episomally maintained expression cassettes can vary in size and autonomy, and ranges from self-replicating pDNA to fully functional minichromosomes (MC). Self-replicating plasmids derived from episomally maintained animal viruses such as SV40, bovine papillomavirus (BPV) and Epstein-Barr Virus (EBV) utilize both cis- and trans-acting factors as replicon and nuclear retention factors. The cis-acting sequence elements provide an origin of replication where it is bound by trans-acting protein factor, which replicates the vector through either a replicase type activity or through the recruitment of the core replication machinery [52-54]. Trans-acting factors can further facilitate binding to metaphase chromosome, providing a piggy-back mechanism to enhance nuclear retention and mitotic stability of the vector [55,56]. Not only are the oriP/EBNA1-based episomal vectors able to extend the expression timeframe from days to months, they also exhibit enhanced nuclear import and enhanced transgene expression [57-60]. Despite their high level and persistence of expression in animal models, hybrid vectors with viral replicons currently have limited utility in human gene therapy due to their cell transforming and immune stimulating nature ([61-65]).

The second class of episomally maintained expression cassettes is derived from mammalian sequences and does not require trans-acting factors for maintenance. Human ACs (HAC) and MCs have been applied to achieve long-term expression in a variety of settings [66-69]. HAC are constructed by a bottom-up approach where individual constituent DNA elements, such as telomere, centromere, replication origin, are retrofitted into a yeast or bacterial-based AC vector [70,71]. MC on the other hand, are constructed by a top-down approach via the de-construction of natural chromosome by irradiation to introduce double strand break, or by telomere fragmentation to generate size-reduced derivative [72,73]. The major advantage of HAC and MC over other episomal vectors is their stability throughout mitotic and meiotic events, without compromising genomic integrity. HAC also has essentially unlimited size insert capacity that can accommodate both the transgene and all of its regulatory elements to preserve wild type expression profile [74-76]. Despite their theoretical superior features, ACs are currently limited to a few niche applications. For one, the sizes of both HAC and MC are in the range of mega basepair, which requires specialized delivery protocols such as the microcell-mediated chromosome transfer or pronuclear injection [77]. Even with these delivery approaches, the establishment of stably expressing cells is difficult at present. Furthermore, insertion of transgene into the AC vector require site-specific recombination, which can be technically cumbersome, making AC difficult to produce for widespread application [78,79].

The third class of episomally maintained system is based on the inclusion of sequences found in the scaffold matrix attachment region (S/MAR). In higher eukaryotes, replication of the genome is tightly associated with the nuclear matrix; the onset of S-phase is often preceded by the binding of the replication origin to the nuclear scaffold or nuclear matrix [80]. The nuclear matrix/scaffold has been implicated to function in genome organization, gene expression, and transcription regulation [81,82]. S/MARs

are AT-rich sequences that define the boundary of independent chromatin domain through the formation of chromatin loops [24]. Based on these characteristics, *S/MAR* sequences have been cloned into expression cassettes to assess its role on transgene expression. The prototype vector pEPI-1, demonstrated persistence in a wide range of mammalian cell lines [83,84] and was even capable of propagating meiotically to generate transgenic animals [85]. The cassette replicates once per cell cycle during early S-phase with initiation starting at random sites throughout the cassette. Sustained reporter gene expression and long-term propagation of the cassette appears to depend exclusively on the transcription unit 5' to the *S/MAR* sequence [86,87]. Sub-cellular fractionation analysis determined that *S/MAR*-containing expression cassettes bind to the nuclear matrix by interaction with the matrix protein SAF-A and associate with chromosome during mitosis [88,89]. Despite the improved nuclear retention and mitotic stability imparted by *S/MAR* sequences, transgene silencing as a result of promoter inactivation seems unavoidable in certain cells [83]. Furthermore, the establishment of stable clones from transfected cells is at present, inefficient, with success rate ranging from 0.5 to 5% [74]. It is becoming increasingly clear that the generation of stable transgenic cell line using episomal vectors is not exclusively dependent on primary DNA sequence or particular chromatin make-up, but rather, involves a series of stochastic epigenetic events yet to be described [90]. Nevertheless, the size, safety and activity afforded by *S/MAR*-based vectors appear to be the most promising for facilitating long-term expression in nonviral delivery.

D.4 Evading silencing for sustained transgene expression

Removal or replacement of undesirable sequences can further contribute to long-term expression of the transgene. This involves either replacement of attenuated promoters, removal of non-expressing bacterial derived vector backbone and/or inclusion of

insulator elements to prevent chromatinization. Highly active virally derived promoters, such as the intermediate early gene promoter from CMV, are known to be subjected to epigenetic silencing. The abundance of cytosine-guanine repeats (CpG) within the promoter sequence is prone to methylation by cellular methyl transferases, which attenuate its transcriptional activity [91]. Constitutively expressed or tissue-specific promoter of mammalian origins, on the other hand, are less prone to hypermethylation and have been shown to be successful in avoiding transcriptional silencing [34,92-94].

The highly immunogenic CpG sequences (discussed in the section Immune responses to nucleic acid and complexes) can abolish long-term transgene expression through induction of innate and humoral responses. It can also render the pDNA in a repressed chromatin state through binding with heterochromatin-associated histones. Extending the duration of transgene expression through reduction of immune reactivity to CpG sequences can be conferred by either methylation of the nucleotides or removal of the bacterial backbone [95-97]. The bacterial derived backbone can be excised through site-specific integrase-mediated intracellular recombination technology [98,99]. The resulting truncated minicircle DNA showed a more robust and persistent transgene expression than its full-length parental molecule in vivo [100].

Shielding of pDNA heterochromatinization can be accomplished through incorporation of genetic insulators [101]. Genetic insulators are boundary elements that can act as enhancer-blocker and silencing-barrier to shield transcriptional units from being affected by neighboring regulatory elements, such as the spread of heterochromatin [102]. Its incorporation in expression cassette provides a mean to maintain the transgene in an open euchromatin state to sustain transcriptional activity [25,103]. However, it is important to note that genetic insulators act as boundary

elements, thus their activity can be both inductive and repressive - the directionality of insulator activity may depend on neighboring genes and nearby regulatory elements. Another genetic element that has been used in transgene construct is the recently identified locus control region (LCR). LCR are transcriptional regulators with enhancer activity related to genes linked in cis and have the ability to overcome position effect to maintain an open chromatin structure at the domain level [104]. Inclusion of the human β -globin LCR in an EBV-based vector was shown to extend the expression of the β -globin transgene for up to 2 months in the absence of selection [105]. Furthermore, a combinatorial use of the cHS4 insulator and the α -globin LCR (HS40) in retroviral vectors resulted in long-term expression of human gamma globin gene in a mouse bone marrow transduction and transplantation model, with retention rate of transfected cells increased from 2–5 to 49% [106]. Numerous LCR has been discovered to date ([107]. However, LCR exhibit tissue-specificity and thus a universal construct may not be feasible to wide spread application, though, this may be viewed as an advantage to further maintain targeted expression in a tissue-specific manner.

D.5 References

- [1] Miller A. M., and Dean D. A., 2009, "Tissue-specific and transcription factor-mediated nuclear entry of DNA," *Adv Drug Deliv Rev*, **61**(7-8), pp. 603–613.
- [2] Dean D. A., 1997, "Import of plasmid DNA into the nucleus is sequence specific," *Exp. Cell Res.*, **230**(2), pp. 293–302.
- [3] Dean D. A., Strong D. D., and Zimmer W. E., 2005, "Nuclear entry of nonviral vectors," *Gene Ther*, **12**(11), pp. 881–890.
- [4] Degiulio J. V., Kaufman C. D., and Dean D. A., 2010, "The SP-C promoter facilitates alveolar type II epithelial cell-specific plasmid nuclear import and gene expression," *Gene Ther*, **17**(4), pp. 541–549.
- [5] Chan C. K., and Jans D. A., 2001, "Enhancement of MSH receptor- and GAL4-mediated gene transfer by switching the nuclear import pathway," *Gene Ther*, **8**(2), pp. 166–171.
- [6] Toscano M. G., Romero Z., Muñoz P., Cobo M., Benabdellah K., and Martin F., 2011, "Physiological and tissue-specific vectors for treatment of inherited diseases," *Gene Ther*, **18**(2), pp. 117–127.
- [7] Follenzi A., Sabatino G., Lombardo A., Boccaccio C., and Naldini L., 2002, "Efficient gene delivery and targeted expression to hepatocytes in vivo by improved lentiviral vectors," *Hum Gene Ther*, **13**(2), pp. 243–260.
- [8] Le M., Okuyama T., Cai S. R., Kennedy S. C., Bowling W. M., Flye M. W., and Ponder K. P., 1997, "Therapeutic levels of functional human factor X in rats after retroviral-mediated hepatic gene therapy," *Blood*, **89**(4), pp. 1254–1259.
- [9] Gregorevic P., Blankinship M. J., Allen J. M., Crawford R. W., Meuse L., Miller D. G., Russell D. W., and Chamberlain J. S., 2004, "Systemic delivery of genes to striated muscles using adeno-associated viral vectors," *Nat. Med.*, **10**(8), pp. 828–834.
- [10] Londrigan S. L., Brady J. L., Sutherland R. M., Hawthorne W. J., Thomas H. E., Jhala G., Cowan P. J., Kay T. W. H., O'Connell P. J., and Lew A. M., 2007,

"Evaluation of promoters for driving efficient transgene expression in neonatal porcine islets," *Xenotransplantation*, **14**(2), pp. 119–125.

- [11] Mount J. D., Herzog R. W., Tillson D. M., Goodman S. A., Robinson N., McClelland M. L., Bellinger D., Nichols T. C., Arruda V. R., Lothrop C. D., and High K. A., 2002, "Sustained phenotypic correction of hemophilia B dogs with a factor IX null mutation by liver-directed gene therapy," *Blood*, **99**(8), pp. 2670–2676.
- [12] Salva M. Z., Himeda C. L., Tai P. W., Nishiuchi E., Gregorevic P., Allen J. M., Finn E. E., Nguyen Q. G., Blankinship M. J., Meuse L., Chamberlain J. S., and Hauschka S. D., 2007, "Design of tissue-specific regulatory cassettes for high-level rAAV-mediated expression in skeletal and cardiac muscle," *Mol Ther*, **15**(2), pp. 320–329.
- [13] Toscano M. G., Frecha C., Benabdellah K., Cobo M., Blundell M., Thrasher A. J., García-Olivares E., Molina I. J., and Martin F., 2008, "Hematopoietic-specific lentiviral vectors circumvent cellular toxicity due to ectopic expression of Wiskott-Aldrich syndrome protein," *Hum Gene Ther*, **19**(2), pp. 179–197.
- [14] Yamaguchi H., and Condeelis J., 2007, "Regulation of the actin cytoskeleton in cancer cell migration and invasion," *Biochim Biophys Acta*, **1773**(5), pp. 642–652.
- [15] Martin F., Toscano M. G., Blundell M., Frecha C., Srivastava G. K., Santamaría M., Thrasher A. J., and Molina I. J., 2005, "Lentiviral vectors transcriptionally targeted to hematopoietic cells by WASP gene proximal promoter sequences," *Gene Ther*, **12**(8), pp. 715–723.
- [16] Dupré L., Trifari S., Follenzi A., Marangoni F., Lain de Lera T., Bernad A., Martino S., Tsuchiya S., Bordignon C., Naldini L., Aiuti A., and Roncarolo M.-G., 2004, "Lentiviral vector-mediated gene transfer in T cells from Wiskott-Aldrich syndrome patients leads to functional correction," *Mol Ther*, **10**(5), pp. 903–915.
- [17] Kelly E. J., and Russell S. J., 2009, "MicroRNAs and the regulation of vector tropism," *Mol Ther*, **17**(3), pp. 409–416.
- [18] Brown B. D., Venneri M. A., Zingale A., Sergi Sergi L., and Naldini L., 2006,

- "Endogenous microRNA regulation suppresses transgene expression in hematopoietic lineages and enables stable gene transfer," *Nat. Med.*, **12**(5), pp. 585–591.
- [19] Brown B. D., Cantore A., Annoni A., Sergi L. S., Lombardo A., Valle Della P., D'Angelo A., and Naldini L., 2007, "A microRNA-regulated lentiviral vector mediates stable correction of hemophilia B mice," *Blood*, **110**(13), pp. 4144–4152.
- [20] Papapetrou E. P., Kovalovsky D., Beloeil L., Sant'angelo D., and Sadelain M., 2009, "Harnessing endogenous miR-181a to segregate transgenic antigen receptor expression in developing versus post-thymic T cells in murine hematopoietic chimeras," *J. Clin. Invest.*, **119**(1), pp. 157–168.
- [21] Butler J. E. F., and Kadonaga J. T., 2002, "The RNA polymerase II core promoter: a key component in the regulation of gene expression," *Genes Dev.*, **16**(20), pp. 2583–2592.
- [22] Blackwood E. M., and Kadonaga J. T., 1998, "Going the distance: a current view of enhancer action," *Science*, **281**(5373), pp. 60–63.
- [23] Bulger M., Sawado T., Schübeler D., and Groudine M., 2002, "ChIPs of the beta-globin locus: unraveling gene regulation within an active domain," *Curr. Opin. Genet. Dev.*, **12**(2), pp. 170–177.
- [24] Bode J., Benham C., Knopp A., and Mielke C., 2000, "Transcriptional augmentation: modulation of gene expression by scaffold/matrix-attached regions (S/MAR elements)," *Crit. Rev. Eukaryot. Gene Expr.*, **10**(1), pp. 73–90.
- [25] Furlan-Magaril M., Rebollar E., Guerrero G., Fernández A., Moltó E., González-Buendía E., Cantero M., Montoliu L., and Recillas-Targa F., 2011, "An insulator embedded in the chicken α -globin locus regulates chromatin domain configuration and differential gene expression," *Nucleic Acids Res*, **39**(1), pp. 89–103.
- [26] Gomos-Klein J., Harrow F., Alarcón J., and Ortiz B. D., 2007, "CTCF-independent, but not CTCF-dependent, elements significantly contribute to TCR-alpha locus control region activity," *J. Immunol.*, **179**(2), pp. 1088–1095.

- [27] Brunner M., and Bujard H., 1987, "Promoter recognition and promoter strength in the Escherichia coli system.," *EMBO J.*, **6**(10), pp. 3139–3144.
- [28] Weeratna R. D., Wu T., Efler S. M., Zhang L., and Davis H. L., 2001, "Designing gene therapy vectors: avoiding immune responses by using tissue-specific promoters.," *Gene Ther*, **8**(24), pp. 1872–1878.
- [29] Pringle I. A., McLachlan G., Collie D. D. S., Sumner-Jones S. G., Lawton A. E., Tennant P., Baker A., Gordon C., Blundell R., Varathalingam A., Davies L. A., Schmid R. A., Cheng S. H., Porteous D. J., Gill D. R., and Hyde S. C., 2007, "Electroporation enhances reporter gene expression following delivery of naked plasmid DNA to the lung.," *J Gene Med*, **9**(5), pp. 369–380.
- [30] Walther W., and Stein U., 1996, "Cell type specific and inducible promoters for vectors in gene therapy as an approach for cell targeting.," *J. Mol. Med.*, **74**(7), pp. 379–392.
- [31] Zheng C., and Baum B. J., 2005, "Evaluation of viral and mammalian promoters for use in gene delivery to salivary glands.," *Mol Ther*, **12**(3), pp. 528–536.
- [32] Qin J. Y., Zhang L., Clift K. L., Hular I., Xiang A. P., Ren B.-Z., and Lahn B. T., 2010, "Systematic comparison of constitutive promoters and the doxycycline-inducible promoter.," *PLoS ONE*, **5**(5), p. e10611.
- [33] Foecking M. K., and Hofstetter H., 1986, "Powerful and versatile enhancer-promoter unit for mammalian expression vectors.," *Gene*, **45**(1), pp. 101–105.
- [34] Magnusson T., Haase R., Schlee M., Wagner E., and Ogris M., 2011, "Sustained, high transgene expression in liver with plasmid vectors using optimized promoter-enhancer combinations.," *J Gene Med*, **13**(7-8), pp. 382–391.
- [35] Laurie K. L., Blundell M. P., Baxendale H. E., Howe S. J., Sinclair J., Qasim W., Brunsberg U., Thrasher A. J., Holmdahl R., and Gustafsson K., 2007, "Cell-specific and efficient expression in mouse and human B cells by a novel hybrid immunoglobulin promoter in a lentiviral vector.," *Gene Ther*, **14**(23), pp. 1623–1631.
- [36] Yasuda M., Domaradzki M. E., Armentano D., Cheng S. H., Bishop D. F., and

- Desnick R. J., 2007, "Acute intermittent porphyria: vector optimization for gene therapy," *J Gene Med*, **9**(9), pp. 806–811.
- [37] Schlabach M. R., Hu J. K., Li M., and Elledge S. J., 2010, "Synthetic design of strong promoters," *Proc Natl Acad Sci USA*, **107**(6), pp. 2538–2543.
- [38] Jackson R. J., and Standart N., 1990, "Do the poly(A) tail and 3' untranslated region control mRNA translation?," *Cell*, **62**(1), pp. 15–24.
- [39] Schambach A., Wodrich H., Hildinger M., Bohne J., Kräusslich H. G., and Baum C., 2000, "Context dependence of different modules for posttranscriptional enhancement of gene expression from retroviral vectors," *Mol Ther*, **2**(5), pp. 435–445.
- [40] Goodwin E. C., and Rottman F. M., 1992, "The 3'-flanking sequence of the bovine growth hormone gene contains novel elements required for efficient and accurate polyadenylation," *J Biol Chem*, **267**(23), pp. 16330–16334.
- [41] Pandey N. B., Chodchoy N., Liu T. J., and Marzluff W. F., 1990, "Introns in histone genes alter the distribution of 3' ends," *Nucleic Acids Res*, **18**(11), pp. 3161–3170.
- [42] Schmidt E. V., Christoph G., Zeller R., and Leder P., 1990, "The cytomegalovirus enhancer: a pan-active control element in transgenic mice," *Mol. Cell. Biol.*, **10**(8), pp. 4406–4411.
- [43] Zufferey R., Donello J. E., Trono D., and Hope T. J., 1999, "Woodchuck hepatitis virus posttranscriptional regulatory element enhances expression of transgenes delivered by retroviral vectors," *J. Virol.*, **73**(4), pp. 2886–2892.
- [44] van den Hoff M. J., Labruyère W. T., Moorman A. F., and Lamers W. H., 1993, "Mammalian gene expression is improved by use of a longer SV40 early polyadenylation cassette," *Nucleic Acids Res*, **21**(21), pp. 4987–4988.
- [45] Proudfoot N. J., 1986, "Transcriptional interference and termination between duplicated alpha-globin gene constructs suggests a novel mechanism for gene regulation," *Nature*, **322**(6079), pp. 562–565.

- [46] Kim D., Kim J. D., Baek K., Yoon Y., and Yoon J., 2003, "Improved mammalian expression systems by manipulating transcriptional termination regions," *Biotechnol. Prog.*, **19**(5), pp. 1620–1622.
- [47] Arendt M. L., Nasir L., and Morgan I. M., 2009, "A novel two-step transcriptional activation system for gene therapy directed toward epithelial cells," *Mol. Cancer Ther.*, **8**(12), pp. 3244–3254.
- [48] Ochiai H., Harashima H., and Kamiya H., 2010, "Positive feedback system provides efficient and persistent transgene expression," *Mol Pharm.*, **7**(4), pp. 1125–1132.
- [49] Dzojic H., Cheng W.-S., and Essand M., 2007, "Two-step amplification of the human PPT sequence provides specific gene expression in an immunocompetent murine prostate cancer model," *Cancer Gene Ther.*, **14**(3), pp. 233–240.
- [50] Hattori Y., and Maitani Y., 2006, "Two-step transcriptional amplification-lipid-based nanoparticles using PSMA or midkine promoter for suicide gene therapy in prostate cancer," *Cancer Sci.*, **97**(8), pp. 787–798.
- [51] Zhang L., Adams J. Y., Billick E., Ilagan R., Iyer M., Le K., Smallwood A., Gambhir S. S., Carey M., and Wu L., 2002, "Molecular engineering of a two-step transcription amplification (TSTA) system for transgene delivery in prostate cancer," *Mol Ther.*, **5**(3), pp. 223–232.
- [52] Friedrich T., Bedner E., Darzynkiewicz Z., and Lehman J., 2005, "Distinct patterns of MCM protein binding in nuclei of S phase and rereplicating SV40-infected monkey kidney cells," *Cytom Part A*, **68A**(1), pp. 10–18.
- [53] Ravnan J. B., Gilbert D. M., Hagen Ten K. G., and Cohen S. N., 1992, "Random-choice replication of extrachromosomal bovine papillomavirus (BPV) molecules in heterogeneous, clonally derived BPV-infected cell lines," *J. Virol.*, **66**(12), pp. 6946–6952.
- [54] Wang J., and Sugden B., 2005, "Origins of bidirectional replication of Epstein-Barr virus: models for understanding mammalian origins of DNA synthesis," *J. Cell. Biochem.*, **94**(2), pp. 247–256.

- [55] Zheng P.-S., Brokaw J., and McBride A. A., 2005, "Conditional mutations in the mitotic chromosome binding function of the bovine papillomavirus type 1 E2 protein.," *J. Virol.*, **79**(3), pp. 1500–1509.
- [56] Ito S., Gotoh E., Ozawa S., and Yanagi K., 2002, "Epstein-Barr virus nuclear antigen-1 is highly colocalized with interphase chromatin and its newly replicated regions in particular.," *J. Gen. Virol.*, **83**(Pt 10), pp. 2377–2383.
- [57] Mazda O., 2002, "Improvement of nonviral gene therapy by Epstein-Barr virus (EBV)-based plasmid vectors.," *Curr Gene Ther.*, **2**(3), pp. 379–392.
- [58] Aliño S. F., Crespo A., and Dasí F., 2003, "Long-term therapeutic levels of human alpha-1 antitrypsin in plasma after hydrodynamic injection of nonviral DNA.," *Gene Ther.*, **10**(19), pp. 1672–1679.
- [59] Min K. A., Oh S. T., Yoon K. H., Kim C. K., and Lee S. K., 2003, "Prolonged gene expression in primary porcine pancreatic cells using an Epstein-Barr virus-based episomal vector.," *Biochem Biophys Res Commun.*, **305**(1), pp. 108–115.
- [60] Sclimenti C. R., Neviasser A. S., Baba E. J., Meuse L., Kay M. A., and Calos M. P., 2003, "Epstein-Barr virus vectors provide prolonged robust factor IX expression in mice.," *Biotechnol. Prog.*, **19**(1), pp. 144–151.
- [61] Valls E., la Cruz de X., and Martínez-Balbás M. A., 2003, "The SV40 T antigen modulates CBP histone acetyltransferase activity.," *Nucleic Acids Res.*, **31**(12), pp. 3114–3122.
- [62] Strayer D. S., and Zern M. A., 1999, "Gene delivery to the liver using simian virus 40-derived vectors.," *Semin. Liver Dis.*, **19**(1), pp. 71–81.
- [63] Lampela P., Ustav E., Ustav M., Niskanen M., Männistö P. T., and Raasmaja A., 2001, "Efficient transfection of novel bovine papillomavirus 1 expression plasmids.," *Plasmid.*, **46**(3), pp. 163–169.
- [64] Taylor G. S., Haigh T. A., Gudgeon N. H., Phelps R. J., Lee S. P., Steven N. M., and Rickinson A. B., 2004, "Dual stimulation of Epstein-Barr Virus (EBV)-specific CD4+ and CD8+ T-cell responses by a chimeric antigen construct: potential therapeutic vaccine for EBV-positive nasopharyngeal carcinoma.," *J. Virol.*,

78(2), pp. 768–778.

- [65] Humme S., Reisbach G., Feederle R., Delecluse H.-J., Bousset K., Hammerschmidt W., and Schepers A., 2003, "The EBV nuclear antigen 1 (EBNA1) enhances B cell immortalization several thousandfold," *Proc Natl Acad Sci USA*, **100**(19), pp. 10989–10994.
- [66] Katoh M., Ayabe F., Norikane S., Okada T., Masumoto H., Horike S.-I., Shirayoshi Y., and Oshimura M., 2004, "Construction of a novel human artificial chromosome vector for gene delivery," *Biochem Biophys Res Commun*, **321**(2), pp. 280–290.
- [67] Vanderbyl S. L., Sullenbarger B., White N., Perez C. F., MacDonald G. N., Stodola T., Bunnell B. A., Ledebur H. C., and Lasky L. C., 2005, "Transgene expression after stable transfer of a mammalian artificial chromosome into human hematopoietic cells," *Exp. Hematol.*, **33**(12), pp. 1470–1476.
- [68] Kennard M. L., 2011, "Engineered mammalian chromosomes in cellular protein production: future prospects," *Methods Mol Biol*, **738**, pp. 217–238.
- [69] Auriche C., Carpani D., Conese M., Caci E., Zegarra-Moran O., Donini P., and Ascenzioni F., 2002, "Functional human CFTR produced by a stable minichromosome," *EMBO Rep.*, **3**(9), pp. 862–868.
- [70] Mejía J. E., Alazami A., Willmott A., Marschall P., Levy E., Earnshaw W. C., and Larin Z., 2002, "Efficiency of de novo centromere formation in human artificial chromosomes," *Genomics*, **79**(3), pp. 297–304.
- [71] Grimes B. R., Rhoades A. A., and Willard H. F., 2002, "Alpha-satellite DNA and vector composition influence rates of human artificial chromosome formation," *Mol Ther*, **5**(6), pp. 798–805.
- [72] Basu J., and Willard H. F., 2005, "Artificial and engineered chromosomes: non-integrating vectors for gene therapy," *Trends Mol Med*, **11**(5), pp. 251–258.
- [73] Kakeda M., Hiratsuka M., Nagata K., Kuroiwa Y., Kakitani M., Katoh M., Oshimura M., and Tomizuka K., 2005, "Human artificial chromosome (HAC) vector provides long-term therapeutic transgene expression in normal human

primary fibroblasts," *Gene Ther*, **12**(10), pp. 852–856.

- [74] Ehrhardt A., Haase R., Schepers A., Deutsch M. J., Lipps H. J., and Baiker A., 2008, "Episomal Vectors for Gene Therapy," *Curr Gene Ther*, **8**(3), pp. 147–161.
- [75] Suzuki N., Nishii K., and Okazaki T., 2006, "Human artificial chromosomes constructed using the bottom-up strategy are stably maintained in mitosis and efficiently transmissible to progeny mice," *Journal of Biological Chemistry*.
- [76] Carlson S., Rudgers G., Zieler H., and Mach J., 2007, "Meiotic transmission of an in vitro-assembled autonomous maize minichromosome," *PLoS Genetics*.
- [77] Killary A. M., and Fournier R. E., 1995, "Microcell fusion," *Meth. Enzymol.*, **254**, pp. 133–152.
- [78] Werdien D., Peiler G., and Ryffel G. U., 2001, "FLP and Cre recombinase function in *Xenopus* embryos," *Nucleic Acids Res*, **29**(11), pp. E53–3.
- [79] Kuroiwa Y., Tomizuka K., Shinohara T., Kazuki Y., Yoshida H., Ohguma A., Yamamoto T., Tanaka S., Oshimura M., and Ishida I., 2000, "Manipulation of human minichromosomes to carry greater than megabase-sized chromosome inserts," *Nat Biotechnol*, **18**(10), pp. 1086–1090.
- [80] Cook P. R., 1999, "The organization of replication and transcription," *Science*, **284**(5421), pp. 1790–1795.
- [81] Laemmli U. K., Käs E., Poljak L., and Adachi Y., 1992, "Scaffold-associated regions: cis-acting determinants of chromatin structural loops and functional domains," *Curr. Opin. Genet. Dev.*, **2**(2), pp. 275–285.
- [82] Schübeler D., Mielke C., Maass K., and Bode J., 1996, "Scaffold/matrix-attached regions act upon transcription in a context-dependent manner," *Biochemistry*, **35**(34), pp. 11160–11169.
- [83] Papapetrou E. P., Ziros P. G., Micheva I. D., Zoumbos N. C., and Athanassiadou A., 2006, "Gene transfer into human hematopoietic progenitor cells with an episomal vector carrying an S/MAR element," *Gene Ther*, **13**(1), pp. 40–51.
- [84] Schaarschmidt D., Baltin J., Stehle I. M., Lipps H. J., and Knippers R., 2004, "An

episomal mammalian replicon: sequence-independent binding of the origin recognition complex.” *EMBO J.*, **23**(1), pp. 191–201.

- [85] Manzini S., Vargiolu A., Stehle I. M., Bacci M. L., Cerrito M. G., Giovannoni R., Zannoni A., Bianco M. R., Forni M., Donini P., Papa M., Lipps H. J., and Lavitrano M., 2006, “Genetically modified pigs produced with a nonviral episomal vector.” *Proc Natl Acad Sci USA*, **103**(47), pp. 17672–17677.
- [86] Stehle I. M., Scinteie M. F., Baiker A., Jenke A. C. W., and Lipps H. J., 2003, “Exploiting a minimal system to study the epigenetic control of DNA replication: the interplay between transcription and replication.” *Chromosome Res.*, **11**(5), pp. 413–421.
- [87] Jenke A. C. W., Stehle I. M., Herrmann F., Eisenberger T., Baiker A., Bode J., Fackelmayer F. O., and Lipps H. J., 2004, “Nuclear scaffold/matrix attached region modules linked to a transcription unit are sufficient for replication and maintenance of a mammalian episome.” *Proc Natl Acad Sci USA*, **101**(31), pp. 11322–11327.
- [88] Baiker A., Maercker C., Piechaczek C., Schmidt S. B., Bode J., Benham C., and Lipps H. J., 2000, “Mitotic stability of an episomal vector containing a human scaffold/matrix-attached region is provided by association with nuclear matrix.” *Nat. Cell Biol.*, **2**(3), pp. 182–184.
- [89] Jenke A. C. W., Eisenberger T., Baiker A., Stehle I. M., Wirth S., and Lipps H. J., 2005, “The nonviral episomal replicating vector pEPI-1 allows long-term inhibition of bcr-abl expression by shRNA.” *Hum Gene Ther*, **16**(4), pp. 533–539.
- [90] Jackson D. A., Juranek S., and Lipps H. J., 2006, “Designing nonviral vectors for efficient gene transfer and long-term gene expression.” *Mol Ther*, **14**(5), pp. 613–626.
- [91] Brooks A. R., Harkins R. N., Wang P., Qian H. S., Liu P., and Rubanyi G. M., 2004, “Transcriptional silencing is associated with extensive methylation of the CMV promoter following adenoviral gene delivery to muscle.” *J Gene Med*, **6**(4), pp. 395–404.

- [92] Wooddell C. I., Reppen T., Wolff J. A., and Herweijer H., 2008, "Sustained liver-specific transgene expression from the albumin promoter in mice following hydrodynamic plasmid DNA delivery," *J Gene Med*, **10**(5), pp. 551–563.
- [93] Gill D. R., Smyth S. E., Goddard C. A., Pringle I. A., Higgins C. F., Colledge W. H., and Hyde S. C., 2001, "Increased persistence of lung gene expression using plasmids containing the ubiquitin C or elongation factor 1alpha promoter," *Gene Ther*, **8**(20), pp. 1539–1546.
- [94] Nguyen A. T., Dow A. C., Kupiec-Weglinski J., Busuttill R. W., and Lipshutz G. S., 2008, "Evaluation of gene promoters for liver expression by hydrodynamic gene transfer," *J. Surg. Res.*, **148**(1), pp. 60–66.
- [95] Hodges B. L., Taylor K. M., Joseph M. F., Bourgeois S. A., and Scheule R. K., 2004, "Long-term transgene expression from plasmid DNA gene therapy vectors is negatively affected by CpG dinucleotides," *Mol Ther*, **10**(2), pp. 269–278.
- [96] Reyes-Sandoval A., and Ertl H. C. J., 2004, "CpG methylation of a plasmid vector results in extended transgene product expression by circumventing induction of immune responses," *Mol Ther*, **9**(2), pp. 249–261.
- [97] Huang M., Chen Z., Hu S., Jia F., Li Z., Hoyt G., Robbins R. C., Kay M. A., and Wu J. C., 2009, "Novel minicircle vector for gene therapy in murine myocardial infarction," *Circulation*, **120**(11 Suppl), pp. S230–7.
- [98] Mayrhofer P., Blaesen M., Schleef M., and Jechlinger W., 2008, "Minicircle-DNA production by site specific recombination and protein-DNA interaction chromatography," *J Gene Med*, **10**(11), pp. 1253–1269.
- [99] Chen Z. Y., He C.-Y., Ehrhardt A., and Kay M. A., 2003, "Minicircle DNA vectors devoid of bacterial DNA result in persistent and high-level transgene expression in vivo," *Mol Ther*, **8**(3), pp. 495–500.
- [100] Osborn M. J., McElmurry R. T., Lees C. J., Defeo A. P., Chen Z. Y., Kay M. A., Naldini L., Freeman G., Tolar J., and Blazar B. R., 2011, "Minicircle DNA-based gene therapy coupled with immune modulation permits long-term expression of α -L-iduronidase in mice with mucopolysaccharidosis type I," *Mol Ther*, **19**(3), pp. 450–460.

- [101] Chen Z. Y., He C. Y., Meuse L., and Kay M. A., 2004, "Silencing of episomal transgene expression by plasmid bacterial DNA elements in vivo.," *Gene Ther*, **11**(10), pp. 856–864.
- [102] Raab J. R., and Kamakaka R. T., 2010, "Insulators and promoters: closer than we think.," *Nat Rev Genet*, **11**(6), pp. 439–446.
- [103] Macarthur C. C., Xue H., Van Hoof D., Lieu P. T., Dudas M., Fontes A., Swistowski A., Touboul T., Seerke R., Laurent L. C., Loring J. F., German M. S., Zeng X., Rao M. S., Lakshmiathy U., Chesnut J. D., and Liu Y., 2011, "Chromatin Insulator Elements Block Transgene Silencing in Engineered Human Embryonic Stem Cell Lines at a Defined Chromosome 13 Locus.," *Stem Cells Dev*.
- [104] Li Q., Peterson K. R., Fang X., and Stamatoyannopoulos G., 2002, "Locus control regions.," *Blood*, **100**(9), pp. 3077–3086.
- [105] Chow C.-M., Athanassiadou A., Raguz S., Psiouri L., Harland L., Malik M., Aitken M. A., Grosveld F., and Antoniou M., 2002, "LCR-mediated, long-term tissue-specific gene expression within replicating episomal plasmid and cosmid vectors.," *Gene Ther*, **9**(5), pp. 327–336.
- [106] Emery D. W., Yannaki E., Tubb J., Nishino T., Li Q., and Stamatoyannopoulos G., 2002, "Development of virus vectors for gene therapy of beta chain hemoglobinopathies: flanking with a chromatin insulator reduces gamma-globin gene silencing in vivo.," *Blood*, **100**(6), pp. 2012–2019.
- [107] Bonifer C., 2000, "Developmental regulation of eukaryotic gene loci: which cis-regulatory information is required?," *Trends Genet*, **16**(7), pp. 310–315.